Channel Estimation and Performance Analysis of MIMO-OFDM Communications using Space-Time and Space-Frequency Coding Schemes

Fabien Delestre

A thesis submitted in partial fulfilment of the requirements of the University of Hertfordshire for the degree of Doctor of Philosophy

The programme of research was carried out in the Science and Technology Research Institute (STRI), University of Hertfordshire,

United Kingdom.

June 2011

Abstract

This thesis is concerned with channel estimation and data detection of MIMO-OFDM communication systems using Space-Time Block Coding (STBC) and Space-Frequency Block Coding (SFBC) under frequency selective channels. A new iterative joint channel estimation and signal detection technique for both STBC-OFDM and SFBC-OFDM systems is proposed. The proposed algorithm is based on a processive sequence of events for space time and space frequency coding schemes where pilot subcarriers are used for channel estimation in the first time instant, and then in the second time instant, the estimated channel is used to decode the data symbols in the adjacent data subcarriers. Once data symbols are recovered, the system recursively performs a new channel estimation using the decoded data symbols as pilots. The iterative process is repeated until all MIMO-OFDM symbols are recovered. In addition, the proposed channel estimation technique is based on the maximum likelihood (ML) approach which offers linearity and simplicity of implementation. Due to the orthogonality of STBC and SFBC, high computation efficiency is achieved since the method does not require any matrix inversion for estimation and detection at the receiver. Another major novel contribution of the thesis is the proposal of a new group decoding method that reduces the processing time significantly via the use of sub-carrier grouping for transmitted data recovery. The OFDM symbols are divided into groups to which a set of pilot subcarriers are assigned and used to initiate the channel estimation process. Designated data symbols contained within each group of the OFDM symbols are decoded simultaneously in order to improve the decoding duration. Finally, a new mixed STBC and SFBC channel estimation and data

detection technique with a joint iterative scheme and a group decoding method is proposed. In this technique, STBC and SFBC are used for pilot and data subcarriers alternatively, forming the different combinations of STBC/SFBC and SFBC/STBC. All channel estimation and data detection methods for different MIMO-OFDM systems proposed in the thesis have been simulated extensively in many different scenarios and their performances have been verified fully.

Acknowledgements

First, I would like to express my sincere gratitude to my supervisor, Professor Yichuang Sun for his guidance, support, advice and encouragement during my research project. This thesis would not have been possible without his help, especially with regards to the financial support to conduct this project.

I would also like to thank EPSRC for the financial support provided during my research under the award number 06001434. Due acknowledgement must also be given to Mr. Chris Lay, Managing Director of GigaSat for funding the early part of my research work. In addition, many thanks go to Andy Slaney who introduced me to the company.

I owe a great deal of thanks to my family, for their constant support and encouragement throughout the duration of my study.

Finally, I would like to thank my friends and colleagues, especially Mr. Gbenga Owojaiye and Dr. Ali Gliwan for their help and for the enjoyable time I have experienced during my study at the University.

Table of Contents

List of Figures

List of Tables

Abbreviations

3G-LTE	3rd Generation-Long Term Evolution
4G	4th Generation
CP	Cyclic Prefix
CSI	Channel State Information
DSTBC	Differential Space Time Block Coding
FFT	Fast Fourier Transform
FPGA	Field Programmable Gate Array
IEEE	Institute of Electrical and Electronics Engineers
IFFT	Inverse Fast Fourier Transform
ISI	Inter-Symbol Interference
LDPC	Low Density Parity Check
LOS	Line of Sight
MIMO	Multiple Input Multiple Output
ML	Maximum Likelihood
MMSE	Minimum Mean Square Error
MRC	Maximal Ratio Combining

NLOS	Non Line of Sight
OFDM	Orthogonal Frequency Division Multiplexing
PAM	Pulse Amplitude Modulation
PAPR	Peak to Average Power Reduction
QAM	Quadrature Amplitude Modulation
QOSTBC	Quasi-Orthogonal Space Time Block Codes
QPSK	Quadrature Phase-Shift Keying
rms	root mean square
SFBC	Space Frequency Block Coding
SISO	Single Input Single Output
SNR	Signal to Noise Ratio
STBC	Space Time Block Coding
STFBC	Space-Time-Frequency Block Coding
SUI	Stanford University Interim
WLAN	Wireless Local area Network

Declaration

The following papers have been published and parts of their materials are included in the thesis:

Published Papers:

[1] F. Delestre, E. Masoud, Y. Sun and A. Slaney, "Detection scheme for space-time block codes wireless communications without channel state information," in *11th IEEE Singapore International Conference on Communication Systems(ICCS)*, pp. 77-81, 2008.

[2] F. Delestre and Y. Sun, "Pilot Aided Channel Estimation for MIMO-OFDM Systems,"in *London Communications Symposium (LCS)*, UCL , 2009.

[3] F. Delestre and Y. Sun, "A channel estimation method for MIMO-OFDM Mobile WiMax systems," in *7th International Symposium on Wireless Communication Systems (ISWCS)*, pp. 956-960, 2010.

[4] G. Owojaiye, F. Delestre and Y.Sun, "Source-assisting strategy for distributed space-time block codes," in *7th International Symposium on Wireless Communication Systems (ISWCS)*, pp. 174-178, 2010.

[5] F. Delestre and Y.Sun, "MIMO-OFDM with pilot-aided channel estimation for WiMax systems," in *6th IEEE International Conference on Wireless and Mobile Computing, Networking and Communications (WiMob)*, pp. 586-590, 2010.

Accepted Papers:

[1] F. Delestre and Y.Sun, "Performance of SFBC-OFDM System with Pilot Aided Channel Estimation" in *the 7th International Conference on Wireless Communications and Mobile Computing (IWCMC),* Istanbul, 2011.

[2] E. Masoud, Y. Sun, F. Delestre, and N. Nwanekezie, "A Detection Method for Space-Time Codes with No Channel State Information", in *the 12th Annual Post Graduate Symposium on the Convergence of Telecommunications, Networking and Broadcasting (PGNet2011),* Liverpool, 2011.

[3] A.Bannour, M. L. Ammari, Y. Sun, F. Delestre and R. Bouallegue, "Pilot-Aided Channel Estimation and Performance of ASTC-MIMO-OFDM System in a Correlated Rayleigh Frequency-Selective Channel", in the *7th International Conference on Wireless Advanced (WiAd 2011),* London, 2011

1 Introduction

This chapter provides a brief introduction of the thesis. This includes background of research, research scope and objectives, original contributions and organisation of the thesis.

1.1 Background of Research

High spectral efficiency and high transmission speed due to the applications of audio, video and internet services [1-4] are the challenging requirements of future wireless broadband communications. In a multipath wireless channel environment, the deployment of Multiple Input Multiple Output (MIMO) systems which enhance channel capacity enormously has led to the achievement of high data rate transmission without increasing the total transmission power or bandwidth. MIMO systems have been under high consideration since Alamouti introduced the well known Space-Time Block Codes (STBC) in [5] which consists of data coded through space and time to improve the reliability of the transmission, as redundant copies of the original data are sent over independent fading channels. .Research on STBC has been intensive over the past years [6-8]. MIMO and especially STBC have also been adopted in IEEE 802.11n standard [9] to achieve higher data rate and to provide more reliable reception than traditional single antenna communications [10, 11].

In practice, wireless communications channels are time varying or frequency selective especially for broadband and mobile applications. To address these challenges, a promising combination has been exploited, namely, MIMO with

Orthogonal Frequency Division Multiplexing (OFDM), which has already been adopted for present and future broadband communication standards such as LTE or WiMax [12-14]. OFDM can reduce the effect of frequency selective channel. This is because in OFDM, the data stream that is to be transmitted is divided into multiple parallel streams and the wideband channel is divided into a number of parallel narrowband subchannels and thus each subchannel has a lower rate data stream. OFDM is also used for its simplicity of implementation in the digital domain by the use of DFT. Moreover, OFDM is bandwidth efficient since the parallel subcarriers are orthogonal to each other and as a result overlaps each other without causing interference. With the use of cyclic prefix, OFDM has also been proven as a robust modulation technique under multipath frequency selective fading environment [3, 15].

One popular combination of MIMO and OFDM is the STBC-OFDM which was first proposed in [16, 17]. In addition to spatial and temporal diversity, the combination of MIMO-OFDM offers a third dimension of coding which achieves frequency diversity. These coding schemes known as Space-Frequency Block Coding (SFBC) and Space-Time-Frequency Block Coding (STFBC), which are respectively capable of achieving two dimensional coding over space and frequency and three dimensional coding over space, time and frequency have recently been proposed in the literature [18-22]. In addition, coding through spatial and frequency dimension offers implementation advantages [4]. MIMO-OFDM has already been adopted by several standards such as IEEE 802.11n, IEEE802.16a and 3GPP [12, 23, 24]. However, in both STBC-OFDM and SFBC-OFDM, channel parameters need to be known at the receiver to recover the transmitted symbols. Therefore, channel estimation with acceptable level of

accuracy and hardware complexity has become an important research topic for MIMO-OFDM systems.

Two approaches for channel estimation have been proposed in the literature. Blind channel estimation [25, 26] which relies on the exploitation of the statistical information of the received symbols, is very attractive due to its bandwidth-saving advantage. However, the blind technique is limited to slow time varying channels and has higher complexity at the receiver. On the other hand, pilot aided channel estimation [27-30] using pilot sequences scattered in the transmitted signal and known at the receiver is simpler to implement and can be applied to different types of channels although the use of pilots affect the data rate. As low complexity is required with a trade-off between bandwidth efficiency and accurate estimation, in many applications, researcher have paid much attention to propose low complexity pilot aided channel estimation methods for MIMO-OFDM [31, 32].

1.2 Research Scope and Objectives

With the constant demand of high spectral efficiency and high transmission speed for audio, video and internet applications, MIMO-OFDM has become the most promising technology combination for present and future wireless communications. MIMO offers spatial diversity and therefore increase the capacity while OFDM allow systems to work in time varying or frequency selective environment. While intensive research has been conducted on channel estimation for STBC-OFDM systems, to date there has been little work on joint iterative channel estimation and data detection techniques for MIMO-OFDM systems. The aim of this research is therefore to propose an iterative channel

estimation and signal detection technique for MIMO-OFDM systems for fixed and mobile communications.

A joint iterative scheme will first be proposed for STBC-OFDM systems using orthogonal STBC at pilot subcarriers for channel estimation and the scheme will then be extended for SFBC-OFDM with SFBC used for pilots. Further, in order to take advantage of the three dimensions offered by MIMO-OFDM; space, time and frequency, the research will also adapt the proposed channel estimation method to mixed STBC and SFBC MIMO-OFDM systems with pilot and data subcarriers being coded by different STBC and SFBC respectively. Due to the orthogonality of STBC and SFBC, both channel estimation and data detection become simple, as no computational intensive matrix inversion is needed.

This research will also propose a new decoding method for MIMO-OFDM to reduce complexity and computation by reducing the decoding duration of the received data according to the number of pilot symbols used. OFDM symbols are divided into groups, which are decoded simultaneously, according to the number of pilot subcarriers used. Once the number of groups is defined, each group is assigned a specific number of pilot subcarriers equal to the number of frequency slots required to transmit one STBC or SFBC coded training block. The grouping approach employed in this work reduces the number of computations which is linearly proportional to the number of pilot subcarriers used.

1.3 Original Contributions

The thesis contains several unique contributions:

- ✓ A new iterative joint channel estimation and data detection scheme for STBC-OFDM is proposed
- ✓ A new decoding algorithm using groups to improve the processing time of STBC-OFDM systems.
- ✓ Generalisation of the new iterative joint scheme proposed for STBC-OFDM to SFBC-OFDM systems.
- ✓ Generalisation of the group decoding technique to SFBC-OFDM systems.
- ✓ A new MIMO-OFDM technique with iterative channel estimation and simultaneous group decoding, where STBC and SFBC are alternatively used for pilot and data subcarriers.
- ✓ All the proposed techniques and algorithms are suitable for any modulation order, any number of transmit or receive antennas, any number of subcarriers and can be used for any wireless communication standards such as LTE, WiMax and WLAN.

1.4 Structure of Thesis

The thesis is organised in the following way:

Chapter 2 provides a detailed overview of MIMO systems including performance analysis and design criteria of STBC. First, the chapter covers channel theory for systems employing various diversity techniques. Then, STBC is discussed in details and performances are evaluated assuming that Channel

State Information (CSI) is known at the receiver and that data is transmitted through flat Rayleigh fading channel. Further, Quasi-Orthogonal Space-Time Block Coding and Differential Space-Time Block Coding are briefly introduced and comparison with original STBC is made in the last part of the chapter.

Chapter 3 reviews MIMO-OFDM systems under multipath frequency selective channels. The basic principle of OFDM is demonstrated through simulations and the combination of MIMO systems with OFDM is then described, leading to the presentation of two coding techniques known as STBC-OFDM and SFBC-OFDM where data is coded through 'space and time' and 'space and frequency' respectively. Performance of both schemes are compared for different number of transmit and receive antennas and different modulation orders.

Chapter 4 presents the new iterative joint channel estimation and data decoding method for STBC-OFDM systems. Derivations of the proposed technique are given and software simulations are presented for different number of transmit and receive antennas, different channel conditions and different number of pilot subcarriers. In addition, a technique decoding multiple STBC sets of data symbols simultaneously by the division of the OFDM symbols into groups is introduced.

Chapter 5 develops the joint channel estimation and data detection scheme for SFBC-OFDM and compares its performances with STBC-OFDM. Simulations were conducted in mobile environments for SFBC-OFDM to show the advantage of SFBC. Simulation results have been obtained for different number of transmit and receive antennas, different modulation orders, different numbers of pilot subcarriers and different Doppler shifts.

Chapter 6 brings together STBC-OFDM and SFBC-OFDM to propose a new joint channel estimation and data detection technique for mixed MIMO-OFDM systems. Estimation of channel parameters and decoding of data signals are jointly performed by using STBC and SFBC for pilot and data subcarriers alternatively. STBC is used for pilots to estimate channel parameters of SFBC-OFDM data symbols while for STBC-OFDM data symbols, SFBC pilots are used for channel estimation. Obtained results of the new combinations are compared with those of the MIMO-OFDM systems in Chapter 4 and 5 where the same STBC or SFBC is used for both data and pilot subcarriers.

Chapter 7 concludes the thesis and proposes the future work.

2 Space-Time Block Codes: an Overview

This chapter introduces space-time block codes. After some background information on wireless channel models, the simple Alamouti encoding using 2 transmit antennas and one receive antenna is presented. Space-time block codes for general MIMO systems are then described and tested for different number of transmit and receive antennas. Further, Quasi-orthogonal space-time block coding and differential space-time block coding techniques are discussed and their performance comparison with the original space-time block coding technique is also provided.

2.1 Introduction

In the past years, Multiple-Input Multiple-Output (MIMO) wireless communications has received much interest [33]. Multiple antennas are employed at both the receiver and the transmitter in a MIMO communication system to enhance channel capacity. Shannon Capacity Limit is difficult to be reached for Single Input Single Output (SISO) systems. It has been demonstrated in [34] that further increases in channel capacity can be gained by the use of MIMO systems. Under ideal propagation conditions, Foschini and Telatar have shown that the capacity limit grows linearly with the number of antennas [34, 35]. Space-time block coding (STBC) has emerged as one of the major techniques to exploit the MIMO benefit. Both spatial and temporal diversity are achieved in STBC. STBC

also offers simple decoding with the use of maximum likelihood detection algorithm at the receiver [5, 36-38].

Other types of codes based on STBC have then emerged and are of most interest as both full rate and full diversity can be achieved contrary to the STBC where full rate cannot be achieved for more than two transmit antennas. Those codes are known as Quasi-Orthogonal Space Time Block Codes (QOSTBC) [39, 40]. QOSTBC however has more complex decoding and therefore research is focusing on improving the complexity of the algorithm in order for the QOSTBC to be easier to implement [41-43].

Aforementioned codes are of much interest but require that channel parameters are known at the receiver to recover the transmitted data signal. Therefore, to counteract the need for channel estimation, codes based on differential modulation where the next transmitted symbol is phase shifted compared to the previously transmitted symbol, has been proposed by Tarokh et al in [44]. Detection and demodulation is based on the same principle, the phase of the received signal is compared with the phase of the previously received signal. Such codes are called Differential Space Time Block codes (DSTBC). The most distinct feature of DSTBC is that it does not require channel estimation. However, similar to the case of QOSTBC, complexity is of some concern to researchers [45].

In this chapter, these three coding techniques are described in detail and performance results of each scheme are analysed and compared. STBC offers lower complexity at the transmitter and receiver for full diversity codes, while QOSTBC has full rate as well and DSTBC require no channel information.

2.2 Wireless Channel Models

2.2.1 Fading Channels

In wireless mobile communications, surrounding objects, such as houses, buildings, trees and mountains provoke reflection, diffraction, scattering and shadowing of the transmitted signals and causes multipath propagation. This multipath effect causes the transmitted signals to arrive at the receiver with different phase angles, different amplitude and at different time intervals. The sum of the received signals is combined in a destructive or constructive way to recover the transmitted signal. The amplitude fluctuation of the received signal is called signal fading and is caused by the frequency selective or time variant characteristics of the multipath channel.

Signal amplitude and phase are subject to numerous scattering components during transmission. When these components are of similar strength, the fading process is described as following a Rayleigh probability distribution, while if some of the scattering components are stronger than others, the fading is no longer following a Rayleigh distribution but a Rician probability distribution and referred as Rician fading.

Figure 2-1 illustrates a transmission where the strongest components are the Line of Sight (LOS) components which are directly transmitted from the transmitter to receiver without any reflection, while other components which are reflected are referred to as Non Line of Sight (NLOS) or scattering components. Therefore, with the description of Rayleigh and Rician distributions, the probability density function of the received signal follows a Rician distribution in

a LOS environment Figure 2-1(a), while a Rayleigh distribution is followed in a NLOS environment Figure 2-1(b).

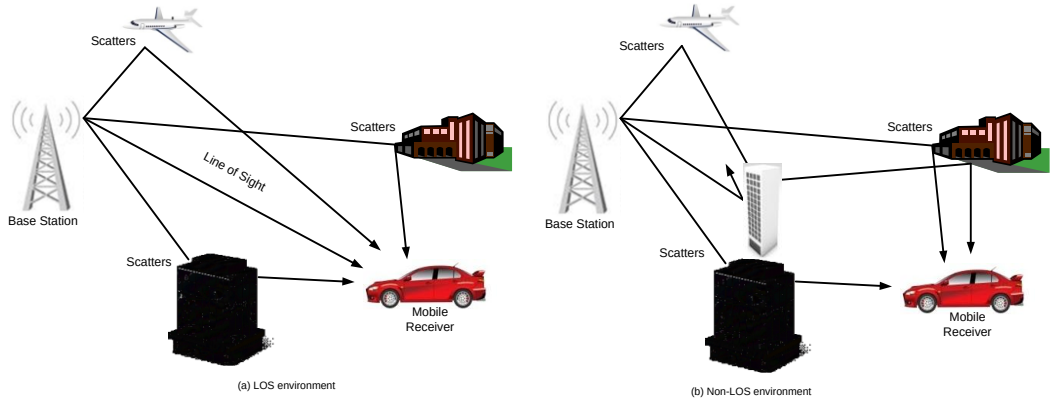

Figure 2-1: Signal Propagation in a Wireless Environment, with and without LOS

According to the type of dispersion, time or frequency, frequency-selective fading or time-selective fading is induced respectively.

2.2.2 Frequency Non Selective Channel

The transmitted wireless signal is subject to multipath time delay spread or Doppler spread. Multipath channels with time delay spread can be divided into two categories: frequency non selective channel or frequency selective channel.

Under time dispersion, received signals undergo frequency non selective channels also known as flat fading, when the channel bandwidth is much larger than the bandwidth of the transmitted signal. Since the bandwidth of the applied signal is narrower than the channel bandwidth, flat fading channels are often referred to as narrowband channels. Flat fading characteristics can be found in Figure 2-2.

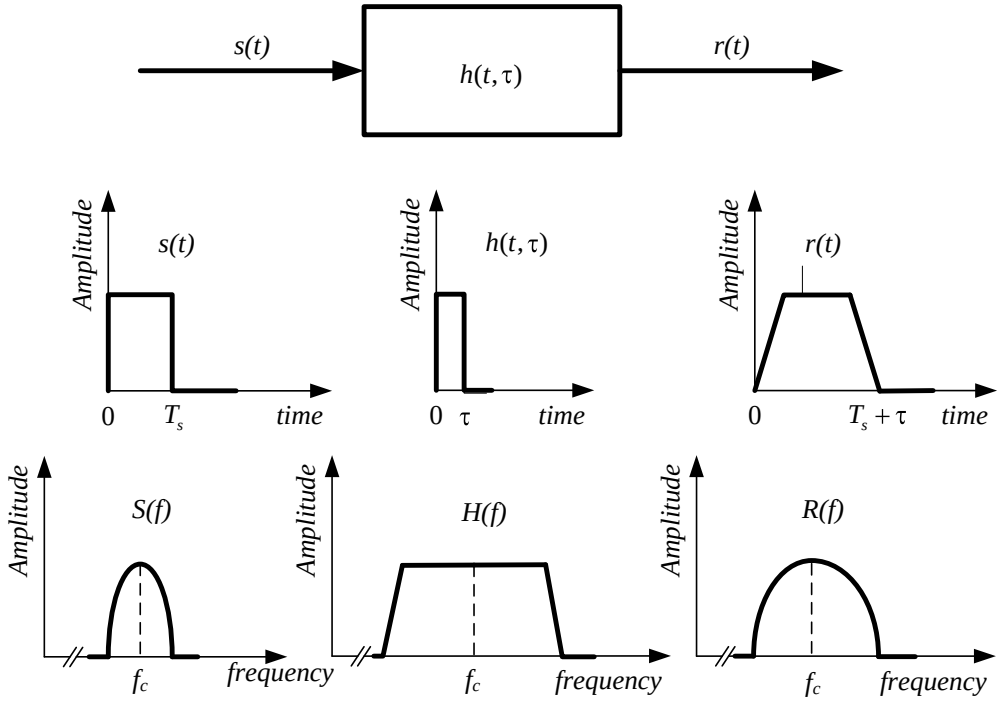

Figure 2-2: Frequency Non Selective Fading Channel Characteristics [46]

From Figure 2-2, it can be seen that symbol period T_s is greater than the delay spread τ of the channel $h(t,\tau)$, implying that inter-symbol interference (ISI) is not significant. To summarize the above observations, a signal is affected by a flat fading channel if:

$$B_s \ll B_c \quad and \; T_s \gg \sigma_\tau \tag{2.1}$$

where B_s and T_s represent respectively the bandwidth and symbol period of the transmitted signal and B_c and σ_τ represent the coherence bandwidth and root mean square (rms) delay spread of the channel respectively.

In this chapter, different space-time block codes and simulations are based on flat fading channels.

2.3 Space-Time Block Codes

MIMO systems have been under high consideration since Alamouti introduced the well known STBC in [5] for two transmit and one receive antenna. STBC consists of data coded through space and time to improve the reliability of the transmission. Later, Tarokh et al [36, 37] introduced orthogonal space-time block coding which generalizes Alamouti's transmission scheme to an arbitrary number of transmit antennas and is able to achieve the full diversity promised by the multiple transmit and receive antennas. Like Alamouti scheme, these generalised codes have a very simple maximum likelihood decoding algorithm based only on linear processing at the receiver.

2.3.1 Alamouti's Space-Time Block Codes

Historically, the first STBC to provide full diversity with full rate matrix and simple decoding algorithm was proposed by Alamouti in [5]. A block diagram of Alamouti STBC encoder can be found in Figure 2-3.

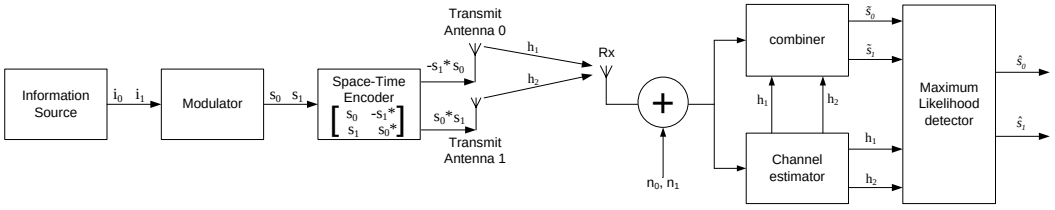

Figure 2-3: A Block Diagram of Alamouti's STBC

As it can be seen from Figure 2-3, *M*-ary modulated symbols s_0 and s_1 are passed through the STBC encoder and complex matrix S is generated such that symbols s_0 and s_1 are coded through space and time. Indeed, replicas of s_0 and s_1 for Alamouti coding are sent through two transmit antennas and over two time slots. Complex matrix S can be found in (2.2).

$$S_2^c = \begin{bmatrix} s_0 & s_1 \\ -s_1^* & s_0^* \end{bmatrix} \tag{2.2}$$

where the superscript * represents the complex conjugate operation.

Here, the number of columns corresponds to the number of transmit antennas M_t and the number of rows to the number of time slots or number of symbols transmitted per antenna n_t. It can be seen from the matrix in (2.2) that at time t, s_0 and s_1 are sent simultaneously from antenna 1 and 2 respectively and at time t+T, where T is the symbol duration, is transmitted from antenna 1 and is simultaneously transmitted from antenna 2. Moreover, from (2.2), it can be seen that full diversity is accomplished as one symbol is transmitted from each antenna during each time slot. Finally, the rate (*R*) of STBC achieved by Alamouti's code defined as is full as the number of different symbols transmitted per antenna n_s (here n_s=2 because of the two symbols s_0 and s_1) divided by the number of time slots n_t (here n_t=2) is giving the full rate of one.

An interesting key feature of Alamouti's scheme is that the sequence transmitted from the different antennas are orthogonal since the matrix of S times the Hermitian matrix S is equal to the identity matrix such as:

$$\begin{aligned} S_2^c . S_2^{cH} &= \begin{bmatrix} s_0 & s_1 \\ -s_1^* & s_0^* \end{bmatrix} . \begin{bmatrix} s_0^* & -s_1 \\ s_1^* & s_0 \end{bmatrix} \\ &= \left|s_0\right|^2 + \left|s_1\right|^2 \; I \end{aligned} \tag{2.3}$$

where the superscript ^{H} represents the Hermitian matrix of S which is the transpose and conjugate of the matrix S and *I* is a 2x2 identity matrix.

Assuming that the channel parameters are constant over two consecutive symbols, thus:

$$\begin{aligned} h_1(t) &= h_1(t+T) = h_1 = |h_1| e^{-j\theta_1} \\ h_2(t) &= h_2(t+T) = h_2 = |h_2| e^{-j\theta_2} \end{aligned} \tag{2.4}$$

where and , with i=1,2 are the amplitude and phase shift respectively. At the receiver, the received signals at time t and t+T can be expressed as in (2.5). The received signal will be denoted by r_1 and r_2 at time t and t+T respectively.

$$\begin{aligned} r_1 = r(t) &= h_1 s_0 + h_2 s_1 + n_1 \\ r_2 = r(t+T) &= -h_1 s_1^* + h_2 s_0^* + n_2 \end{aligned} \tag{2.5}$$

where n_1 and n_2 represent the white Gaussian noise samples. Originally, STBC channel parameters were assumed known at the receiver. Therefore, transmitted symbols s_0 and s_1 can be recovered by combining the received signal r_1 and r_2 as:

$$\begin{aligned} \tilde{s}_0 &= r_1 h_1^* + r_2^* h_2 = (|h_1|^2 + |h_2|^2) s_0 + h_1^* n_1 + h_2 n_2^* \\ \tilde{s}_1 &= h_2^* r_1 - h_1 r_2^* = (|h_1|^2 + |h_2|^2) s_1 - h_1 n_2^* + h_2^* n_1 \end{aligned} \tag{2.6}$$

As it can be seen from (2.5) and (2.6), and due to the orthogonality of the transmitted matrix, cancellation of the unwanted signal s_1 to recover s_0 and s_0 to recover s_1 is possible. Both signals are then passed through the maximum likelihood (ML) detector as described in Figure 2-3 to determine the most likely transmitted symbols.

The decision rule is based on choosing s_i if and only if:

$$(h_1^2 + h_2^2 - 1)|s_i|^2 + d^2(\tilde{s}_0, s_i) \leq (h_1^2 + h_2^2 - 1)|s_k|^2 + d^2(\tilde{s}_0, s_k) \tag{2.7}$$

where i≠k and $d^2(.)$ represents the Euclidean distance between the two signals. From (2.7), it can be seen that the transmitted symbol is the one with the minimum Euclidean distance from the combined output signal.

The performance of Alamouti transmit diversity scheme is evaluated under slow fading channels by simulation [5, 47]. Channel coefficients have been assumed known at the receiver. Moreover, independent fading from each transmit to each receive antenna and similar transmit power for every case have been assumed. The performance of Alamouti scheme has been evaluated in terms of bit error rate (BER) against signal to noise ratio (SNR) with BPSK modulation.

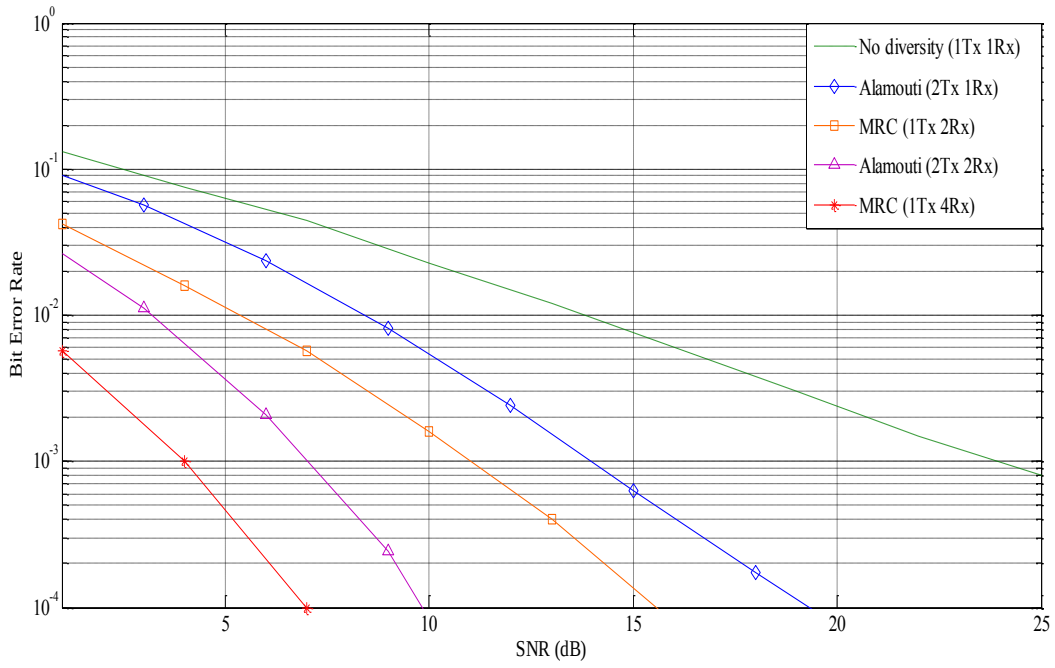

Figure 2-4: BER Performance of the Alamouti Scheme with BPSK

The simulation results show that for similar diversity, a two-branch maximal ratio combining (MRC) receive diversity performs better than the Alamouti scheme with two transmit antennas and one receive antenna. The difference is due to the fact that same total power has been used to transmit data from both

schemes. Alamouti scheme would achieve performance similar to MRC scheme if the power used at each transmit antenna was similar to the power used for the transmit antenna of the MRC scheme. Generally, a 2 by N_r Alamouti scheme would achieve performance similar to a 1 by N_r MRC scheme.

2.3.2 Generalised STBC

STBC is generally regarded as a generalisation of the Alamouti coding. Based on the previous Subsection where simple ML can be achieved due to the orthogonality of the design scheme, Tarokh et al generalised STBC to an arbitrary number of transmit and receive antennas in [37]. STBC can achieve full rate and full diversity which as stated earlier is specified by the number of different symbols to transmit and the number of time slots required to transmit the entire STBC block. In addition, STBC allows a very simple decoding algorithm based on the ML decoding described in the previous Subsection.

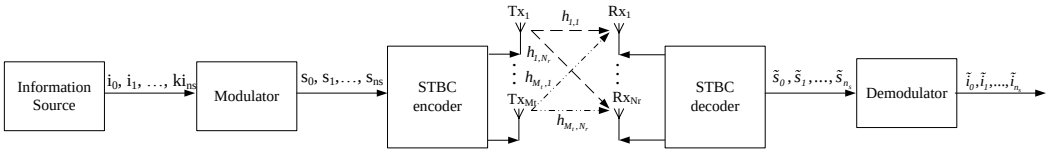

Figure 2-5: A Block Diagram of STBC Communications

Figure 2-5 shows a block diagram of the generalised STBC communication link. Like Alamouti case, data is first mapped by a 2^k points modulator resulting in n_s data symbols passed to the STBC encoder. At the receiver, the data is decoded with the STBC decoder including channel estimation, combiner and ML detector.

Based on the type of modulation used, STBC can be classified in two categories known as real and complex constellations. STBC with real-

constellation can be found when Pulse Amplitude Modulation (PAM) or Binary Phase Shift Keying (BPSK) modulation is applied to the information signal, while STBC with complex-constellation is used with M-PSK or M-QAM modulation.

2.3.3 STBC for Real-Constellations

For STBC with real-constellations, if an M_t x n_t transmission matrix with variables $s_0, s_1, \ldots, s_{ns}$ satisfies [37, 47]:

$$S_{M_t} \cdot S_{M_t}^T = c \left(|s_0|^2 + |s_1|^2 + \ldots + |s_{n_s}|^2 \right) I_{M_t} \tag{2.8}$$

where c is a constant and I_{Mt} is a Mt x Mt identity matrix, STBC can achieve a full diversity order of . Square STBC matrix S_{Mt} with real-constellation exist if and only if the number of transmit antennas M_t=2, 4 or 8 [37]. These codes offer full transmit diversity of M_t due to their full rate R=1. The real transmission matrices for 2, 4 and 8 transmit antennas are given by:

$$S_2 = \begin{bmatrix} s_0 & s_1 \\ -s_1 & s_0 \end{bmatrix} \qquad S_4 = \begin{bmatrix} s_0 & s_1 & s_2 & s_3 \\ -s_1 & s_0 & -s_3 & s_2 \\ -s_2 & s_3 & s_0 & -s_1 \\ -s_3 & -s_2 & s_1 & s_0 \end{bmatrix}$$

$$S_8 = \begin{bmatrix} s_0 & s_1 & s_2 & s_3 & s_4 & s_5 & s_6 & s_7 \\ -s_1 & s_0 & s_3 & -s_2 & s_5 & -s_4 & -s_7 & s_6 \\ -s_2 & -s_3 & s_0 & s_1 & s_6 & s_7 & -s_4 & -s_5 \\ -s_3 & s_2 & -s_1 & s_0 & s_7 & -s_6 & s_5 & -s_4 \\ -s_4 & -s_5 & -s_6 & -s_7 & s_0 & s_1 & s_2 & s_3 \\ -s_5 & s_4 & -s_7 & s_6 & -s_1 & s_0 & -s_3 & s_2 \\ -s_6 & s_7 & s_4 & -s_5 & -s_2 & s_3 & s_0 & -s_1 \\ -s_7 & -s_6 & s_5 & s_4 & -s_3 & -s_2 & s_1 & s_0 \end{bmatrix}$$

At the receiver side, the received equations are based on Alamouti's model with the simplicity of having only real symbols and therefore no conjugate symbol

in the equations. Thus, the received equations for two and four transmit antennas and any number of received antennas can be found in (2.9) and (2.10) respectively.

$$\begin{aligned} r_{1,j} &= r_j \quad t \quad = h_{1,j}\, s_0 + h_{2,j}\, s_1 + n_{1,j} \\ r_{2,j} &= r_j \quad t+T \quad = -h_{1,j}\, s_1 + h_{2,j}\, s_0 + n_{2,j} \end{aligned} \tag{2.9}$$

$$\begin{aligned} r_{1,j} &= r_j \quad t \quad = h_{1,j}\, s_0 + h_{2,j}\, s_1 + h_{3,j}\, s_2 + h_{4,j}\, s_3 + n_{1,j} \\ r_{2,j} &= r_j \quad t+T \quad = -h_{1,j}\, s_1 + h_{2,j}\, s_0 - h_{3,j}\, s_3 + h_{4,j}\, s_2 + n_{2,j} \\ r_{3,j} &= r_j \quad t+2T \quad = -h_{1,j}\, s_2 + h_{2,j}\, s_3 + h_{3,j}\, s_0 - h_{4,j}\, s_1 + n_{3,j} \\ r_{4,j} &= r_j \quad t+3T \quad = -h_{1,j}\, s_3 - h_{2,j}\, s_2 + h_{3,j}\, s_1 + h_{4,j}\, s_0 + n_{4,j} \end{aligned} \tag{2.10}$$

where $n_{1,j}$, $n_{2,j}$, $n_{3,j}$ and $n_{4,j}$ are independent noise samples and j denotes the j-th receive antenna.

Received signals are then combined for two and four transmit antennas as given in (2.11) and (2.12) respectively.

$$\begin{aligned} \tilde{s}_0 &= \sum_{j=1}^{N_r} r_{1,j}\, h_{1,j} + r_{2,j}\, h_{2,j} \\ \tilde{s}_1 &= \sum_{j=1}^{N_r} r_{1,j}\, h_{2,j} - r_{2,j}\, h_{1,j} \end{aligned} \tag{2.11}$$

$$\begin{aligned} \tilde{s}_0 &= \sum_{j=1}^{N_r} r_{1,j}\, h_{1,j} + r_{2,j}\, h_{2,j} + r_{3,j}\, h_{3,j} + r_{4,j}\, h_{4,j} \\ \tilde{s}_1 &= \sum_{j=1}^{N_r} r_{1,j}\, h_{2,j} - r_{2,j}\, h_{1,j} - r_{3,j}\, h_{4,j} + r_3\, h_{3,j} \\ \tilde{s}_2 &= \sum_{j=1}^{N_r} r_{1,j}\, h_{3,j} + r_{2,j}\, h_{4,j} - r_{3,j}\, h_{1,j} - r_{4,j}\, h_{2,j} \\ \tilde{s}_3 &= \sum_{j=1}^{N_r} r_{1,j}\, h_{4,j} - r_{2,j}\, h_{3,j} + r_{3,j}\, h_{2,j} - r_{4,j}\, h_{1,j} \end{aligned} \tag{2.12}$$

Finally, the combined signals are sent to the ML detection in order to recover the transmitted signal.

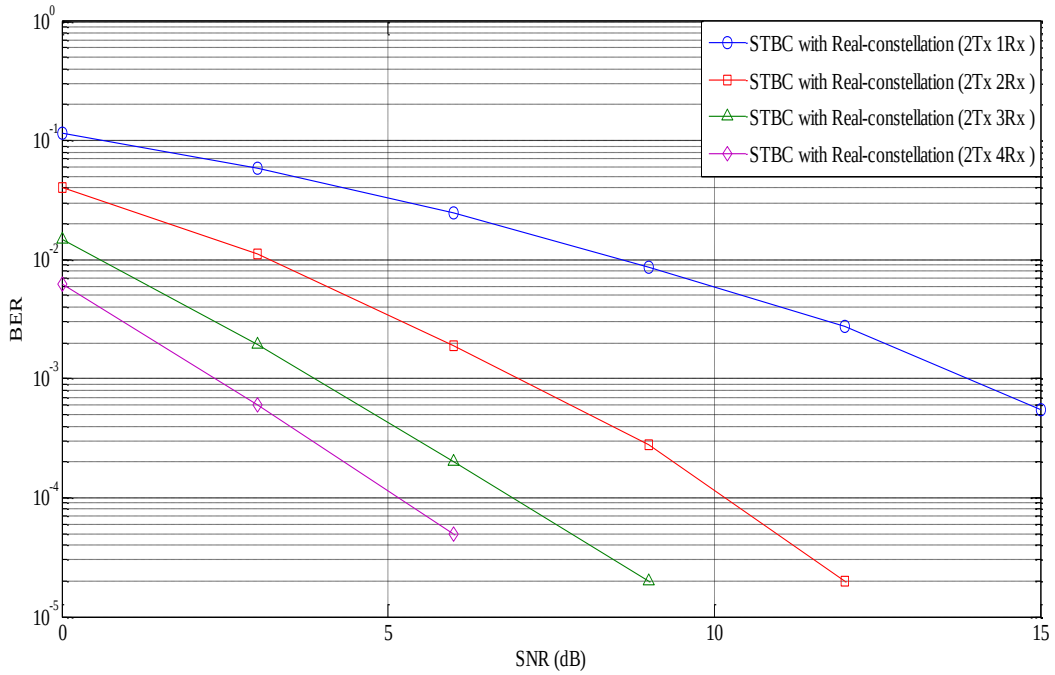

Figure 2-6: Performance of Real-Constellation for 2 Transmit Antennas under BPSK

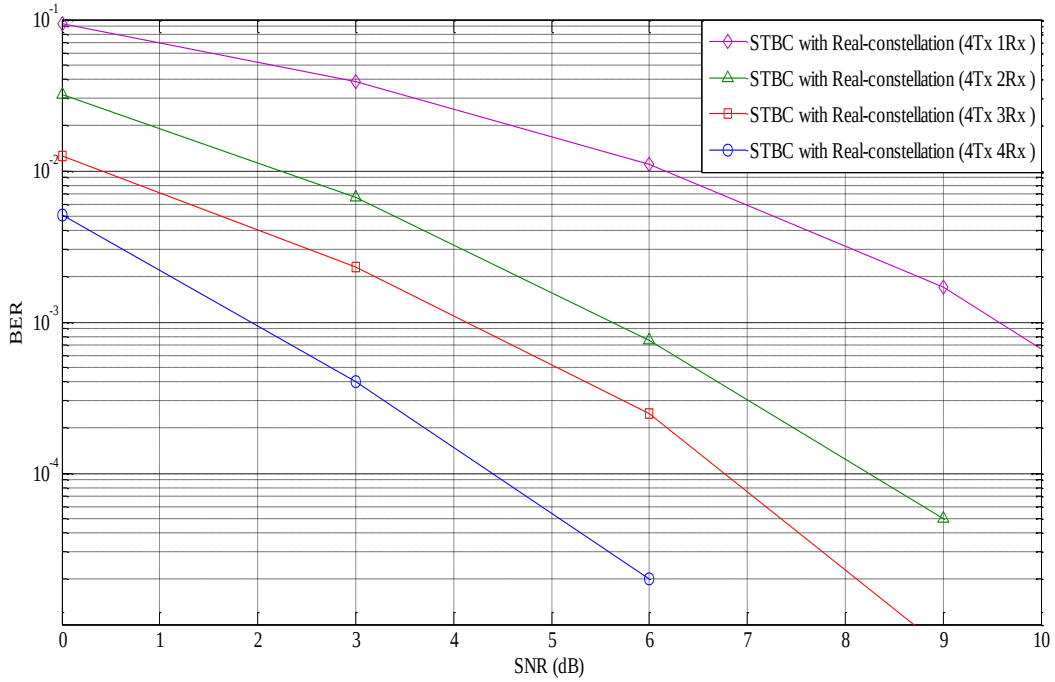

Figure 2-7: Performance of Real-Constellation for 4 Transmit Antennas under BPSK

Figure 2-6 and Figure 2-7 show the BER performance for two and four transmit antennas with 1, 2, 3 and 4 receive antennas for STBC of 1bit/s/Hz. The spectral efficiency of the STBC is calculated based on the following equation:

$$R = \frac{mn_s}{n_t} \tag{2.13}$$

where m represents the number of bit per symbol.

From the simulation results, it can be seen that better BER performance can be achieved by the use of more receive antennas owing to the fact that MIMO works well in multipath fading and that multiple antenna systems achieve better performance than single antenna systems. Furthermore, it can be noticed from Figure 2-4 and Figure 2-6, that real and complex coding for two transmit and one receive antennas achieve similar results. This is due to the fact that Alamouti's codes allow full diversity and full rate, in both real and complex constellations. Therefore Alamouti's codes are equivalent to the use of real matrix at the particularity that it is possible to use higher modulation order. Moreover, it can be seen that the performance of STBC improves when either the number of transmit or receive antennas is increased. Indeed, by comparing Figure 2-6 and Figure 2-7, a system of two transmit antennas to one receive antenna has a higher BER than the scheme of two transmit antennas to two receive antennas or four transmit antennas to one receive antenna.

2.3.4 STBC for Complex-Constellations

In general, for STBC with complex-constellations, if an M_t x n_t transmission matrix with variables s_0, s_1, …,s_{ns} satisfies [37, 47]:

$$S_{M_t} \cdot S_{M_t}^T = c \left(|s_0|^2 + |s_1|^2 + \ldots + |s_{n_s}|^2 \right) I_{M_t} \tag{2.14}$$

where c is a constant and I_{Mt} is a M_t x M_t identity matrix, STBC can achieve a full diversity order of .

The introduced by Alamouti is considered as the simplest STBC with complex constellation and it is also the only M_t x M_t STBC code with complex-constellations. In addition, Alamouti code is the only STBC achieving full rate of 1 for a full diversity of 2. The aim of using higher number of transmit antennas on generalised STBC is to achieve high rate with full diversity, minimum coding delay (minimise n_s) and minimum decoding complexity.

Examples of half rate complex transmission matrices achieving full diversity for three ( ) and four ( ) transmit antennas are given below [37, 47]:

$$S_3^C = \begin{bmatrix} s_0 & s_1 & s_2 \\ -s_1 & s_0 & -s_3 \\ -s_2 & s_3 & s_0 \\ -s_3 & -s_2 & s_1 \\ s_0^* & s_1^* & s_2^* \\ -s_1^* & s_0^* & -s_3^* \\ -s_2^* & s_3^* & s_0^* \\ -s_3^* & -s_2^* & s_1^* \end{bmatrix}$$

$$S_4^C = \begin{bmatrix} s_0 & s_1 & s_2 & s_3 \\ -s_1 & s_0 & -s_3 & s_2 \\ -s_2 & s_3 & s_0 & -s_1 \\ -s_3 & -s_2 & s_1 & s_0 \\ s_0^* & s_1^* & s_2^* & s_3^* \\ -s_1^* & s_0^* & -s_3^* & s_2^* \\ -s_2^* & s_3^* & s_0^* & -s_1^* \\ -s_3^* & -s_2^* & s_1^* & s_0^* \end{bmatrix}$$

For both schemes, flat fading channels are assumed to be constant over 8 symbol periods. Thus, following the real-constellation derivations, the received signal for three transmit antennas can be expressed as:

$$
\begin{aligned}
r_{1,j} &= r_j(t) = h_{1,j}\,s_0 + h_{2,j}\,s_1 + h_{3,j}\,s_2 + n_{1,j}\\
r_{2,j} &= r_j(t+T) = -h_{1,j}\,s_1 + h_{2,j}\,s_0 - h_{3,j}\,s_3 + n_{2,j}\\
r_{3,j} &= r_j(t+2T) = -h_{1,j}\,s_2 + h_{2,j}\,s_3 + h_{3,j}\,s_0 + n_{3,j}\\
r_{4,j} &= r_j(t+3T) = -h_{1,j}\,s_3 - h_{2,j}\,s_2 + h_{3,j}\,s_1 + n_{4,j}\\
r_{5,j} &= r_j(t+4T) = h_{1,j}\,s_0^* + h_{2,j}\,s_1^* + h_{3,j}\,s_2^* + n_{5,j}\\
r_{6,j} &= r_j(t+5T) = -h_{1,j}\,s_1^* + h_{2,j}\,s_0^* - h_{3,j}\,s_3^* + n_{6,j}\\
r_{7,j} &= r_j(t+6T) = -h_{1,j}\,s_2^* + h_{2,j}\,s_3^* + h_{3,j}\,s_0^* + n_{7,j}\\
r_{8,j} &= r_j(t+7T) = -h_{1,j}\,s_3^* - h_{2,j}\,s_2^* + h_{3,j}\,s_1^* + n_{8,j}
\end{aligned}
\tag{2.15}
$$

where $n_{1,j}$, $n_{2,j}$, …, $n_{8,j}$ are independent noise samples. Received signals are then combined to retrieve the original transmitted symbols:

$$
\begin{aligned}
\tilde{s}_1 &= \sum_{j=1}^{N_r} h_{0,j}^*\,r_{1,j} + h_{1,j}^*\,r_{2,j} + h_{2,j}^*\,r_{3,j} + h_{0,j}\,r_{5,j}^* + h_{1,j}\,r_{6,j}^* + h_{2,j}\,r_{7,j}^*\\
\tilde{s}_2 &= \sum_{j=1}^{N_r} h_{1,j}^*\,r_{1,j} - h_{0,j}^*\,r_{2,j} + h_{2,j}^*\,r_{4,j} + h_{1,j}\,r_{5,j}^* - h_{0,j}\,r_{6,j}^* + h_{2,j}\,r_{8,j}^*\\
\tilde{s}_3 &= \sum_{j=1}^{N_r} \left(h_{2,j}^*\,r_{1,j} - h_{0,j}^*\,r_{3,j} - h_{1,j}^*\,r_{4,j} + h_{2,j}\,r_{5,j}^* - h_{0,j}\,r_{7,j}^* - h_{1,j}\,r_{8,j}^*\right)\\
\tilde{s}_4 &= \sum_{j=1}^{N_r} \left(-h_{2,j}^*\,r_{2,j} + h_{1,j}^*\,r_{3,j} - h_{0,j}^*\,r_{4,j} - h_{2,j}\,r_{6,j}^* + h_{1,j}\,r_{7,j}^* - h_{0,j}\,r_{8,j}^*\right)
\end{aligned}
\tag{2.16}
$$

The transmission matrix is just an extension of . Using j received antennas, the received signals can be expressed as:

$$
\begin{aligned}
r_{1,j} &= r_j(t) = h_{1,j}\,s_0 + h_{2,j}\,s_1 + h_{3,j}\,s_2 + h_{4,j}\,s_3 + n_{1,j}\\
r_{2,j} &= r_j(t+T) = -h_{1,j}\,s_1 + h_{2,j}\,s_0 - h_{3,j}\,s_3 + h_{4,j}s_2 + n_{2,j}\\
r_{3,j} &= r_j(t+2T) = -h_{1,j}\,s_2 + h_{2,j}\,s_3 + h_{3,j}\,s_0 - h_{4,j}s_1 + n_{3,j}\\
r_{4,j} &= r_j(t+3T) = -h_{1,j}\,s_3 - h_{2,j}\,s_2 + h_{3,j}\,s_1 + h_{4,j}s_0 + n_{4,j}\\
r_{5,j} &= r_j(t+4T) = h_{1,j}\,s_0^* + h_{2,j}\,s_1^* + h_{3,j}\,s_2^* + h_{4,j}s_3^* + n_{5,j}\\
r_{6,j} &= r_j(t+5T) = -h_{1,j}\,s_1^* + h_{2,j}\,s_0^* - h_{3,j}\,s_3^* + h_{4,j}\,s_2^* + n_{6,j}\\
r_{7,j} &= r_j(t+6T) = -h_{1,j}\,s_2^* + h_{2,j}\,s_3^* + h_{3,j}\,s_0^* - h_{4,j}s_1^* + n_{7,j}\\
r_{8,j} &= r_j(t+7T) = -h_{1,j}\,s_3^* - h_{2,j}\,s_2^* + h_{3,j}\,s_1^* + h_{4,j}s_0^* + n_{8,j}
\end{aligned}
\tag{2.17}
$$

where $n_{1,j}$, $n_{2,j}$, …, $n_{8,j}$ are independent noise samples. Following the decoding equations of , it can be deduced for four transmit antennas:

$$\begin{aligned}
\tilde{s}_1 &= \sum_{j=1}^{N_r} h_{0,j}^* r_{1,j} + h_{1,j}^* r_{2,j} + h_{2,j}^* r_{3,j} + h_{3,j}^* r_{4,j} + h_{0,j} r_{5,j}^* + h_{1,j} r_{6,j}^* + h_{2,j} r_{7,j}^* + h_{3,j} r_{8,j}^* \\
\tilde{s}_2 &= \sum_{j=1}^{N_r} h_{1,j}^* r_{1,j} - h_{0,j}^* r_{2,j} - h_{3,j}^* r_{3,j} + h_{2,j}^* r_{4,j} + h_{1,j} r_{5,j}^* - h_{0,j} r_{6,j}^* - h_{3,j} r_{7,j}^* + h_{2,j} r_{8,j}^* \\
\tilde{s}_3 &= \sum_{j=1}^{N_r} \left(h_{2,j}^* r_{1,j} + h_{3,j}^* r_{2,j} - h_{0,j}^* r_{3,j} - h_{1,j}^* r_{4,j} + h_{2,j} r_{5,j}^* + h_{3,j} r_{6,j}^* - h_{0,j} r_{7,j}^* - h_{1,j} r_{8,j}^* \right) \\
\tilde{s}_4 &= \sum_{j=1}^{N_r} \left(h_{3,j}^* r_{1,j} - h_{2,j}^* r_{2,j} + h_{1,j}^* r_{3,j} - h_{0,j}^* r_{4,j} + h_{3,j} r_{5,j}^* - h_{2,j} r_{6,j}^* + h_{1,j} r_{7,j}^* - h_{0,j} r_{8,j}^* \right)
\end{aligned} \tag{2.18}$$

As it can be noticed through the different examples given above, the complexity at the receiver side increases linearly with the number of transmit-antennas and receive-antennas. Indeed, for x receive antennas, the equations of will have x times more terms than it has now.

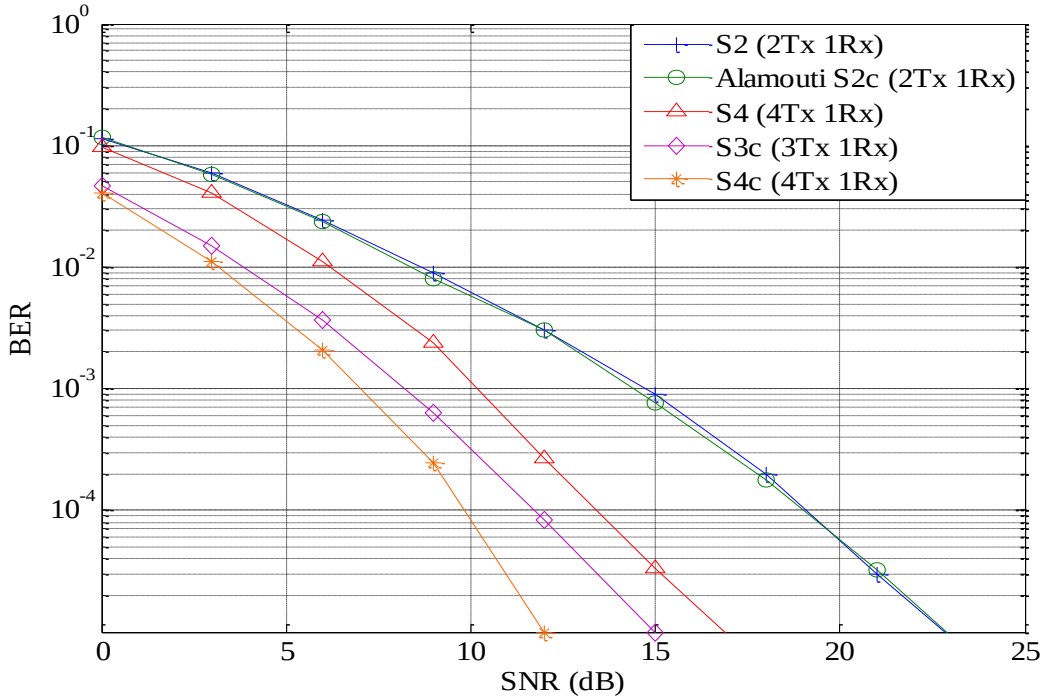

Figure 2-8: Comparison of STBC Designs with Real and Complex Matrices

A performance comparison between the real and complex constellation schemes is shown in Figure 2-8. Comparison of the two types of STBC is only possible for the specific case of BPSK modulation as it can be treated as a real constellation when used with a phase difference of π. Indeed, BPSK is considered as a complex digital modulation but when used in the real axis, modulated symbols can be considered as real symbols.

While Alamouti code achieves the same performance for real and complex constellations, the real and complex scheme of four transmit antennas with one receive antenna achieve different performances. In the case of Alamouti code, results were predictable as the rate and diversity of the matrix remain the same in both cases. Results were also expected in the case of four transmit antennas as the matrix rate was full for STBC with real constellation while it was only 1/2 rate for STBC with complex constellations. Lower rate implies higher number of replicas transmitted to the receiver and therefore higher probability of recovering the signal accurately. Finally, similar conclusions can be drawn in terms of diversity, higher number of transmit antennas result in an improvement in performance.

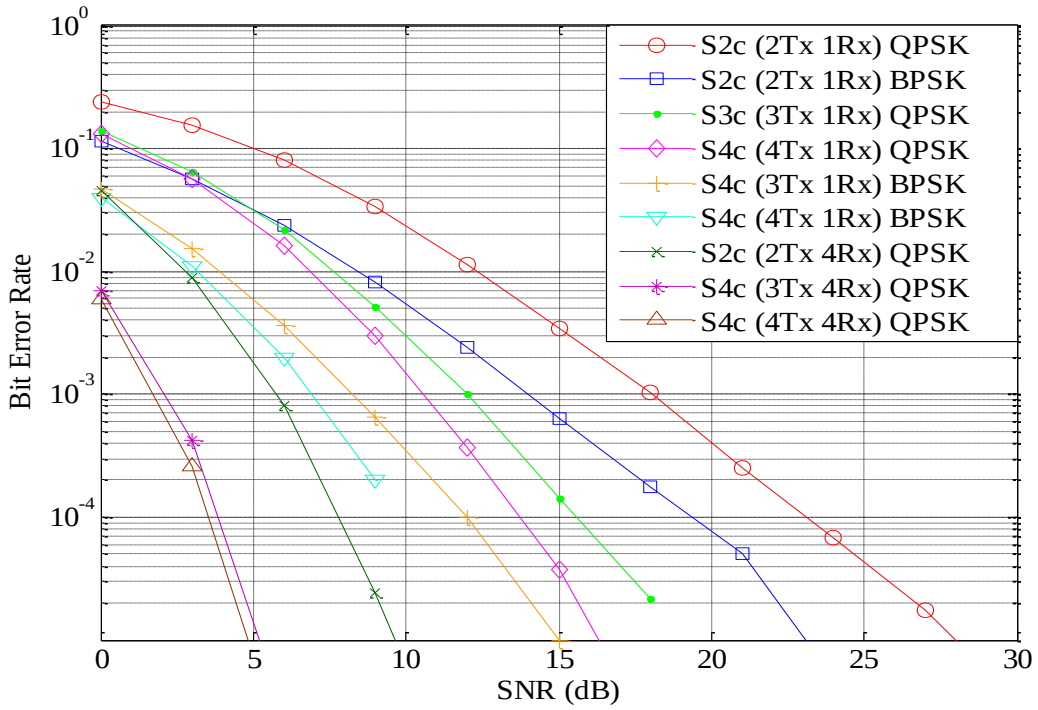

Figure 2-9: Performance Comparison of Complex Matrix with BPSK and QPSK

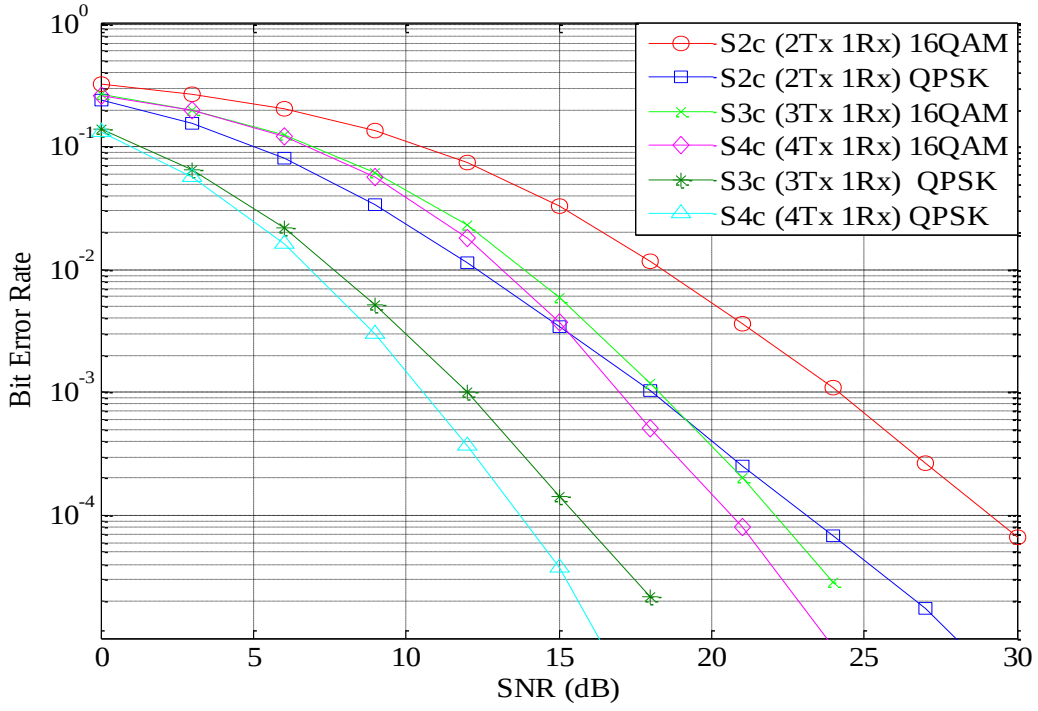

Figure 2-10: Performance Comparison of Complex Matrix with QPSK and 16-QAM

Figure 2-9 and Figure 2-10 show the performance of STBC for complex constellation matrices of 1bit/s/Hz, 2bit/s/Hz and 4bit/s/Hz for 2 transmit antennas

and ½ bit/s/Hz, 1bit/s/Hz and 2bit/s/Hz for three and four transmit antennas. Spectral efficiency of each type of matrices according to the modulation used is summarized in Table 2-1 with the help of (2.13) .

Table 2-1: Spectral Efficiency per Number of Transmit Antennas

Modulation / Number of Tx	BPSK (1 bit/symbol)	QPSK (2 bits/symbol)	16-QAM (4 bits/symbol)
2 Tx	1 bit/s/Hz	2 bits/s/Hz	4 bits/s/Hz
3 Tx	1/2 bit/s/Hz	1 bit/s/Hz	2 bits/s/Hz
4 Tx	1/2 bit/s/Hz	1 bit/s/Hz	2 bits/s/Hz

The simulation results show that increasing the order of modulation will result in a significant SNR loss. From the above figures, it can be seen that by comparing identical STBC structures, the gain difference between BPSK and QPSK modulation is about 3-4dB and that the gain difference between QPSK and 16-QAM modulation is about 6dB regardless of the number of transmit antennas used. Therefore, it can be said that for higher order of modulation order, the system will have higher BER. A trade-off needs to be found between the modulation used and the number of transmit and receive antennas, knowing that in a real life system, higher number of antennas imply higher power consumption.

Finally, it can be noticed that and achieve similar performance for low order modulation. However, as it can be seen from Figure 2-10, this similarity is not valid anymore when the modulation order increases. The two matrices transmit similar amount of data symbols and achieve similar rate which justify the obtained results.

2.4 Quasi-Orthogonal Space-Time Block Codes

Full rate STBC using complex symbols in its transmission matrix are not possible to achieve as mentioned in Section 2.3. Indeed, only the particular case of Alamouti code presented in Section 2.3.1 can achieve full rate with full diversity.

Full diversity and simple decoding are the rules of orthogonal design. Jafarkhani in [39] proposed a new STBC technique called Quasi-Orthogonal-Space-Time Block codes (QOSTBC) which achieved full rate at the cost of higher complexity decoding. Quasi-orthogonal designs are attractive because they achieve higher code-rate than orthogonal designs and lower decoding complexity than non-orthogonal designs.

Jafarkhani's coded matrix is given as:

$$S_{4Q} = \begin{bmatrix} S_2^c \ \ s_1, s_2 & S_2^c \ \ s_3, s_4 \\ -S_2^{c*} \ \ s_3, s_4 & S_2^{c*} \ \ s_1, s_2 \end{bmatrix} = \begin{bmatrix} s_1 & s_2 & s_3 & s_4 \\ -s_2^* & s_1^* & -s_4^* & s_3^* \\ -s_3^* & -s_4^* & s_1^* & s_2^* \\ s_4 & -s_3 & -s_2 & s_1 \end{bmatrix} \tag{2.19}$$

where a matrix is the complex conjugate of the matrix as demonstrated in (2.20) for the matrix.

$$S_2^{c*} \ \ s_0, s_1 \ = S_2^c \ \ s_0^*, s_1^* \ = \begin{bmatrix} s_0^* & s_1^* \\ -s_1 & s_0 \end{bmatrix} \tag{2.20}$$

Now, by using V_i with i=1, 2, 3, 4 representing the *i*th column of , it can be seen that:

(2.1)

where is the inner product of the vector and .

Therefore the subspace created by and is orthogonal to the subspace created by and .

This orthogonality allows the calculation of the maximum likelihood decision metric which minimizes the following sum:

$$f_{14}\ s_1, s_4\ + f_{23}\ s_2, s_3 \tag{2.21}$$

where:

$$\begin{aligned} f_{14}\ s_1, s_4\ &= \sum_{j=1}^{Nr}\Bigg[\ |s_1|^2 + |s_4|^2\ \left(\sum_{n_t=1}^{4}\left|h_{n_t,j}\right|^2\right) \\ &+2\mathcal{R}e\Big\{\ -h_{1,j}r_{1,j}^* - h_{2,j}^* r_{2,j} - h_{3,j}^* r_{3,j} - h_{4,j} r_{4,j}^*\ \ s_1 \\ &+\ -h_{4,j} r_{1,j}^* + h_{3,j}^* r_{2,j} + h_{2,j}^* r_{3,j} - h_{1,j} r_{4,j}^*\ \ s_4 \\ &+\ h_{1,j}h_{4,j}^* - h_{2,j}^* h_{3,j} - h_{2,j} h_{3,j}^* + h_{1,j}^* h_{4,j}\ \ s_1 s_4^*\Big\}\Bigg] \end{aligned} \tag{2.22}$$

and:

$$\begin{aligned} f_{23}\ s_2, s_3\ &= \sum_{j=1}^{N_r}\Bigg[\ |s_2|^2 + |s_3|^2\ \left(\sum_{n_t=1}^{4}\left|h_{n_t,j}\right|^2\right) \\ &+2\mathcal{R}e\Big\{\ -h_{2,j}r_{1,j}^* + h_{1,j}^* r_{2,j} - h_{4,j}^* r_{3,j} + h_{3,j} r_{4,j}^*\ \ s_2 \\ &+(-h_{3,j}r_{1,j}^* - h_{4,j}^* r_{2,j} + h_{1,j}^* r_{3,j} + h_{2,j} r_{4,j}^*)s_3 \\ &+\ h_{2,j}h_{3,j}^* - h_{1,j}^* h_{4,j} - h_{1,j} h_{4,j}^* + h_{2,j}^* h_{3,j}\ \ s_2 s_3^*\Big\}\Bigg] \end{aligned} \tag{2.23}$$

and are independent of and respectively and are decoded separately. Indeed, the maximum likelihood detection is to find the pair which minimises over all possible values of and . The same logic is applied in parallel or after the decoding of and for where the maximum likelihood is applied to find the pair which gives the minimum value of amongst all combination of pairs . As it can

be seen, the complexity of the decoder is increased compared to the STBC decoder presented earlier. However, complexity of QOSTBC systems does not grow linearly as for STBC but exponentially with the number of transmit and receive antennas. Many QOSTBC have been proposed in the literature following the same properties as described by Jafarkhani [48]. For four transmit antennas, the matrix proposed by Jafarkhani can be adapted such as:

$$S_{4Q} = \begin{bmatrix} S_2^c\ s_1, s_2 & S_2^c\ s_3, s_4 \\ -S_2^{c*}\ s_3, s_4 & S_2^{c*}\ s_1, s_2 \end{bmatrix} = \begin{bmatrix} S_2^c\ s_1, s_2 & S_2^c\ s_3, s_4 \\ -S_2^c\ s_3, s_4 & S_2^c\ s_1, s_2 \end{bmatrix} = \begin{bmatrix} S_2^c\ s_1, s_2 & S_2^c\ s_3, s_4 \\ S_2^c\ s_3, s_4 & -S_2^c\ s_1, s_2 \end{bmatrix} = \begin{bmatrix} S_2^c\ s_1, s_2 & S_2^c\ s_3, s_4 \\ S_2^{c*}\ s_3, s_4 & -S_2^{c*}\ s_1, s_2 \end{bmatrix} \tag{2.24}$$

In addition, QOSTBC code with different rate and higher number of transmit antennas have also been proposed, for example the ¾ rate coded matrix for eight transmit antennas:

$$S_{8Q} = \begin{bmatrix} s_0 & s_1 & s_2 & 0 & s_3 & s_4 & s_5 & 0 \\ -s_1^* & s_0^* & 0 & -s_2 & s_4^* & -s_3^* & 0 & s_5 \\ s_2^* & 0 & -s_0^* & -s_1 & -s_5^* & 0 & s_3^* & s_4 \\ 0 & -s_2^* & s_1^* & -s_0 & 0 & s_5^* & -s_4^* & s_3 \\ -s_3 & -s_4 & -s_5 & 0 & s_0 & s_1 & s_2 & 0 \\ -s_4^* & s_3^* & 0 & s_5 & -s_1^* & s_0^* & 0 & s_2 \\ s_5^* & 0 & -s_3^* & s_4 & s_2^* & 0 & -s_0^* & s_1 \\ 0 & s_5^* & -s_4^* & -s_3 & 0 & s_2^* & -s_1^* & -s_0 \end{bmatrix} \tag{2.25}$$

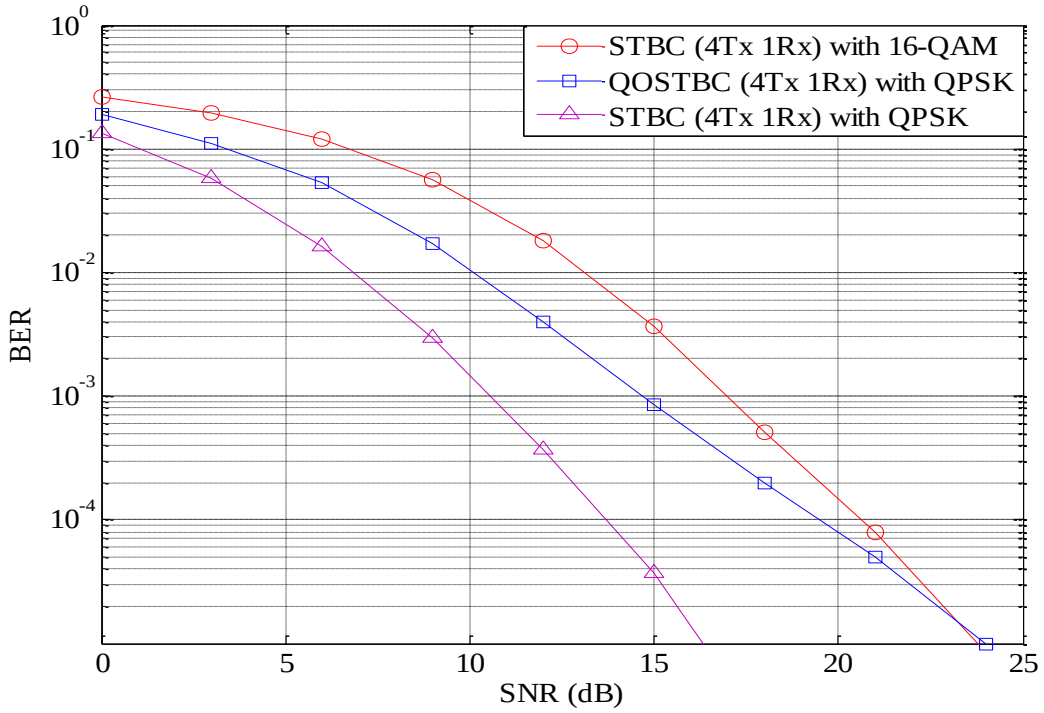

Figure 2-11: Comparison Results of STBC and QOSTBC for 4 Transmit Antennas

The performance of the QOSTBC scheme proposed by Jafarkhani and STBC for four transmit antennas is illustrated in Figure 2-11. As shown, for the same modulation order, STBC achieves better performance than QOSTBC. However, in order to have a comparison in term of rate, STBC with 16-QAM is also presented. Simulation results reveal that quasi orthogonal design performs better than orthogonal STBC for similar transmission rate of 2 bits/s/Hz. An improvement of up to 3 dB can be noticed at a SNR value of 10dB. From Figure 2-11, it can also be seen that STBC transmission achieves lower BER than QOSTBC for a SNR higher than 22dB. The QOSTBC transmission provides full rate and full diversity. However, it can be noticed that orthogonal design can decode symbols separately while quasi-orthogonal design decodes symbols in pairs which leads to an increase of complexity at the decoder.

2.5 Differential Space-Time Block Codes

Primary focus of previous Subsections was on diversity and coding rate for systems assuming channel parameters known at the receiver. When the coherence time of the channel is large enough, pilot sequence can be sent prior to the data symbols to acquire channel parameters via channel estimation. However, in some situation such as high-mobility environment or when channel conditions change rapidly, accurate channel estimation might be costly and complex. Therefore, a new STBC technique known as Differential-STBC (DSTBC), based on differential modulation has been proposed by Tarokh and Jafarkhani in [44].

Differential STBC can recover the transmitted sequence without the need of channel estimation [49-51]. Two consecutive transmitted symbols are encoded into phase differences and the receiver recovers the transmitted information by comparing the phase of the current symbol with the previously received symbol.

2.5.1 System Model

The block diagram of the differential STBC encoder based on orthogonal design is given in Figure 2-12. For the simple case of two transmit and one receive antenna, the transmitter starts by sending two arbitrary symbols s_0 and s_1 used to initiate the system. These first symbols are encoded according to Alamouti's model such that s_0 and s_1 are simultaneously transmitted at time 1 from antenna 1 and 2 respectively. At time 2, is transmitted from antenna 1 while simultaneously, is transmitted from antenna 2. The following data symbols are then encoded according to differential modulation.

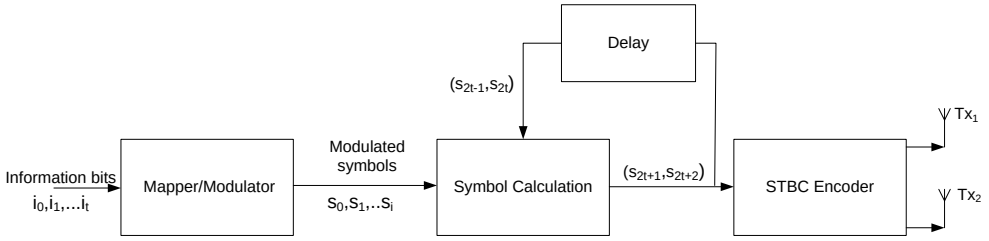

Figure 2-12: Block Diagram of DSTBC

At the i_{th} transmission interval, a block of 2m information bits from an m=$\log_2 M$ signal constellation where M is the modulation order is generated. From this block of bits, two complex co-efficient R1 and R2 are calculated and used with the previous information bits at (i-1)-*th* transmission interval to compute the information bits of the next transmission interval such as:

$$s_{2t+1}, s_{2t+2} = R_1 \; s_{2t-1}, s_{2t} + R_2(-s_{2t}^*, s_{2t-1}^*) \tag{2.26}$$

where s_{2t-1} and s_{2t} are the symbols transmitted simultaneously from antennas 1 and 2 respectively at time 2t-1 and that symbols - and are sent from antennas 1 and 2 respectively at time 2t. In addition, the coefficients R_1 and R_2 can be expressed as:

$$\begin{aligned} R_1 &= s_{2t+1}s_{2t-1}^* + s_{2t+2}s_{2t}^* \\ R_2 &= -s_{2t+1}s_{2t} + s_{2t+2}s_{2t-1} \end{aligned} \tag{2.27}$$

2.5.2 System Encoding

In order to describe the design of DSTBC efficiently, explanations on the encoding sequence are made for the simple case of Alamouti code under BPSK modulation. With this modulation scheme, modulated symbols can be assigned to one of the two signal point or . The coefficient vector set is computed using (2.27) in [47] as:

$$V = \left[R_1, R_2 \right] = \quad 1,0 \ , \ 0,1 \ , \ -1,0 \ , \ 0,-1 \tag{2.28}$$

The next set of bits is sent in a second time to the mapper/modulator where data symbols are first modulated using BPSK and then mapped according to [44] as:

$$M \quad 00 \ , \ 10 \ , \ 01 \ , \ 11 \quad = \quad 1,0 \ , \ 0,1 \ , \ -1,0 \ , \ 0,-1 \tag{2.29}$$

Assuming that the training symbols transmitted from antenna 1 and 2 at time *2t*-1 are — and — respectively and at time 2t, — and — transmitted from antenna 1 and 2 respectively.

If the information bits at 2t+1 are 01, using the mapping function given in (2.29), the computed value of R_1 and R_2 are equal to 0 and -1 respectively. Thus using (2.26), it can be deduced:

$$\begin{aligned} s_{2t+1}, s_{2t+2} \quad &= 0\left(-\frac{1}{\sqrt{2}}, -\frac{1}{\sqrt{2}} \right) + (-1)\left(+\frac{1}{\sqrt{2}}, -\frac{1}{\sqrt{2}} \right) \\ &= \left(-\frac{1}{\sqrt{2}}, +\frac{1}{\sqrt{2}} \right) \end{aligned} \tag{2.30}$$

Hence, at 2t+1, — and — are sent from antenna 1 and 2 simultaneously followed by — and — respectively.

A summary of the value of and for all possible combinations of s_3 and s_4 can be found in Table 2-2.

Table 2-2: Possible Values of and According to s_3 and s_4

s_3, s_4	R_1, R_2	,
0, 0	1, 0	$-\frac{1}{\sqrt{2}}, -\frac{1}{\sqrt{2}}$
0, 1	0, -1	$-\frac{1}{\sqrt{2}}, \frac{1}{\sqrt{2}}$
1, 0	0, 1	$\frac{1}{\sqrt{2}}, -\frac{1}{\sqrt{2}}$
1, 1	-1, 0	$\frac{1}{\sqrt{2}}, \frac{1}{\sqrt{2}}$

2.5.3 System Decoding

For simplicity reasons, it is assumed that only one receive antenna is used. As done previously, received signals will be denoted according to the time at which data is received. At time t, the received symbol will be r_t. Channels or fading coefficients will be denoted as h_1 and h_2 from transmit antennas 1 and 2 respectively. Therefore received signals at time 2t-1, 2t, 2t+1, 2t+2 can be represented by:

$$\begin{aligned} r_{2t-1} &= h_1 s_{2t-1} + h_2 s_{2t} + n_{2t-1} \\ r_{2t} &= -h_1 s_{2t}^* + h_2 s_{2t-1}^* + n_{2t} \\ r_{2t+1} &= h_1 s_{2t+1} + h_2 s_{2t+2} + n_{2t+1} \\ r_{2t+2} &= -h_1 s_{2t+2}^* + h_2 s_{2t+1}^* + n_{2t+2} \end{aligned} \tag{2.31}$$

For simplicity reasons, equation (2.31) can be written considering a vector representation of the received signal such as:

$$\begin{aligned} (r_{2t-1}, r_{2t}^*) &= (s_{2t-1}, s_{2t})H + N_{2t-1} \\ (r_{2t+1}, r_{2t+2}^*) &= (s_{2t+1}, s_{2t+2})H + N_{2t+1} \\ (r_{2t}, -r_{2t-1}^*) &= (-s_{2t}^*, s_{2t-1}^*)H + N_{2t} \end{aligned} \tag{2.32}$$

where H can be represented by the matrix:

$$H = \begin{bmatrix} h_1 & h_2^* \\ h_2 & -h_1^* \end{bmatrix} \tag{2.33}$$

and where N_i are the noisy terms and can be expressed as:

$$\begin{aligned} N_{2t-1} &= n_{2t-1}, n_{2t}^* \\ N_{2t+1} &= n_{2t+1}, n_{2t+2}^* \\ N_{2t} &= n_{2t}, -n_{2t-1}^* \end{aligned} \tag{2.34}$$

Moreover, the decision static is defined as the inner product of the two received signal vectors in (2.32) and is given as:

$$\begin{aligned} \tilde{R}_1 &= (r_{2t+1}, r_{2t+2}^*).(r_{2t-1}, r_{2t}^*) \\ &= (s_{2t+1}, s_{2t+2})HH^H(s_{2t-1}^*, s_{2t}) + (s_{2t+1}, s_{2t+2})HN_{2t-1}^H \\ &\quad + N_{2t+1}H^H(s_{2t-1}, s_{2t})^H + N_{2t+1}N_{2t-1}^H \end{aligned} \tag{2.35}$$

It can be deduced:

$$\begin{aligned} \tilde{R}_1 &= (r_{2t+1}, r_{2t+2}^*).(r_{2t-1}, r_{2t}^*) \\ &= r_{2t+1}r_{2t-1}^* + r_{2t+2}^* r_{2t} = \left|h_1\right|^2 + \left|h_2\right|^2 \quad s_{2t+1}s_{2t-1}^* + s_{2t+2}s_{2t}^* \\ &\quad + (s_{2t+1}, s_{2t+2})HN_{2t-1}^H + N_{2t+1}H^H(s_{2t-1}, s_{2t})^H + N_{2t+1}N_{2t-1}^H \end{aligned} \tag{2.36}$$

To simplify the notation, we denote:

$$\tilde{N}_1 = (s_{2t+1}, s_{2t+2})HN_{2t-1}^H + N_{2t+1}H^H(s_{2t-1}, s_{2t})^H + N_{2t+1}N_{2t-1}^H \tag{2.37}$$

Therefore, it leads to the simplification of (2.35) such as:

$$\tilde{R}_1 = \left|h_1\right|^2 + \left|h_2\right|^2 \; R_1 + \tilde{N}_1 \tag{2.38}$$

Next, the second decision statistics denoted by is constructed as the inner product of the two received signals r_{2t} and . Following the same procedure as , it can be deduced:

$$\tilde{R}_2 = \left|h_1\right|^2 + \left|h_2\right|^2 \; R_2 + \tilde{N}_2 \tag{2.39}$$

where $\tilde{N}_2$ can be expressed by:

$$\tilde{N}_2 = (s_{2t+1}, s_{2t+2})HN_{2t}^H + N_{2t+1}H^H(-s_{2t}^*, s_{2t-1}^*)^H + N_{2t+1}N_{2t}^H \tag{2.40}$$

Finally, and can be summarised in a single vector as:

$$\tilde{R}_1, \tilde{R}_2 \; = (\left|h_1\right|^2 + |\, h_2\,|^2)(R_1, R_2) + (N_1, N_2) \tag{2.41}$$

Due to the equal length of the elements of V, the receiver computes the closest vector V to (. Once the vector is computed, inverse mapping is applied and the transmitted bits are recovered.

Through all the derivations carried out in this Section, it can be seen that channel information is not needed in order to recover the transmitted data.

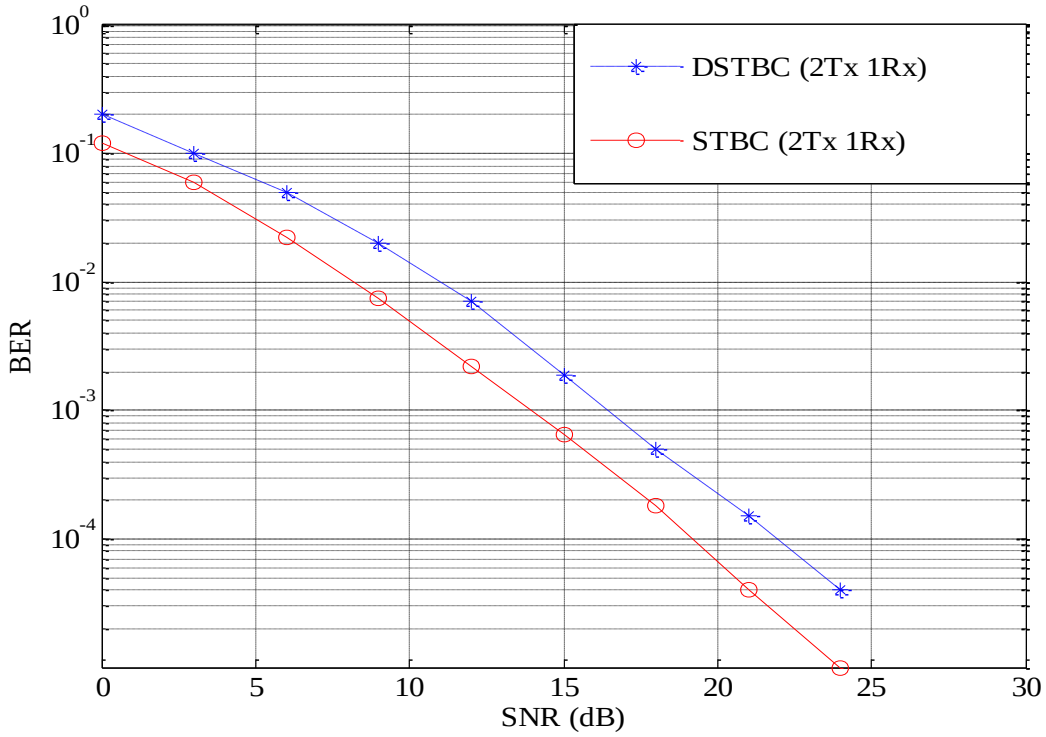

Figure 2-13: Performance Comparison of DSTBC with STBC under BPSK

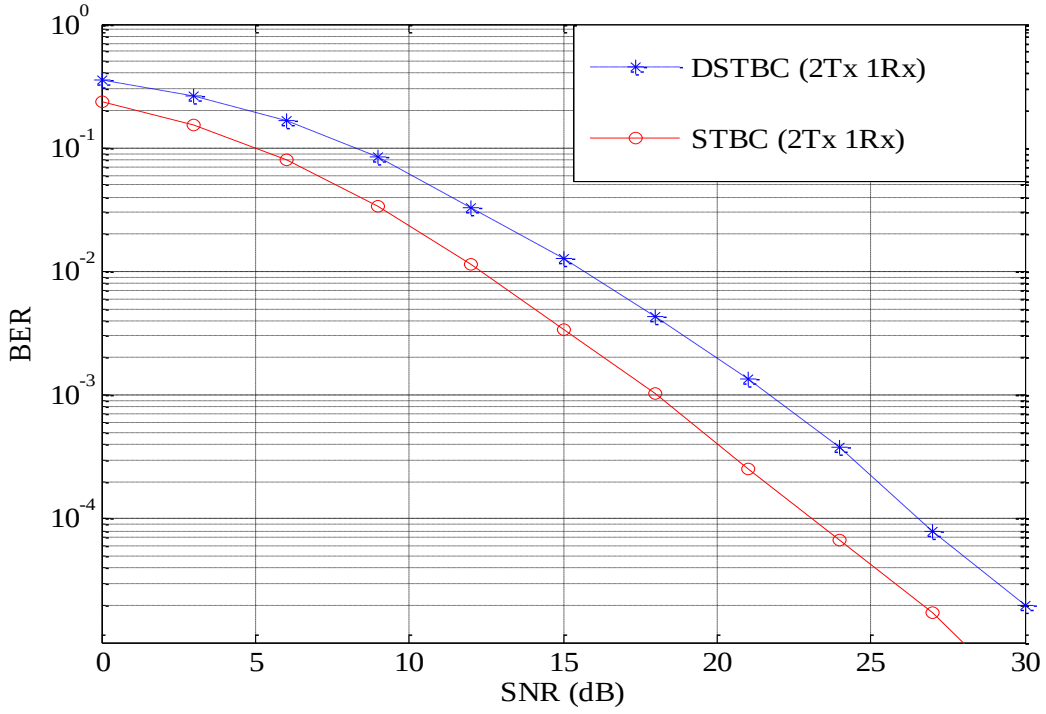

Figure 2-14: Performance Comparison of DSTBC with STBC under QPSK

The performance of the differential STBC scheme with two transmit antennas and one receive antenna are evaluated under slow fading channel. Figure 2-13 and Figure 2-14 show the performance comparison of DSTBC and STBC for BPSK and QPSK respectively. From the figures, it can be noticed that DSTBC gives a 3dB penalty when compared with STBC.

The 3dB penalty can be explained by the low impact of the multiplicative terms $N_{2t+1}N_{2t-1}^{H}$ at high SNR in (2.37). By ignoring the multiplicative terms due to its low impact in high SNR compared to the two remaining terms, it can be seen that the power of noise is twice the one of coherent detection where channel parameters are known at the receiver.

2.6 Conclusions

STBC is a relatively well known coding technique to enhance the capacity of wireless communication systems without affecting the bandwidth efficiency. Three coding schemes have been discussed in this chapter.

STBC achieves full diversity but full rate only for the case of two transmit antennas, while QOSTBC achieves both full rate and full diversity for two and four transmit antennas. However, decoding complexity of QOSTBC grows exponentially with the number of antennas used, whereas STBC decoding complexity grows linearly with the number of transmit and receive antennas.

Low complexity is also the main advantage of STBC compared to DSTBC. The coded transmission matrices are similar with the exception that in DSTBC the modulation of the input symbol is based on the previously transmitted symbol. In addition, the decoding of the symbols is similarly achieved, by looking at the

phase difference of the received symbol with the previously received one. In DSTBC, channel parameters are not required to decode the transmitted data, but DSTBC will suffer 3dB loss in SNR compared with STBC.

Due to the promising performances achieved by STBC in wireless communications, many wireless standards such as IEEE802.11n, IEEE802.16 and LTE are now incorporating these coding ideas. Current research is mainly focused on the use of STBC with OFDM in frequency selective environment and on the implementation using Field Programmable Gate Array (FPGA).

3 MIMO-OFDM Systems

STBC was first introduced for wireless systems operating in flat fading environments. However, with the recent advances in wireless communications, present and future wireless systems are now required to operate in frequency selective environments. In this chapter, a brief introduction to Orthogonal Frequency Division Multiplexing (OFDM) is given. The combination of OFDM with MIMO systems is then described. The two major coding techniques proposed in the literature namely, STBC-OFDM where data is coded through 'space and time', and SFBC-OFDM where data is coded through 'space and frequency', are described via mathematical derivations and simulation results. In addition, the performance of both coding techniques are compared for different number of transmit and receive antennas.

3.1 Introduction

Originally, STBC were proposed for non-frequency selective channels. However, present and future wideband wireless transmissions are expected to operate in frequency selective environments [52] where the propagation delay of the channel exceeds the transmission time of the symbols. With this development, it has become necessary to design new STBC codes for wideband systems operating in multipath frequency selective environments. In contrast to non-frequency selective channels, the design of STBC for frequency selective channels is not straightforward due to the attenuation of the signals in space and time. In order to maintain the decoding simplicity of STBC and with the help of original

generalised codes designed for flat fading channels, most researchers [53, 54] utilize a two-step approach to enhance the spectrum efficiency of the transmitted signal. First, their algorithms are able to cancel the effect of inter-symbols interference (ISI) by converting frequency selective channels into non-frequency selective channels. Secondly, the STBC encoder and decoder employed in their work are designed to be adaptive to non-frequency selective channels. One of the first methods proposed by researchers to combat the effect of ISI was the use of equalisers at the receiver to convert the channel in a temporal ISI-free channel [55, 56]. Another approach proposed in [17, 57] achieved lower decoding complexity at the receiver. The concept exploits one of the properties of OFDM which converts frequency selective channels into multiple parallel flat fading channels.

The combination of STBC with OFDM, termed 'STBC-OFDM' was first proposed by Agrawal in [16]. Following this development, various researchers have focused on designs for scenarios where the channel is assumed to be known at the receiver, for example, the designs proposed in [24, 58-60]. The results from these works are consistent with the findings in [29] which indicate that the combination of MIMO techniques with OFDM improves the transmission rate, range and reliability. Moreover, frequency diversity can be achieved in addition to the space and time diversity exploited by STBC. Hence, the combination of MIMO with OFDM led to codes known as Space-Frequency Block coding (SFBC) or SFBC-OFDM and Space-Time-Frequency Block OFDM coding (STFBC-OFDM) which exploit the maximum diversity available in MIMO channels [61]. In STBC-OFDM, the information symbols are coded across multiple antennas and time via the use of multiple consecutive OFDM symbols

[59], whereas, SFBC symbols are coded across multiple antennas and multiple OFDM subcarriers [62]. STFBC is a combination of STBC-OFDM and SFBC-OFDM, in this concept, the information symbols are coded though space, time and frequency by the use of multiple subcarriers [21].

The combination of MIMO-OFDM have been adopted in different standards like WiMax, 3G-LTE and 4G due to their ability to enable high data rate transmission over multipath and frequency selective fading channels. The additional advantages of STBC-OFDM are the simple linear decoding and low complexity receiver which have made them a popular choice for future wireless communications.

In this chapter, OFDM modulation is first presented, and its advantages and disadvantages are discussed. Then, STBC-OFDM and SFBC-OFDM are introduced, simulation results are presented and analysed for different number of transmit and receive antennas. Comparison between the STBC-OFDM and SFBC-OFDM coding schemes are made for different number of subcarriers, different number of antennas, different modulation orders and different cyclic prefix lengths.

3.2 Wireless Channel Models

3.2.1 Frequency Selective Channel

Received signals suffer from frequency selective fading when the constant amplitude and linear phase response of the wireless channel is narrower than the signal bandwidth. Under such conditions, the channel impulse response has a larger multipath delay spread than the symbol period of the transmitted signal.

Due to the short duration of the transmitted symbols in relation to the multipath delay spread, multiple attenuated and time delayed versions of the transmitted signal are received which induces inter-symbol interference. In contrast to flat fading channels, in frequency selective channels the amplitude of the frequency response of the transmitted signal varies with frequency.

Figure 3-1 shows the characteristics of a frequency selective fading channel. Frequency selective fading channels are also known as wideband channels since the channel delay spread τ is much greater than the symbol period *Ts* of the transmitted signal. Thus, the coherence bandwidth of the channel is smaller than that of the transmitted signal which leads to a gain variation in the frequency domain.

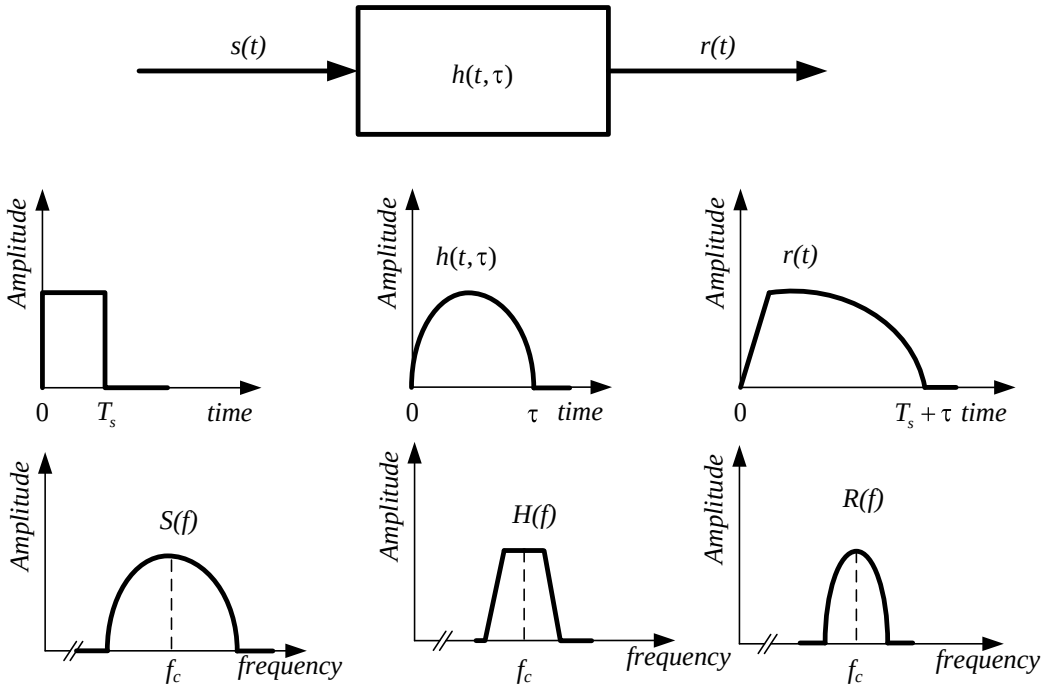

Figure 3-1: Frequency Selective Channel Characteristics [46]

To summarize the above observations, a signal is affected by a frequency selective channel if:

$$B_s > B_c \quad and \; T_s < \sigma_\tau \tag{3.1}$$

Even if it depends on the modulation scheme, a channel is commonly considered as frequency selective when $\sigma_\tau = 0.1 T_s$.

This thesis mainly focuses on channel estimation algorithms for fixed and mobile broadband wireless system. Thus, simulation results are proposed for IEEE 802.16 channel models [63]. This work thus provides channel parameters for systems operating in such scenarios. The channel parameters are related to terrain type, delay spread, and antenna directionality.

The modified Stanford University Interim (SUI) channel models consist of a set of 6 typical channels used to simulate three typical terrain types which are hilly terrain with moderate to heavy tree densities (category A), minimum path loss with flat terrain (category C) and intermediate path loss (category B). Table 3-1 summarized the parametric of the SUI channels according to the terrain type.

Table 3-1: Summary of the Channels Parametric in term of Terrain Type

Terrain Type	SUI Channels
Category A	SUI-1, SUI-2
Category B	SUI-3, SUI-4
Category B	SUI-5, SUI-6

Each SUI channel model is characterised by three taps (or channel path) which are defined by seven major parameters identified as the delay spread, the relative power, the K-factor (when K>0, Rician distribution is assumed, while for K=0 a Rayleigh distribution is assumed), the Doppler shift, the antenna correlation, the gain reduction and the normalisation factor. In this thesis, SUI-1 and SUI-3 are the channel models used as they represent two terrain types and both models are subject to low delay spread. Parameters of these two SUI channel models can be found in Table 3-2 and Table 3-3 respectively.

Table 3-2: SUI-1 Channel Model Parameters

SUI-1 Channel				
	Tap 1	**Tap 2**	**Tap 3**	**Units**
Delay	0	0.4	0.9	μs
Power (omni. ant.)	0	-15	-20	dB
K factor (omni. ant.)	4	0	0	
Doppler	0.4	0.3	0.5	Hz
Antenna Correlation:		ρ_{ENV}=0.7		
Gain Reduction Factor:		GRF=0dB		
Normalisation Factor:		F=-1.1771dB		

Table 3-3: SUI-3 Channel Model Parameters

SUI-3 Channel				
	Tap 1	**Tap 2**	**Tap 3**	**Units**
Delay	0	0.4	0.9	μs
Power (omni. ant.)	0	-5	-10	dB
K factor (omni. ant.)	1	0	0	
Doppler	0.4	0.3	0.5	Hz
Antenna Correlation:	ρ_{ENV}=0.4			
Gain Reduction Factor:	GRF=3dB			
Normalisation Factor:	F=-1.5113dB			

3.2.2 Doppler Shift

Spread in the frequency domain relative to a variation in the time domain is often related to movement of the transmitter or the receiver. Variation in the time domain of the received signal caused by the motion of the transmitter or receiver is called the *Doppler shift*. Based on the mobility of the transmitter, the received signal undergoes fast or slow fading. In fast fading, where the transmitter or receiver is mobile, the coherence time is smaller than the symbol period.

Let f_d denote the Doppler shift of the received signal, where θ is the angle of arrival of the transmitted signal with respect to the direction of the vehicle. Given that fc is the carrier frequency of the transmitted signal, the Doppler shift of the received signal can be given as:

$$f_d = \frac{vf_c}{c}\cos\theta \tag{3.2}$$

where v is the vehicle speed and c is the speed of light. In a multipath propagation environment, the bandwidth of the multipath waves is spread by the Doppler shift within the range f_c+f_{dmax}, where f_{dmax} is the maximum Doppler shift given in (3.3).

$$f_{d\max} = \frac{vf_c}{c} \tag{3.3}$$

The maximum Doppler shift is also referred to as the maximum fade rate.

3.3 OFDM modulation

3.3.1 Principle

Contrary to a single carrier systems where data is modulated on a single carrier of rate R_s, multicarrier systems such as OFDM transmit data simultaneously on N_s subcarriers modulated at a rate R_s/N_s. The total rate remains similar to that of single carrier systems but in this case each subcarrier is less sensitive to the delay spread of the channel.

The block diagram of a baseband OFDM transmitter after coding can be found in Figure 3-2. Once generated, bits are modulated using complex constellation and coded using STBC, SFBC or STFBC. The OFDM symbols undergo two operations. First, an IFFT is done in order to obtain symbols in the time domain from its image in the frequency domain. Then, a guard interval or cyclic prefix is added to the obtained signal. This interval is the copy of the last symbols of the transmitted data added at the beginning of the stream. The

extension of the stream is made in the time domain and its length must be larger than the delay spread of the channel.

Complex symbols $S_{i\ \ i=1,2...}$ are successively regrouped into blocks of length N_s (due to serial to parallel conversion) of transmission time $N_s T_s$. From this a single OFDM symbol of length T_{sym} (where $T_{sym} = N_s T_s$) is formed. Let $g_{l,k}(t)$ denote the OFDM signal sent on the N_s, $f_{k\ \ k=-N_s/2...N_s/2-1}$ in order to generate the output signal.

During the time $[iT_s,(i+1)T_s]$, the generated OFDM signal can be expressed as:

$$x_l(t) = \sum_{k=-N_s/2}^{N_s/2-1} S_{l,k}\, g(t-(i+1)T_s)\, e^{j2\pi f_k t} \tag{3.4}$$

It represents the *l-th* OFDM symbol, while $S_{l,k\ \ k=-N_s/2...N_s/2-1}$ represents the N_s complex symbols S_i it carries.

The received signal can be expressed as:

$$r(t) = \sum_{l=1}^{\infty} \sum_{k=-N_s/2}^{N_s/2-1} S_{l,k}\, g(t-(i+1/2)T_s)\, e^{j2\pi f_k t} + n_k(t) \tag{3.5}$$

where $n_k(t)$ represents the white Gaussian noise at the *k-th* subcarrier.

Transmitted symbols can be recovered with the help of an appropriate filter at the receiver followed by an appropriate sampler.

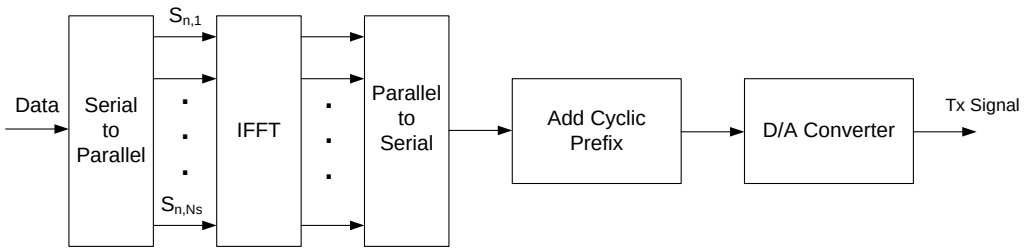

Figure 3-2: Block Diagram of an OFDM Transmitter

3.3.2 Orthogonality

The spectral efficiency of a system is defined by the transmitted bit rate in the frequency domain. In a multicarrier transmission, the spacing between two subcarriers is important in order to have a bandwidth efficient system.

If the spacing between the subcarriers is large, a higher bandwidth will be required to transmit a signal with similar rate and hence the spectral efficiency is lower. As it can be seen in Figure 3-3, preventing subcarriers from overlapping eliminates the inter-channel interference at the cost of bandwidth inefficiency.

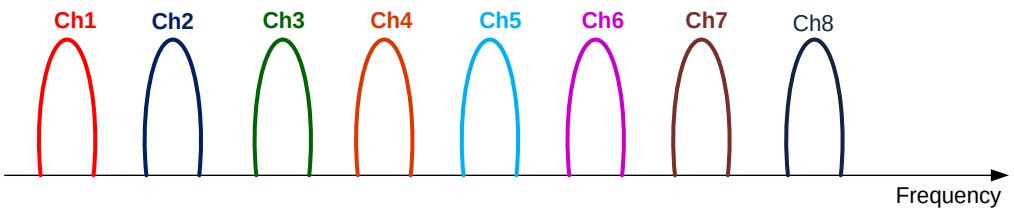

Figure 3-3: Conventional Multicarrier Technique

To solve the bandwidth inefficiency, OFDM has been introduced where the centre of one subcarrier is positioned such that it lands into the null of the neighbouring subcarrier as shown in Figure 3-4. The notion of orthogonality was first been introduced by Chang in [64]. As shown in Figure 3-4, almost 50% of the bandwidth is saved by allowing the subcarriers to overlap.

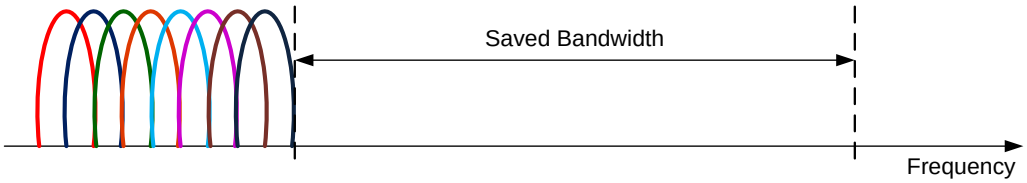

Figure 3-4: Orthogonal Multicarrier Modulation Technique

3.3.3 Cyclic Prefix

The introduction of cyclic prefix (CP) between two consecutive OFDM symbols is used in terrestrial systems in order to reduce the effect of the delay spread of the multipath channels. In order to simplify the synchronisation, a copy of the end of the transmitted OFDM symbols is added before the data stream, after the IFFT operation. The length of the CP is adjustable and must be set in order to keep a bandwidth efficient system.

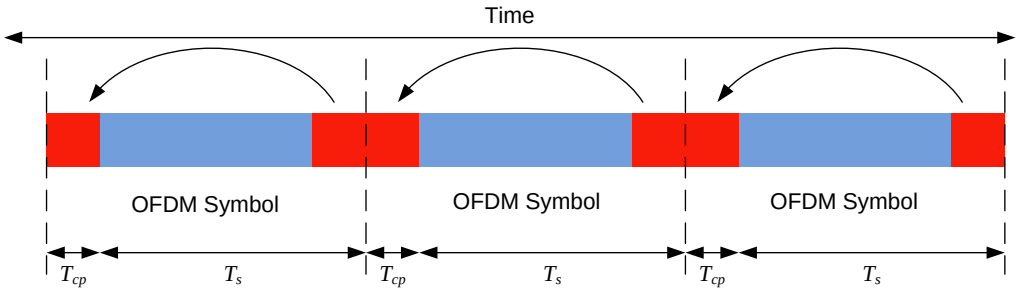

Figure 3-5: Temporal Representation of OFDM Symbols

Let D denote the last set of symbols of the OFDM symbol where N_s is the total number of subcarriers. The length of the CP depends on 4 factors:

1. **The length of the channel:** in order to ensure a perfect equalization, the length of the channel, L, must be smaller than the length of the CP, D, that is $D>L$.

2. **System performance:** as the CP represents a redundancy of the end of the OFDM symbol, the spectrum efficiency is reduced and is given by $N_s/(N_s+D)$. In order to get a spectral efficiency close to 1, N_s must tend to infinity.
3. **Complexity:** the FFT operations are made on blocks of size N_s, therefore, in order to have a feasible system, the value of N_s cannot be increased indefinitely. In such cases, a trade-off between complexity and spectral efficiency must be reached. Generally, the value of N_s is chosen equal to 4D, which gives a spectral efficiency of 25%.
4. **Channel type:** in order to obtain the circularity of the convolution, the channel must remain constant during the transmission of one OFDM symbol. In such cases, the diversity brought by the system cannot be increased even if N_s increase. Thus, the choice of N_s depends on the channel type (channel diversity, fast or slow fading).

3.3.4 Advantages and Drawbacks of OFDM

Single carrier transmission may not be useful in wideband wireless systems because it requires high complexity equalizer to deal with the ISI problem of the multipath frequency selective channels. Moreover, in Section 3.3.1, it has been shown that OFDM is easy to implement with the use of FFT. OFDM is also a bandwidth efficient modulation technique since the parallel subcarriers overlap but are orthogonal to each other without causing interference. In Section 3.3.3, it has been shown that the use of cyclic prefix helps the system to combat the effect of multipath fading and minimize the effects of ISI. Another advantage of OFDM

is that each subcarrier can be modulated using different modulation techniques M-PSK or M-QAM according to the requirement of the system.

OFDM appears to be a very powerful modulation technique for systems working under frequency selective channels. On the other hand, OFDM is more sensitive to frequency offset and phase noise. Furthermore, OFDM has a relatively large Peak to Average Power Ratio (PAPR) which tends to reduce the power efficiency of the RF amplifier.

As a result of the aforementioned advantages, OFDM is a very powerful and useful modulation technique for wireless communications. Up till now, OFDM is of great interest to researchers as they try to reduce PAPR effects using clipping, peak windowing and compression techniques hence making OFDM even better [65, 66].

3.4 MIMO-OFDM System Model

Application of STBC to MIMO systems using OFDM modulation is made in a similar way to conventional OFDM modulation. However, instead of sending one STBC block over n_t time slots, N_s blocks are simultaneously transmitted over the N_s subcarriers over n_t OFDM symbols. Similar to STBC-OFDM, another coding technique known as SFBC-OFDM where symbols are coded through frequency over multiple subcarriers within only one OFDM symbol, has been proposed in [18, 67]. In SFBC-OFDM, N_s/ n_t block coded symbols are simultaneously sent from the transmit antennas instead of one block of length n_t.

The block diagram of the STBC/SFBC-OFDM system using OFDM modulation is given in Figure 3-6. As stated in Chapter 2, Section 2.3.1, data bits

are first modulated using M-PSK or M-QAM complex constellation and then encoded using the STBC/SFBC encoder. The encoder receives p_s sequences of $2N_s$ symbols for STBC and N_s symbols for SFBC which are coded such that the output gives $d_s n_t$ sequences of length N_s transmitted over n_t OFDM symbols. Therefore, the coding rate is given by $R_c=p_s/d_s$. Finally, each sequence is passed through the OFDM modulator of its respective antennas.

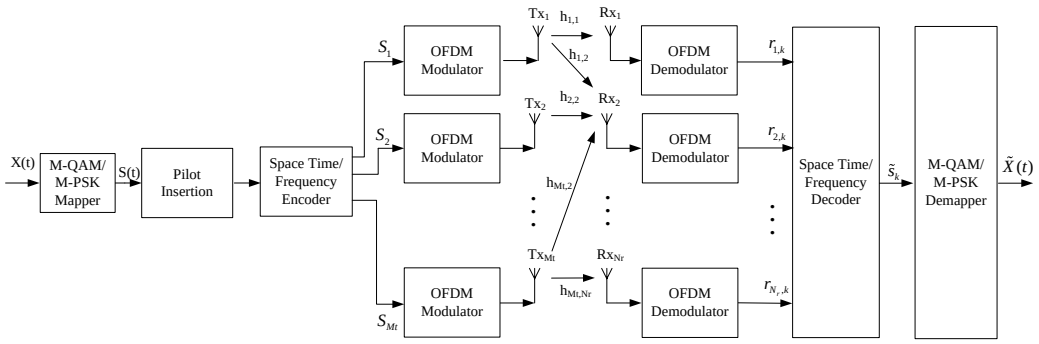

Figure 3-6: Block Diagram of a STBC/SFBC-OFDM System

It is assumed that OFDM symbols are transmitted over a Rayleigh multipath channel from the *i*-th transmit antenna to the *j*-th receive antenna. Rayleigh fading multipath channel can be described as:

$$h_{i,j}(\tau,t)=\sum_{l=0}^{L_{i,j}}\gamma_{i,j,l}(t)\delta(\tau-\tau_{i,j,l}) \tag{3.6}$$

where L is the number of paths, $\tau_{i,j,l}$ is the delay of the l-th path, $\gamma_{i,j,l}(t)$ is the corresponding gain, $\delta(t)$ is the Dirac function. All paths $\gamma_{i,j,l}(t)$ are assumed to be independent of each other.

The discrete channel response of subcarriers between the *i*-th transmit antenna and the *j*-th receive antenna can be expressed as:

$$H_{i,j,k}(t) = \sum_{l=0}^{L_{i,j}} \gamma_{i,j,l}(t) e^{-\frac{j2\pi k \tau_{i,j,l}}{N_{FFT}}} \tag{3.7}$$

where N_{FFT} is the Fast Fourier Transform (FFT) size and k is the subcarrier.

At the receiver, an equivalent procedure is followed. Data is received and down converted, cyclic prefix is removed and FFT operation is performed. STBC and SFBC encoding schemes offer a simple decoding algorithm when channel parameters are known at the receiver.

The transmitted sequence from transmit antenna 1 to M_t passes through a fast frequency selective channel with adaptive white Gaussian noise so that the received signal between the *i*-th transmit antenna and the *j*-th receive antenna, once the OFDM demodulation is applied, can be expressed in matrix form as:

$$R_{j,k} = \sum_{i=1}^{M_t} H_{i,j,k} S_{i,k} + N_{j,k} \tag{3.8}$$

where $N_{j,k}$ represents the white Gaussian noise with variance per dimension, $H_{i,j,k}$ is the time varying channel tap between the *i*-th transmit antenna and the *j*-th receive antenna and $S_{i,k}$ represents the transmitted signal from the *i*-th antenna.

Once the data has been decoded, the output of the combiner is fed to the ML detector which computes the optimum ML decision metric J_m over the set *s* and decides in favour of the symbol group that minimizes the metric J_m [68]:

$$J_m = \sum_{j=1}^{N_r} \sum_{k=1}^{N_C - 1} \left\| r_{j,k} - \sum_{i=1}^{M_t} h_{i,j,k} s_{i,k} \right\|^2 \tag{3.9}$$

At the receiver side, inverse operations are conducted where OFDM demodulation is first achieved, followed by a space time decoder. Finally data is demodulated using the appropriate modulation order.

3.5 STBC-OFDM

3.5.1 STBC-OFDM for 2 Transmit Antennas

In this Section, data transmission is considered using N_s subcarriers over two transmit and N_r receive antennas. The channel parameters are assumed known at the receiver.

As described in Section 3.4, data is encoded through space, time and frequency with the help of the space time encoder and OFDM modulation. From Subsection 2.3.4, it can be seen that two time slots are required to transmit the matrix $G_{2,c}$. Therefore, each antenna of the STBC-OFDM system is fed with a data stream of length $2N_s$ transmitted over $n_t=2$ OFDM symbols.

For a two transmit antenna STBC-OFDM, vectors $S_1(n)$ and $S_1(n+1)$ are transmitted alternatively form antenna 1. Simultaneously, $S_2(n)$ and $S_2(n+1)$ are similarly transmitted from antenna 2. Each vector is composed of symbols coded according to STBC rules described Subsection 2.3.2.

Figure 3-7 shows the organisation of the data through space, time and frequency. Assuming $h_{i,j,k}(n) = h_{i,j,k}(n+1)$ the received equation at the output of the FFT, for the case of two transmit and N_r receive antenna can be expressed as:

$$
\begin{aligned}
R_j(n) &= \sum_{j=1}^{Nr} H_{1,j}(n)S_1(n) + H_{2,j}(n)S_2(n) + N_j(n) \\
R_j(n+1) &= \sum_{j=1}^{Nr} H_{1,j}(n+1)S_1(n+1) + H_{2,j}(n+1)S_2(n+1) + N_j(n+1) \\
&= \sum_{j=1}^{Nr} -H_{1,j}(n)S_2^*(n) + H_{2,j}(n)S_1^*(n) + N_j(n+1)
\end{aligned}
\tag{3.10}
$$

where $R_j(n)$, $S_i(n)$ and $N_j(n)$ are the received symbols, transmitted vector symbols and the Gaussian noise sample respectively; *n* refers to the *n*-th OFDM symbol and *j* to the *j*-th receive antenna.

In addition, $S_1(n)$ and $S_2(n)$ are the vectors given after the serial to parallel operation at transmit antennas 1 and 2 respectively, and given for the OFDM symbol *n* and *n*+1 by the following equations:

$$
\begin{aligned}
S_1(n) &= \left[s_0,\ s_2,\ \ldots,\ s_{2k}, \ldots, s_{2Ns-4}, s_{2Ns-2} \right]^T \\
S_2(n) &= \left[s_1,\ s_3,\ \ldots,\ s_{2k+1}, \ldots, s_{2Ns-3},\ s_{2Ns-1} \right]^T \\
S_1(n+1) &= \left[-s_1^*,\ -s_3^*,\ \ldots, -s_{2k+1}^*, \ldots,\ -s_{2Ns-3}^*, s_{2Ns-1}^* \right]^T = -S_2^*(n) \\
S_2(n+1) &= \left[s_0^*,\ s_2^*,\ \ldots,\ s_{2k}^*,\ \ldots,\ s_{2Ns-4}^*,\ s_{2Ns-2}^* \right]^T = S_1^*(n)
\end{aligned}
\tag{3.11}
$$

with *k*=0, 1, …, *Ns*-1 and *n* represent the *n*-th OFDM symbols.

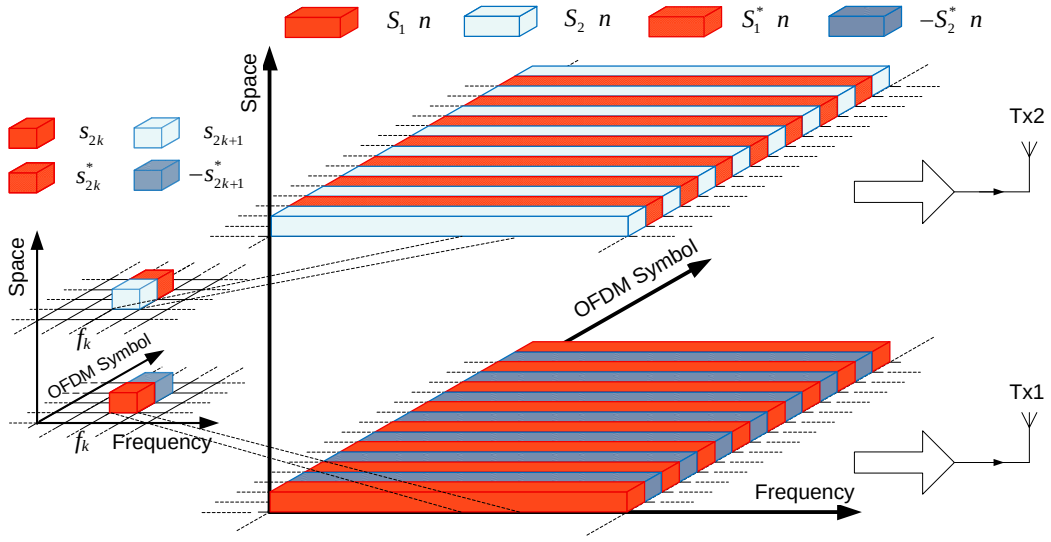

Figure 3-7 : Symbols Organisation of a STBC-OFDM

With the help of Figure 3-7 and equation (3.11), it can be seen that at OFDM symbol n, s_{2k} and s_{2k+1} are transmitted simultaneously at subcarrier k from antenna 1 and 2 respectively and in the second OFDM symbol n+1 at the same subcarrier k, $-s_{2k+1}^*$ is transmitted from antenna 1 while simultaneously, s_{2k}^* is transmitted from antenna 2.

At the receiver, the signal is first demodulated by an FFT demodulator and data is recovered by the space time decoder. For an ideal transmission where the channel is known at the receiver and according to the equations given in [5] for single carrier system, the following can be derived for multicarrier systems:

$$\begin{aligned}
\tilde{S}_{1,k}(n) &= \sum_{j=1}^{N_r}\left(H_{1,j,k}(n)R_{j,k}(n) + H_{2,j,k}(n)R_{j,k}(n+1)\right) \\
&= \tilde{s}_{2k} = \sum_{j=1}^{N_r}\left(h_{1,j,k}^* r_{j,2k} + h_{2,j,k} r_{j,2k+1}^*\right) \\
\tilde{S}_{2,k}(n) &= \sum_{j=1}^{N_r}\left(H_{2,j,k}^*(n)R_{j,k}(n) + H_{1,j,k}(n)R_{j,k}^*(n+1)\right) \\
&= \tilde{s}_{2k+1} = \sum_{j=1}^{N_r}\left(h_{2,j,k}^* r_{j,2k} - h_{1,j,k} r_{j,2k+1}^*\right)
\end{aligned} \tag{3.12}$$

with k=1, 2, ...,Ns, representing the symbol number, j represent the j-th receive antenna and $\tilde{S}_{i,k}$ and, $\tilde{s}_{2k}$ and $\tilde{s}_{2k+1}$ are the decoded signal and symbols respectively.

3.5.2 STBC-OFDM for 4 Transmit Antennas

In this Section, data is transmitted using N_s subcarriers over four transmit and N_r receive antennas. Similar to Subsection 3.5.1, the channel parameters are assumed known at the receiver.

As described in Section 3.4, data is encoded through space, time and frequency with the help of the space time encoder and OFDM modulator. From Subsection 2.3.4, it can be seen that 8 time slots are required to transmit the matrix S_4^c. As described in Figure 3-8, each antenna of the STBC-OFDM system is fed with a data stream of length $4N_s$ transmitted over n_t =8 OFDM symbols.

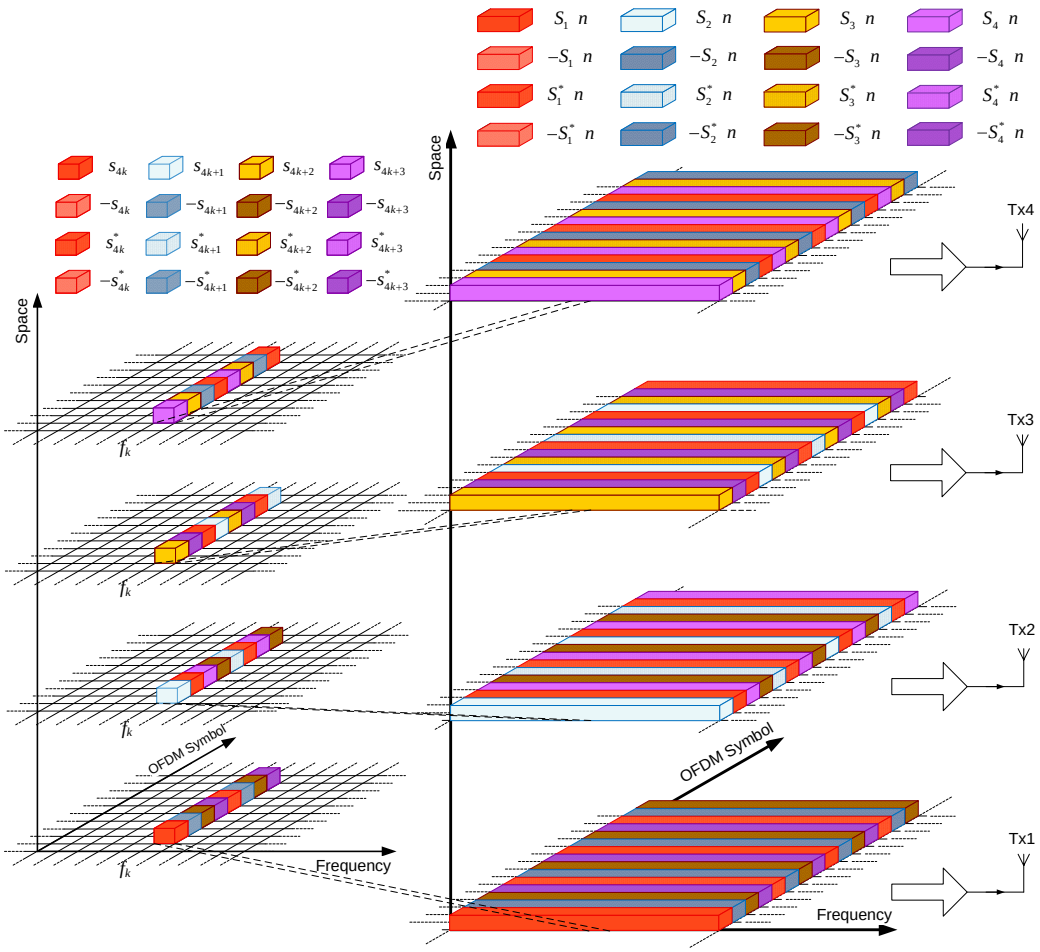

Figure 3-8: Symbols Organisation for 4 Transmit Antennas STBC-OFDM Systems

Figure 3-8 shows the organisation of the data through space, time and frequency. Assuming that channel parameters remain constant over 8 OFDM symbols, $h_{i,j,k}(n) = h_{i,j,k}(n+d)$ where d=1, 2, …, 8, the received equations at the output of the FFT are given as:

$$
\begin{aligned}
R_j(n) &= \sum_{j=1}^{Nr} H_{1,j}(n)S_1(n) + H_{2,j}(n)S_2(n) + H_{3,j}(n)S_3(n) + H_{4,j}(n)S_4(n) + N_{1,j}(n) \\
R_j(n+1) &= \sum_{j=1}^{Nr} -H_{1,j}(n)S_2(n) + H_{2,j}(n)S_1(n) - H_{3,j}(n)S_4(n) + H_{4,j}(n)S_3(n) + N_{1,j}(n+1) \\
R_j(n+2) &= \sum_{j=1}^{Nr} \left(-H_{1,j}(n)S_3(n) + H_{2,j}(n)S_4(n) + H_{3,j}(n)S_1(n) - H_{4,j}(n)S_2(n) + N_{1,j}(n+2)\right) \\
R_j(n+3) &= \sum_{j=1}^{Nr} \left(-H_{1,j}(n)S_4(n) - H_{2,j}(n)S_3(n) + H_{3,j}(n)S_2(n) + H_{4,j}(n)S_1(n) + N_{1,j}(n+3)\right) \\
R_j(n+4) &= \sum_{j=1}^{Nr} \left(H_{1,j}(n)S_1^*(n) + H_{2,j}(n)S_2^*(n) + H_{3,j}(n)S_3^*(n) + H_{4,j}(n)S_4^*(n) + N_{1,j}(n+4)\right) \\
R_j(n+5) &= \sum_{j=1}^{Nr} \left(-H_{1,j}(n)S_2^*(n) + H_{2,j}(n)S_1^*(n) - H_{3,j}(n)S_4^*(n) + H_{4,j}(n)S_3^*(n) + N_{1,j}(n+5)\right) \\
R_j(n+6) &= \sum_{j=1}^{Nr} \left(-H_{1,j}(n)S_3^*(n) + H_{2,j}(n)S_4^*(n) - H_{3,j}(n)S_1^*(n) + H_{4,j}(n)S_2^*(n) + N_{1,j}(n+6)\right) \\
R_j(n+7) &= \sum_{j=1}^{Nr} \left(-H_{1,j}(n)S_4^*(n) - H_{2,j}(n)S_3^*(n) + H_{3,j}(n)S_2^*(n) + H_{4,j}(n)S_1^*(n) + N_{1,j}(n+7)\right)
\end{aligned} \tag{3.13}
$$

where $R_j(n)$, $S_i(n)$ and $N_j(n)$ are the received symbols, transmitted vectors and the Gaussian noise sample respectively; *n* refers to the *n*-th OFDM symbol and *j* to the *j*-th receive antenna. In addition, *i*=1, 2, 3 and 4, which leads to the derivation of the vectors $S_i(n)$ given by:

$$
\begin{aligned}
S_1(n) &= \left[s_0,\ s_4,\ \ldots,\ s_{4k},\ldots,\ s_{4Ns-8}, s_{2Ns-4}\right]^T \\
S_2(n) &= \left[s_1,\ s_5,\ \ldots,\ s_{4k+1},\ldots,s_{4Ns-7},\ s_{2Ns-3}\right]^T \\
S_3(n) &= \left[s_2,\ s_6,\ \ldots,\ s_{4k+2},\ldots,\ s_{4Ns-6}, s_{2Ns-2}\right]^T \\
S_4(n) &= \left[s_3,\ s_7,\ \ldots,\ s_{4k+3},\ldots,\ s_{4Ns-5},\ s_{2Ns-1}\right]^T
\end{aligned} \tag{3.14}
$$

where *k*=0, 1, …, *Ns*-1.

Finally, due to the fact that channel parameters are known at the receiver, the transmitted signal is recovered by combining the receive signals as follows:

$$
\begin{aligned}
\tilde{s}_{4k} &= \sum_{j=1}^{N_r} (h^*_{1,j,k} r_{j,4k} + h^*_{2,j,k} r_{j,4k+1} + h^*_{3,j,k} r_{j,4k+2} + h^*_{4,j,k} r_{j,4k+3} + \\
&\qquad h_{1,j,k} r^*_{j,4k+4} + h_{2,j,k} r^*_{j,4k+5} + h_{3,j,k} r^*_{j,4k+6} + h_{4,j,k} r^*_{j,4k+7}) \\
\tilde{s}_{4k+1} &= \sum_{j=1}^{N_r} (h^*_{2,j,k} r_{j,4k} - h^*_{1,j,k} r_{j,4k+1} - h^*_{4,j,k} r_{j,4k+2} + h^*_{3,j,k} r_{j,4k+3} + \\
&\qquad h_{2,j,k} r^*_{j,4k+4} - h_{1,j,k} r^*_{j,4k+5} - h_{4,j,k} r^*_{j,4k+6} + h_{3,j,k} r^*_{j,4k+7}) \\
\tilde{s}_{4k+2} &= \sum_{j=1}^{N_r} (h^*_{3,j,k} r_{j,4k} + h^*_{4,j,k} r_{j,4k+1} - h^*_{1,j,k} r_{j,4k+2} - h^*_{2,j,k} r_{j,4k+3} + \\
&\qquad h_{3,j,k} r^*_{j,4k+4} + h_{4,j,k} r^*_{j,4k+5} - h_{1,j,k} r^*_{j,4k+6} - h_{2,j,k} r^*_{j,4k+7}) \\
\tilde{s}_{4k+3} &= \sum_{j=1}^{N_r} (h^*_{4,j,k} r_{j,4k} - h^*_{3,j,k} r_{j,4k+1} + h^*_{2,j,k} r_{j,4k+2} - h^*_{1,j,k} r_{j,4k+3} + \\
&\qquad h_{4,j,k} r^*_{j,4k+4} - h_{3,j,k} r^*_{j,4k+5} + h_{2,j,k} r^*_{j,4k+6} - h_{1,j,k} r^*_{j,4k+7})
\end{aligned}
\tag{3.15}
$$

where $h_{i,j,k}$ represents the channel parameter between *i*-th transmit antenna and the *j*-th receive antenna at subcarrier *k*. The signal is then sent to the ML detector and demodulated.

3.5.3 Simulation Results

The STBC-OFDM system presented in Subsection 3.5.1 and 3.5.2 have been simulated under frequency selective channels. System parameters have been set as described in Table 3-4. Simulations have been performed using Matlab. In the proposed results, two and four transmit antennas have been used with one and two receive antennas and with different modulation orders.

Table 3-4: Simulation Parameters for MIMO-OFDM Systems

FFT Size (Nfft)	256
Number of Active Subcarriers (N_{used})	192
Number of Guard Subcarriers	28 low, 27 high
Channel Bandwidth	3.5MHz
Sampling Rate (Fs)	2.28MHz (n=57/50)
Distance between Adjacent Subcarriers (Δf)	8.9kHz
Useful Symbol Duration (T_b)	0.112ms
Guard Time (T_g)	28.07μs
Total Symbol Duration (T_s)	140 μs
Modulation	QPSK, 16 QAM
SUI	1
Transmit Antenna	2, 4
Receive Antenna	1 and 2

Simulations have been performed under multipath frequency selective channels and results are obtained in terms of BER versus SNR. In addition, the impulse response of the channel was generated based on SUI 1 channel model (see subsection 3.2.1). Channel parameters of two and eight adjacent OFDM symbols have been assumed constant for two and four transmit antennas respectively.

Simulation results presented in Figure 3-9 and Figure 3-10 show the performances of STBC-OFDM systems for different CP lengths. It can be seen that as the length of the CP reduces, the BER value increases. Moreover, simulation results show that between CP length of 1/4 and 1/32 of the data stream,

2 dB can be saved at the cost of extra bandwidth usage. The 2dB loss was expected as stated in Subsection 3.3.3 because the CP length must be longer than the delay spread of the channel in order to ensure perfect equalisation.

From the performance results, it can be seen that the BER reduces with the number of transmit and receive antennas. Finally, as stated in Chapter 2, BER is increasing as the modulation order increases.

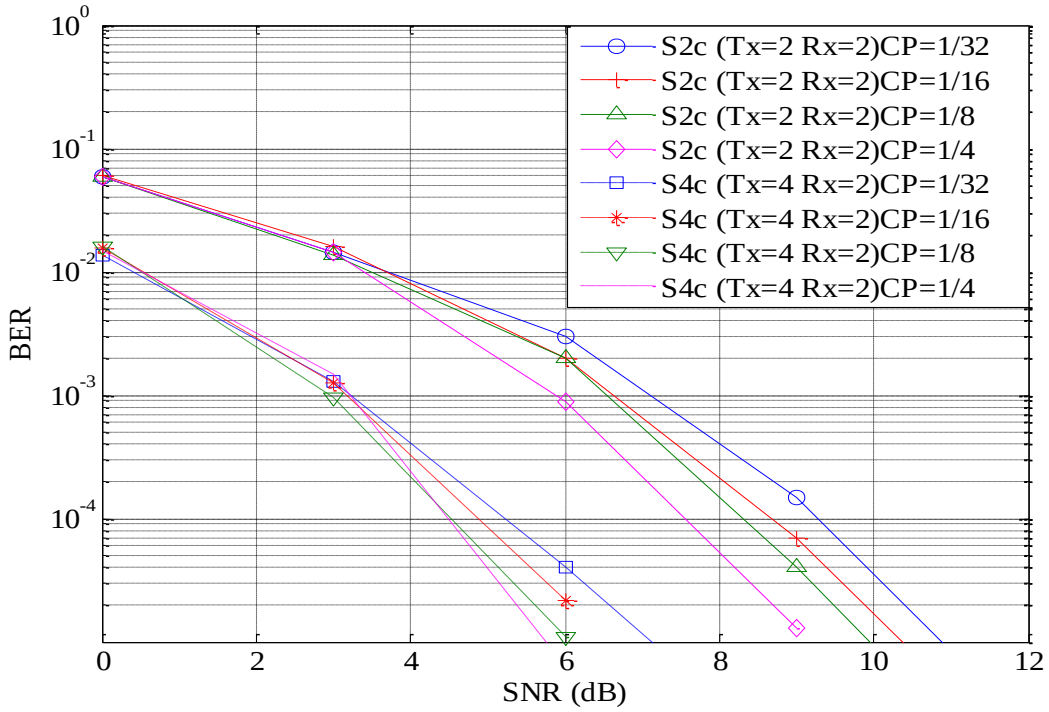

Figure 3-9: Cyclic Prefix Performance Results of STBC-OFDM System under QPSK

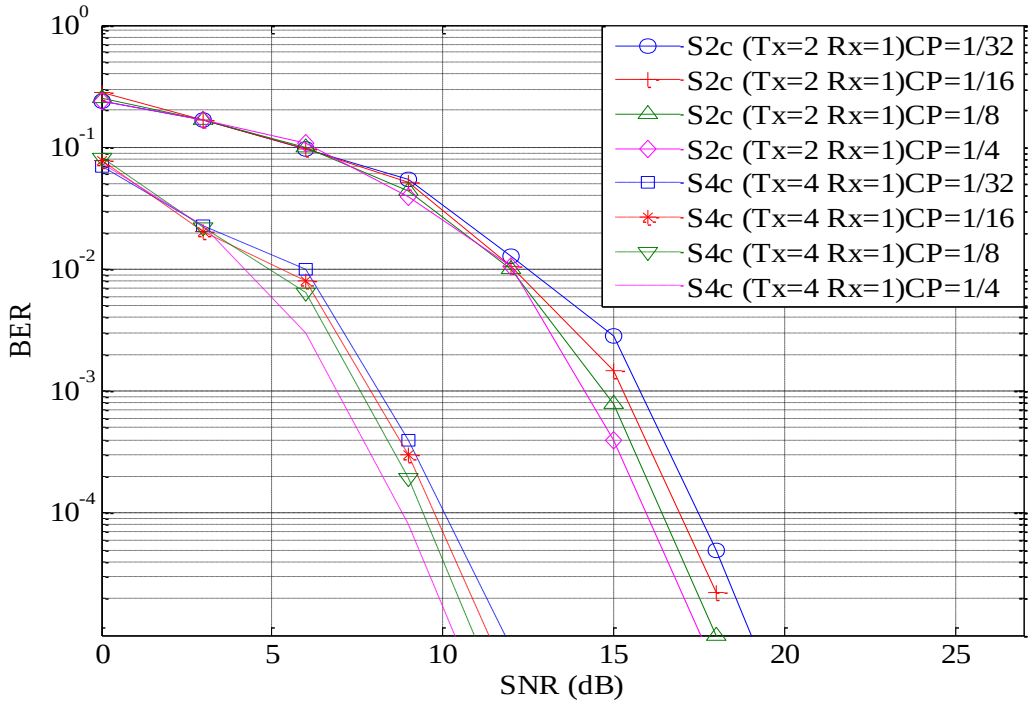

Figure 3-10: Cyclic Prefix Performance Results of STBC-OFDM under 16QAM

3.6 SFBC-OFDM

3.6.1 SFBC-OFDM for 2 Transmit Antennas

Similar to STBC-OFDM presented in Section 3.5, SFBC-OFDM for two transmit antennas requires two time slots to transmit the S_{2c} matrix. However, in contrast with STBC-OFDM, only one OFDM symbol is required as data is coded across subcarriers.

Figure 3-11 shows the organisation of the data through space, time and subcarriers. As it can be seen, symbol s_k and $-s_{k+1}^*$ are transmitted alternatively from antenna 1 while s_{k+1} and s_k^* are transmitted in a similar way from antenna 2.

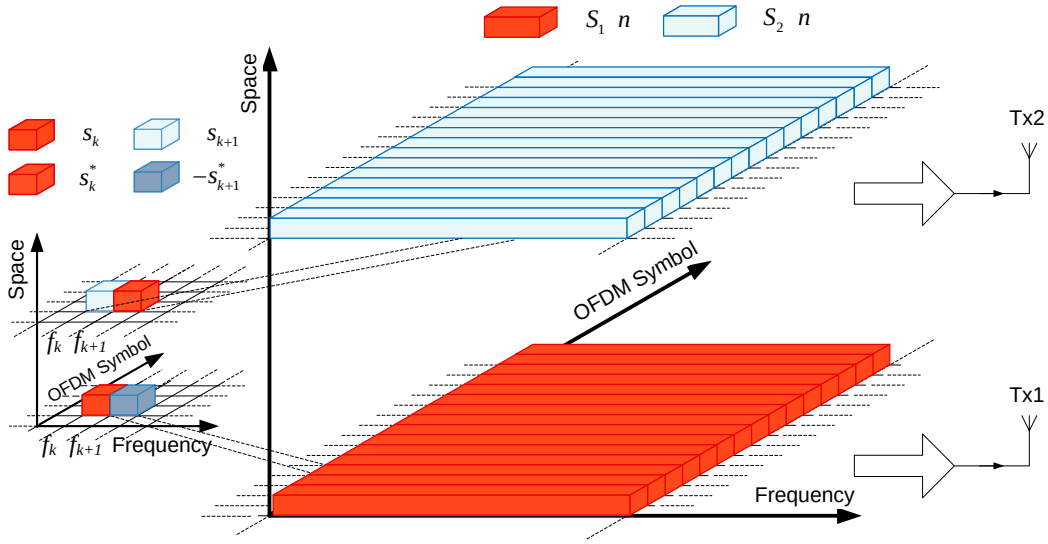

Figure 3-11: Data Organisation of SFBC-OFDM

Due to the fact that data symbols are transmitted within one OFDM symbol, the received signal can be expressed as:

$$R_j(n) = \sum_{j=1}^{Nr} H_{1,j}(n)S_1(n) + H_{2,j}(n)S_2(n) + N_j(n) \tag{3.16}$$

where $N_j(n)$ is the white Gaussian noise. Data vector $S_1(n)$ and $S_2(n)$ can also be expressed as:

$$\begin{aligned} S_1 &= [s_0,\ -s_1^*,\ \ldots,\ s_k,\ -s_{k+1}^*,\ldots,\ s_{Ns-2},-s_{Ns-1}^*]^T \\ S_2 &= [s_1,\ s_0^*,\ \ldots,\ s_{k+1},\ s_k^*,\ldots,\ s_{Ns-1},\ s_{Ns-2}^*]^T \end{aligned} \tag{3.17}$$

where k=0, 2,…, Ns-1.

Data symbols can be recovered using only one OFDM symbol, therefore, *n* has been omitted and will be omitted for the rest of this Section.

Assuming that channel parameters remain constant over two consecutive subcarriers and that channel parameters are known at the receiver. After FFT

operation is performed, received data is sent to the SFBC decoder. Following the derivation of the single carrier STBC case, it can be derived that:

$$\begin{aligned}\tilde{s}_k &= \sum_{j=1}^{N_r} (h_{1,j,k}^{*} r_{j,k} + h_{2,j,k} r_{j,k+1}^{*}) \\ \tilde{s}_{k+1} &= \sum_{j=1}^{N_r} (h_{2,j,k}^{*} r_{j,k} - h_{1,j,k} r_{j,k+1}^{*})\end{aligned} \tag{3.18}$$

Data is then sent to the ML decoder and to the demapper to recover the transmitted stream.

3.6.2 SFBC-OFDM for 4 Transmit Antennas

In this Section, SFBC-OFDM for four transmit and N_r receive antennas is described. Again all the mentioned assumptions above in Subsection 3.6.1 are applied.

The transmitter codes the data through space, time and frequency based on the S_{4c} matrix of Chapter 2. Figure 3-12 shows the organisation of the data symbols through space, time and frequency.

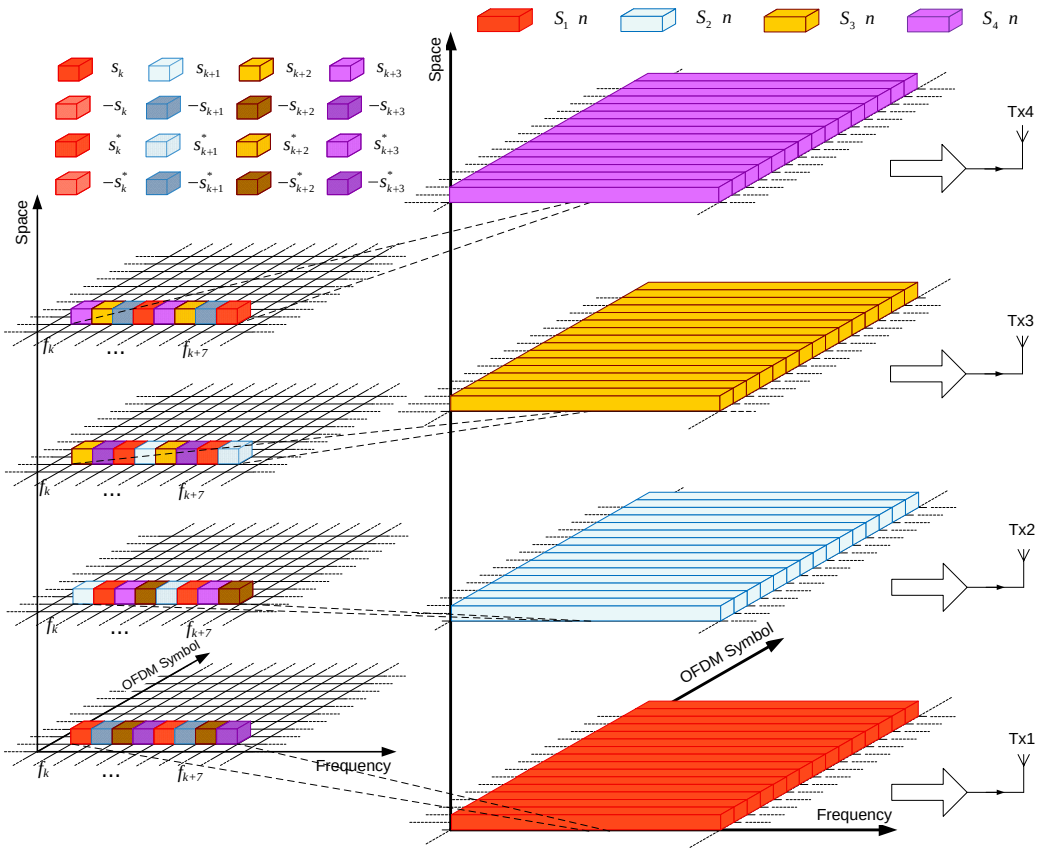

Figure 3-12: Organisation of Data Symbol for 4 Transmit Antennas SFBC-OFDM Systems

At the receiver, after the FFT operation, the received signal can be expressed as:

$$R_j = \sum_{j=1}^{Nr} H_{1,j}S_1 + H_{2,j}S_2 + H_{3,j}S_3 + H_{4,j}S_4 + N_j \qquad (3.19)$$

where N_j is the white Gaussian noise, $H_{i,j}$ and S_i are the channel between the i-th transmit antenna and the j-th receive antenna and the transmitted signal from the i-th transmit antenna respectively. The transmitted vectors can be expressed as:

$$
\begin{aligned}
S_1 &= [s_0,\ -s_1,\ -s_2,\ -s_3, s_0^*,\ -s_1^*, -s_2^*, -s_3^* \ldots, \\
&\quad s_{Ns/2-4},\ -s_{Ns/2-3},\ -s_{Ns/2-2},\ -s_{Ns/2-1,} s_{Ns/2-4}^*,\ -s_{Ns/2-3}^*,\ -s_{Ns/2-2}^*, -s_{Ns/2-1}^*]^T \\
S_2 &= [s_1, s_0, s_{3,} -s_{2,}\ s_1^*, s_0^*,\ s_3^*,\ -s_2^*\ \ldots, \\
&\quad s_{Ns/2-3},\ s_{Ns/2-4},\ s_{Ns/2-1},\ -s_{Ns/2-2}, s_{Ns/2-3}^*,\ s_{Ns/2-4}^*,\ s_{Ns/2-1}^*,\ -s_{Ns/2-2}^*]^T \\
S_3 &= [s_2,\ -s_3, s_{0,} s_{1,}\ s_2^*,\ -s_3^*,\ s_0^*,\ s_1^*\ \ldots, \\
&\quad s_{Ns/2-2},\ -s_{Ns/2-1},\ s_{Ns/2-4}, s_{Ns/2-3},\ s_{Ns/2-2}^*,\ -s_{Ns/2-1}^*,\ s_{Ns/2-4}^*,\ s_{Ns/2-3}^*]^T \\
S_4 &= [s_3,\ s_2,\ -s_1,\ s_0,\ s_3^*,\ s_2^*,\ -s_1^*,\ s_0^*\ \ldots, \\
&\quad s_{Ns/2-1},\ s_{Ns/2-2},\ -s_{Ns/2-3}, s_{Ns/2-4},\ s_{Ns/2-1}^*,\ s_{Ns/2-2}^*,\ -s_{Ns/2-3}^*,\ s_{Ns/2-4}^*]^T
\end{aligned}
\tag{3.20}
$$

The receiver then combines the received signals and the channel parameters to recover the transmitted data. Equation of the combination can be found in (3.21).

$$
\begin{aligned}
\tilde{s}_k &= \sum_{j=1}^{N_r} (h_{1,j,k}^* r_{j,k} + h_{2,j,k}^* r_{j,k+1} + h_{3,j,k}^* r_{j,k+2} + h_{4,j,k}^* r_{j,k+3} + \\
&\qquad h_{1,j,k} r_{j,k+4}^* + h_{2,j,k} r_{j,k+5}^* + h_{3,j,k} r_{j,k+6}^* + h_{4,j,k} r_{j,k+7}^*) \\
\tilde{s}_{k+1} &= \sum_{j=1}^{N_r} (h_{2,j,k}^* r_{j,k} - h_{1,j,k}^* r_{j,k+1} - h_{4,j,k}^* r_{j,k+2} + h_{3,j,k}^* r_{j,k+3} + \\
&\qquad h_{2,j,k} r_{j,k+4}^* - h_{1,j,k} r_{j,k+5}^* - h_{4,j,k} r_{j,k+6}^* + h_{3,j,k} r_{j,k+7}^*) \\
\tilde{s}_{k+2} &= \sum_{j=1}^{N_r} (h_{3,j,k}^* r_{j,k} + h_{4,j,k}^* r_{j,k+1} - h_{1,j,k}^* r_{j,k+2} - h_{2,j,k}^* r_{j,k+3} + \\
&\qquad h_{3,j,k} r_{j,k+4}^* + h_{4,j,k} r_{j,k+5}^* - h_{1,j,k} r_{j,k+6}^* - h_{2,j,k} r_{j,k+7}^*) \\
\tilde{s}_{k+3} &= \sum_{j=1}^{N_r} (h_{4,j,k}^* r_{j,k} - h_{3,j,k}^* r_{j,k+1} + h_{2,j,k}^* r_{j,k+2} - h_{1,j,k}^* r_{j,k+3} + \\
&\qquad h_{4,j,k} r_{j,k+4}^* - h_{3,j,k} r_{j,k+5}^* + h_{2,j,k} r_{j,k+6}^* - h_{1,j,k} r_{j,k+7}^*)
\end{aligned}
\tag{3.21}
$$

where k=0, 4,…, Ns-3.

As it can be seen, equations of SFBC-OFDM are similar to the equations given for STBC-OFDM, the difference being that symbols are coded through frequency instead of time for the former. As for single carrier systems, complexity increases linearly with the number of transmit and receive antennas.

3.6.3 Simulation Results

The performance of SFBC-OFDM systems have been evaluated according to the specifications described in Table 3-4 of Subsection 3.5.3. As done for STBC-OFDM, simulations have been performed for two and four transmit antennas and one and two receive antennas. Different values of CP have been tested for the different scenarios using QPSK and 16QAM. Channel parameters of two and eight adjacent subcarriers have been assumed constant for two and four transmit antennas respectively.

Figure 3-13 and Figure 3-14 show the performance results of two and four transmit antennas for different CP lengths. It can be noticed from the two figures that similar to STBC-OFDM, longer CP lengths achieve lower BER than shorter CP lengths. Moreover, it can be noticed that the dB loss between the biggest CP= 1/4 and the shortest CP=1/32, is around 2dB. As in the case of STBC-OFDM, the error is due to the fact that the CP needs to be longer than the delay spread of the channel in order to allow effective equalisation.

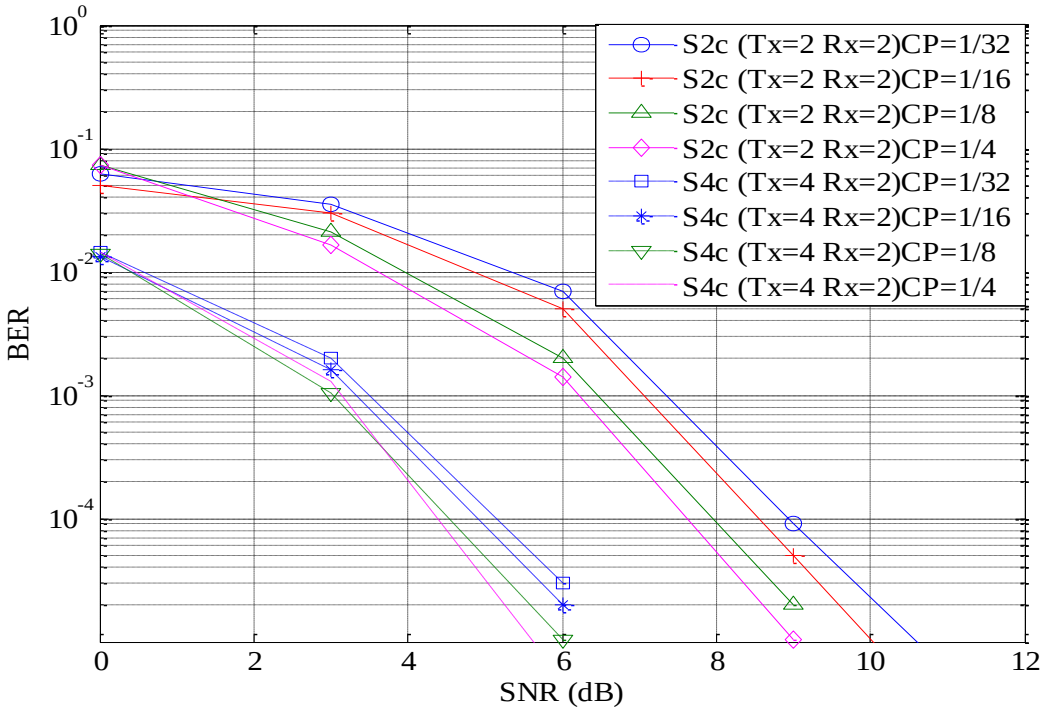

Figure 3-13: Cyclic Prefix Performance Results of SFBC-OFDM System under QPSK

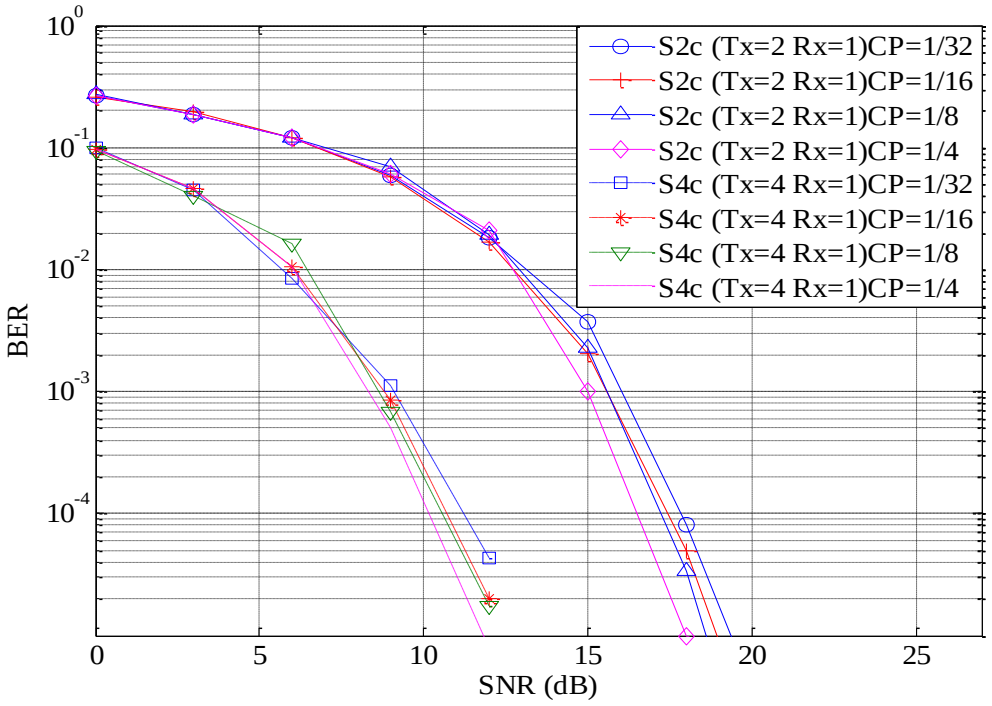

Figure 3-14: Cyclic Prefix Performance Results of SFBC-OFDM System under 16QAM

A performance comparison between STBC-OFDM and SFBC-OFDM systems is shown in Figure 3-15 and Figure 3-16 for QPSK and 16QAM

respectively. From the performance results, it can be seen that STBC-OFDM and SFBC-OFDM systems achieve similar performance under similar condition when channel parameters are known at the receiver. Such results were expected because similar assumptions have been made and that the coding technique is similar with the exception that STBC-OFDM symbols are coded over OFDM symbols while SFBC-OFDM symbols are coded over subcarriers.

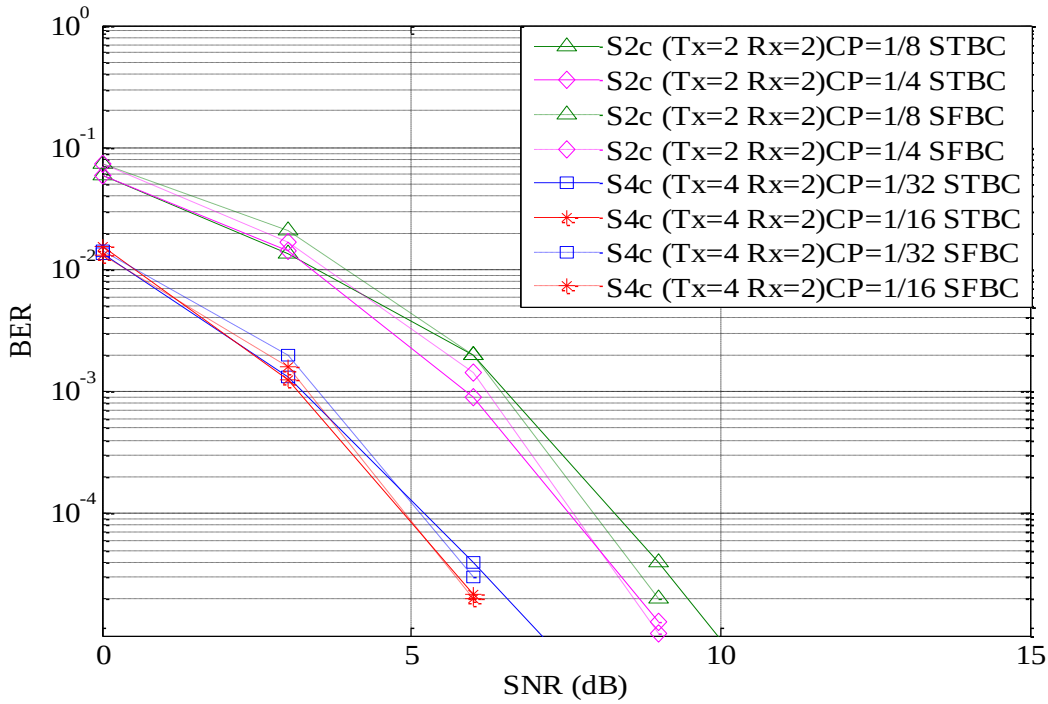

Figure 3-15: Comparison Results between STBC-OFDM and SFBC-OFDM under QPSK

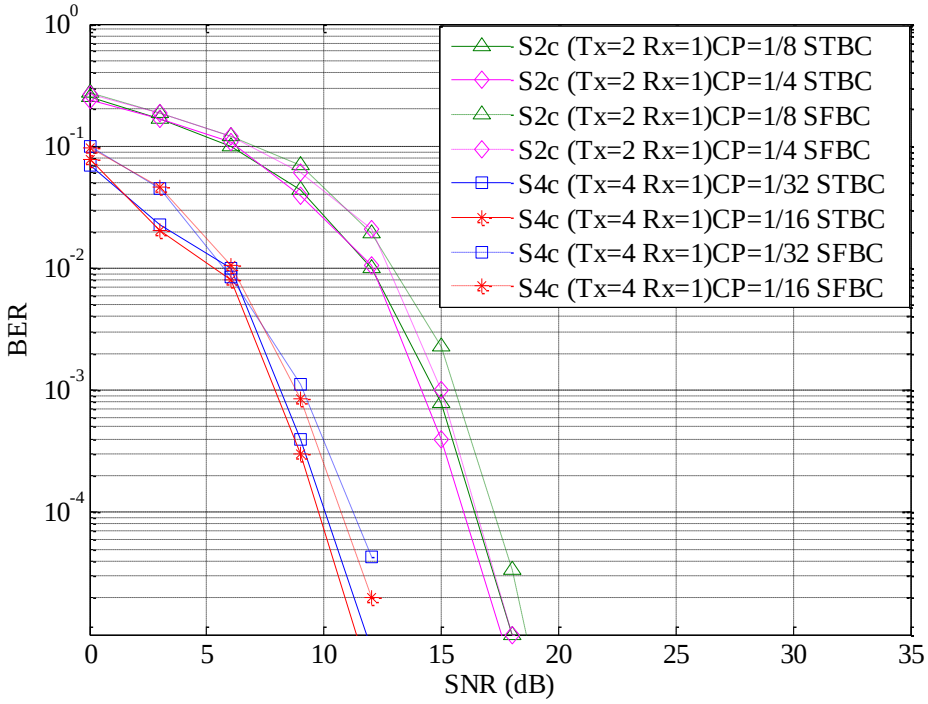

Figure 3-16: Comparison Results between STBC-OFDM and SFBC-OFDM under 16QAM

3.7 Conclusions

The combination of OFDM with STBC, allowed the creation of codes known as STBC-OFDM and SFBC-OFDM offering low decoding complexity and bandwidth efficiency as realised in STBC for single carrier systems. STBC-OFDM and SFBC-OFDM systems have been adopted by standard such as WiMax and 4G and have been under extensive investigation by researchers.

In this chapter, a comprehensive investigation of OFDM and in particular MIMO-OFDM systems was conducted. Two coding schemes, STBC-OFDM and SFBC-OFDM, have been described in detail and simulation results for both schemes have been presented for different number of transmit and receive antennas and under various modulation schemes. A comparison of the 2 schemes

has also been made which led to the conclusions that STBC-OFDM and SFBC-OFDM achieve similar performances. Moreover, investigation on the effect of CP on MIMO-OFDM systems was made and it has been noticed for both schemes that the BER increases as the CP length decreases.

For both STBC and SFBC scheme, similar coding has been used where symbols are coded through different OFDM symbols and different subcarriers for STBC and SFBC respectively. Moreover, in both cases, channel parameters have been assumed known at the receiver. Therefore, using known channel parameter and same type of coding; results were expected to be the same. Finally, the effect of CP on both schemes was expected as increasing CP reduces the BER due to the fact that CP length must be longer than the delay spread of the channel in order to ensure perfect equalisation.

At the early stage of research, perfect knowledge of channel parameters was assumed at the receiver which in real wireless communication system is not the case. Therefore, a new channel estimation technique for STBC/SFBC-OFDM systems is proposed in Chapter 4.

4 Joint Channel Estimation and Data Detection for STBC-OFDM

Combination of STBC with OFDM has gained considerable interest and seems to be a promising technique for future wireless communications. However, such systems require the knowledge of the Channel State Information (CSI) at the receiver. In this chapter, a new channel estimation approach is proposed using dedicated pilot subcarriers defined at fixed intervals to estimate the channel parameters. Once channel parameters at the pilot subcarriers have been estimated using known pilot symbols at the receiver, the iterative channel estimation process is initiated, and data symbols positioned at adjacent data subcarriers are recovered. Subsequently, the recovered data symbols become the new set of pilots which are then used to re-estimate the channel parameters and recover the next adjacent STBC block. The performance of the proposed method has been investigated via extensive computer simulations.

4.1 Introduction

Orthogonal Frequency Division Multiplexing (OFDM) is a technique that has attracted a lot of attention because of its ability to achieve higher data rates over wireless channels. The principal reasons behind the wide study of OFDM are its design simplicity and its distinctive ability to resist frequency selective channels. This is achieved by dividing the entire channel into many narrow parallel sub-channels which thereby reduces Inter-Symbol Interference (ISI). Combination of

Multiple Input Multiple Output (MIMO) wireless communication systems with OFDM has gained considerable interest and seems to be a promising technique for future wireless communications [14, 69, 70]. However, such systems require the knowledge of the CSI at the receiver.

CSI must be known at the receiver side in order to recover the transmitted data. Two approaches for channel estimation have been proposed in the literature. Blind channel estimation [71-73] relies on the exploitation of the statistical information of the received symbols and has the bandwidth-saving advantage. However, the blind technique is limited to slow time varying channels and has higher complexity at the receiver. On the other hand, pilot aided channel estimation uses pilot sequences sent as a preamble of each data frame and these pilot sequences are known at the receiver. Apart from the fact that the use of pilots affects the data rate [27, 29, 30, 74], this approach is simple to implement and can be applied to different types of channels. As a result, this research is mainly focused on pilot-aided channel estimation.

In the literature many techniques have been proposed to estimate the channel parameters of MIMO-OFDM systems [68, 75-77]. In such systems, a complete OFDM frame composed of training symbols is first sent in order to estimate the channel parameters. The channel is therefore assumed constant for the next set of STBC blocks until a new estimation is performed. In fast fading environments, performance degradation would arise as a result of the outdated channel estimation. As a matter of fact, estimation performed in the time domain would be more appropriate as impulse response contains fewer parameters than frequency response.

In this Chapter, a new iterative joint channel estimation technique is proposed where channel parameters at the pilot subcarriers are first estimated and used to recover data symbols at adjacent data subcarriers. Once recovered, the data symbols at adjacent subcarriers are used as new set of pilot in order to re-estimate the channel parameters and recover the successive STBC block located at the next adjacent data subcarrier. The process is then repeated until all data symbols are decoded. In addition a decoding method based on group decoding is proposed where each set of OFDM symbols is divided into groups which are decoded simultaneously. In this method, the number of groups varies according to the number of pilot subcarriers used. Once the number of groups is defined, each one of them is assigned to a pilot subcarrier. The use of groups reduces the number of computations linearly with respect to the number of pilot subcarriers used and therefore reduces the processing time at the decoder.

These algorithms have been investigated via extensive computer simulations and results have been presented for different number of transmit and receive antennas, different modulation order, different number of pilot subcarriers and different channel conditions.

4.2 STBC-OFDM Systems Architecture

A STBC-OFDM system with Mt transmit antennas and Nr receive antennas is shown in Figure 4-1.

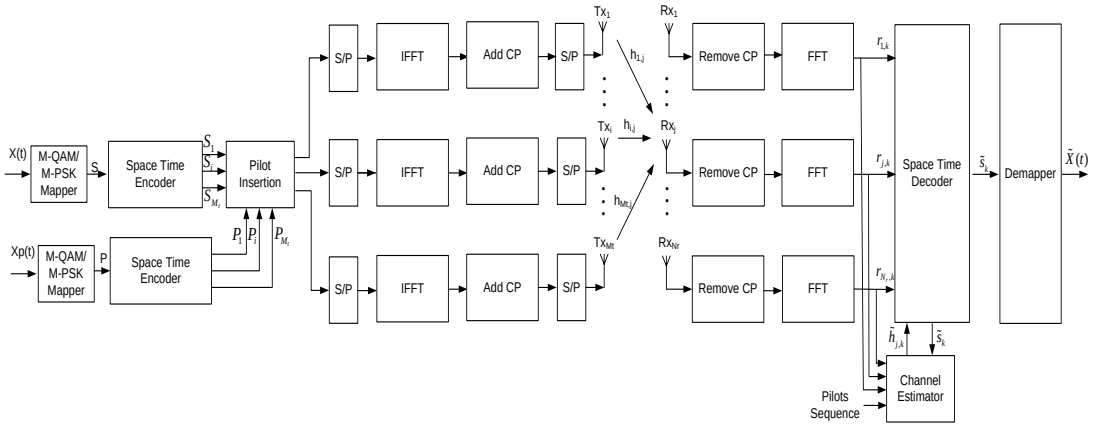

Figure 4-1: Block Diagram of the STBC-OFDM System

At time t, a modulated pilot sequence of length 2Np is scattered into a modulated data sequence of length 2Ns, where Np and Ns represent the number of pilot and data subcarriers respectively. Each block of data is then sent to the STBC-OFDM encoder where data is encoded in space, time and frequency. Finally, CP longer than the delay spread of the channel is added to each OFDM symbol and data is transmitted simultaneously from different antennas.

It is assumed that OFDM symbols are transmitted over a Rayleigh multipath channel from the *i*-th transmit antenna to the *j*-th receive antenna. Multipath Rayleigh fading channel is described in Chapter 3 Section 3.4.

At the receiver, an inverse procedure is implemented. CP is first removed and FFT operation is performed. STBC encoding offers simple decoding algorithms when channel parameters are known at the receiver. Therefore, once OFDM demodulation is applied, the received signal can be expressed as:

$$R_{j,k} = \sum_{i=1}^{Mt} S_{i,k} H_{i,j,k} + N_{i,j,k} \qquad (4.1)$$

where k=1, 2,…, Ns and $N_{j,k}$ represents the white Gaussian noise with variance per dimension, $H_{i,j,k}$ is the time varying channel tap between the *i*-th transmit antenna and the *j*-th receive antenna and $S_{i,k}$ represents the transmitted signal from the *i*-th antenna. Once decoded, data symbols are sent to the ML detector similar to the procedure in Chapter 3 Section 3.4.

4.3 Basic Principle of Pilot Design and Channel Estimation

Figure 4-2 shows the organisation of OFDM symbols and the two-step procedure undertaken by the channel estimation technique proposed in this Chapter. The first step occurs at the transmitter where a group of data subcarriers is assigned to a pilot subcarrier. The number of groups within the OFDM symbols is determined by the number of pilot subcarriers used such that $N_{group}=N_s/L_{sub/group}=N_p$ where $L_{sub/group}$ represents the length of each group and is defined as $L_{sub/group}=N_s/N_p$.

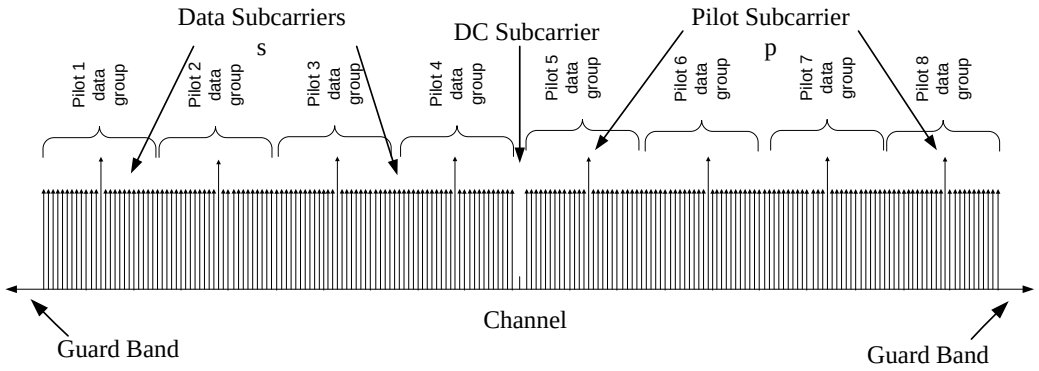

Figure 4-2: First-Step of the STBC-OFDM Channel Estimation Method

Once the number of data subcarriers per group has been determined, a pilot subcarrier is positioned in the middle of that group in order to carry out the

estimation of the channel parameter at the pilot subcarrier. Once the channel parameters at the pilot subcarrier have been estimated, the estimated channel parameter is used to initiate the iterative channel estimation process for that group at the receiver. Figure 4-2 shows 8 groups of data subcarriers with one pilot subcarrier positioned in the middle of each group but the method can be adapted to any number of pilot subcarriers, data subcarriers and any number of transmit antennas. In STBC-OFDM, one block of symbols (S_{2c}, S_{4c}, …) is transmitted through multiple OFDM symbols according to the rate of the matrix (n_t=2 and n_t=8 for S_{2c} and S_{4c} respectively). Therefore, only one pilot subcarrier per group is required to estimate the channel parameters and initiate the iterative process. For a similar number of pilot and data subcarriers, various number of transmit antennas can be used. The number of groups will remain and so will the number of data subcarriers per group because only the number of OFDM symbols required to transmit a STBC block will vary (from 2 OFDM symbols for two antennas to n_t OFDM symbols according to the rate of the STBC block).

The second step of the method occurs at the receiver side. The pilot sequence known at the receiver is used to estimate the channel parameter of the corresponding subcarriers. Then, assuming that channel parameters remain constant over n_t OFDM symbols (n_t is equal to the number of time slots required to transmit one STBC matrix) and over two adjacent subcarrier, the estimated channel parameters at the pilot subcarriers are used to recover the data symbols located at the data subcarriers adjacent to the pilot subcarriers. Once channel estimation at pilot subcarrier kp has been performed, channel parameters are used to decode adjacent data subcarriers k and k+1 as described in Figure 4-3. A pilot subcarrier has been positioned in the middle of each group in order to recover two

set of symbols at a time per group; at subcarriers k and k+1. Therefore, for two antennas in group X, s_{2k} and s_{2k+1} will be recovered for subcarrier k and s_{2k+2} and s_{2k+3} at subcarrier k+1.

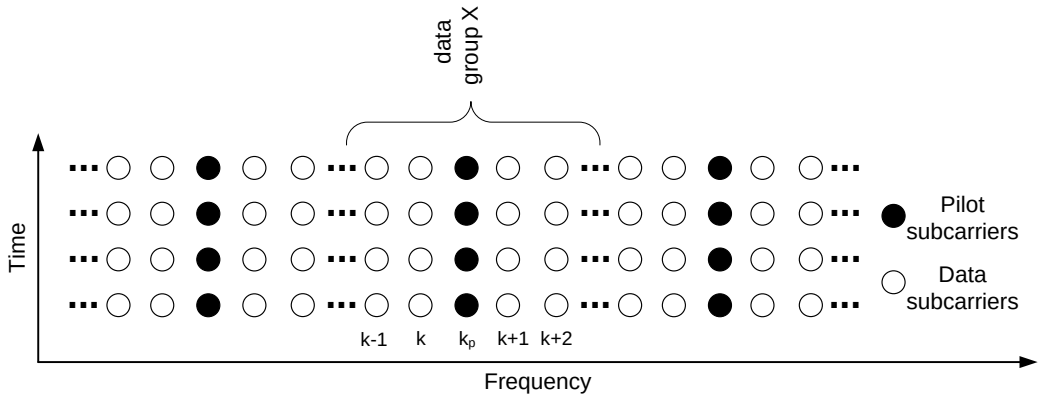

Figure 4-3: Second-Step of the Proposed Method for STBC-OFDM

Once symbols at data subcarriers adjacent to the pilot subcarriers have been recovered, the channel parameters of the corresponding subcarriers can be estimated and used to recover the next set of STBC symbols. For example, in the lower side, once symbols at subcarrier k have been recovered, channel estimation can be performed and used to recover the next adjacent data at subcarrier k-1. In a similar way, in the upper side, once data symbols at subcarrier k+1 have been recovered, channel parameters of those subcarriers can be estimated and with the assumption that channel parameters remain constant over two adjacent subcarriers, data symbols at subcarrier k+2 can be recovered. The process is then repeated in a joint iterative way to decode all the data symbols of the group. The advantages of the technique reside in the simplicity and computation efficiency due to the use of groups which increases the decoding speed as all groups are decoded simultaneously.

4.4 STBC-OFDM Systems for 2 Transmit Antennas

Assuming that the pilot sequence is known at the receiver and that channel parameters remain constant over two adjacent subcarriers and over n_t OFDM symbols, channel estimation is performed at the pilot subcarriers and used to decode adjacent data subcarriers as described in Section 4.3. In this Section, the proposed channel estimation strategy is described for subcarriers located in the lower side of the pilot subcarrier of each group but proposed equations are also simultaneously used for the upper side.

Based on (4.1), received pilot and data subcarriers signal after FFT can be expressed as:

$$\begin{aligned} \bar{R}p_j &= \sum_{j=1}^{N_r} \bar{P}\bar{H}p_j + \bar{N}p_j \\ \bar{R}_j &= \sum_{j=1}^{N_r} \bar{S}\bar{H}_j + \bar{N}_j \end{aligned} \tag{4.2}$$

where $\bar{R}p_j$ and $\bar{R}_j$ represent the received pilot and data signal at the *j*-th antenna respectively. $\bar{P}$ and $\bar{S}$ are the pilot and data signals respectively, $\bar{H}p_j$, $\bar{H}_j$ and $\bar{N}p_j$, $\bar{N}_j$ represent the channel parameters and the white Gaussian noise between the two transmit antennas and the Nr receive antennas for pilot and data signals respectively. The pilot elements of (4.2) can be expressed as:

$$\begin{aligned}
\bar{R}p_j &= \left[Rp_{j,kp}(n) \quad Rp_{j,kp}(n+1) \right]^T \\
\bar{H}p_j &= \begin{bmatrix} Hp_{1,j,kp}(n) \\ Hp_{2,j,kp}(n) \end{bmatrix} \\
\bar{P} &= \begin{bmatrix} P_{1,kp}(n) & P_{2,kp}(n) \\ -P^*_{2,kp}(n) & P^*_{1,kp}(n) \end{bmatrix}, \quad \bar{N}p_j = \begin{bmatrix} Np_{1,j,kp}(n) \\ Np_{2,j,kp}(n) \end{bmatrix}
\end{aligned} \tag{4.3}$$

where kp=0,1,…, N_p-1.While the data elements are given as:

$$\begin{aligned}
\bar{R}_j &= \left[R_{j,k}(n) \quad R_{j,k}(n+1) \right]^T \\
\bar{H}_j &= \begin{bmatrix} H_{1,j,k}(n) \\ H_{2,j,k}(n) \end{bmatrix} \\
\bar{S} &= \begin{bmatrix} S_{1,k}(n) & S_{2,k}(n) \\ -S^*_{2,k}(n) & S^*_{1,k}(n) \end{bmatrix}, \quad \bar{N}p_j = \begin{bmatrix} N_{1,j,k}(n) \\ N_{2,j,k}(n) \end{bmatrix}
\end{aligned} \tag{4.4}$$

where k=0,1,…, N_s-1.

Transmitted pilot and data signals are encoded in space, time and frequency as described in Figure 4-4. Therefore, $P_1(n)$ and $P_2(n)$ transmitted in OFDM symbol n and $P_1(n+1)$ and $P_2(n+1)$ transmitted during the second OFDM symbol n+1 can be expressed by (4.5).

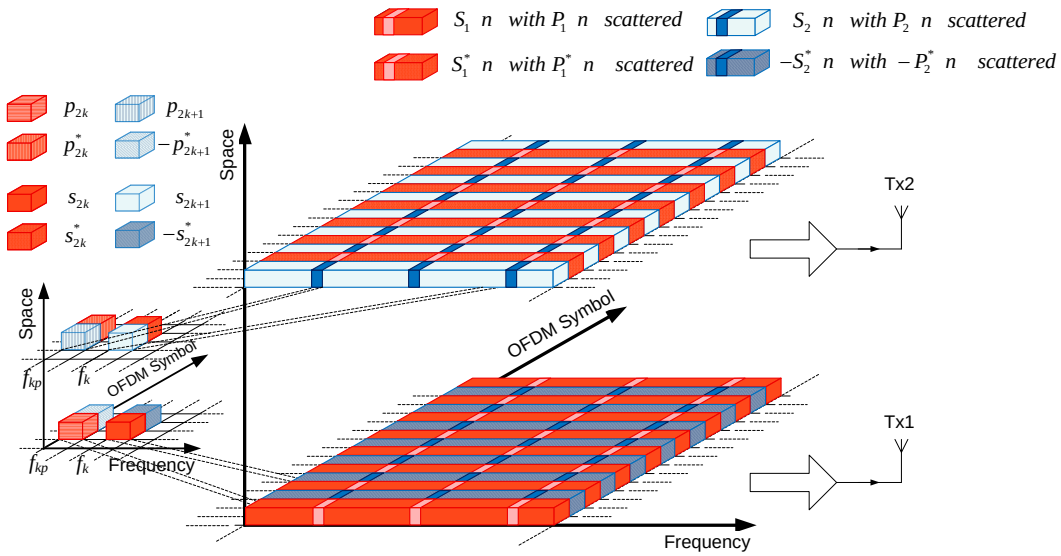

Figure 4-4: Transmitted OFDM Symbols Organisation for 2 Transmit Antennas

$$
\begin{aligned}
P_1(n) &= \left[\, p_0,\ p_2,\ \ldots,\ p_{2kp}, \ldots, p_{2Np-4},\ p_{2Np-2} \,\right]^T \\
P_2(n) &= \left[\, p_1,\ p_3,\ \ldots,\ p_{2kp+1}, \ldots, p_{2Np-3},\ p_{2Np-1} \,\right]^T \\
P_1(n+1) &= \left[\, -p_1^*,\ -p_3^*,\ \ldots, -p_{2kp+1}^*, \ldots,\ -p_{2Np-3}^*,\ p_{2Np-1}^* \,\right]^T = -P_2^*(n) \\
P_2(n+1) &= \left[\, p_0^*,\ p_2^*,\ \ldots,\ p_{2kp}^*,\ \ldots,\ p_{2Np-4}^*,\ p_{2Np-2}^* \,\right]^T = P_1^*(n) \\
S_1(n) &= \left[\, s_0,\ s_2,\ \ldots,\ s_{2k}, \ldots, s_{2Ns-4}, s_{2Ns-2} \,\right]^T \\
S_2(n) &= \left[\, s_1,\ s_3,\ \ldots,\ s_{2k+1}, \ldots, s_{2Ns-3},\ s_{2Ns-1} \,\right]^T \\
S_1(n+1) &= \left[\, -s_1^*,\ -s_3^*,\ \ldots, -s_{2k+1}^*, \ldots,\ -s_{2Ns-3}^*, s_{2Ns-1}^* \,\right]^T = -S_2^*(n) \\
S_2(n+1) &= \left[\, s_0^*,\ s_2^*,\ \ldots,\ s_{2k}^*,\ \ldots,\ s_{2Ns-4}^*,\ s_{2Ns-2}^* \,\right]^T = S_1^*(n)
\end{aligned}
\tag{4.5}
$$

The received vector Rp_j and R_j at OFDM symbols n and n+1 can be expressed as:

$$
\begin{aligned}
Rp_j(n) &= [\, rp_{j,0},\ rp_{j,2},\ \ldots,\ rp_{j,2Np-4},\ rp_{j,2Np-2} \,]^T \\
Rp_j(n+1) &= [\, rp_{j,1},\ rp_{j,3},\ \ldots,\ rp_{j,2Np-3},\ rp_{j,2Np-1} \,]^T \\
R_j(n) &= [\, r_{j,0},\ r_{j,2},\ \ldots,\ r_{j,2Ns-4},\ r_{j,2Ns-2} \,]^T \\
R_j(n+1) &= [\, r_{j,1},\ r_{j,3},\ \ldots,\ r_{j,2Ns-3},\ r_{j,2Ns-1} \,]^T
\end{aligned}
\tag{4.6}
$$

At the receiver side, as stated in Section 4.3, channel parameters of two consecutive OFDM symbols are assumed constant therefore $\tilde{H}p_{i,j,kp}(n) = \tilde{H}p_{i,j,kp}(n+1)$ and the receiver uses the pilot sequence in (4.2) to estimate the channel coefficients using the minimum mean square error (MMSE) as in (4.7).

$$\tilde{H}p_j = \begin{bmatrix} \tilde{H}p_{1,j,kp}(n) \\ \tilde{H}p_{2,j,kp}(n) \end{bmatrix} = \begin{bmatrix} \tilde{H}p_{1,j,kp}(n+1) \\ \tilde{H}p_{2,j,kp}(n+1) \end{bmatrix} = \bar{P}^{-1}\bar{R}p_j = \begin{bmatrix} \dfrac{rp_{j,2kp}p^*_{2kp} - rp_{j,2kp+1}p_{2kp+1}}{|p_{2kp}|^2 + |p_{2kp+1}|^2} \\ \dfrac{rp_{j,2kp}p^*_{2kp+1} + rp_{j,2kp+1}p_{2kp}}{|p_{2kp}|^2 + |p_{2kp+1}|^2} \end{bmatrix} \quad (4.7)$$

Once channel parameters are evaluated, the receiver can detect the upper and lower data symbols of the adjacent data subcarrier. Using $\tilde{H}p_j$ in (4.7) and $\bar{R}_j$ in (4.4), the receiver constructs a new channel matrix $\ddot{H}p_j$ and a new receive matrix $\ddot{R}_j$ given as:

$$\ddot{H}p_j = \begin{bmatrix} \tilde{H}p^*_{1,j,kp} & \tilde{H}p_{2,j,kp} \\ \tilde{H}p^*_{2,j,kp} & -\tilde{H}p_{1,j,kp} \end{bmatrix}$$
$$\ddot{R}_j = \begin{bmatrix} R_{j,k}(n) & R^*_{j,k}(n+1) \end{bmatrix}^T \quad (4.8)$$

The receiver uses the constructed channel matrix $\ddot{H}p_j$ and the constructed received data vector $\ddot{R}_j$ for the combining scheme. Assuming that channel parameters of two adjacent subcarriers and two consecutive OFDM symbols remain constant $\tilde{H}p_{i,j,kp}(n) = \tilde{H}_{i,j,k}(n) = \tilde{H}_{i,j,k}(n+1)$, the combined signals can be expressed as:

$$\tilde{S} = \begin{bmatrix} \tilde{s}_{2k} \\ \tilde{s}_{2k+1} \end{bmatrix} = \sum_{j=1}^{N_r} \ddot{H}p_j \ddot{R}_j = \begin{bmatrix} \sum_{j=1}^{N_r} (\tilde{h}p^*_{1,j,kp} r_{j,2k} + \tilde{h}p_{2,j,kp} r^*_{j,2k+1}) \\ \sum_{j=1}^{N_r} (\tilde{h}p^*_{2,j,kp} r_{j,2k} - \tilde{h}p_{1,j,kp} r^*_{j,2k+1}) \end{bmatrix} \quad (4.9)$$

Once the data signals that are adjacent to the pilot subcarriers have been recovered, the process is repeated for adjacent lower and upper data subcarriers using the recovered data symbols $\tilde{s}_{2k}$, $\tilde{s}_{2k+1}$ and $\tilde{s}_{2k+2}$, $\tilde{s}_{2k+3}$ as the new pilot sequence. Therefore, the first pair of decoded data and become the pilot sequence and to be used to recover the data and in the next iteration. Similarly, the second pair of decoded data and become the pilot sequence and to be used to recover the data and in the next iteration. In other words, each pair of decoded symbols yield a pair of pilot sequence each, this pilot sequence is then used in the next iteration to recover the adjacent pair of symbols. The iterative joint process is repeated until all the data of the group have been recovered. Each group is decoded simultaneously which, when compared with classic decoding where only one set of data is decoded at a time, leads to a decoding speed which increases linearly with the number of pilots subcarriers used.

From the above derivations, it can be seen that the proposed iterative channel estimation technique does not require any matrix inversion, which enhances the simplicity of the system and therefore reduces the cost without affecting the performance.

4.5 STBC-OFDM Systems for 4 Transmit Antennas

In this Section, the iterative joint channel estimation technique and data detection for four transmit antennas and Nr receive antennas is described. Similar assumptions like that of Section 4.4 are made, however, instead of assuming that channel parameters are constant over 2 OFDM symbols, in this section, channel parameters are assumed constant over 8 OFDM symbols due to the use of matrix S_{4c} which requires 8 time slots to be fully transmitted [37]. Following Section 4.4, the received signal can be expressed as:

$$\begin{aligned} \bar{R}p_j &= \sum_{j=1}^{N_r} \bar{P}\bar{H}p_j + \bar{N}p_j \\ \bar{R}_j &= \sum_{j=1}^{N_r} \bar{S}\bar{H}_j + \bar{N}_j \end{aligned} \tag{4.10}$$

where $\bar{R}p_j$, $\bar{R}_j$ and $\bar{P}$, $\bar{S}$ represent the received pilot and data signals, and the transmitted pilot and data signals respectively. Also, $\bar{H}p_j$, $\bar{H}_j$ and $\bar{N}p_j$, $\bar{N}_j$ represent the channel parameters and the white Gaussian noise for pilot and data signals respectively. Pilot and data elements of (4.10) are given in (4.11) and (4.12) respectively.

$$\bar{R}p_j = \begin{bmatrix} Rp_{j,kp}(n) \\ Rp_{j,kp}(n+1) \\ Rp_{j,kp}(n+2) \\ Rp_{j,kp}(n+3) \\ Rp_{j,kp}(n+4) \\ Rp_{j,kp}(n+5) \\ Rp_{j,kp}(n+6) \\ Rp_{j,kp}(n+7) \end{bmatrix}, \bar{H}p_j = \begin{bmatrix} Hp_{1,j,kp}(n) \\ Hp_{2,j,kp}(n) \\ Hp_{3,j,kp}(n) \\ Hp_{4,j,kp}(n) \end{bmatrix}, \bar{N}p_j = \begin{bmatrix} Np_{1,j,kp}(n) \\ Np_{2,j,kp}(n) \\ Np_{3,j,kp}(n) \\ Np_{4,j,kp}(n) \\ Np_{5,j,kp}(n) \\ Np_{6,j,kp}(n) \\ Np_{7,j,kp}(n) \\ Np_{8,j,kp}(n) \end{bmatrix}$$

$$\bar{P} = \begin{bmatrix} P_{1,kp}(n) & P_{2,kp}(n) & P_{3,kp}(n) & P_{4,kp}(n) \\ -P_{2,kp}(n) & P_{1,kp}(n) & -P_{4,kp}(n) & P_{3,kp}(n) \\ -P_{3,kp}(n) & P_{4,kp}(n) & P_{1,kp}(n) & -P_{2,kp}(n) \\ -P_{4,kp}(n) & -P_{3,kp}(n) & P_{2,kp}(n) & P_{1,kp}(n) \\ P^*_{1,kp}(n) & P^*_{2,kp}(n) & P^*_{3,kp}(n) & P^*_{4,kp}(n) \\ -P^*_{2,kp}(n) & P^*_{1,kp}(n) & -P^*_{4,kp}(n) & P^*_{3,kp}(n) \\ -P^*_{3,kp}(n) & P^*_{4,kp}(n) & P^*_{1,kp}(n) & -P^*_{2,kp}(n) \\ -P^*_{4,kp}(n) & -P^*_{3,kp}(n) & P^*_{2,kp}(n) & P^*_{1,kp}(n) \end{bmatrix} \quad (4.11)$$

$$\bar{R}_j = \begin{bmatrix} R_{j,k}(n) \\ R_{j,k}(n+1) \\ R_{j,k}(n+2) \\ R_{j,k}(n+3) \\ R_{j,k}(n+4) \\ R_{j,k}(n+5) \\ R_{j,k}(n+6) \\ R_{j,k}(n+7) \end{bmatrix}, \bar{H}_j = \begin{bmatrix} H_{1,j,k}(n) \\ H_{2,j,k}(n) \\ H_{3,j,k}(n) \\ H_{4,j,k}(n) \end{bmatrix}, \bar{N}_j = \begin{bmatrix} N_{1,j,k}(n) \\ N_{2,j,k}(n) \\ N_{3,j,k}(n) \\ N_{4,j,k}(n) \\ N_{5,j,k}(n) \\ N_{6,j,k}(n) \\ N_{7,j,k}(n) \\ N_{8,j,k}(n) \end{bmatrix}$$

$$\bar{S} = \begin{bmatrix} S_{1,k}(n) & S_{2,k}(n) & S_{3,k}(n) & S_{4,k}(n) \\ -S_{2,k}(n) & S_{1,k}(n) & -S_{4,k}(n) & S_{3,k}(n) \\ -S_{3,k}(n) & S_{4,k}(n) & S_{1,k}(n) & -S_{2,k}(n) \\ -S_{4,k}(n) & -S_{3,k}(n) & S_{2,k}(n) & S_{1,k}(n) \\ S^*_{1,k}(n) & S^*_{2,k}(n) & S^*_{3,k}(n) & S^*_{4,k}(n) \\ -S^*_{2,k}(n) & S^*_{1,k}(n) & -S^*_{4,k}(n) & S^*_{3,k}(n) \\ -S^*_{3,k}(n) & S^*_{4,k}(n) & S^*_{1,k}(n) & -S^*_{2,k}(n) \\ -S^*_{4,k}(n) & -S^*_{3,k}(n) & S^*_{2,k}(n) & S^*_{1,k}(n) \end{bmatrix} \quad (4.12)$$

where $P_{i,kp}(n)$ and $S_{i,k}(n)$ represent the pilot and data symbols encoded through space, time and frequency as defined in (4.13) and (4.14) respectively. Figure 4-5 shows the organisation of the pilot and data symbols.

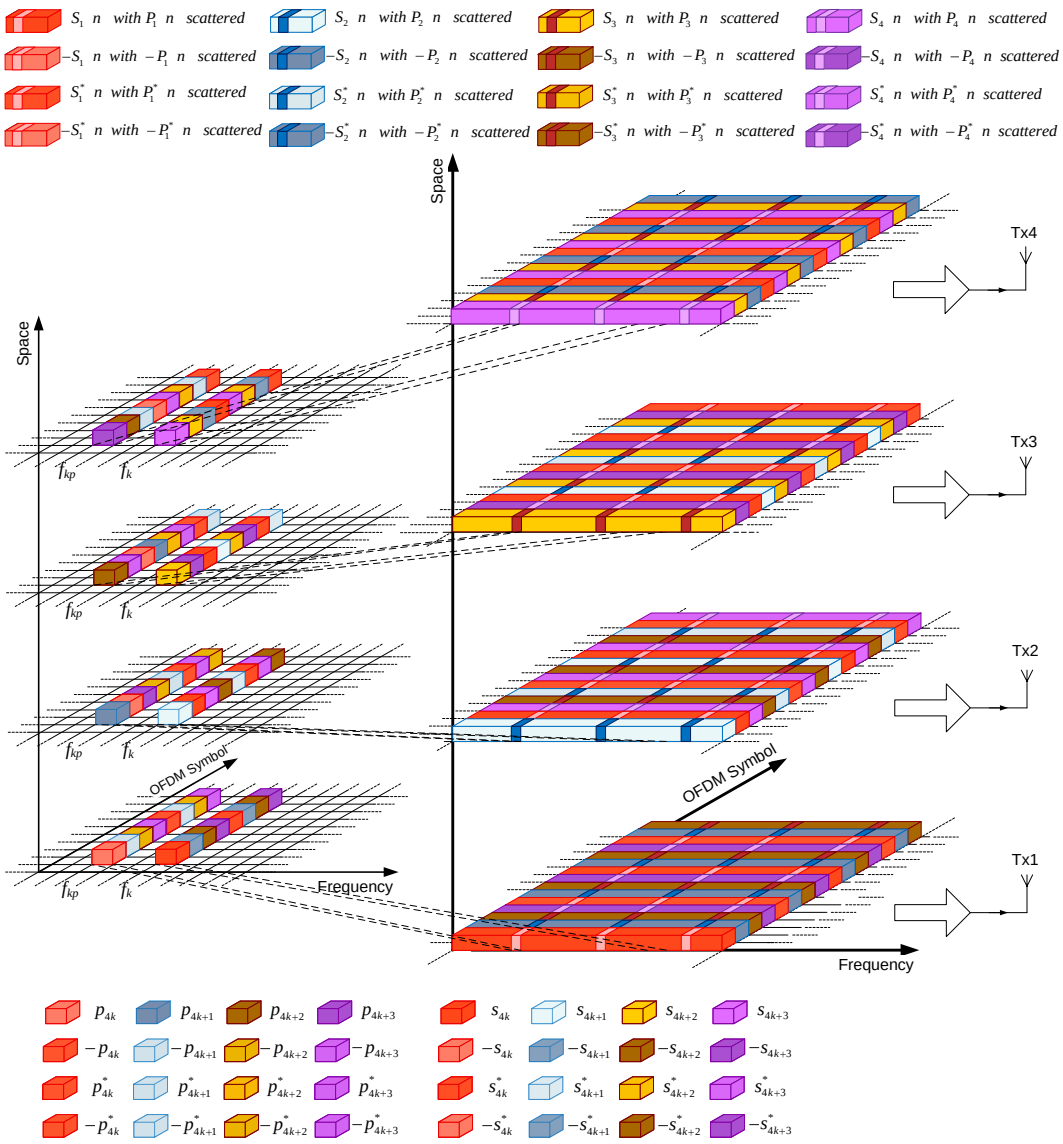

Figure 4-5: Organisation of the Pilot and Data Sequence for 4 Transmit Antennas

$$P_1(n) = \left[\, p_0,\ p_4,\ \ldots,\ p_{4kp}, \ldots, p_{4Np-8},\ p_{4Np-4} \,\right]^T$$
$$P_2(n) = \left[\, p_1,\ p_5,\ \ldots,\ p_{4kp+1}, \ldots, p_{4Np-7},\ p_{4Np-3} \,\right]^T$$
$$P_3(n) = \left[\, p_2,\ p_6,\ \ldots,\ p_{4kp+2}, \ldots, p_{4Np-6},\ p_{4Np-2} \,\right]^T$$
$$P_4(n) = \left[\, p_3,\ p_7,\ \ldots,\ p_{4kp+3}, \ldots, p_{4Np-5},\ p_{4Np-1} \,\right]^T$$
$$P_1(n+1) = -P_2(n);\ \ P_2(n+1) = P_1(n);\qquad P_3(n+1) = -P_4(n);\ P_4(n+1) = P_3(n);$$
$$P_1(n+2) = -P_3(n);\ P_2(n+2) = P_4(n);\qquad P_3(n+2) = P_1(n);\ \ P_4(n+2) = -P_2(n); \quad (4.13)$$
$$P_1(n+3) = -P_4(n);\ P_2(n+3) = -P_3(n);\ \ P_3(n+3) = P_2(n);\ \ P_4(n+3) = P_1(n);$$
$$P_1(n+4) = P_1^*(n);\ \ P_2(n+4) = P_2^*(n);\qquad P_3(n+4) = P_3^*(n);\ \ P_4(n+4) = P_4^*(n);$$
$$P_1(n+5) = -P_2^*(n);\ P_2(n+5) = P_1^*(n);\qquad P_3(n+5) = -P_4^*(n);\ P_4(n+5) = P_3^*(n);$$
$$P_1(n+6) = -P_3^*(n);\ P_2(n+6) = P_4^*(n);\ \ P_3(n+6) = P_1^*(n);\ \ P_4(n+6) = -P_2^*(n);$$
$$P_1(n+7) = -P_4^*(n);\ P_2(n+7) = -P_3^*(n);\ P_3(n+7) = P_2^*(n);\ \ P_4(n+7) = P_1^*(n);$$

$$S_1(n) = \left[\, s_0,\ s_4,\ \ldots,\ s_{4k}, \ldots, s_{4Ns-8},\ s_{4Ns-4} \,\right]^T$$
$$S_2(n) = \left[\, s_1,\ s_5,\ \ldots,\ s_{4k+1}, \ldots, s_{4Ns-7},\ s_{4Ns-3} \,\right]^T$$
$$S_3(n) = \left[\, s_2,\ s_6,\ \ldots,\ s_{4k+2}, \ldots, s_{4Ns-6},\ s_{4Ns-2} \,\right]^T$$
$$S_4(n) = \left[\, s_3,\ s_7,\ \ldots,\ s_{4k+3}, \ldots, s_{4Ns-5},\ s_{4Ns-1} \,\right]^T$$
$$S_1(n+1) = -S_2(n);\ S_2(n+1) = S_1(n);\qquad S_3(n+1) = -S_4(n);\ S_4(n+1) = S_3(n);$$
$$S_1(n+2) = -S_3(n);\ S_2(n+2) = S_4(n);\ \ S_3(n+2) = S_1(n);\ \ S_4(n+2) = -S_2(n); \quad (4.14)$$
$$S_1(n+3) = -S_4(n);\ S_2(n+3) = -S_3(n);\ S_3(n+3) = S_2(n);\ \ S_4(n+3) = S_1(n);$$
$$S_1(n+4) = S_1^*(n);\ \ S_2(n+5) = S_2^*(n);\ \ S_3(n+4) = S_3^*(n);\ S_4(n+4) = S_4^*(n);$$
$$S_1(n+5) = -S_2^*(n);\ S_2(n+6) = S_1^*(n);\ \ S_3(n+5) = -S_4^*(n);\ S_4(n+5) = S_3^*(n);$$
$$S_1(n+6) = -S_3^*(n);\ S_2(n+7) = S_4^*(n);\ \ S_3(n+6) = S_1^*(n);\ \ S_4(n+6) = -S_2^*(n);$$
$$S_1(n+7) = -S_4^*(n);\ S_2(n+8) = -S_3^*(n);\ S_3(n+7) = S_2^*(n);\ S_4(n+7) = S_1^*(n);$$

where kp=0, 1, …, Np-1 and k=0, 1, …, Ns-1.

As mentioned for two transmit antennas, the proposed channel estimation technique first focuses on the estimation of the channel at the pilot subcarriers. It then uses this estimation to initiate the joint iterative process. Under the assumption that the fade remains constant over 2 adjacent subcarriers, adjacent data symbols are decoded and used to generate new channel estimation in order to

decode the next set of STBC coded symbols. The process is then repeated until all the data blocks of the group are decoded. Due to the fact that all the groups are decoded simultaneously, 8 data symbols multiplied by 2 STBC block are decoded simultaneously per group.

Pilot sequence is known at the receiver and following the description given for two transmit antennas, channel parameters can be assumed constant over 8 OFDM symbols therefore $hp_{i,j,kp}(n)=hp_{i,j,kp}(n+x)$, with x=1, 2, …, 8 as 8 time slots are required to transmit the matrix S_{4c}. Thus with the help of (4.10), (4.11) and (4.13), the following channel estimation equations can be derived:

$$\tilde{\mathrm{H}}\mathrm{p}_{\mathrm{j}} = \begin{bmatrix} \tilde{\mathrm{H}}\mathrm{p}_{1,\mathrm{j},\mathrm{kp}} \\ \tilde{\mathrm{H}}\mathrm{p}_{2,\mathrm{j},\mathrm{kp}} \\ \tilde{\mathrm{H}}\mathrm{p}_{3,\mathrm{j},\mathrm{kp}} \\ \tilde{\mathrm{H}}\mathrm{p}_{4,\mathrm{j},\mathrm{kp}} \end{bmatrix} = \bar{\mathrm{P}}^{\mathrm{H}}\bar{\mathrm{P}}^{-1}\bar{\mathrm{P}}\bar{\mathrm{R}}\mathrm{p}_{\mathrm{j}} = \frac{1}{2\sum_{\mathrm{x}=\mathrm{kp}}^{\mathrm{kp}+4}\left|\mathrm{P}_{\mathrm{j,x}}(\mathrm{n})\right|^{2}}\bar{\mathrm{P}}^{\mathrm{H}}\bar{\mathrm{R}}\mathrm{p}_{\mathrm{j}} \tag{4.15}$$

where the superscript H represents the Hermitian operation which is the transpose and conjugate operation. After estimating the channel coefficient vector as in (4.15), the receiver then uses it to construct the channel matrix $\ddot{\mathrm{H}}\mathrm{p}_{\mathrm{j}}$ such that:

$$\ddot{\mathrm{H}}\mathrm{p}_{\mathrm{j}} = \begin{bmatrix} \tilde{\mathrm{H}}\mathrm{p}^{*}_{1,\mathrm{j},\mathrm{kp}} & \tilde{\mathrm{H}}\mathrm{p}^{*}_{2,\mathrm{j},\mathrm{kp}} & \tilde{\mathrm{H}}\mathrm{p}^{*}_{3,\mathrm{j},\mathrm{kp}} & \tilde{\mathrm{H}}\mathrm{p}^{*}_{4,\mathrm{j},\mathrm{kp}} & \tilde{\mathrm{H}}\mathrm{p}_{1,\mathrm{j},\mathrm{kp}} & \tilde{\mathrm{H}}\mathrm{p}_{2,\mathrm{j},\mathrm{kp}} & \tilde{\mathrm{H}}\mathrm{p}_{3,\mathrm{j},\mathrm{kp}} & \tilde{\mathrm{H}}\mathrm{p}_{4,\mathrm{j},\mathrm{kp}} \\ \tilde{\mathrm{H}}\mathrm{p}^{*}_{2,\mathrm{j},\mathrm{kp}} & -\tilde{\mathrm{H}}\mathrm{p}^{*}_{1,\mathrm{j},\mathrm{kp}} & -\tilde{\mathrm{H}}\mathrm{p}^{*}_{4,\mathrm{j},\mathrm{kp}} & \tilde{\mathrm{H}}\mathrm{p}^{*}_{3,\mathrm{j},\mathrm{kp}} & \tilde{\mathrm{H}}\mathrm{p}_{2,\mathrm{j},\mathrm{kp}} & -\tilde{\mathrm{H}}\mathrm{p}_{1,\mathrm{j},\mathrm{kp}} & -\tilde{\mathrm{H}}\mathrm{p}_{4,\mathrm{j},\mathrm{kp}} & \tilde{\mathrm{H}}\mathrm{p}_{3,\mathrm{j},\mathrm{kp}} \\ \tilde{\mathrm{H}}\mathrm{p}^{*}_{3,\mathrm{j},\mathrm{kp}} & \tilde{\mathrm{H}}\mathrm{p}^{*}_{4,\mathrm{j},\mathrm{kp}} & -\tilde{\mathrm{H}}\mathrm{p}^{*}_{1,\mathrm{j},\mathrm{kp}} & -\tilde{\mathrm{H}}\mathrm{p}^{*}_{2,\mathrm{j},\mathrm{kp}} & \tilde{\mathrm{H}}\mathrm{p}_{3,\mathrm{j},\mathrm{kp}} & \tilde{\mathrm{H}}\mathrm{p}_{4,\mathrm{j},\mathrm{kp}} & -\tilde{\mathrm{H}}\mathrm{p}_{1,\mathrm{j},\mathrm{kp}} & -\tilde{\mathrm{H}}\mathrm{p}_{2,\mathrm{j},\mathrm{kp}} \\ \tilde{\mathrm{H}}\mathrm{p}^{*}_{4,\mathrm{j},\mathrm{kp}} & -\tilde{\mathrm{H}}\mathrm{p}^{*}_{3,\mathrm{j},\mathrm{kp}} & \tilde{\mathrm{H}}\mathrm{p}^{*}_{2,\mathrm{j},\mathrm{kp}} & -\tilde{\mathrm{H}}\mathrm{p}^{*}_{1,\mathrm{j},\mathrm{kp}} & \tilde{\mathrm{H}}\mathrm{p}_{4,\mathrm{j},\mathrm{kp}} & -\tilde{\mathrm{H}}\mathrm{p}_{3,\mathrm{j},\mathrm{kp}} & \tilde{\mathrm{H}}\mathrm{p}_{2,\mathrm{j},\mathrm{kp}} & -\tilde{\mathrm{H}}\mathrm{p}_{1,\mathrm{j},\mathrm{kp}} \end{bmatrix} \tag{4.16}$$

The receiver also constructs the vector $\ddot{\mathrm{R}}_{\mathrm{j}}$ from the data equation (4.10) and can be expressed as:

$$\begin{aligned} \ddot{\mathrm{R}}_{\mathrm{j}} = [&\mathrm{R}_{\mathrm{j,k}}(\mathrm{n}) \quad \mathrm{R}_{\mathrm{j,k}}(\mathrm{n}+1) \quad \mathrm{R}_{\mathrm{j,k}}(\mathrm{n}+2) \quad \mathrm{R}_{\mathrm{j,k}}(\mathrm{n}+3) \\ &\mathrm{R}^{*}_{\mathrm{j,k}}(\mathrm{n}+4) \quad \mathrm{R}^{*}_{\mathrm{j,k}}(\mathrm{n}+5) \quad \mathrm{R}^{*}_{\mathrm{j,k}}(\mathrm{n}+6) \quad \mathrm{R}^{*}_{\mathrm{j,k}}(\mathrm{n}+7)]^{\mathrm{T}} \end{aligned} \tag{4.17}$$

The receiver uses the constructed matrix $\ddot{H}p_j$ and the constructed vector $\ddot{R}_j$ for the combining purposes. Assuming that channel parameters remain constant over two adjacent subcarrier, $\ddot{H}p_j = \ddot{H}_j$, the combined scheme can be expressed by:

$$\tilde{S} = \begin{bmatrix} \tilde{s}_{4k} \\ \tilde{s}_{4k+1} \\ \tilde{s}_{4k+2} \\ \tilde{s}_{4k+3} \end{bmatrix} = \sum_{j=1}^{N_r} \ddot{H}p_j \ddot{R}_j \tag{4.18}$$

where $\tilde{s}_{4k}$, $\tilde{s}_{4k+1}$, $\tilde{s}_{4k+2}$ and $\tilde{s}_{4k+3}$ can be derived as:

$$\begin{aligned}
\tilde{s}_{4k} &= \sum_{j=1}^{N_r} (\tilde{h}^*_{1,j,k} r_{j,4k} + \tilde{h}^*_{2,j,k} r_{j,4k+1} + \tilde{h}^*_{3,j,k} r_{j,4k+2} + \tilde{h}^*_{4,j,k} r_{j,4k+3} + \\
&\qquad \tilde{h}_{1,j,k} r^*_{j,4k+4} + \tilde{h}_{2,j,k} r^*_{j,4k+5} + \tilde{h}_{3,j,k} r^*_{j,4k+6} + \tilde{h}_{4,j,k} r^*_{j,4k+7}) \\
\tilde{s}_{4k+1} &= \sum_{j=1}^{N_r} (\tilde{h}^*_{2,j,k} r_{j,4k} - \tilde{h}^*_{1,j,k} r_{j,4k+1} - \tilde{h}^*_{4,j,k} r_{j,4k+2} + \tilde{h}^*_{3,j,k} r_{j,4k+3} + \\
&\qquad \tilde{h}_{2,j,k} r^*_{j,4k+4} - \tilde{h}_{1,j,k} r^*_{j,4k+5} - \tilde{h}_{4,j,k} r^*_{j,4k+6} + \tilde{h}_{3,j,k} r^*_{j,4k+7}) \\
\tilde{s}_{4k+2} &= \sum_{j=1}^{N_r} (\tilde{h}^*_{3,j,k} r_{j,4k} + \tilde{h}^*_{4,j,k} r_{j,4k+1} - \tilde{h}^*_{1,j,k} r_{j,4k+2} - \tilde{h}^*_{2,j,k} r_{j,4k+3} + \\
&\qquad \tilde{h}_{3,j,k} r^*_{j,4k+4} + \tilde{h}_{4,j,k} r^*_{j,4k+5} - \tilde{h}_{1,j,k} r^*_{j,4k+6} - \tilde{h}_{2,j,k} r^*_{j,4k+7}) \\
\tilde{s}_{4k+3} &= \sum_{j=1}^{N_r} (\tilde{h}^*_{4,j,k} r_{j,4k} - \tilde{h}^*_{3,j,k} r_{j,4k+1} + \tilde{h}^*_{2,j,k} r_{j,4k+2} - \tilde{h}^*_{1,j,k} r_{j,4k+3} + \\
&\qquad \tilde{h}_{4,j,k} r^*_{j,4k+4} - \tilde{h}_{3,j,k} r^*_{j,4k+5} + \tilde{h}_{2,j,k} r^*_{j,4k+6} - \tilde{h}_{1,j,k} r^*_{j,4k+7})
\end{aligned} \tag{4.19}$$

The new combined signals are then sent to the maximum-likelihood detector to detect $S_{1,k}(n), S_{2,k}(n), S_{3,k}(n)$ and $S_{4,k}(n)$. The receiver saves the received user data vector as the new pilot sequence and uses (4.15) to re-estimate the channel parameters but this time at subcarrier k and k+1 simultaneously. Then, the estimation is in a similar process used to recover data symbols at subcarrier k-1 and k+2. Once these sets of symbols are decoded, they will be used as the next

set of pilots. This process is repeated simultaneously for each group until all data symbols have been decoded.

4.6 Simulation Results

The performance of the proposed iterative channel estimation technique has been evaluated according to the specifications described in the WiMax standard for fixed wireless communications [78]. Simulations were realized for two and four transmit antennas and one and two receive antennas. Moreover, the method has been tested using different number of pilot subcarriers, different channel environments and different modulation orders.

QAM modulation with index 16 and 64 have been employed for the simulation scenario as well as M_t=2, 4 and N_r=1, 2. The system has a 3.5 MHz channel bandwidth and a carrier frequency of 2.5GHz. Specific simulation parameters are presented in Table 4-1.

Allocation of the subcarriers of the OFDM frame is made according to the IEEE802.16e (WiMax) standard [78]; indices of -128~-101 and 101~127 are reserved for guard interval, 0 is for the DC subcarrier, -100~-1 and 1~100 are defined as the chosen subcarriers in which -88, -63, -38, -13, 13, 38, 63 and 88 are pilot subcarriers and the remaining are specified as data subcarriers.

Table 4-1: Simulation Parameters for STBC-OFDM Systems

FFT Size (Nfft)	256
Number of Active Subcarriers (N_{used})	200 (192 for data, 8 for pilot)
Number of Guard Subcarriers	28 low, 27 high
Channel Bandwidth	3.5MHz
Sampling Rate (Fs)	2.28MHz (n=57/50)
Distance between Adjacent Subcarrier (Δf)	8.9kHz
Useful Symbol Duration (T_b)	0.112ms
Guard Time (T_g)	28.07μs
Total Symbol Duration (T_s)	140 μs
Cyclic Prefix length (CP)	1/4
Modulation	BPSK, 16 QAM, 64QAM
SUI	1,3
Transmit Antenna	2, 4
Receive Antenna	1, 2

Figure 4-6 and Figure 4-7 show simulation results of the proposed channel estimation technique for 2 and 4 transmit antennas with one and two receive antennas for different number of pilot subcarriers and different modulation orders. The results illustrate the performance for both the proposed method, and the ideal case where channel state information (CSI) is known at the receiver.

Simulations have been conducted under Stanford University Interim (SUI) channel model 1 as defined in [79]. In the results, the performance of the proposed channel estimation technique is compared with the performance of the perfect CSI case where channel parameters are known at the receiver.

The simulation results for 2 and 4 transmit antennas and 1 and 2 receive antennas show that the proposed channel estimation technique experiences 4-8dB degradation compared to the case where channel parameters are known at the receiver. The STBC-OFDM system has also been tested using different number of pilot subcarriers. From the simulation results, it can be noticed that as the number of pilot subcarriers increase, the performance of the proposed method tends towards the case where channel parameters are known at the receiver. Thus, from the simulation results, performance has been improved by 1 to 3dB by increasing the number of pilot subcarriers from 8 to 24. Performance of the STBC-OFDM system for different number of pilot subcarriers has been obtained by keeping the number of data subcarriers fixed at 192 and by reducing the guard interval according to the number of pilots required. Despite the fact that system performance improves when more pilot sub-carriers are utilized, the use of higher number of pilot subcarriers is bandwidth inefficient.

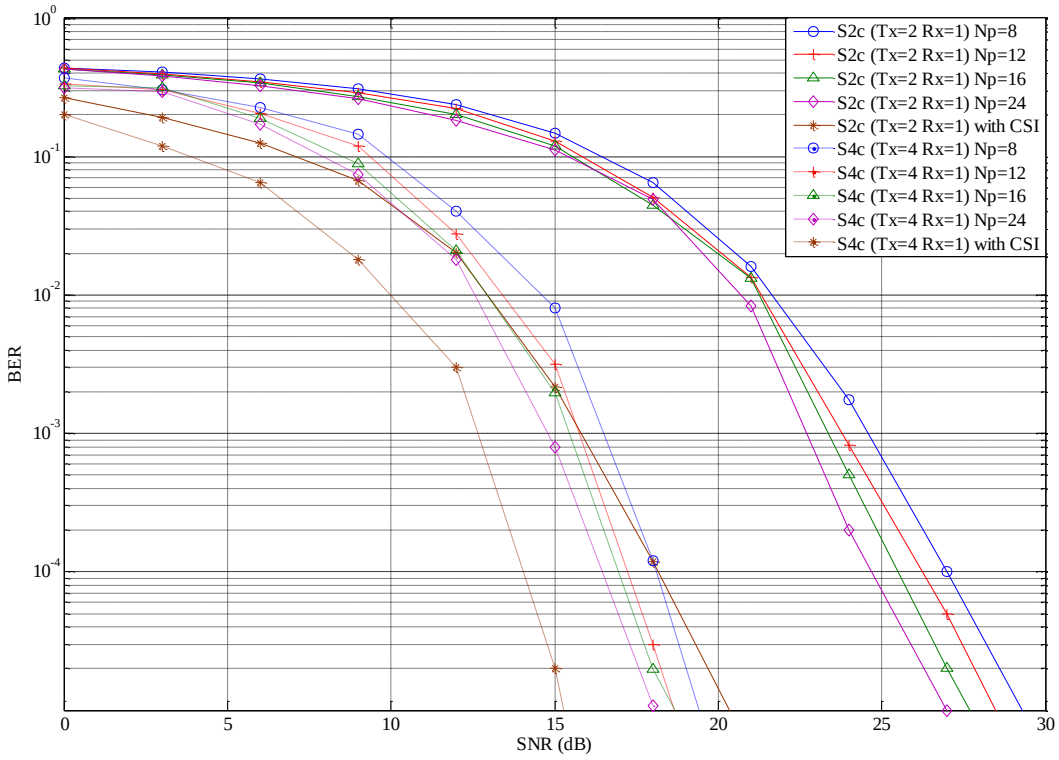

Figure 4-6: Simulation Results for 2 and 4 Transmit Antennas with 1 Receive Antennas with 16QAM under SUI1

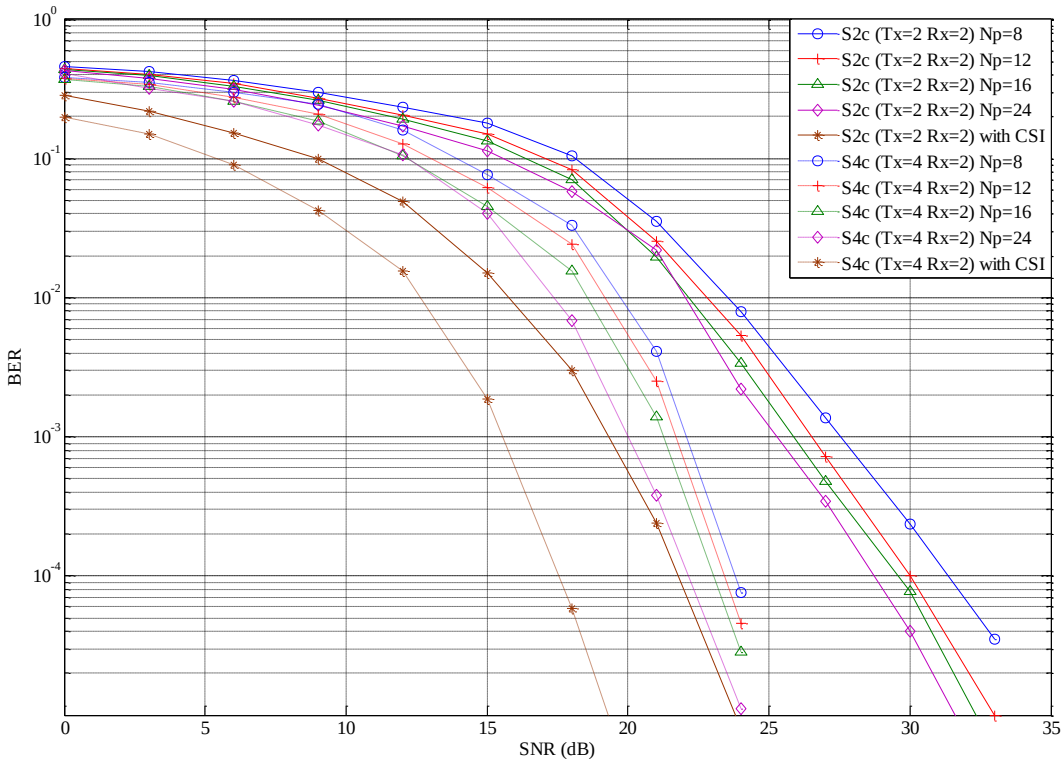

Figure 4-7: Simulation Results for 2 and 4 Transmit Antennas with 2 Receive Antennas with 64QAM under SUI1

BER can also be improved by using different modulation orders for pilot and data subcarriers. In contrast to most proposed work where the modulation order utilized by the pilot sequence is fixed, in this work, we have considered two types of modulation orders for the pilot sequence. Throughout the analysis in this part, 16QAM and 64QAM modulation are used for the data subcarriers while the pilot subcarriers utilize either BPSK, 16QAM or 64QAM modulation. For example in Figure 4-8, for two transmit antennas and one receive antenna, BPSK denotes the modulation order for the pilot symbols and 16QAM denotes the modulation order for the data symbols (BPSK/16QAM).

From this, it has been observed from Figure 4-8 to Figure 4-11, that when the pilot subcarriers are modulated using a lower modulation order than that used by the data subcarriers, channel estimation is more accurate. It is also observed that this approach results in a better BER performance for the same SNR when compared to the case where the modulation order for both pilot and data subcarriers is the same. Thus, from the results, it is evident that in contrast to scenarios where the same modulation order is used for both pilot and data subcarriers, using BPSK modulation for the pilot subcarriers improves the performance by 1 to 3dB.

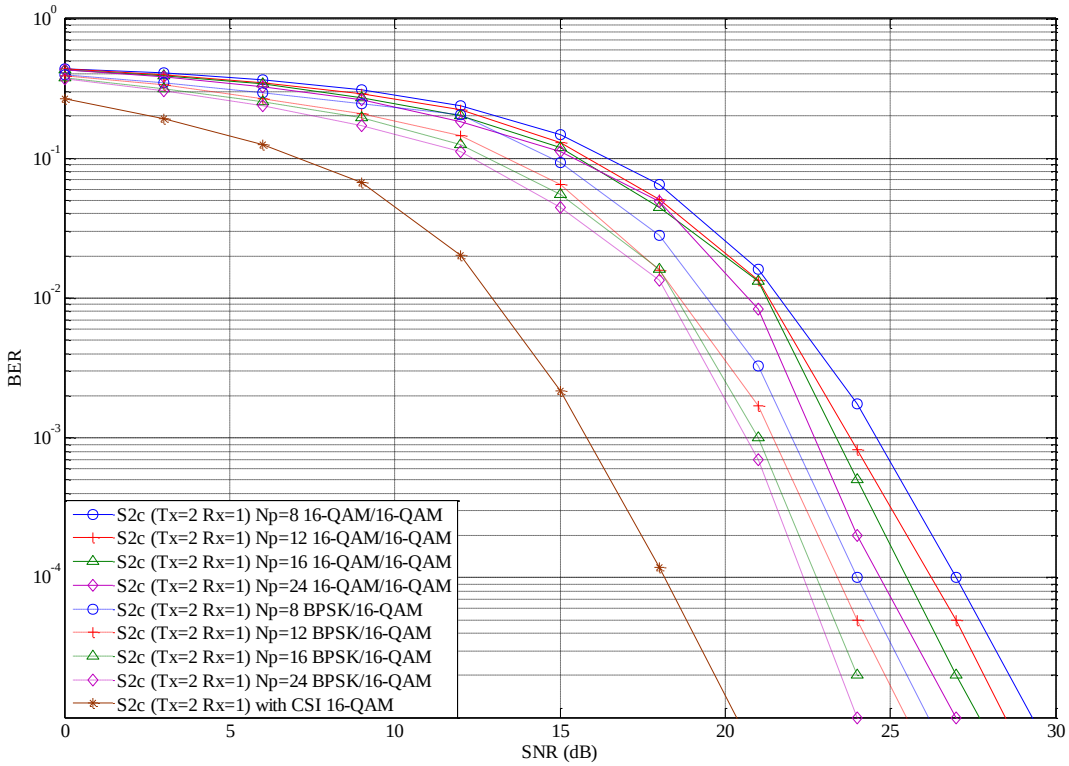

Figure 4-8: Simulation Results for 2 Transmit and 1 Receive Antennas for Different Pilot Modulation

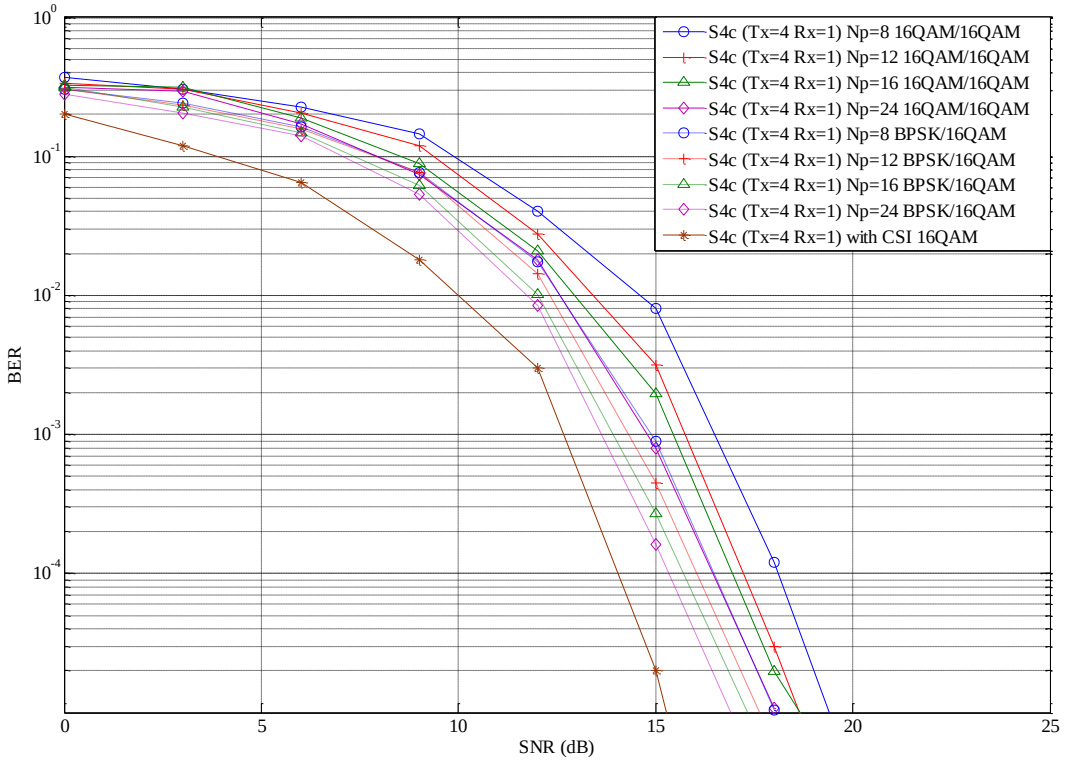

Figure 4-9: Simulation Results for 4 Transmit and 1 Receive Antennas for Different Pilot Modulation

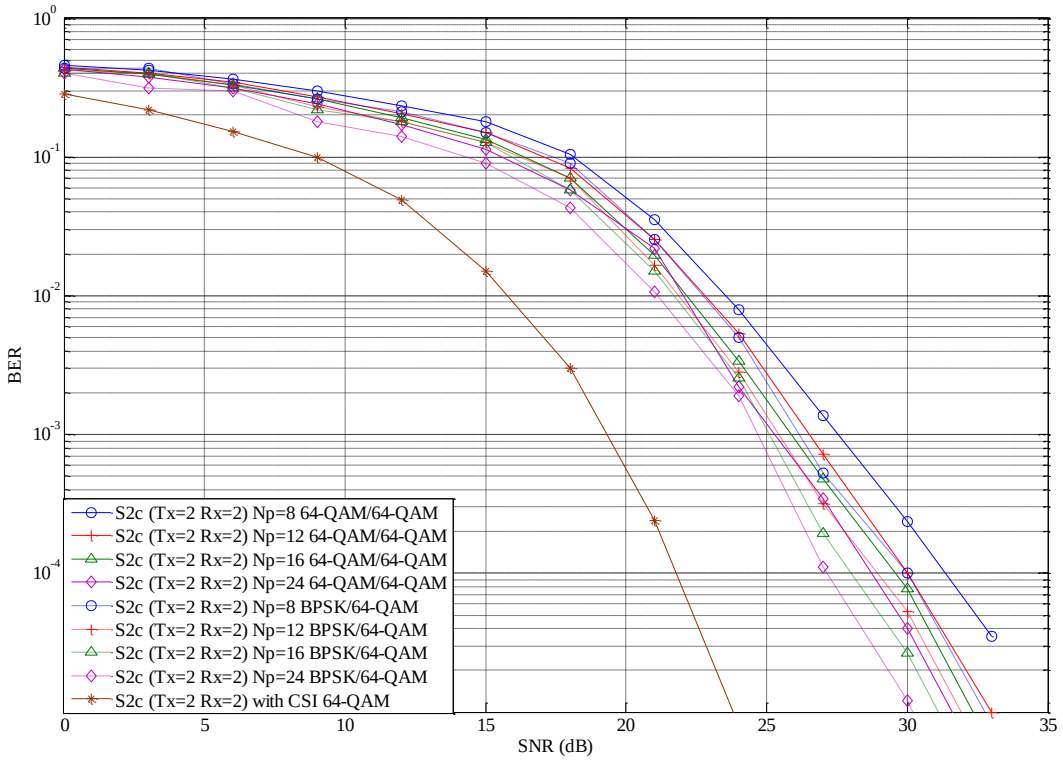

Figure 4-10: Simulation Results for 2 Transmit and 2 Receive Antennas for Different Pilot Modulation

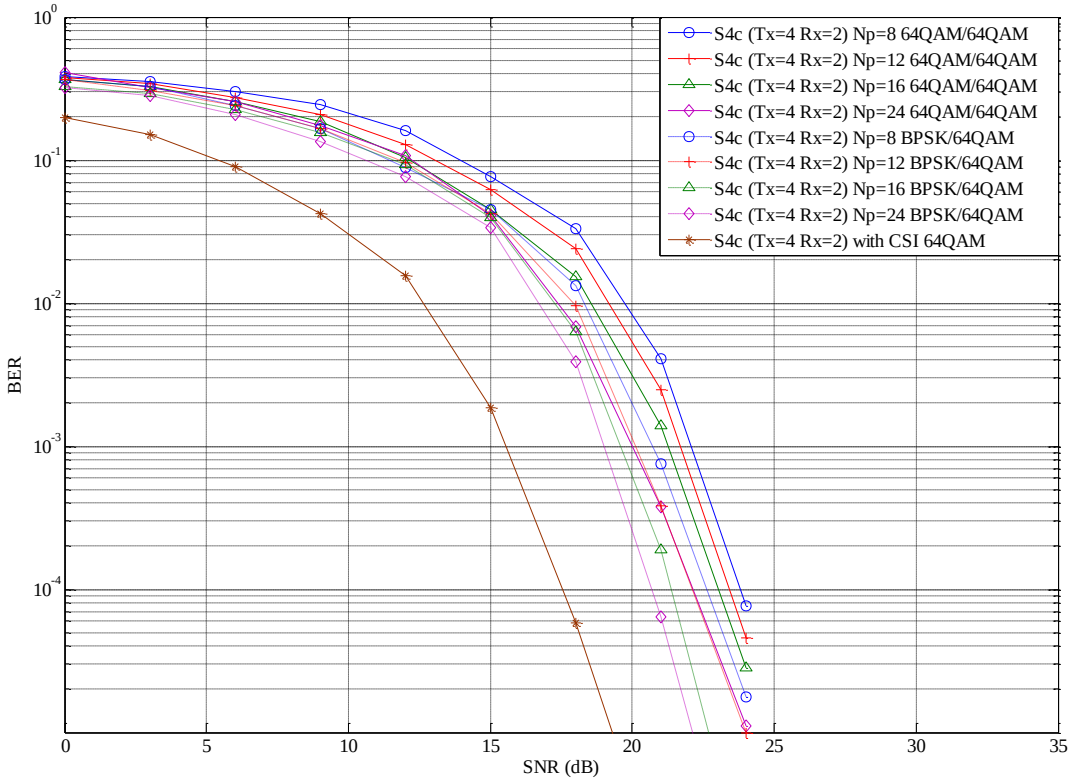

Figure 4-11: Simulation Results for 4 Transmit and 2 Receive Antennas for Different Pilot Modulation

In addition to the above simulation results, the proposed channel estimation technique has also been tested under different channel conditions. From Figure 4-12 and Figure 4-13, it can be noticed that the results obtained from the proposed channel estimation technique are similar under SUI1 and SUI3. However, it can be noticed that the system achieves lower BER under SUI1 due to the lower delay spread in SUI1 channels. Moreover, it can be seen that as stated in Chapter 2, higher number of transmit or receive antennas give lower BER. It can also be noticed that using a higher modulation order gives worse performance than using a lower modulation order.

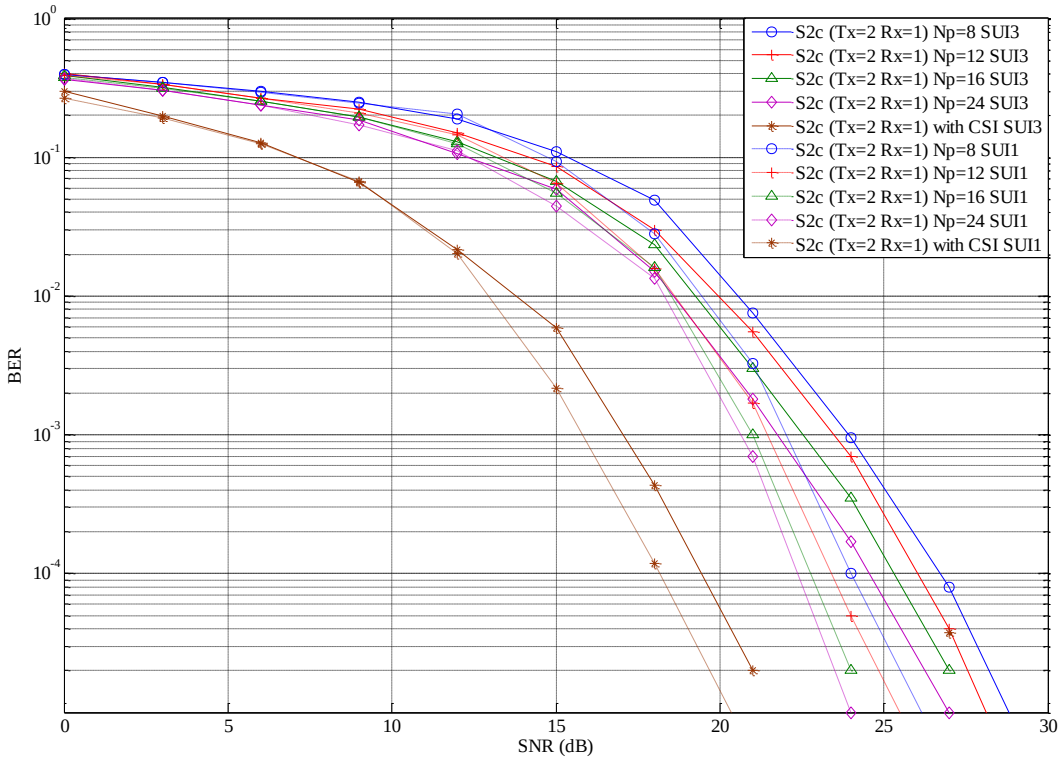

Figure 4-12: Comparison for 2 Transmit Antennas and 1 Receive Antenna under SUI1 and SUI3 with 16-QAM

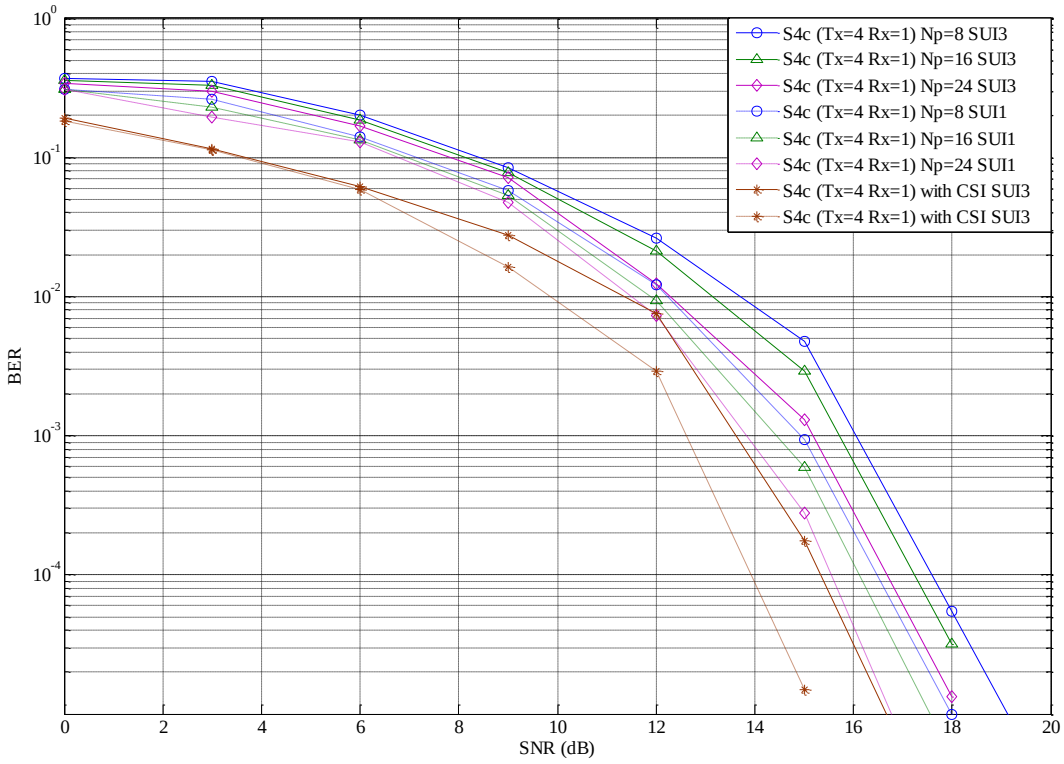

Figure 4-13: Comparison for 4 Transmit Antennas and 1 Receive Antenna under SUI1 and SUI3 with 16-QAM

With the proposed iterative channel estimation technique, the grouping of symbols improves the computational efficiency of the system. When the number of pilot symbols is increased, the number of groups is also increased. This means that the decoding time is also reduced as two sets of STBC-OFDM symbols are decoded concurrently in each group. Table 4-2 shows the simulation time to perform the decoding of one STBC-OFDM block which occurs over 2 and 8 OFDM symbols for 2 (n_t=2) and 4 (n_t=8) transmit antennas respectively.

From Table 4-2 and Figure 4-14, it can be seen that the decoding time increases with the number of transmit and receive antennas while it decreases with the number of pilot subcarriers used. Moreover, it can be noticed that the decoding time for 4 transmit antennas is high due to the use of 8 received signals to decode 4 data symbols. Finally, from Figure 4-14, it can be seen that the decoding time saved compared to the case where 2 and 4 symbols are decoded at a time for 2 and

4 transmit antennas respectively, increases exponentially with the number of pilot subcarriers.

Table 4-2: Decoding Time per STBC-OFDM Block

Number of Pilot Subcarriers	Decoding Subcarrier per Subcarrier	8 Pilot Subcarriers	12 Pilot Subcarriers	16 Pilot Subcarriers	24 Pilot Subcarriers
Tx=2 Rx=1	3.1s	0.48s	0.2s	0.16s	0.1s
Tx=2 Rx=2	4.7s	0.6s	0.22s	0.17s	0.11s
Tx=4 Rx=1	5.8s	0.69s	0.48s	0.35s	0.23s
Tx=4 Rx=2	9.76s	1.2s	0.83s	0.63s	0.42s

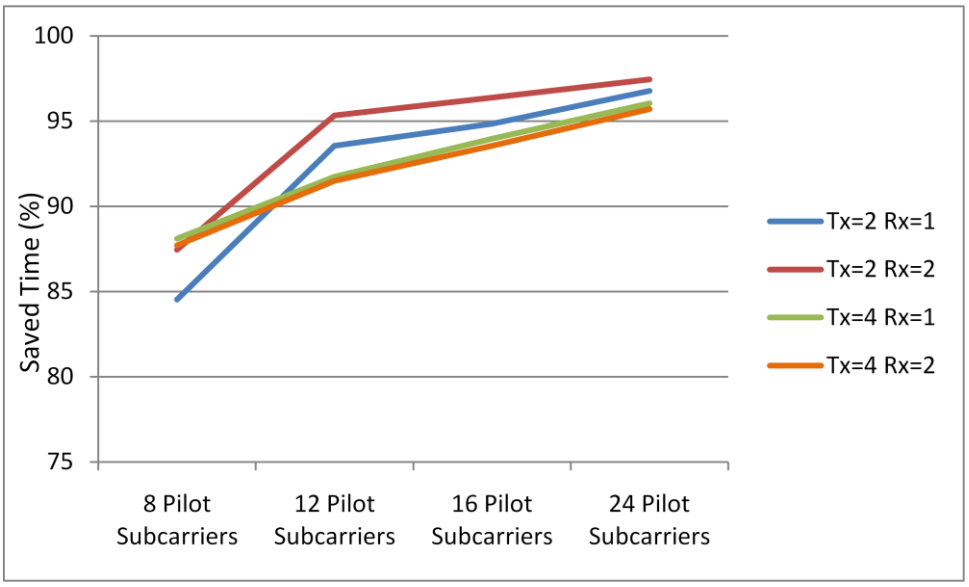

Figure 4-14: Saved Decoding Time per Number of Pilot Subcarriers Used

4.7 Conclusions

The combination of OFDM with STBC offers codes with low decoding complexity and bandwidth efficiency. However, most works in the literature propose a combination of STBC-OFDM codes for scenarios where channel

parameters are assumed to be known at the receiver. With the introduction of new channel estimation methods, real life conditions are simulated and analysed in order to propose methods suitable for future wireless technology such as 4G.

In this chapter, the proposed channel estimation technique for STBC-OFDM systems was intensively investigated using different number of transmit and receive antennas, different modulation order for pilot and data subcarriers, different number of pilot subcarriers and different channel conditions. Simulation results for 2 and 4 transmit antennas and 1 and 2 receive antennas have been presented and the channel estimation algorithm was compared with the ideal case where channel parameters are assumed to be known at the receiver. Moreover, investigations on the effects of group decoding have been conducted by looking at the decoding time of a single STBC-OFDM block and by looking at the time saved to decode the entire group of data blocks.

In this chapter, a new channel estimation technique using a group decoding method is proposed for STBC-OFDM. From simulation results, it can be observed that the proposed technique has the advantages of improving the computational efficiency of the system by reducing the computation time while increasing the number of pilot subcarriers. Moreover, using the group decoding technique allows the system to be more robust against error propagation. Indeed, in traditional schemes using iterative technique where channel estimation is performed at the beginning of the transmission, error propagation is of critical importance as an error in the estimation of the channel parameter would result in inaccurate data decoding. Consequently, this would initiate the propagation of the error in the next set of data due to the iterative process. Therefore, a higher number of groups would achieve better performance as the error would only propagate within the

group without affecting the rest of the transmitted data. Simulation results also show that higher number of groups result in better computation time. However, a trade-off needs to be found between BER and bandwidth efficiency as higher number of pilot subcarriers would result in lower number of transmitted data per OFDM symbols or smaller guard interval which would allow ISI.

At this stage of research, a new joint channel estimation and data detection has been proposed. The method offers simplicity, cost and computation efficiency due to its simplicity and due to the fact that the technique does not require matrix inversion at the receiver in contrast to other techniques proposed in the literature. In this Chapter, the STBC-OFDM system has been designed for static communication systems. A channel estimation technique for STBC-OFDM systems will be proposed in Chapter 5 for non-static wireless mobile communications.

5 Joint Channel Estimation and Data Detection for SFBC-OFDM

MIMO-OFDM systems have been suggested for future wireless communication systems such as 4G due to their ability to provide freedom in the spatial, temporal and frequency domains. A new iterative joint channel estimation method for STBC-OFDM was proposed in Chapter 4. In this chapter, a channel estimation method which exploits spatial and frequency diversity is proposed. The proposed method is based on the maximum likelihood (ML) approach which offers linearity and simplicity of implementation. In addition, the method is suitable for the next generation of broadband wireless communications systems. The performance of the proposed algorithm has been tested using different levels of Doppler shift for high frequency selective channels and for different number of transmit and receive antennas. Simulation results have proven that the proposed method is capable of tracking the channel parameter under high frequency selective channels and that the error margin between slow and high speed receivers is minimised compared to similar ML methods.

5.1 Introduction

The development and practical implementation of channel estimation algorithms for STBC can be a real challenge, especially under frequency selective multipath channels. Therefore, one of the solutions to support high data rate transmission in severe frequency selective environments is the use of OFDM in combination with STBC. Such integration allows systems to combat the problem

of long channel impulse response by transmitting parallel symbols over many orthogonal subcarriers, thus yielding unique reduced complexity and enhanced physical layer capabilities [80]. Shifting from time to frequency domain offers the possibility of coding which results in the development of SFBC [81]. STBC-OFDM and SFBC-OFDM have shown similar performance in slow fading environments under the assumption that the channel parameters are known at the receiver, whereas in environments where the propagation experiences high Doppler shift, SFBC-OFDM has shown better performance than STBC-OFDM [67, 82]. Furthermore, given a total transmission bandwidth, the efficiency of SFBC can be increased with the use of a higher number of subcarriers. Another advantage of SFBC-OFDM systems is that only half of the decoder memory is required compared to STBC-OFDM where the decoding is performed within only one OFDM symbol [82].

Channel estimation is crucial for the performance of a real MIMO-OFDM system and has therefore attracted much attention since the pioneering work of [68]. More work was done later in [28-30, 83-85] for STBC-OFDM and recently for SFBC-OFDM [82, 86]. Amongst the proposed methods, Discrete Fourier Transform (DFT) based channel estimation using Maximum Likelihood (ML) decoding has been the most popular. This method is implemented in OFDM systems that utilize preamble sequence [87] and Minimum Mean Square Error (MMSE) channel estimators [62, 77]. Both techniques have been shown to be competent they however incur additional cost because of the high complexity involved in calculating the pseudo inverse of the matrix. Hence, lower complexity channel estimation methods have been proposed [88, 89]. However, the downside

of these methods is that they introduce performance degradation and they have limited areas of application.

In this Chapter, a robust iterative channel estimation technique is proposed for high mobility SFBC-OFDM systems. The channel estimation algorithm presented in our work is a SFBC-OFDM technique based on ML decoding. As opposed to the methods proposed in the literature, this method does not require any matrix inversion at the receiver. As a result of the orthogonal property of SFBC, it has been possible to derive exact and simple analytical expressions to estimate the unknown channel parameters. Another advantage of the method is that the estimation technique is suitable for present and future technologies such as 3G-LTE, 4G or WiMax. The method can also support any number of transmit or receive antennas, any number of pilot and data subcarriers as well as any type of modulation. Finally, with the proposed method, each set of OFDM symbols is divided into groups, which are decoded simultaneously, according to the number of pilot subcarriers used. Once the number of groups is defined, each group is assigned a number of pilot subcarriers equal to the number of frequency slots (n_t) required to transmit one SFBC coded training block. The use of groups reduces the number of computations linearly with respect to the number of pilot subcarriers used.

5.2 SFBC-OFDM Systems Architecture

5.2.1 Transmitter

A SFBC-OFDM system with M_t transmit antennas and N_r receive antennas is shown in Figure 5-1. At time t, a binary data block X(t) of q bits is scrambled and mapped using a set of predefined constellation diagram (BPSK, QPSK, 16-QAM,

64-QAM, 256-QAM) resulting in a symbol stream

with N_s being the number of data subcarriers and N_{FS} being the number of frequency slots required per SFBC coded data. A modulated pilot sequence

where N_p is the number of pilot subcarriers which must be a multiple of N_{FS}, are scattered in the data signals at regular intervals. Each block of data is then sent to the SFBC encoder which is based on Alamouti's encoding method [5]. Data is then split to the different antennas according to SFBC encoding such that . For each antenna, an N-point Inverse Fast Fourier Transform (IFFT) is applied to convert the coded data from frequency domain to time domain. SFBC-OFDM becomes more efficient as the number of subcarriers increases for a given bandwidth [90]. Finally, cyclic prefix is added to each OFDM symbol and data is transmitted simultaneously from different antennas.

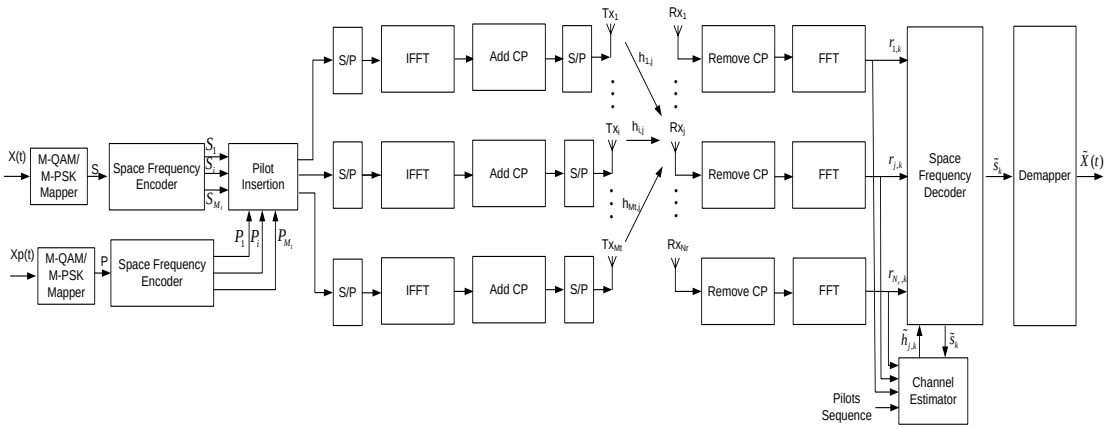

Figure 5-1: Block Diagram of the SFBC-OFDM System

In this paper, it is assumed that OFDM symbols are transmitted over a Rayleigh multipath channel from transmit antenna *i* to receive antenna *j* as described in Chapter 3 Section 3.4.

5.2.2 Receiver

At the receiver, an equivalent procedure is followed. Data is received and down converted, cyclic prefix is removed and FFT operation is performed. Alamouti's encoding scheme offers a simple decoding algorithm when channel parameters are known at the receiver. Therefore, extra attention has been paid to the channel estimation.

The transmitted sequence from transmit antenna 1 to M_t passes through a fast frequency selective channel with white Gaussian noise so that the received signal between the *i*-th transmit antenna and the *j*-th receive antenna, once the OFDM demodulation is applied, can be expressed in the matrix form as:

$$R_{j,k} = \sum_{i=1}^{M_t} H_{i,j,k} S_{i,k} + N_{j,k} \tag{5.1}$$

where $S_{i,k}=[s_0, s_1,...s_{Ns-1}]$ and $S_{i,k}=[s_0, s_1,...s_{Ns/2-1}]$ for two and four transmit antennas respectively. $N_{j,k}$ represents the white Gaussian noise with variance per dimension, $H_{i,j,k}$ is the time varying channel tap between the *i*-th transmit antenna and the *j*-th receive antenna and $S_{i,k}$ represents the transmitted signal from the *i*-th antenna.

Once the data has been decoded, the output of the combiner is fed to the ML detector.

5.3 Basic Principle of Pilot Design and Channel Estimation

Similarly to STBC-OFDM, the channel estimation technique proposed in this Chapter is based on a two-step procedure which is described in Figure 5-2. The first step occurs at the transmitter side where according to the application used, a specific number of subcarriers N_s and N_p are assigned for data and pilot transmission respectively. In this technique, each OFDM symbol is divided into groups, where the length of each group varies according to the number of pilot subcarriers. Due to SFBC encoding, pilot subcarriers are regrouped in pairs for two or more transmit antennas according to the number of frequency slots (N_{FS}) needed for SFBC encoding. As it can be seen from Figure 5-2, for OFDM symbols composed of N_s subcarriers, the length of each group of OFDM symbol is equal to $L_{sub/group}=N_s/(N_p/ N_{FS})$ which results in a number of groups per OFDM symbol equal to $N_{group/OFDM}= N_s/ L_{sub/group}$.

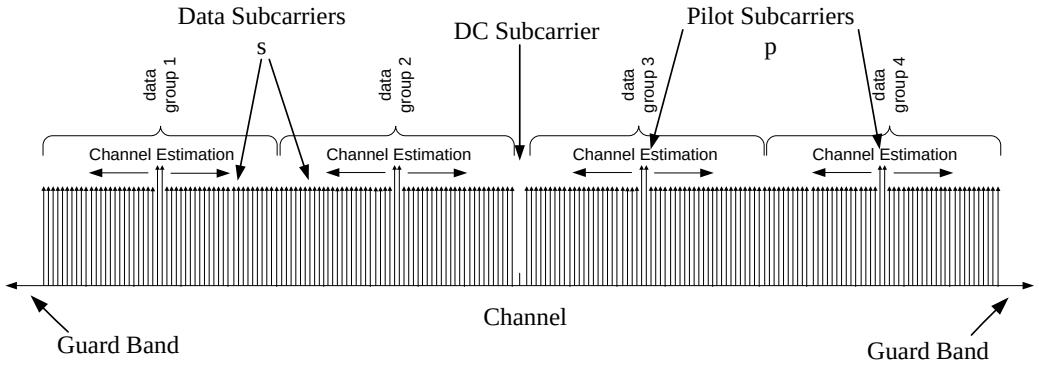

Figure 5-2: Description of the First Step of the Channel Estimation for 2 Transmit Antennas

Once the number of groups has been determined, a number of pilot subcarriers equal to the number of frequency slots needed for SFBC coding are assigned to each group. Pilot subcarriers are positioned in the middle of each

group in order to have equivalent number of data subcarriers on both sides. The number of pilot subcarriers per group will vary according to the number of transmit antennas and according to the rate of the matrix used for SFBC coding. With the help of Figure 5-2 for example, it can be seen that for two transmit antennas with 160 data subcarriers and 8 pilot subcarriers, that 4 groups will be created as $N_{group/OFDM}= N_s/ L_{sub/group}$. Also, due to the fact that for two transmit antennas, SFBC requires 2 frequency slots to transmit the data. Moreover, the number of data subcarriers per group would be equal to 40 which results in positioning the pilot subcarriers between data subcarrier 20 and 21 of each group. By doing so, an equivalent number of 20 subcarriers can be found on each side of the pilot subcarriers which will be decoded simultaneously at the receiver and therefore reduce the computational complexity of the system.

The second step occurs at the receiver side, the pilot sequence known at the receiver is used to estimate the channel frequency response of the corresponding subcarriers. Then, under the assumption that the channel parameters for two adjacent SFBC blocks are similar, the channel estimated by the pilot subcarriers is used to recover the adjacent SFBC-coded data subcarriers. Using the earlier example, channel parameters for pilot subcarriers between data subcarriers 20 and 21 of each group can be estimated and then used simultaneously to decode adjacent SFBC coded data subcarriers 19, 20 and 21, 22. Once adjacent data subcarriers have been recovered, frequency channel parameters for the corresponding data subcarrier can be estimated and used to decode the next adjacent SFBC data subcarriers 17, 18 and 23, 24. The estimated data becomes the new pilot sequence, and is therefore used to estimate the channel parameters which will be used to recover the next data symbols. With the assumption that the

channels remain constant for two adjacent SFBC blocks, the next pair of symbol can be estimated in the lower side of the pilot subcarriers as well as in the upper side. With the use of groups, the entire OFDM symbol is decoded faster than a traditional SFBC-OFDM decoder. This new decoding method improves the computation and memory efficiency of the system.

5.4 SFBC-OFDM Systems for 2 Transmit Antennas

As mentioned in the previous section, pilot sequence is assumed known at the receiver and therefore channel estimation of the pilot subcarriers is first performed. Then, once channel frequency responses of pilot subcarriers have been estimated, decoding of adjacent data subcarriers is performed assuming constant fading conditions for two adjacent SFBC coded data blocks (decoding of subcarriers k and k+1 is performed using the adjacent estimated channel frequency response of pilot subcarriers kp and kp+1 with k=0, 2,..., N_s-2 and kp=0, 2,..., N_p-2). Using equation (5.1), received pilot and data subcarriers can be expressed as:

$$\begin{aligned} rp_{j,kp} &= hp_{1,j,kp}\,p_{kp} + hp_{2,j,kp}\,p_{kp+1} + np_{j,kp} \\ rp_{j,kp+1} &= -hp_{1,j,kp+1}\,p^{*}_{kp+1} + hp_{2,j,kp+1}\,p^{*}_{kp} + np_{j,kp+1} \end{aligned} \tag{5.2}$$

$$\begin{aligned} r_{j,k} &= h_{1,j,k}\,s_k + h_{2,j,k}\,s_{k+1} + n_{j,k} \\ r_{j,k+1} &= -h_{1,j,k+1}\,s^{*}_{k+1} + h_{2,j,k+1}\,s^{*}_{k} + n_{j,k+1} \end{aligned} \tag{5.3}$$

where p_{kp}* denotes the complex conjugate of p_{kp}, $rp_{j,kp}$, $r_{j,k}$ and $np_{j,kp}$, $n_{j,k}$ represent the received pilot and data information and white Gaussian noise at subcarrier kp and k, $hp_{i,j,kp}$ and $h_{i,j,k}$ represent the channel frequency response of pilot and data subcarrier between the i-th transmit antenna and the j-th receive antenna, p_{kp} and s_k represent the pilot and data information at subcarrier kp and k

respectively. Organisation of pilot and data vectors through space, time and frequency can be seen in Figure 5-3 and can be expressed for antennas 1 and 2 as in (5.4) and (5.5) for pilot and data respectively.

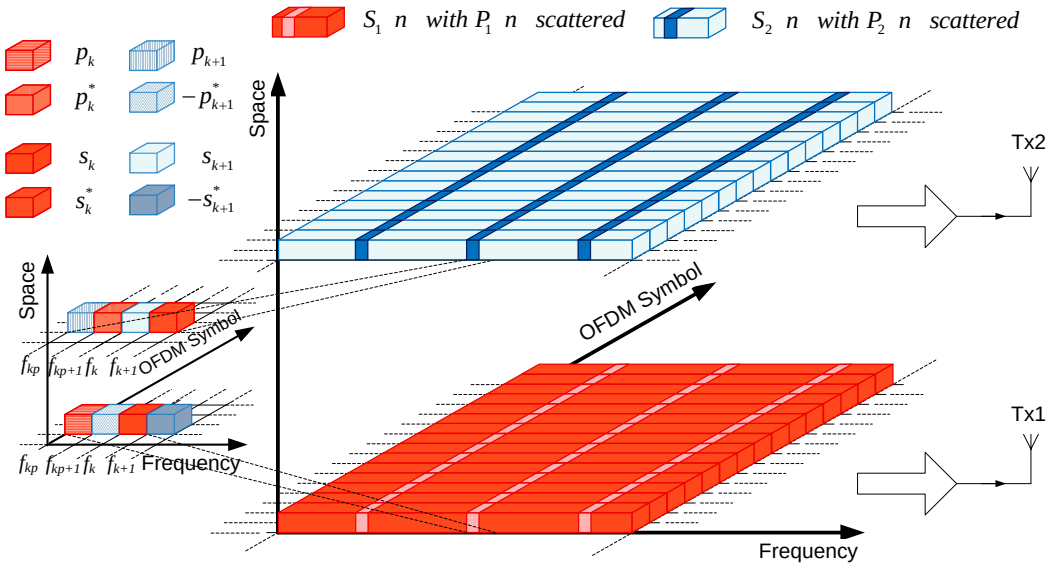

Figure 5-3: Organisation of the Pilot and Data Subcarriers for 2 Transmit Antennas

$$P_1 = [p_0,\ -p_1^*,\ \ldots,\ p_{kp},\ -p_{kp+1}^*, \ldots,\ p_{Np-2},\ -p_{Np-1}^*]^T$$
$$P_2 = [p_1,\ p_0^*,\ \ldots,\ p_{kp+1},\ p_{kp}^*, \ldots,\ p_{Np-1},\ p_{Np-2}^*]^T \quad (5.4)$$

$$S_1 = [s_0,\ -s_1^*,\ \ldots,\ s_k,\ -s_{k+1}^*, \ldots,\ s_{Ns-2}, -s_{Ns-1}^*]^T$$
$$S_2 = [s_1,\ s_0^*,\ \ldots,\ s_{k+1},\ s_k^*, \ldots,\ s_{Ns-1},\ s_{Ns-2}^*]^T \quad (5.5)$$

where k=0, 2, …, Ns-2 and kp=0, 2, …, Np-2.

Pilot sequence is known at the receiver and as stated earlier two adjacent channel frequency responses can be assumed constant therefore $hp_{i,j,kp}=hp_{i,j,kp+1}$ which leads with the help of equation (5.2) for the derivation of the channel estimation :

$$\tilde{hp}_{1,j,kp} = \frac{rp_{j,kp}\,p^{*}_{kp} - rp_{j,kp+1}\,p_{kp+1}}{\left|p_{kp}\right|^2 + \left|p_{kp+1}\right|^2}$$
$$\tilde{hp}_{2,j,kp} = \frac{rp_{j,kp}\,p^{*}_{kp+1} + rp_{j,kp+1}\,p_{kp}}{\left|p_{kp}\right|^2 + \left|p_{kp+1}\right|^2} \qquad (5.6)$$

Once channel estimation is made, it is possible to detect the upper and lower adjacent SFBC data signal by using (5.3). For instance, as shown in Figure 5-4, if the pilot subcarriers were positioned between data subcarriers k+1 and k+2 then the channel estimation formulae given in (5.6) would be used to recover the data subcarriers k and k+1 in the lower side as well as k+2 and k+3 in the upper side.

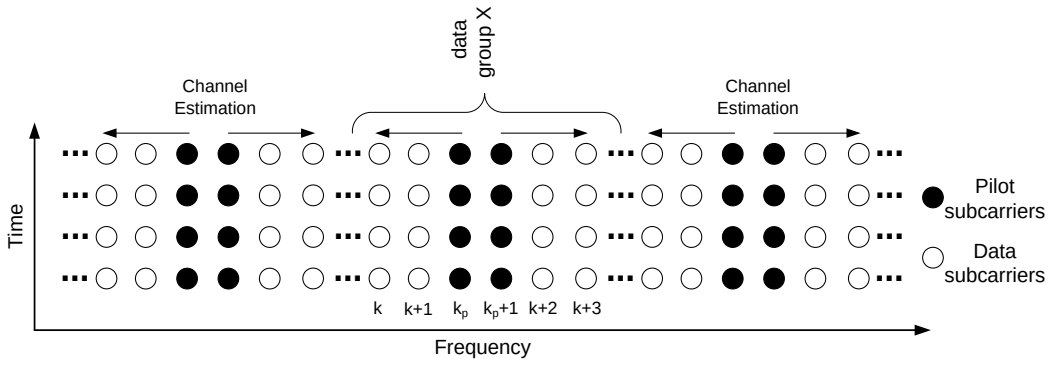

Figure 5-4: Details of the Estimation Technique for 2 Transmit Antennas

Using the estimation made in (5.6), with the help of (5.3) and due to the assumption that $hp_{1,j,kp}=h_{1,j,k}=h_{1,j,k+1}$ and $hp_{2,j,kp}=h_{2,j,k}=h_{2,j,k+1}$, the following combinations can be deduced:

$$\tilde{s}_k = \sum_{j=1}^{N_r} (\tilde{hp}^{*}_{1,j,kp} r_{j,k} + \tilde{hp}_{2,j,kp} r^{*}_{j,k+1})$$
$$\tilde{s}_{k+1} = \sum_{j=1}^{N_r} (\tilde{hp}^{*}_{2,j,kp} r_{j,k} - \tilde{hp}_{1,j,kp} r^{*}_{j,k+1}) \qquad (5.7)$$

Substitution of (5.6) into (5.7) leads to:

$$\begin{aligned}\tilde{s}_k &= \frac{1}{\Delta_p}(Ap^*_{kp+1} + Bp_{kp}) \\ \tilde{s}_{k+1} &= \frac{1}{\Delta_p}(Bp_{kp+1} - Ap^*_{kp})\end{aligned} \tag{5.8}$$

where and A and B are given in (5.9).

$$\begin{aligned}A &= \sum_{j=1}^{N_r}(rp_{j,kp}r^*_{j,k+1} - rp^*_{j,kp+1}r_{j,k}) \\ &= \Delta_h \quad p_{kp+1}s_k - p_{kp}s_{k+1} \quad + N_{j,1} \\ B &= \sum_{j=1}^{N_r}(rp^*_{j,kp}r_{j,k} + rp_{j,kp+1}r^*_{j,k+1}) \\ &= \Delta_h \quad p^*_{kp}s_k + p^*_{kp+1}s_{k+1} \quad + N_{j,2}\end{aligned} \tag{5.9}$$

where $N_{j,1}$ and $N_{j,2}$ are white Gaussian Noise vectors and

.

Substituting (5.9) into (5.8), we obtain:

$$\begin{aligned}\tilde{s}_k &= \Delta_h s_k + N_3 \\ \tilde{s}_{k+1} &= \Delta_h s_{k+1} + N_4\end{aligned} \tag{5.10}$$

where N_3 and N_4 are noise terms. Once the data signals that are adjacent to the pilot subcarriers have been recovered, the process is repeated for the upper and lower data signal using the recovered data , and , as the new pilot sequence. Therefore, the first pair of decoded data and become the pilot sequence and to be used to recover the data and in the next iteration. Similarly, the second pair of decoded data and become the pilot sequence and to be used to recover the data and in the next iteration. In other words, each pair of decoded symbols yield a pair of pilot

sequence each, this pilot sequence is then used in the next iteration to recover the adjacent pair of symbols. The iterative joint process is repeated until all the data of the group have been recovered. Each group is decoded simultaneously which, when compared with classic decoding where only 2 symbols are decoded at a time, leads to a decoding speed which increases linearly with the number of pilots subcarriers used.

From the above derivations, it can be seen that the proposed iterative channel estimation does not require any matrix inversion, which enhances the simplicity of the system and therefore reduces the cost without affecting the performances.

5.5 SFBC-OFDM Systems for 4 Transmit Antennas

In this section, the method of detection for four transmit antennas and one receive antenna is presented. Half-rate complex S_{4c} code [37] is used. The fading channels are assumed to be constant over 16 symbol periods and the received pilot symbols are assumed known at the receiver. From Section 5.4, the following can be written for four transmit antennas:

$$\begin{aligned}
rp_{j,kp} &= hp_{1,j,kp}p_{kp} + hp_{2,j,kp}p_{kp+1} + hp_{3,j,kp}p_{kp+2} + hp_{4,j,kp}p_{kp+3} \\
rp_{j,kp+1} &= -hp_{1,j,kp+1}p_{kp+1} + hp_{2,j,kp+1}p_{kp} - hp_{3,j,kp+1}p_{kp+3} + hp_{4,j,kp+1}p_{kp+2} \\
rp_{j,kp+2} &= -hp_{1,j,kp+2}p_{kp+2} + hp_{2,j,kp+2}p_{kp+3} + hp_{3,j,kp+2}p_{kp} - hp_{4,j,kp+2}p_{kp+1} \\
rp_{j,kp+3} &= -hp_{1,j,kp+3}p_{kp+3} - hp_{2,j,kp+3}p_{kp+2} + hp_{3,j,kp+3}p_{kp+1} + hp_{4,j,kp+3}p_{kp} \\
rp_{j,kp+4} &= hp_{1,j,kp+4}p^*_{kp} + hp_{2,j,kp+4}p^*_{kp+1} + hp_{3,j,kp+4}p^*_{kp+2} + hp_{4,j,kp+4}p^*_{kp+3} \\
rp_{j,kp+5} &= -hp_{1,j,kp+5}p^*_{kp+1} + hp_{2,j,kp+5}p^*_{kp} - hp_{3,j,kp+5}p^*_{kp+3} + hp_{4,j,kp+5}p^*_{kp+2} \\
rp_{j,kp+6} &= -hp_{1,j,kp+6}p^*_{kp+2} + hp_{2,j,kp+6}p^*_{kp+3} + hp_{3,j,kp+6}p^*_{kp} - hp_{4,j,kp+6}p^*_{kp+1} \\
rp_{j,kp+7} &= -hp_{1,j,kp+7}p^*_{kp+3} - hp_{2,j,kp+7}p^*_{kp+2} + hp_{3,j,kp+7}p^*_{kp+1} + hp_{4,j,kp+7}p^*_{kp}
\end{aligned} \tag{5.11}$$

where to are known at the receiver and kp=1, 9, ..., N_p/2-7. The received equations of the adjacent transmitted data subcarriers can be found in (5.12).

$$\begin{aligned}
r_{j,k} &= h_{1,j,k}s_k + h_{2,j,k}s_{k+1} + h_{3,j,k}s_{k+2} + h_{4,j,k}s_{k+3} \\
r_{j,k+1} &= -h_{1,j,k+1}s_{k+1} + h_{2,j,k+1}s_k - h_{3,j,k+1}s_{k+3} + h_{4,j,k+1}s_{k+2} \\
r_{j,k+2} &= -h_{1,j,k+2}s_{k+2} + h_{2,j,k+2}s_{k+3} + h_{3,j,k+2}s_k - h_{4,j,k+2}s_{k+1} \\
r_{j,k+3} &= -h_{1,j,k+3}s_{k+3} - h_{2,j,k+3}s_{k+2} + h_{3,j,k+3}s_{k+1} + h_{4,j,k+3}s_k \\
r_{j,k+4} &= h_{1,j,k+4}s_k^* + h_{2,j,k+4}s_{k+1}^* + h_{3,j,k+4}s_{k+2}^* + h_{4,j,k+4}s_{k+3}^* \\
r_{j,k+5} &= -h_{1,j,k+5}s_{k+1}^* + h_{2,j,k+5}s_k^* - h_{3,j,k+5}s_{k+3}^* + h_{4,j,k+5}s_{k+2}^* \\
r_{j,k+6} &= -h_{1,j,k+6}s_{k+2}^* + h_{2,j,k+6}s_{k+3}^* + h_{3,j,k+6}s_k^* - h_{4,j,k+6}s_{k+1}^* \\
r_{j,k+7} &= -h_{1,j,k+7}s_{k+3}^* - h_{2,j,k+7}s_{k+2}^* + h_{3,j,k+7}s_{k+1}^* + h_{4,j,k+7}s_k^*
\end{aligned} \tag{5.12}$$

where $r_{j,k}$ to $r_{j,k+7}$ are known at the receiver with {k=1, 9, ..., N_s/2-7}.

With the help of Figure 5-5 and according to the well known STBC coding for four antennas, vectors P_1 to P_4 and S_1 to S_4 can be expressed as in (5.13) and (5.14) respectively.

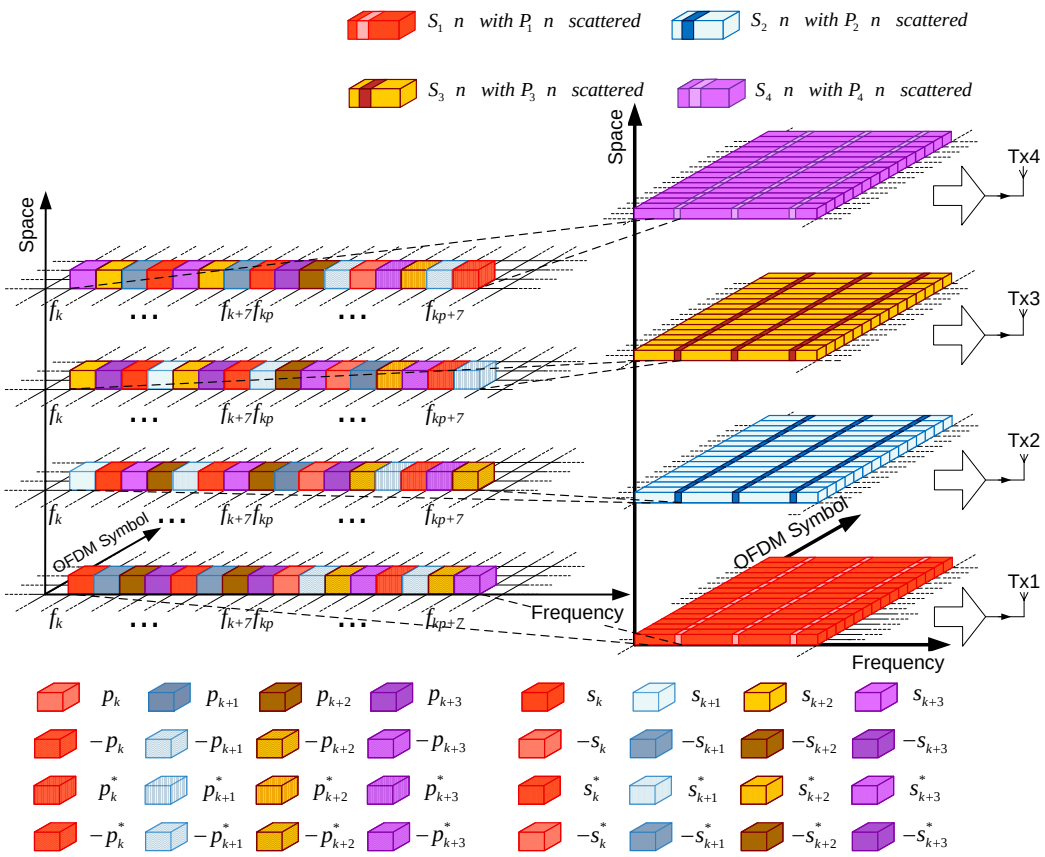

Figure 5-5: Organisation of Data and Pilot Subcarriers through Space, Time and Frequency

$$
\begin{aligned}
P_1 &= [p_0, -p_1, -p_2, -p_3, p_0^*, -p_1^*, -p_2^*, -p_3^*, \ldots, \\
&\quad p_{Np/2-4}, -p_{Np/2-3}, -p_{Np/2-2}, -p_{Np/2-1}, p_{Np/2-4}^*, -p_{2Np/2-3}^*, -p_{Np/2-2}^*, -p_{Np/2-1}^*]^T \\
P_2 &= [p_1, p_0, p_3, -p_4, p_1^*, p_0^*, p_3^*, -p_2^*, \ldots, \\
&\quad p_{Np/2-3}, p_{Np/2-4}, p_{Np/2-1}, -p_{Np/2-2}, p_{Np/2-3}^*, p_{2Np/2-4}^*, p_{Np/2-1}^*, -p_{Np/2-2}^*]^T \\
P_3 &= [p_2, -p_3, p_0, p_1, p_2^*, -p_3^*, p_0^*, p_1^*, \ldots, \\
&\quad p_{Np/2-2}, -p_{Np/2-1}, p_{Np/2-4}, p_{Np/2-3}, p_{Np/2-2}^*, -p_{2Np/2-1}^*, p_{Np/2-4}^*, p_{Np/2-3}^*]^T \\
P_4 &= [p_3, p_2, -p_1, p_0, p_3^*, p_2^*, -p_1^*, p_0^*, \ldots, \\
&\quad p_{Np/2-1}, p_{Np/2-2}, -p_{Np/2-3}, p_{Np/2-4}, p_{Np/2-1}^*, p_{2Np/2-2}^*, -p_{Np/2-3}^*, p_{Np/2-4}^*]^T
\end{aligned}
\tag{5.13}
$$

$$
\begin{aligned}
S_1 &= [s_0,\ -s_1,\ -s_2,\ -s_3, s_0^*,\ -s_1^*, -s_2^*, -s_3^* \ldots, \\
&\quad s_{Ns/2-4},\ -s_{Ns/2-3},\ -s_{Ns/2-2},\ -s_{Ns/2-1,} s_{Ns/2-4}^*,\ -s_{Ns/2-3}^*,\ -s_{Ns/2-2}^*, -s_{Ns/2-1}^*]^T \\
S_2 &= [s_1, s_0, s_{3,} -s_{2,}\ s_1^*, s_0^*,\ s_3^*,\ -s_2^*\ \ldots, \\
&\quad s_{Ns/2-3},\ s_{Ns/2-4},\ s_{Ns/2-1},\ -s_{Ns/2-2}, s_{Ns/2-3}^*,\ s_{Ns/2-4}^*,\ s_{Ns/2-1}^*,\ -s_{Ns/2-2}^*]^T \\
S_3 &= [s_2,\ -s_3, s_{0,} s_{1,}\ s_2^*,\ -s_3^*,\ s_0^*,\ s_1^*\ \ldots, \\
&\quad s_{Ns/2-2},\ -s_{Ns/2-1},\ s_{Ns/2-4}, s_{Ns/2-3},\ s_{Ns/2-2}^*,\ -s_{Ns/2-1}^*,\ s_{Ns/2-4}^*,\ s_{Ns/2-3}^*]^T \\
S_4 &= [s_3,\ s_2,\ -s_1, s_0, s_3^*,\ s_2^*, -s_1^*, s_0^*\ \ldots, \\
&\quad s_{Ns/2-1},\ s_{Ns/2-2},\ -s_{Ns/2-3}, s_{Ns/2-4},\ s_{Ns/2-1}^*,\ s_{Ns/2-2}^*,\ -s_{Ns/2-3}^*,\ s_{Ns/2-4}^*]^T
\end{aligned}
\tag{5.14}
$$

As mentioned for two transmit antennas, the proposed channel estimation technique first focuses on the estimation of the channel at the pilot subcarriers. Then using this estimation and under the assumption that the fade remains constant over 16 symbol periods, adjacent data subcarriers are decoded and used to decode the next SFBC block of 8 symbol periods. Figure 5-6 shows the organisation of the OFDM symbol. First, the pilot subcarrier kp to kp+7, known at the receiver are used to initiate the iterative channel estimation method. Estimation is performed and used to decode the data subcarriers k to k+7 and k+8 to k+15 simultaneously. Each iteration allows the decoding of 16 data subcarriers per group which is equivalent to 8 data symbols multiplied by the number of groups of the OFDM symbols.

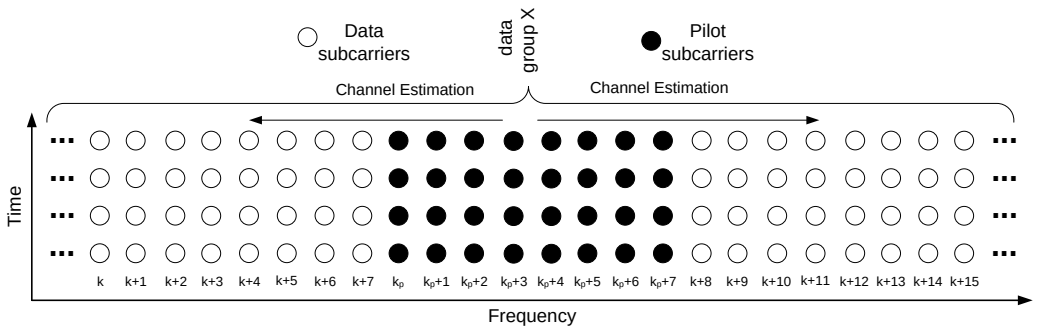

Figure 5-6: Details of the Estimation Technique for 4 Transmit Antennas

Pilot sequence is known at the receiver and following the description given for two transmit antennas, adjacent channel frequency response can be assumed constant therefore $hp_{i,j,kp}=hp_{i,j,kp+sp,}$ with i=1, 2, 3, 4 as 4 transmit antennas are used and sp=0, 1,..., 7 as 8 subcarriers are used for SFBC pilot encoding. Thus with the help of (5.11), the following channel estimation equations can be derived:

$$\begin{aligned}
\tilde{h}p_{1,j,kp} &= \frac{rp_{j,kp}p_{kp}^{*} - rp_{j,kp+1}p_{kp+1}^{*} - rp_{j,kp+2}p_{kp+2}^{*} - rp_{j,kp+3}p_{kp+3}^{*}}{2\left(\left|p_{kp}\right|^2+\left|p_{kp+1}\right|^2+\left|p_{kp+3}\right|^2+\left|p_{kp+4}\right|^2\right)} + \\
&\quad \frac{rp_{j,kp+4}p_{kp} + rp_{j,kp+5}p_{kp+1} + rp_{j,kp+6}p_{kp+2} + rp_{j,kp+7}p_{kp+3}}{2\left(\left|p_{kp}\right|^2+\left|p_{kp+1}\right|^2+\left|p_{kp+3}\right|^2+\left|p_{kp+4}\right|^2\right)} \\
\tilde{h}p_{2,j,kp} &= \frac{rp_{j,kp}p_{kp+1}^{*} + rp_{j,kp+1}p_{kp}^{*} + rp_{j,kp+2}p_{kp+3}^{*} - rp_{j,kp+3}p_{kp+2}^{*}}{2\left(\left|p_{kp}\right|^2+\left|p_{kp+1}\right|^2+\left|p_{kp+3}\right|^2+\left|p_{kp+4}\right|^2\right)} + \\
&\quad \frac{rp_{j,kp+4}p_{kp+1} + rp_{j,kp+5}p_{kp} + rp_{j,kp+6}p_{kp+3} - rp_{j,kp+7}p_{kp+2}}{2\left(\left|p_{kp}\right|^2+\left|p_{kp+1}\right|^2+\left|p_{kp+3}\right|^2+\left|p_{kp+4}\right|^2\right)} \\
\tilde{h}p_{3,j,kp} &= \frac{rp_{j,kp}p_{kp+2}^{*} - rp_{j,kp+1}p_{kp+3}^{*} + rp_{j,kp+2}p_{kp}^{*} + rp_{j,kp+3}p_{kp+1}^{*}}{2\left(\left|p_{kp}\right|^2+\left|p_{kp+1}\right|^2+\left|p_{kp+3}\right|^2+\left|p_{kp+4}\right|^2\right)} + \\
&\quad \frac{rp_{j,kp+4}p_{kp+2} - rp_{j,kp+5}p_{kp+3} + rp_{j,kp+6}p_{kp} + rp_{j,kp+7}p_{kp+1}}{2\left(\left|p_{kp}\right|^2+\left|p_{kp+1}\right|^2+\left|p_{kp+3}\right|^2+\left|p_{kp+4}\right|^2\right)} \\
\tilde{h}p_{4,j,kp} &= \frac{rp_{j,kp}p_{kp+3}^{*} + rp_{j,kp+1}p_{kp+2}^{*} - rp_{j,kp+2}p_{kp+1}^{*} + rp_{j,kp+3}p_{kp}^{*}}{2\left(\left|p_{kp}\right|^2+\left|p_{kp+1}\right|^2+\left|p_{kp+3}\right|^2+\left|p_{kp+4}\right|^2\right)} + \\
&\quad \frac{rp_{j,kp+4}p_{kp+3} + rp_{j,kp+5}p_{kp+2} - rp_{j,kp+6}p_{kp+1} + rp_{j,kp+7}p_{kp}}{2\left(\left|p_{kp}\right|^2+\left|p_{kp+1}\right|^2+\left|p_{kp+3}\right|^2+\left|p_{kp+4}\right|^2\right)}
\end{aligned} \tag{5.15}$$

where k=0, 4, …, Ns-4 and kp=0, 4, …, Np-4.

The detection formulas for the data signals can be derived with the help of (5.12) and (5.15). Assuming $hp_{i,j,kp}= h_{i,j,k} =h_{i,j,k+sp}$, equation (5.16) can be deduced.

$$
\begin{aligned}
\tilde{s}_k &= \sum_{j=1}^{N_r} (\tilde{hp}^*_{1,j,kp} r_{j,k} + \tilde{hp}^*_{2,j,kp} r_{j,k+1} + \tilde{hp}^*_{3,j,kp} r_{j,k+2} + \tilde{hp}^*_{4,j,kp} r_{j,k+3} + \\
&\qquad \tilde{hp}_{1,j,kp} r^*_{j,k+4} + \tilde{hp}_{2,j,kp} r^*_{j,k+5} + \tilde{hp}_{3,j,kp} r^*_{j,k+6} + \tilde{hp}_{4,j,kp} r^*_{j,k+7}) \\
\tilde{s}_{k+1} &= \sum_{j=1}^{N_r} (\tilde{hp}^*_{2,j,kp} r_{j,k} - \tilde{hp}^*_{1,j,kp} r_{j,k+1} - \tilde{hp}^*_{4,j,kp} r_{j,k+2} + \tilde{hp}^*_{3,j,kp} r_{j,k+3} + \\
&\qquad \tilde{hp}_{2,j,kp} r^*_{j,k+4} - \tilde{hp}_{1,j,kp} r^*_{j,k+5} - \tilde{hp}_{4,j,kp} r^*_{j,k+6} + \tilde{hp}_{3,j,kp} r^*_{j,k+7}) \\
\tilde{s}_{k+2} &= \sum_{j=1}^{N_r} (\tilde{hp}^*_{3,j,kp} r_{j,k} + \tilde{hp}^*_{4,j,kp} r_{j,k+1} - \tilde{hp}^*_{1,j,kp} r_{j,k+2} - \tilde{hp}^*_{2,j,kp} r_{j,k+3} + \\
&\qquad \tilde{hp}_{3,j,kp} r^*_{j,k+4} + \tilde{hp}_{4,j,kp} r^*_{j,k+5} - \tilde{hp}_{1,j,kp} r^*_{j,k+6} - \tilde{hp}_{2,j,kp} r^*_{j,k+7}) \\
\tilde{s}_{k+3} &= \sum_{j=1}^{N_r} (\tilde{hp}^*_{4,j,kp} r_{j,k} - \tilde{hp}^*_{3,j,kp} r_{j,k+1} + \tilde{hp}^*_{2,j,kp} r_{j,k+2} - \tilde{hp}^*_{1,j,kp} r_{j,k+3} + \\
&\qquad \tilde{hp}_{4,j,kp} r^*_{j,k+4} - \tilde{hp}_{3,j,kp} r^*_{j,k+5} + \tilde{hp}_{2,j,kp} r^*_{j,k+6} - \tilde{hp}_{1,j,kp} r^*_{j,k+7})
\end{aligned}
\tag{5.16}
$$

Replacing the channels by their estimated expressions obtained in (5.15), (5.16) becomes:

$$
\begin{aligned}
\tilde{s}_k &= \frac{1}{2\Delta_p} (Ap_{kp} + Bp_{kp+1} + Cp_{kp+2} + Dp_{kp+3} + \\
&\qquad Ep^*_{kp} + Fp^*_{kp+1} + Gp^*_{kp+2} + Hp^*_{kp+3}) \\
\tilde{s}_{k+1} &= \frac{1}{2\Delta_p} (-Bp_{1,kp} + Ap_{kp+1} + Dp_{kp+2} - Cp_{kp+3} - \\
&\qquad Fp^*_{kp} + Ep^*_{kp+1} + Hp^*_{kp+2} - Gp^*_{kp+3}) \\
\tilde{s}_{k+3} &= \frac{1}{2\Delta_p} (-Cp_{1,kp} - Dp_{kp+1} + Ap_{kp+2} + Bp_{kp+3} - \\
&\qquad Gp^*_{kp} - Hp^*_{kp+1} + Ep^*_{kp+2} + Fp^*_{kp+3}) \\
\tilde{s}_{k+4} &= \frac{1}{2\Delta_p} (-Dp_{1,kp} + Cp_{kp+1} - Bp_{kp+2} + Ap_{kp+3} - \\
&\qquad Hp^*_{kp} + Gp^*_{kp+1} - Fp^*_{kp+2} + Ep^*_{kp+3})
\end{aligned}
\tag{5.17}
$$

where and A, B, C, D, E, F, G and H are given as:

$$
\begin{aligned}
A &= \sum_{j=1}^{N_r} (r_{j,kp}^{*} r_{j,k} + r_{j,kp+1}^{*} r_{j,k+1} + r_{j,kp+2}^{*} r_{j,k+2} + r_{j,kp+3}^{*} r_{j,k+3} + \\
&\qquad r_{j,kp+4} r_{j,k+4}^{*} + r_{j,kp+5} r_{j,k+5}^{*} + r_{j,kp+6} r_{j,k+6}^{*} + r_{j,kp+7} r_{j,k+7}^{*}) \\
&= 2\Delta_h (p_{kp}^{*} s_k + p_{kp+1}^{*} s_{k+1} + p_{kp+2}^{*} s_{k+2} + p_{kp+3}^{*} s_{k+3}) + N_{j,1} \\
B &= \sum_{j=1}^{N_r} (-r_{j,kp+1}^{*} r_{j,k} + r_{j,kp}^{*} r_{j,k+1} + r_{j,kp+3}^{*} r_{j,k+2} - r_{j,kp+2}^{*} r_{j,k+3} - \\
&\qquad r_{j,kp+5} r_{j,k+4}^{*} + r_{j,kp+4} r_{j,k+5}^{*} + r_{j,kp+7} r_{j,k+6}^{*} - r_{j,kp+6} r_{j,k+7}^{*}) \\
&= 2\Delta_h (p_{kp+1}^{*} s_k - p_{kp}^{*} s_{k+1} + p_{kp+3}^{*} s_{k+2} - p_{kp+2}^{*} s_{k+3}) + N_{j,2} \\
C &= \sum_{j=1}^{N_r} (-r_{j,kp+2}^{*} r_{j,k} - r_{j,kp+3}^{*} r_{j,k+1} + r_{j,kp}^{*} r_{j,k+2} + r_{j,kp+1}^{*} r_{j,k+3} - \\
&\qquad r_{j,kp+6} r_{j,k+4}^{*} - r_{j,kp+7} r_{j,k+5}^{*} + r_{j,kp+4} r_{j,k+6}^{*} + r_{j,kp+5} r_{j,k+7}^{*}) \\
&= 2\Delta_h (p_{kp+2}^{*} s_k - p_{kp+3}^{*} s_{k+1} - p_{kp}^{*} s_{k+2} + p_{kp+1}^{*} s_{k+3}) + N_{j,3} \\
D &= \sum_{j=1}^{N_r} (-r_{j,kp+3}^{*} r_{j,k} + r_{j,kp+2}^{*} r_{j,k+1} - r_{j,kp+1}^{*} r_{j,k+2} + r_{j,kp}^{*} r_{j,k+3} - \\
&\qquad r_{j,kp+7} r_{j,k+4}^{*} + r_{j,kp+6} r_{j,k+5}^{*} - r_{j,kp+5} r_{j,k+6}^{*} + r_{j,kp+4} r_{j,k+7}^{*}) \\
&= 2\Delta_h (p_{kp+3}^{*} s_k + p_{kp+2}^{*} s_{k+1} - p_{kp+1}^{*} s_{k+2} - p_{kp}^{*} s_{k+3}) + N_{j,4} \\
E &= \sum_{j=1}^{N_r} (r_{j,kp+4}^{*} r_{j,k} + r_{j,kp+5}^{*} r_{j,k+1} + r_{j,kp+6}^{*} r_{j,k+2} + r_{j,kp+7}^{*} r_{j,k+3} + \\
&\qquad r_{j,kp} r_{j,k+4}^{*} + r_{j,kp+1} r_{j,k+5}^{*} + r_{j,kp+2} r_{j,k+6}^{*} + r_{j,kp+3} r_{j,k+7}^{*}) \\
&= 2\Delta_h (p_{kp} s_k + p_{kp+1} s_{k+1} + p_{kp+2} s_{k+2} + p_{kp+3} s_{k+3}) + N_{j,5} \\
F &= \sum_{j=1}^{N_r} (-r_{j,kp+5}^{*} r_{j,k} + r_{j,kp+4}^{*} r_{j,k+1} + r_{j,kp+7}^{*} r_{j,k+2} - r_{j,kp+6}^{*} r_{j,k+3} - \\
&\qquad r_{j,kp+1} r_{j,k+4}^{*} + r_{j,kp} r_{j,k+5}^{*} + r_{j,kp+3} r_{j,k+6}^{*} - r_{j,kp+2} r_{j,k+7}^{*}) \\
&= 2\Delta_h (p_{kp+1} s_k - p_{kp} s_{k+1} + p_{kp+3} s_{k+2} - p_{kp+2} s_{k+3}) + N_{j,6} \\
G &= \sum_{j=1}^{N_r} (-r_{j,kp+6}^{*} r_{j,k} - r_{j,kp+7}^{*} r_{j,k+1} + r_{j,kp+4}^{*} r_{j,k+2} + r_{j,kp+5}^{*} r_{j,k+3} - \\
&\qquad r_{j,kp+2} r_{j,k+4}^{*} - r_{j,kp+3} r_{j,k+5}^{*} + r_{j,kp} r_{j,k+6}^{*} + r_{j,kp+1} r_{j,k+7}^{*}) \\
&= 2\Delta_h (p_{kp+2} s_k - p_{kp+3} s_{k+1} - p_{kp} s_{k+2} + p_{kp+1} s_{k+3}) + N_{j,7} \\
H &= \sum_{j=1}^{N_r} (-r_{j,kp+7}^{*} r_{j,k} + r_{j,kp+6}^{*} r_{j,k+1} - r_{j,kp+5}^{*} r_{j,k+2} + r_{j,kp+4}^{*} r_{j,k+3} - \\
&\qquad r_{j,kp+3} r_{j,k+4}^{*} + r_{j,kp+2} r_{j,k+5}^{*} - r_{j,kp+1} r_{j,k+6}^{*} + r_{j,kp} r_{j,k+7}^{*}) \\
&= 2\Delta_h (p_{kp+3} s_k + p_{kp+2} s_{k+1} - p_{kp+1} s_{k+2} - p_{kp} s_{k+3}) + N_{j,8}
\end{aligned}
\tag{5.18}
$$

where and

$N_{j,1}$, $N_{j,2}$, …, $N_{j,8}$ are noise terms.

Substituting (5.18) into (5.17), the final equations for the signal detection can be derived and expressed as:

$$\begin{aligned}\tilde{s}_k &= \Delta_h s_k + N_9 \\ \tilde{s}_{k+1} &= \Delta_h s_{k+1} + N_{10} \\ \tilde{s}_{k+2} &= \Delta_h s_{k+2} + N_{11} \\ \tilde{s}_{k+3} &= \Delta_h s_{k+3} + N_{12}\end{aligned} \tag{5.19}$$

where N_9, N_{10}, N_{11} and N_{12} are noise terms.

Following the same joint iterative process as described in the previous section, detected signals , , and will, in the next iteration, be the new pilots , , and . And with the help of (5.15) channel parameters will be estimated in order to recover , , and according to equations (5.16) to (5.19). Similarly, the second group of decoded data , and will, in the same iteration, be the new pilots , , and and with the help of (5.15), channel parameters will be estimated in order to recover , , and according to equations (5.16) to (5.19).

As it can be noticed, this method is simple, cost and computation effective as two SFBC blocks per group are decoded simultaneously. Hence, decoding using groups increases the decoding speed linearly with the number of pilot subcarriers. For a higher number of pilot subcarriers, a higher number of groups will be generated and therefore, higher number of SFBC blocks will be decoded at a time.

In addition, the method is cost and computation effective because the pilot sequence is scattered in the transmitted OFDM symbol and matrix inversion is not required at the receiver as opposed to other techniques proposed in the literature. Absence of matrix inversion at the receiver simplifies the receiver algorithm as well as the implementation cost. Finally, as demonstrated in the previous sections, the proposed method is suitable for any number of transmit or receive antennas and can be adapted to SFBC codes of different matrix rates.

5.6 Simulation Results

The performance of the proposed channel estimation algorithm is evaluated by computer simulation in a Mobile WiMax environment. Mobile channels used for performance evaluation are multipath channels each experiencing Rayleigh fading with Doppler frequency. The channel parameters were set as defined by the SUI standard [91] .

For the simulation of the algorithm, two and four transmit antennas with one and two receive antennas have been used. In addition, as utilized for the channel estimation algorithm of the STBC-OFDM system in Chapter 4 Section 4.6, an OFDM block of 256 subcarriers defined in the Mobile WiMax standard have been used. This standard includes 192 data tones, 8 pilot tones and 56 guard tones. Allocation of the subcarriers of the OFDM frame is made according to the IEEE802.16e (WiMax) standard [24]; indices of -128~-101 and 101~127 are reserved for guard interval, 0 is for the DC subcarrier, -100~-1 and 1~100 are defined as the chosen subcarriers in which -88, -63, -38, -13, 13, 38, 63 and 88 are pilot subcarriers and the remaining are specified as data subcarriers. However, in order to achieve more accurate channel estimation in fast fading environments and

of because SFBC is utilized, pilot subcarriers have been redefined for this work as -76, -75, -26, -25, 25, 26, 75, and 76 for two transmit antennas. For a higher number of transmit antennas, adjacent tones would also be defined in order to have an equivalent number of data subcarriers on each side of the pilot tone (for example, subcarriers -4, -3, -2, -1, 1, 2, 3 and 4 would be used for four transmit antennas with 8 pilot subcarriers and therefore 96 data subcarriers would be found on each side of the pilot tones). Such values have been defined in order to have pilot tones regrouped to achieve more accurate channel estimation as the channel gains of two adjacent tones can be considered to be approximately equal.

Performance was observed under SUI channels 1 and 3 for 16QAM and 64QAM modulation. The channel bandwidth was set to 3.5MHz with an OFDM block duration of 0.112ms and a guard interval duration of 28.07μs. Finally, the method is proposed for systems operating in mobile environment, therefore, the method has been tested under different levels of Doppler Shift.

Figure 5-7 to Figure 5-10 depict the performance of the proposed channel estimation algorithm for different modulation orders for pilot and data subcarriers and for different number of transmit and receive antennas. The performance of the channel estimation algorithm is compared to the case where CSI is known at the receiver. For a fixed modulation order for pilot and data subcarriers, the channel estimation technique experiences a 4 to 8 dB loss compared to the case where CSI is known at the receiver.

In addition, simulation results for different number of pilot subcarriers are presented for a fixed number of data subcarriers, set to 192. It can be noticed that as the number of pilot subcarriers increase, the BER of the proposed channel

estimation technique decreases. From Figure 5-7 to Figure 5-10, it can be seen that 1 to 2 dB can be saved by increasing the number of pilot subcarriers from 8 to 24. Moreover, the performance of the system has not been evaluated for 12 pilot subcarriers when 4 transmit antennas are used due to the fact that in SFBC-OFDM, the symbols are coded through frequency, implying that a multiple of 8 is required to map G_{4c}.

Finally, from the Figure 5-7 to Figure 5-10, it can be noticed that performance improves when a lower modulation order is used for pilot subcarriers. In contrast to most proposed work where the modulation order utilized by the pilot sequence is fixed, in this work, we have considered two types of modulation orders for the pilot sequence. From this, it has been observed that when the pilot subcarriers are modulated using a lower modulation order than that used by the data subcarriers, a more accurate channel estimation is obtained which leads to an improvement in the BER performance. Thus, from the results, it can be seen that when the modulation order for the pilot sequence is reduced to BPSK, the performance of the estimation method is improved by 1 to 3dB. The modulation order for pilot and data subcarriers is denoted by BPSK/16QAM, this means that the pilot sequence is modulated using BPSK and data sequence is modulated using 16QAM.

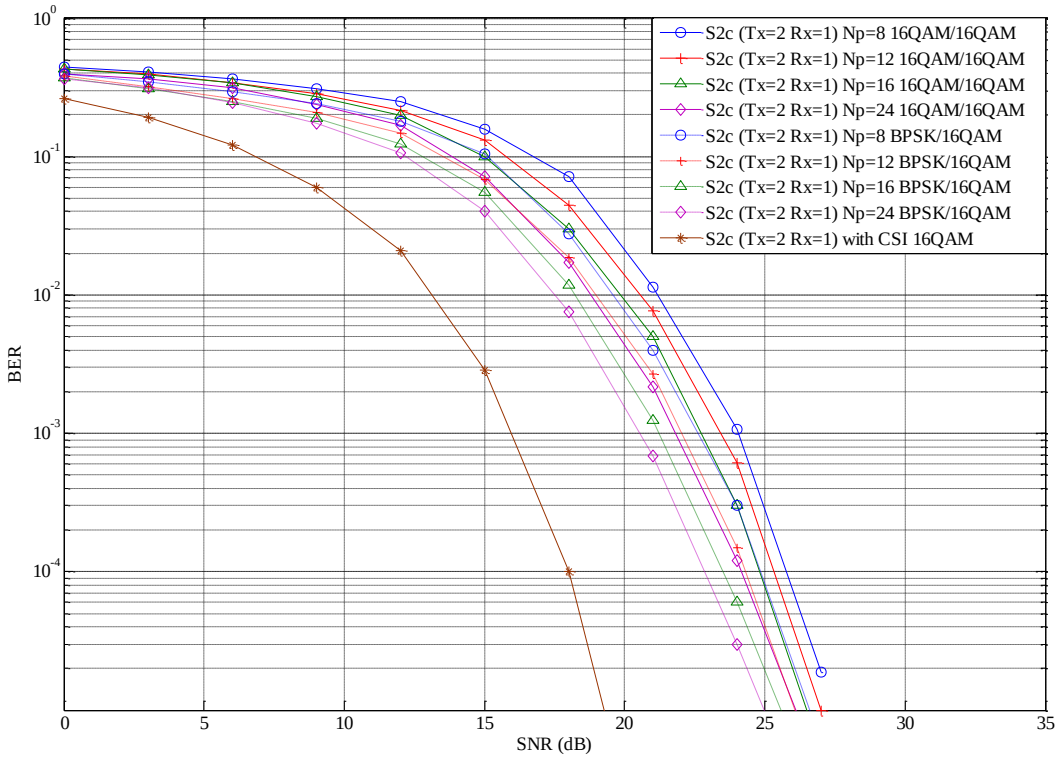

Figure 5-7: Effect of the use of Different Modulation and Pilot length for 2 Transmit and 1 Receive Antennas

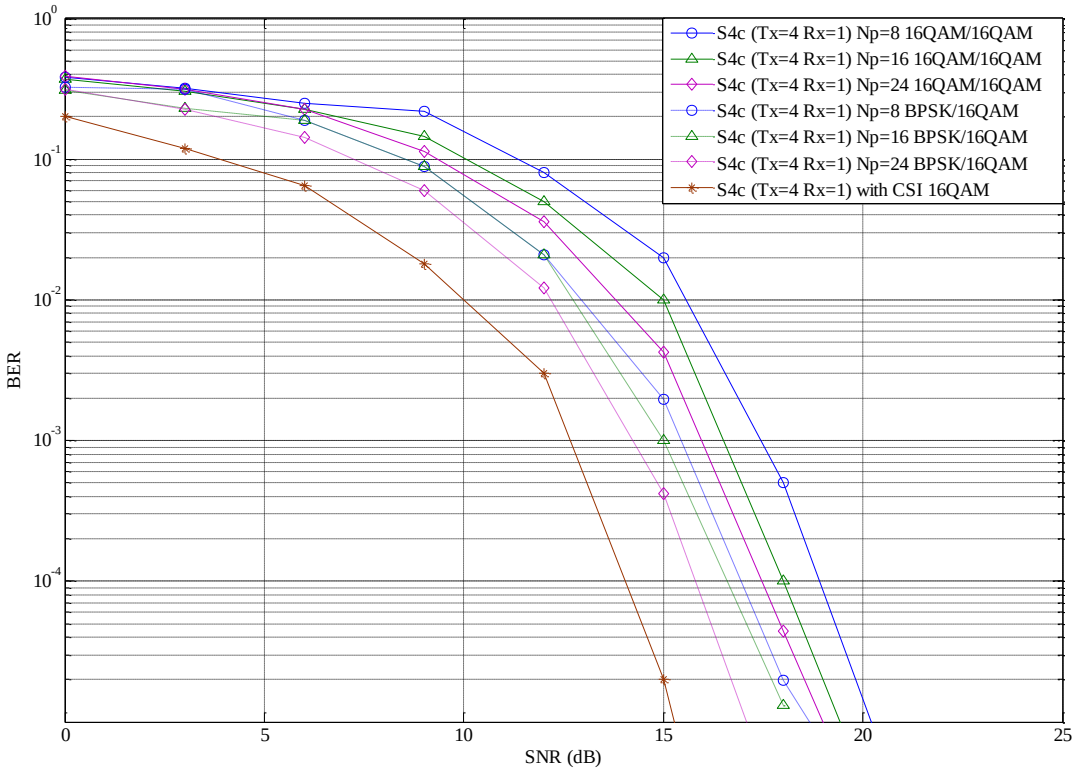

Figure 5-8: Effect of the use of Different Modulation and Pilot Length for 4 Transmit and 1 Receive Antennas

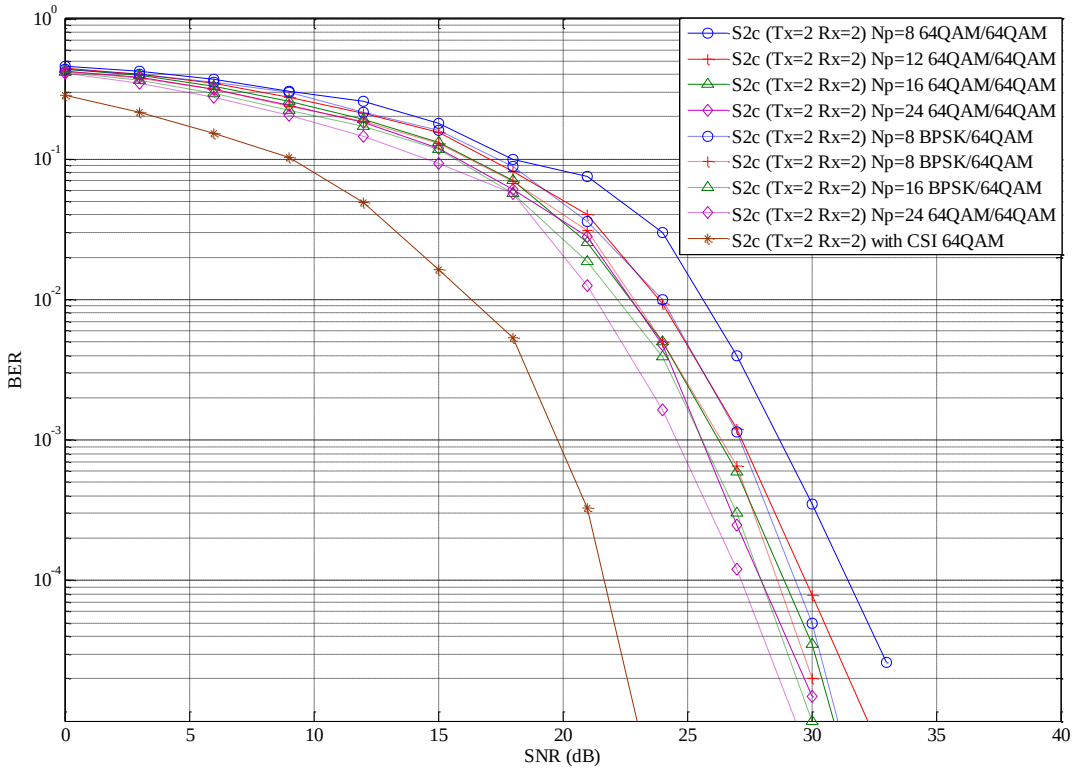

Figure 5-9: Effect of the use of Different Modulation and Pilot Length for 2 Transmit and 2 Receive Antennas

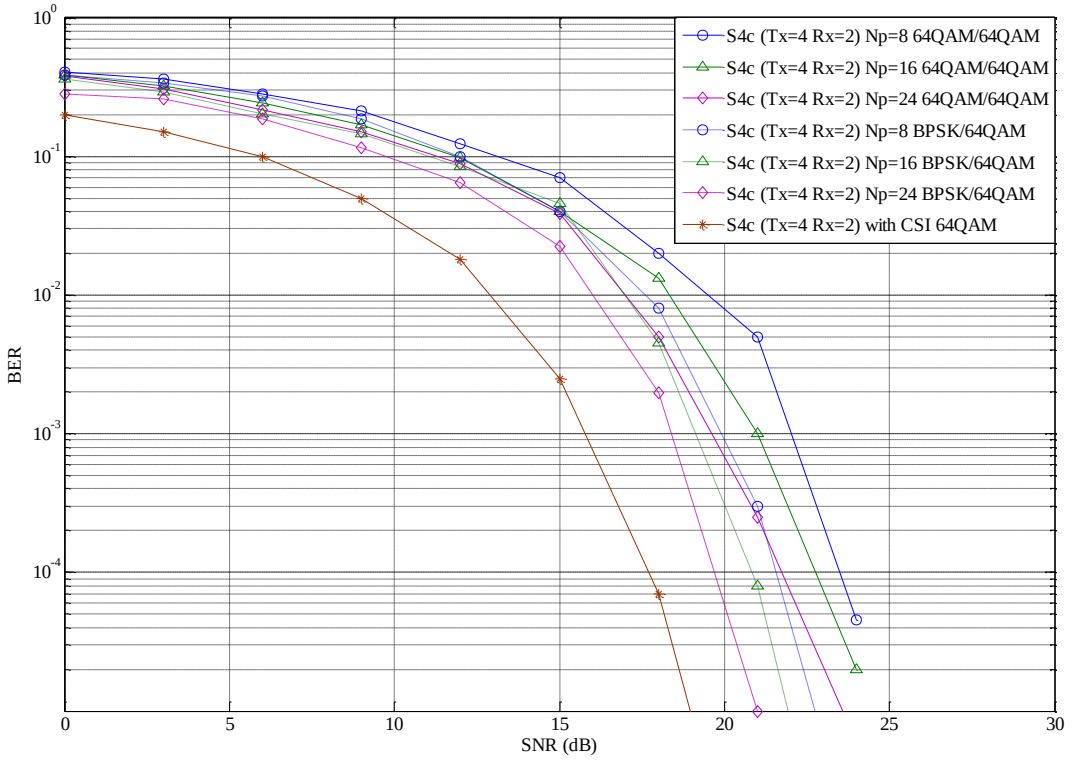

Figure 5-10: Effect of the use of Different Modulation and Pilot Length for 4 Transmit and 2 Receive Antennas

From the case where similar modulation order is used for both pilot and data subcarriers to the case where BPSK is used to modulate pilot subcarriers with the number of pilot subcarriers increased from 8 to 24, a BER reduction of 3 dB can be obtained. However, this result should be considered with caution as a higher number of pilot subcarriers would imply a reduction in the length of the guard interval or an increase in bandwidth use. Significant reduction of the guard interval length would cause ISI, therefore a trade off between number of pilot subcarriers and BER performance needs to be found.

Simulations results presented above have been compared in Figure 5-11 and Figure 5-12 with the results obtained for STBC-OFDM for two and four transmit antennas and one receive antenna. From Figure 5-11 and Figure 5-12, it can be seen that STBC-OFDM and SFBC-OFDM achieve similar performance, with STBC-OFDM achieving 1dB improvement compared to SFBC-OFDM. The reason for this difference is due to the fact that, for example, for 8 pilot subcarriers designed for two transmit antennas, channel estimation will be performed 8 times for STBC-OFDM while it will only be performed 4 times for SFBC-OFDM. This is mainly because STBC-OFDM is coded through multiple OFDM symbols which make the code more vulnerable to mobile environments while SFBC-OFDM is coded through multiple subcarriers. Hence, it can be implied that SFBC-OFDM performs better because for 8 pairs of channel estimations (16 pilot subcarriers), SFBC-OFDM achieves lower BER of 1-2dB compared to STBC-OFDM.

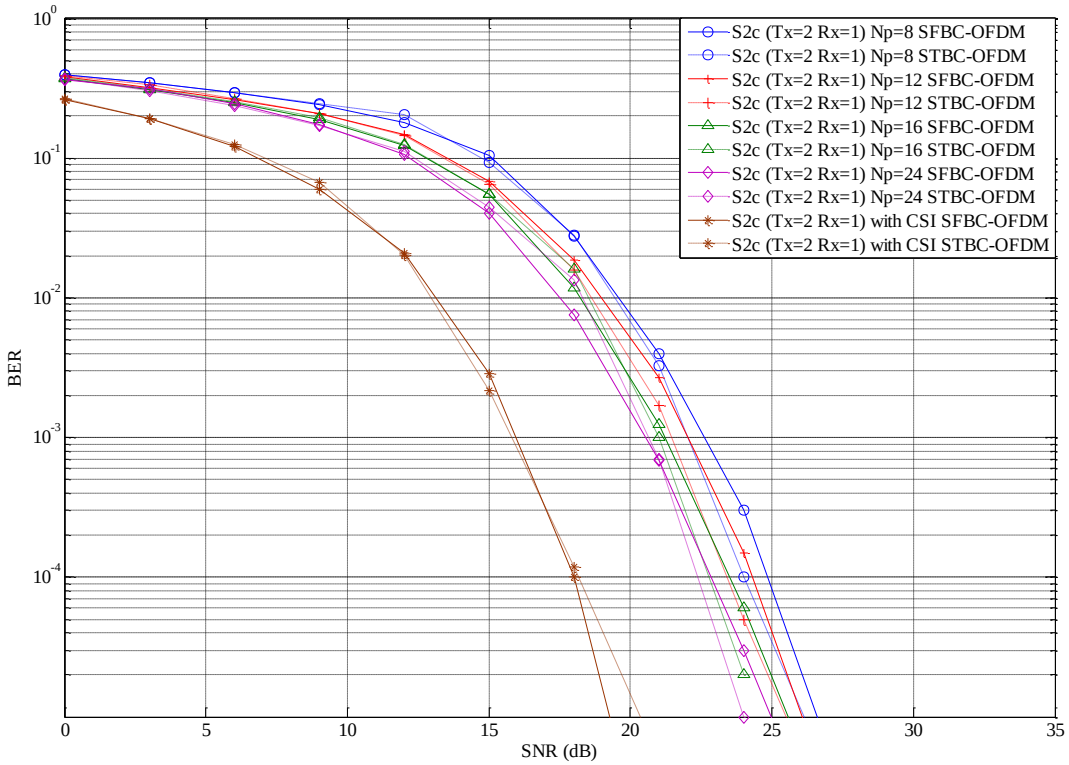

Figure 5-11: Comparison Results for 2 Transmit and 1 Receive Antennas between STBC-OFDM and SFBC-OFDM under BPSK/16QAM

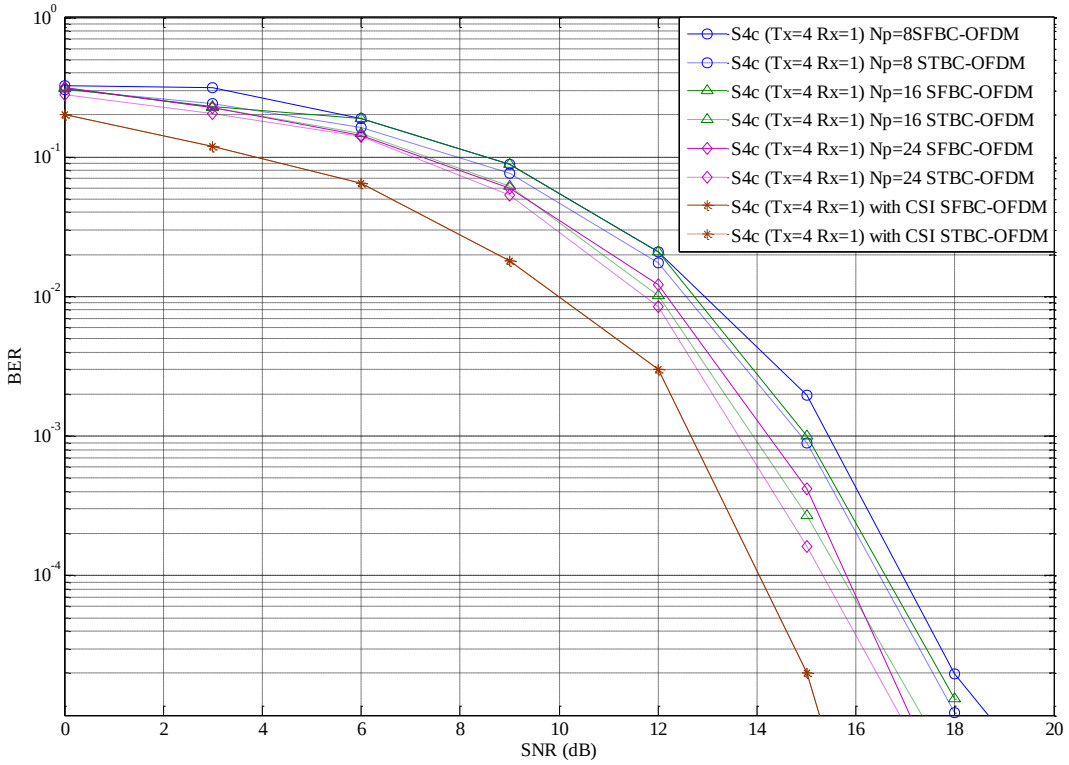

Figure 5-12: Comparison Results for 4 Transmit and 1 Receive Antennas between STBC-OFDM and SFBC-OFDM under BPSK/16QAM

As in Chapter 4 Section 4.6 for STBC-OFDM, simulation of the iterative joint channel estimation were realised under various channel conditions. Figure 5-13 and Figure 5-14 show the performance results of the proposed method under SUI1 and SUI3 for 2 and 4 transmit antennas with one receive antenna respectively. Similar conclusions to the one made earlier in Chapter 4 Section 4.6 for STBC-OFDM occurs, the behaviour of the methods are similar under SUI1 and SUI3, but due to the smaller delay spread of SUI3, SUI3 gives higher BER than SUI1. The difference between the two cases is about 2dB when BPSK modulation is used for pilot subcarriers and 16QAM is used for data subcarriers.

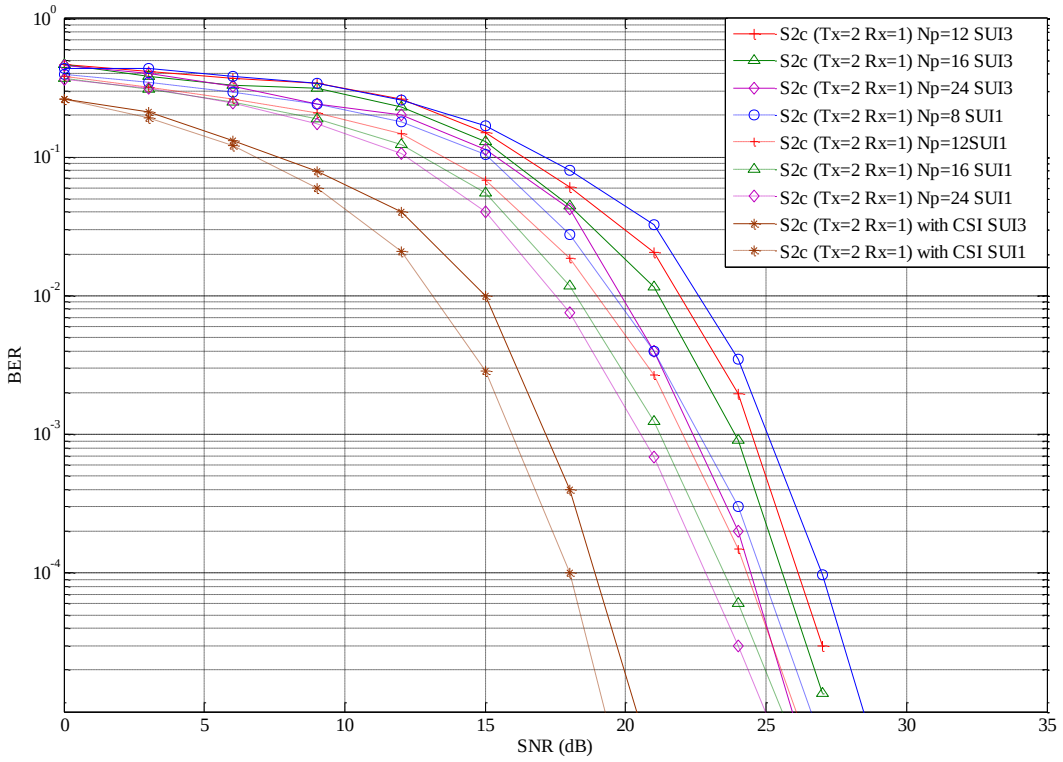

Figure 5-13: Comparison Results between SUI1 and SUI3 for 2 Transmit and 1 Receive Antennas

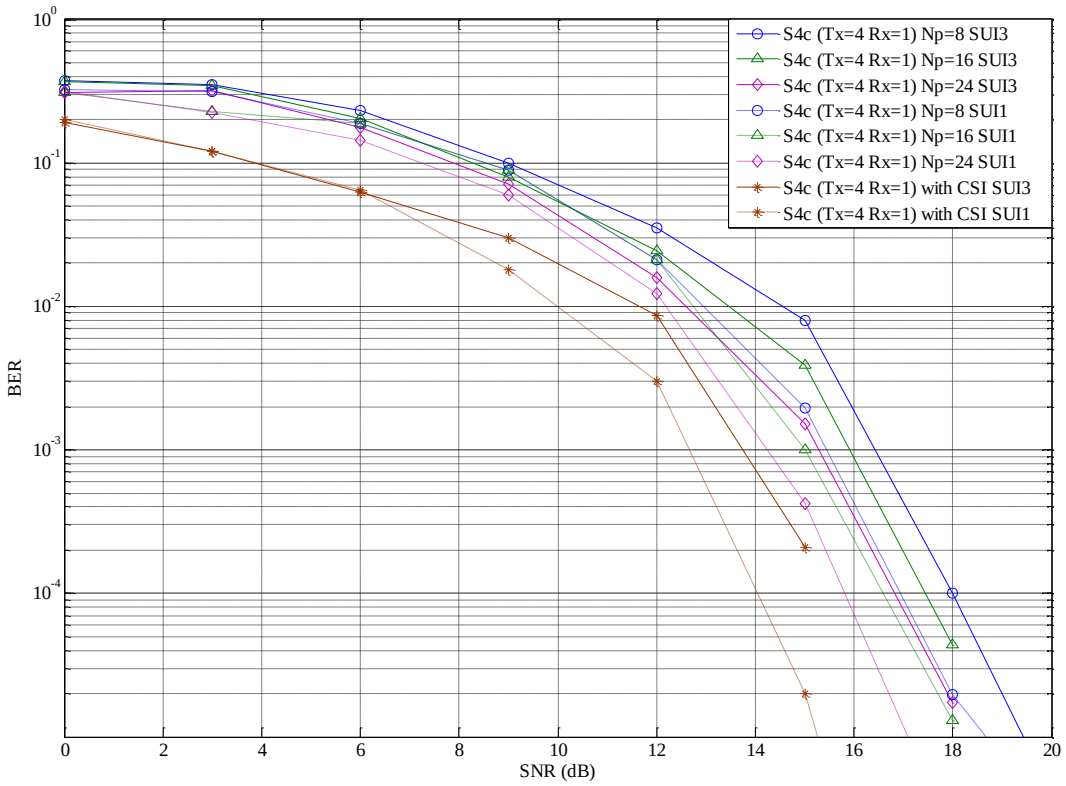

Figure 5-14: Comparison Results between SUI1 and SUI3 for 4 Transmit and 1 Receive Antennas

Simulation results presented in Figure 5-15 to Figure 5-18 were performed for different levels of Doppler shift with a carrier frequency of 2.5GHz. The system was tested for speed varying from 20 km/h to 90 km/h. Results show that as the speed increases, the estimation becomes less accurate. Therefore, performance declines as Doppler shift increases. Higher expected loss can be found when the receiver is mobile. Indeed, as far as the Doppler shift is concerned, a penalty of 3 to 10 dB is observed between the ideal case where the Doppler shift is low and the case where Doppler shift is equal to 200Hz.

According to the Doppler shift and compared to the low mobility scenario, penalty of 1dB to 9dB can be observed. It is thus clear that the proposed method is sensitive to high mobility environments. The results in the proposed method still show better performance than the one given in [92] where performance

degradation observed for 4 transmit antennas ranges from 5dB to more than 10dB as estimation error is increased. In space frequency coding, detection is achieved within one OFDM symbol. Therefore, systems are less susceptible to Doppler interference than STBC-OFDM systems. From [31], it can be seen that STBC-OFDM systems reach their BER limits faster than SFBC-OFDM systems.

From the results, it is also evident that in contrast to scenarios where the modulation order for both pilot and data subcarriers is fixed, using BPSK modulation for the pilot subcarriers improves the performance by 1 to 3dB even in mobile environments.

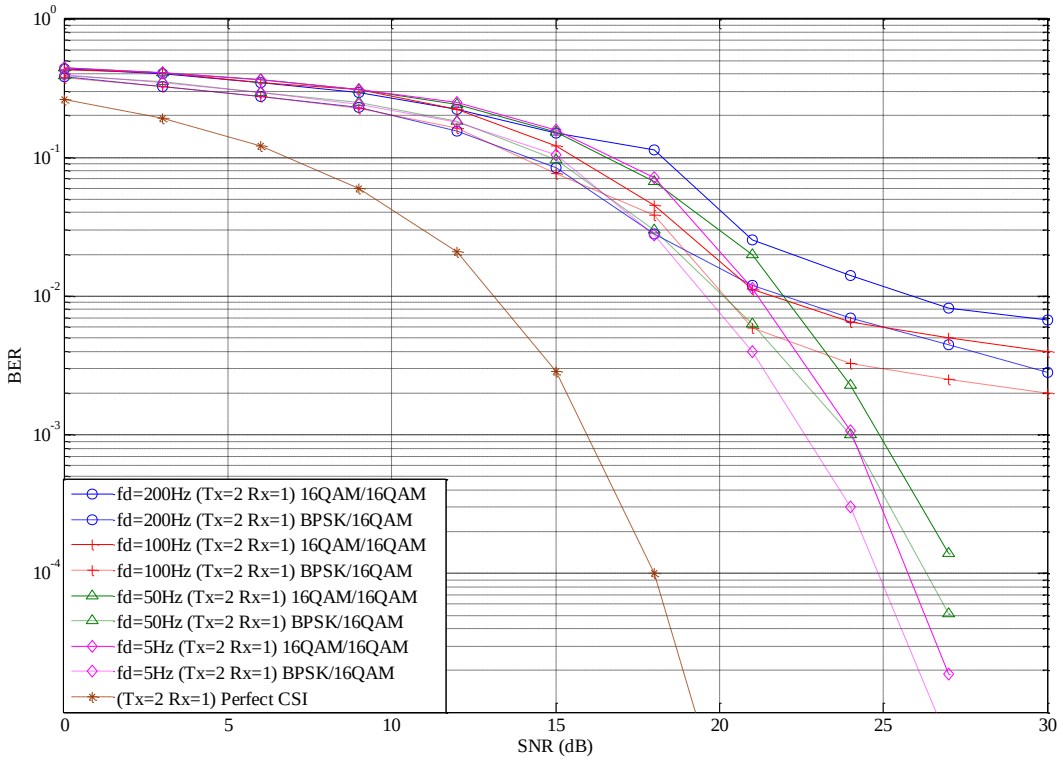

Figure 5-15: Performance of the Proposed Technique under Various Speed for 2 Transmit Antennas and 1 Receive Antenna under 16QAM

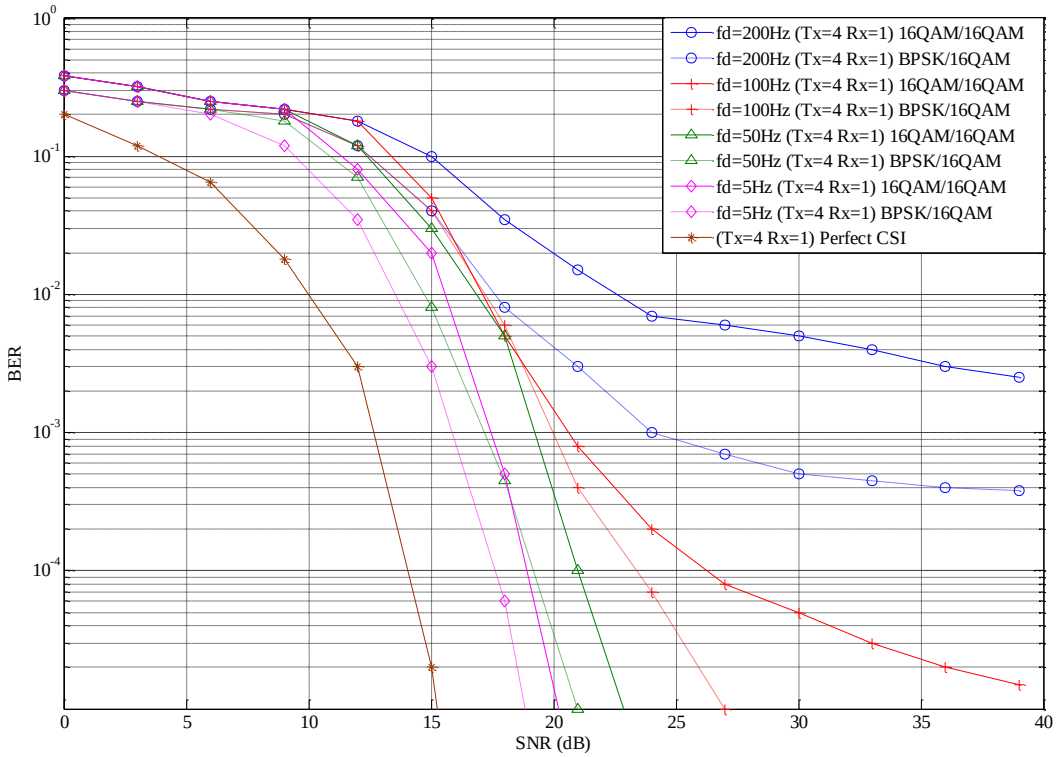

Figure 5-16: Performance of the Proposed Technique under Various Speed for 4 Transmit Antennas and 1 Receive Antenna under 16QAM

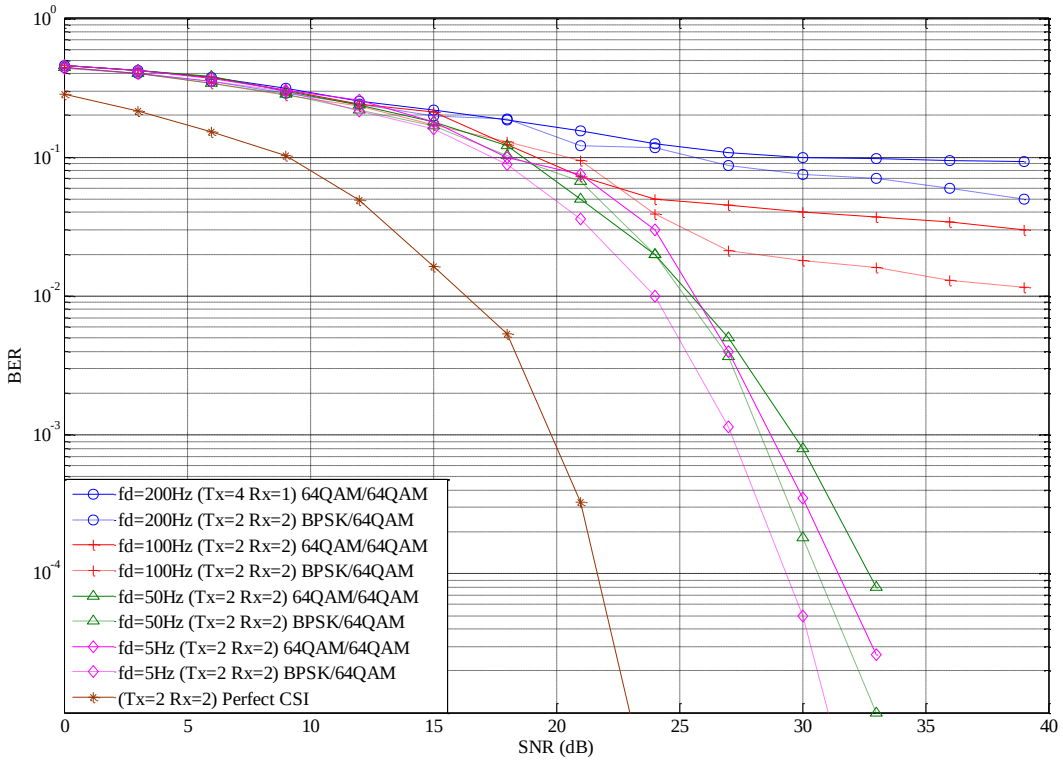

Figure 5-17: Performance of the Proposed Technique under Various Speed for 2 Transmit Antennas and 2 Receive Antennas under 64QAM

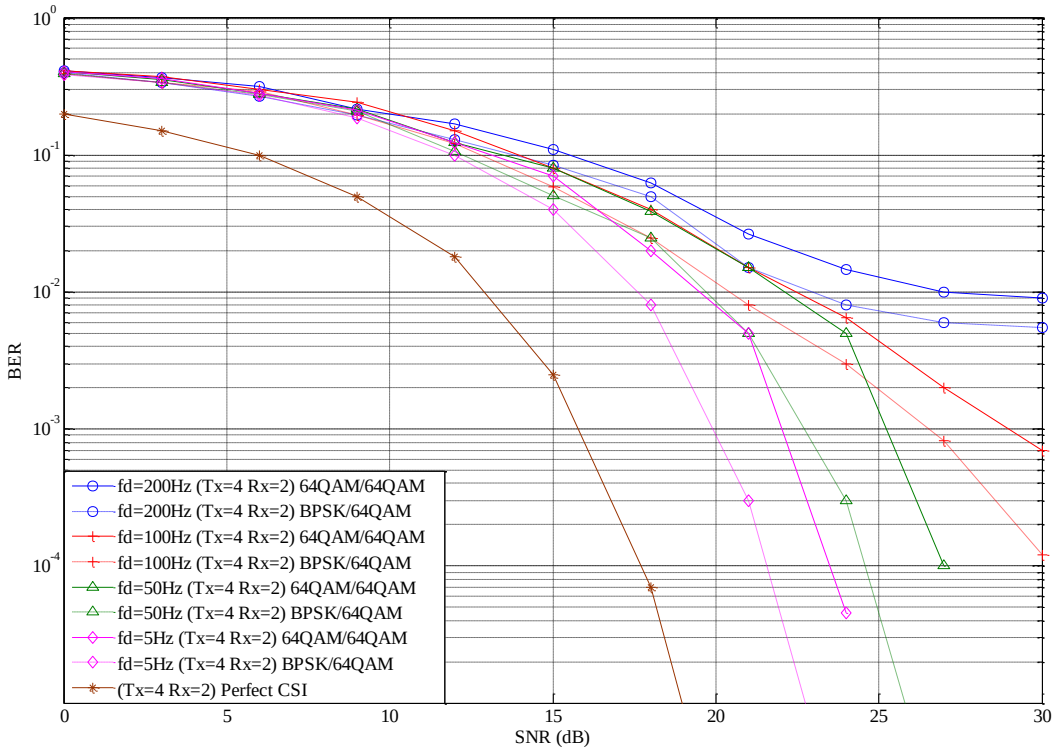

Figure 5-18: Performance of the Proposed Technique under Various Speed for 4 Transmit Antennas and 2 Receive Antennas under 64QAM

With the proposed iterative channel estimation technique, the grouping of symbols improves the computational efficiency of the system. When the number of pilot symbols increase, the number of groups also increases. This means that the decoding time is reduced as two sets of SFBC-OFDM symbols are decoded concurrently in each group. Moreover, with the use of SFBC-OFDM, decoding can take place within one OFDM symbol which when compared to STBC-OFDM, saves half of the memory used. Indeed, in order to decode the data in STBC-OFDM, the system needs to save two OFDM symbols in contrast to SFBC-OFDM where the system needs to save only one OFDM symbol. Thus, it can be concluded that space frequency coded OFDM system is a good candidate for high mobility environments.

Finally, investigation focused on the decoding time required to decode an entire SFBC-OFDM symbols and the percentage time saved. Table 5-1 and Table

5-2 show the decoding time and decoding time saved per SFBC-OFDM symbols respectively for 2 and 4 transmit antennas and 1 and 2 receive antennas. In contrast to STBC-OFDM where there is no relationship between the decoding time and the number of transmit antennas or number of pilot symbols used, from Table 5-1, it is clear that the decoding time per SFBC-OFDM symbol is reducing linearly with the number of antennas. Indeed, by looking at 2 transmit antennas and one receive antenna, it can be noticed that the time to decode the OFDM symbol for 16 pilot subcarriers is half the time to decode the OFDM symbol for 8 pilot subcarriers. In addition the time for 24 pilot subcarriers is a third of the time taken to decode the OFDM symbol with 8 pilot subcarriers. It can also be seen from Table 5-1 that the decoding time depends only on the number of transmit antennas and has no relationship with the number of received antennas used.

Table 5-2 shows the percentage bandwidth saved. Due to the fact that the decoding time has no relationship with the number of receive antennas, it can be seen that percentage value for 2 transmit and 1 and 2 receive antennas are similar, and that similar conclusions can be made for the case of four transmit antennas. Finally, it can be seen that the time saved increases exponentially with the number of pilot used.

Table 5-1: Decoding Time per SFBC-OFDM Symbol

Number of Pilot Subcarriers	Decoding Subcarrier per Subcarrier	8 Pilot Subcarriers	12 Pilot Subcarriers	16 Pilot Subcarriers	24 Pilot Subcarriers
Tx=2 Rx=1	0.75s	0.195s	0.127s	0.096s	0.065s
Tx=2 Rx=2	0.75s	0.199s	0.131s	0.099s	0.066s
Tx=4 Rx=1	1.2s	0.382s	N/A	0.195s	0.128s
Tx=4 Rx=2	1.2s	0.388s	N/A	0.195s	0.132s

Table 5-2: Decoding Time Saved per OFDM Symbol

Number of Pilot Subcarriers	8 Pilot Subcarriers	12 Pilot Subcarriers	16 Pilot Subcarriers	24 Pilot Subcarriers
Tx=2 Rx=1	74%	83%	87.2%	91.3%
Tx=2 Rx=2	73.8%	82.8%	87%	91.3%
Tx=4 Rx=1	68.2%	N/A	83.8%	89.3%
Tx=4 Rx=2	67.9%	N/A	83.9%	89.1%

5.7 Conclusions

In this Chapter, a new channel estimation method is proposed for SFBC-OFDM systems. The effects of channel estimation for mobile SFBC-OFDM systems have been studied. A new iterative channel estimation method using SFBC coded groups of subcarriers has been presented and simulated under high mobility frequency selective channels. In addition, the method has been simulated for various numbers of pilot subcarriers using 2 types of SUI channels.

The system proposed in this paper offers an efficient and computation-effective algorithm where all groups are decoded simultaneously and where the initial training sequence is limited. Limitation of the training sequence offers a trade-off between accurate channel estimation and efficient bandwidth usage as more pilots would allow the algorithm to perform more accurate channel estimation at the cost of less transmitted data or more ISI. Furthermore, low sensitivity of the system to mobile environments has been demonstrated. Performance of the system can be improved by inserting an error correction technique or by inserting a coding technique such as low density parity check (LDPC). One of the most important conclusions of the Chapter is that the proposed method does not require any matrix inversion at the receiver and that the system is not sensitive to mobile environments. Moreover, the algorithm has been demonstrated suitable for any number of transmit or receive antennas and for any modulation order as well as any number of pilot and data subcarriers.

Finally, in this chapter, it has been demonstrated that SFBC-OFDM performs better than STBC-OFDM in terms of computational complexity and robustness in fading. Indeed, from simulation results, it can be noticed that decoding time is less in SFBC-OFDM compared to the one for STBC-OFDM. This is due to the fact that only one OFDM symbol is required in SFBC-OFDM to decode the transmitted data. Moreover, in mobile environments, the performance of STBC-OFDM would be reduced due to the fact that data is coded over multiple OFDM symbols. However, when compared to STBC-OFDM in slow fading environments, for the same number of pilot subcarrier, it can be noticed that STBC performed better. This is due to the fact that in STBC, channel estimation is performed using pilot symbols coded over multiple OFDM symbols and therefore

allows the creation of higher number of groups compared to SFBC-OFDM. On the contrary, when STBC-OFDM and SFBC-OFDM are compared in terms of groups, it can be seen that SFBC-OFDM performed better. Therefore, a new coding combination between STBC and SFBC is proposed in the following chapter.

6 Channel Estimation for SFBC/STBC and STBC/SFBC with OFDM

In this Chapter, an iterative channel estimation algorithm with joint detection is proposed for MIMO-OFDM systems using STBC and SFBC. In Chapter 4 and 5, joint iterative channel estimation was proposed for STBC-OFDM and SFBC-OFDM respectively. From the analysis of the results of the two previous channel estimation methods, it was identified that significant benefits can be achieved when pilot and data symbols are encoded using STBC and SFBC respectively. From Chapter 5, it was identified that SFBC performs better than STBC when the same amount of estimation is used for data recovery. Further modification of the algorithms of Chapter 5 has led to the development of an STBC-SFBC alternating scheme. In this scheme the STBC and SFBC designs are switched between pilot and data subcarriers in order to enhance the performance of SFBC codes without increasing the number of pilot subcarriers. We demonstrate the efficiency of the method through computer simulation and comparison of the simulation results with the results obtained in Chapter 4 and 5.

6.1 Introduction

Since the pioneering work introduced by Li in [68], various channel estimation algorithms have been proposed for STBC/SFBC-OFDM systems [31, 93, 94]. Among these methods, pilot aided channel estimation based on Discrete Fourier

Transform (DFT) using minimum mean square error (MMSE) or Maximum likelihood (ML) have been studied for OFDM systems [31, 95]. For a sufficient number of pilots, the two methods have comparable performance but the ML scheme is simpler to implement than the MMSE. Thus, our focus in this Chapter is on the development of a pilot aided channel estimation algorithm with ML detection.

A pilot aided channel estimation method using ML was proposed in [31] and compared with MMSE method and Kalman filtering method in [96] and [97] respectively. The proposed channel estimation method is applied to STBC-OFDM systems for different number of transmit and receive antennas. Unlike the method proposed in [31], we propose in this Chapter an iterative channel estimation algorithm for STBC-OFDM and SFBC-OFDM. The proposed iterative joint channel estimation and decoding algorithm improves the receiver performance and is specifically suited for mobile environments. This is largely because the algorithm is based on a processive re-estimation of channel parameters immediately after each set of symbols are decoded. The novelty of the proposed algorithm mainly comes from the fact that the method employs a concatenation of STBC and SFBC designs to estimate channel parameters and decode the transmitted data. Hence, an STBC-SFBC alternating scheme for pilot and data subcarriers is proposed. Another significant contribution of this Chapter comes from the fact that the channel estimation technique presented in this work is a STBC/SFBC-OFDM method based on ML detection. Moreover, as an improvement to the methods proposed in the literature; this method does not require any matrix inversion at the receiver. As a result of the orthogonal property of STBC/SFBC, it has been possible to derive exact and simple analytical

expressions to estimate the unknown channel parameters. The method can also support any number of transmit or receive antennas as well as any type of modulation scheme for pilot and data subcarriers. As proposed for STBC-OFDM and SFBC-OFDM, OFDM symbols are divided into groups, which are decoded simultaneously according to the number of pilot subcarriers used. Once the number of groups is defined, each group is assigned a specific number of pilot subcarriers equal to the number of frequency slots required to transmit one STBC/SFBC coded training block. The grouping approach employed in this work reduces the number of computations which is linearly proportional to the number of pilot subcarriers used.

In this Chapter two approaches are described, first, SFBC is used to encode pilot subcarriers while STBC is used to encode data subcarriers. Then in a second part, encoding between pilot and data subcarriers is switched such that STBC is now used for pilot subcarriers while SFBC is used for data subcarriers. The efficiency of the two methods has been tested via computer simulations for various scenarios and comparison with previous proposed methods is given. The proposed methods are suitable for present and future technologies such as 3G-LTE, 4G or WiMax especially those operating in mobile environments.

6.2 Systems Architecture

A MIMO-OFDM system with M_t transmit antennas and N_r receive antennas, employing N_{FFT} subcarriers from which N_s are used to transmit data symbols, N_p are used to transmit pilot symbols and the remaining N_{FFT} - N_s - N_p subcarriers are used as DC subcarrier and guard interval, is shown in Figure 6-1. At time t, a binary data block X(t) of q bits is scrambled and mapped using a set of predefined

constellation diagram (BPSK, QPSK, 16-QAM, 64-QAM, 256-QAM) resulting in a symbol stream $\{S = [s_0, s_1, \ldots, s_k, s_{k+1}, \ldots, s_x]^T\}_{k=0,2,\ldots,x,}$. Simultaneously, a binary data block Xp(t) is modulated resulting in a pilot sequence which is known at the receiver. The value of *x* and *xp* are determined by the encoding type employed, the number of transmit antennas and the rank of the matrix. For example for two transmit antennas, *x*=2Ns-1 (*xp*=2Np-1) and *x*=Ns-1(*xp*=Np-1) for STBC and SFBC respectively. Each block of pilot and data is then sent to the Space-Time and Space-Frequency or Space-Frequency and Space-Time encoder respectively. Encoding is based on the Alamouti scheme [5]. Data is then split to the different antennas according to the encoding used for data and pilot subcarriers such that . Then, once encoded, the known pilot sequence is added to the generated signal and allocated to the different antennas. For each antenna, an N-point inverse Fast Fourier Transform (IFFT) is applied to convert the coded data from frequency domain to time domain. Finally, cyclic prefix is added to each OFDM symbol and data is transmitted simultaneously from different antennas. It is assumed that time and frequency synchronization of the system is perfect.

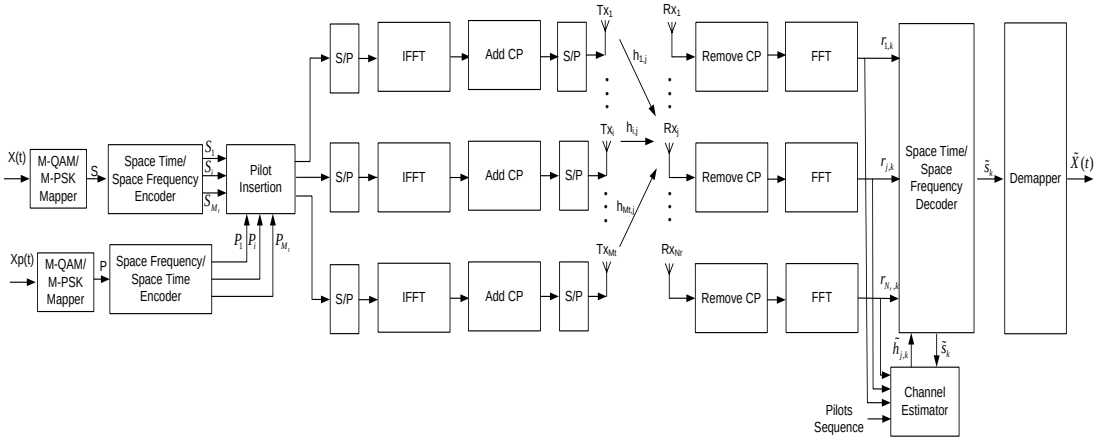

Figure 6-1: Block Diagram of the Proposed Method

At the receiver, an inverse procedure is employed. Data is received and down converted, cyclic prefix is removed and FFT operation is performed. Alamouti's encoding scheme offers a simple decoding algorithm when channel parameters are known at the receiver. Therefore, extra attention has been paid to the channel estimation aspect.

The transmitted sequence across all transmit antennas passes through a fast frequency selective channel with adaptive white Gaussian noise. The received signal between the *i*-th transmit antenna and the *j*-th receive antenna, after OFDM demodulation is applied, can be expressed in matrix form as:

$$R_j(n) = \sum_{i=1}^{M_t} H_{i,j}(n) S_i(n) + N_j(n) \qquad (6.1)$$

where $S_{i,k}(n)=[s_0, s_1,...s_{x-1}]$ and where $N_{j,k}(n)$ represents the white Gaussian noise with variance per dimension, $H_{i,j,k}(n)$ is the time varying channel tap between the *i*-th transmit antenna and the *j*-th receive antenna of the *n*-th OFDM

symbol and $S_{i,k}(n)$ represents the transmitted signal from the *i*-th antenna of the *n*-th OFDM symbol.

Data is then sent to the channel estimator in order to estimate channel parameters at pilot subcarriers. The estimated channel is sent to Space-Time/Frequency Decoder in order to be used to recover the transmitted data sequence which is finally detected using ML.

6.3 Channel Estimation Strategy

An iterative joint channel estimation strategy which is similar to the one proposed for STBC-OFDM and SFBC-OFDM, is proposed in this Chapter. The fact that STBC and SFBC are both orthogonal codes allows the combination of the two coding schemes and allows us to propose the STBC/SFBC-OFDM channel estimation strategy where pilot and data subcarriers are encoded using STBC and SFBC respectively. Also, on the other hand, the SFBC/STBC-OFDM channel estimation strategy is proposed where pilot and data subcarriers are encoded using STBC and SFBC respectively.

As described in Chapter 4 and 5, Np and Ns pilot and data subcarriers are used to estimate the channel parameters and recover the transmitted sequence. A grouping strategy is also applied where the number of data subcarriers per group is pre-determined such that $L_{sub/group}=N_s/N_p$ and the number of groups is equal to $N_{group}=N_s/L_{sub/group}=N_p$ for STBC/SFBC-OFDM. In the case of SFBC/STBC-OFDM, $L_{sub/group}=N_s/(N_p/ N_{FS})$ which results in a number of groups per OFDM symbol equal to $N_{group/OFDM}= N_s/ L_{sub/group}$. According to the encoding scheme used, for two transmit antennas, 1 or 2 pilot subcarriers are assigned to each group for STBC/SFBC-OFDM and SFBC/STBC-OFDM system respectively.

Significant benefits are realized for SFBC-OFDM systems, for example when 8 pilot subcarriers are utilized, the OFDM symbol is divided into 4 groups. On the contrary when STBC/SFBC-OFDM systems are utilized for the same amount of pilot subcarriers, 8 groups of data would be generated. As identified in Chapters 4 and 5, higher number of subcarriers results in a higher number of groups and therefore the channel estimation is more accurate. Indeed, from Chapter 5 it is realized that, SFBC-OFDM achieves better performance than STBC-OFDM when comparison is based on the same number of groups.

The integration of STBC with SFBC-OFDM systems will however lead to the assumption that channel parameters remain constant over n_t OFDM symbols and over n_t adjacent subcarriers which might be a disadvantage in high mobility environments especially when the number of transmit antennas exceed 2. For the scenario where SFBC is integrated with STBC-OFDM systems, the assumption that the channel parameters remain constant over n_t OFDM symbols already exists for STBC-OFDM systems. However, an additional assumption that the channel parameters will remain constant over n_t adjacent subcarriers will be required.

6.4 SFBC Pilot Aided Channel Estimation for STBC-OFDM Systems

In this Section, pilot subcarriers are coded according to the encoding rules of SFBC-OFDM while data subcarriers are coded according to the encoding rules of STBC-OFDM.

6.4.1 SFBC/STBC-OFDM for 2 Transmit Antennas

Details of the organisation of SFBC/STBC symbols combined with OFDM can be found in Figure 6-2.

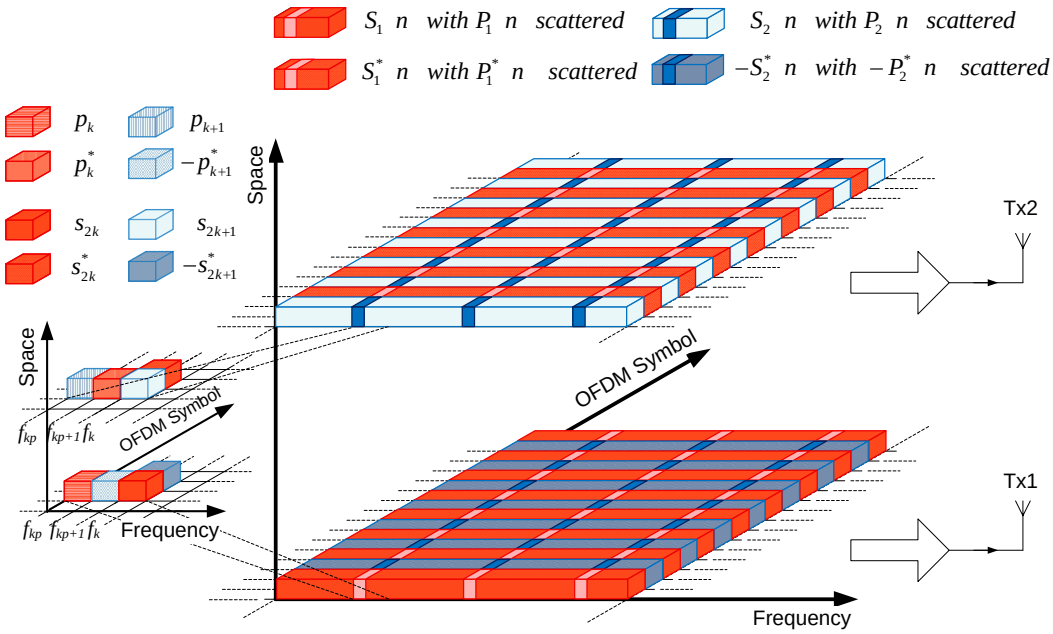

Figure 6-2: Organisation of Pilot and Data Symbol for 2 Transmit Antennas SFBC/STBC-OFDM

Therefore, to transmit two consecutive OFDM symbols, two vectors are required for pilot subcarriers while four vectors are required for the data subcarriers:

$$\begin{aligned} P_1(n) = P_1(n+1) &= [p_0, -p_1^*, \ldots, p_{kp}, -p_{kp+1}^*, \ldots, p_{Np-2}, -p_{Np-1}^*]^T \\ P_2(n) = P_2(n+1) &= [p_1, p_0^*, \ldots, p_{kp+1}, p_{kp}^*, \ldots, p_{Np-1}, p_{Np-2}^*]^T \end{aligned} \tag{6.2}$$

$$\begin{aligned} S_1(n) &= [s_0, s_2, \ldots, s_k, \ldots, s_{2Ns-4}, s_{2Ns-2}]^T \\ S_2(n) &= [s_1, s_3, \ldots, s_{k+1}, \ldots, s_{2Ns-3}, s_{2Ns-1}]^T \\ S_1(n+1) &= [-s_1^*, -s_3^*, \ldots, -s_{k+1}^*, \ldots, -s_{2Ns-3}^*, -s_{2Ns-1}^*]^T = -S_2^*(n) \\ S_2(n+1) &= [s_0^*, s_2^*, \ldots, s_k^*, \ldots, s_{2Ns-4}^*, s_{2Ns-2}^*]^T = S_1^*(n) \end{aligned} \tag{6.3}$$

where k=0, 1,…, Ns-1 and kp=0, 2, …, Np-2.

The received vector Rp_j at OFDM symbols *n* and R_j at OFDM symbols *n* and *n*+1 can be expressed as:

$$\begin{aligned} Rp_{j,kp}(n) &= [rp_{j,0},\ rp_{j,2},\ ...,\ rp_{j,2Np-4},\ rp_{j,2Np-2}]^T \\ Rp_{j,kp+1}(n) &= [rp_{j,1},\ rp_{j,3},\ ...,\ rp_{j,2Np-3},\ rp_{j,2Np-1}]^T \\ R_{j,k}(n) &= [r_{j,0},\ r_{j,2},\ ...,\ r_{j,2Ns-4},\ r_{j,2Ns-2}]^T \\ R_{j,k+1}(n+1) &= [r_{j,1},\ r_{j,3},\ ...,\ r_{j,2Ns-3},\ r_{j,2Ns-1}]^T \end{aligned} \tag{6.4}$$

For the case where SFBC is utilised for pilot subcarriers and STBC for data subcarriers, channel estimation is achieved only for OFDM symbol n and used throughout the n+1 OFDM symbols to recover the STBC coded data symbols. From Chapter 4 and 5, the received signals for pilot and data subcarriers can be written as:

$$\begin{aligned} \bar{\mathrm{R}}\mathrm{p}_\mathrm{j} &= \sum_{\mathrm{j}=1}^{\mathrm{N_r}} \bar{\mathrm{P}}\bar{\mathrm{H}}\mathrm{p}_\mathrm{j} + \bar{\mathrm{N}}\mathrm{p}_\mathrm{j} \\ \bar{\mathrm{R}}_\mathrm{j} &= \sum_{\mathrm{j}=1}^{\mathrm{N_r}} \bar{\mathrm{S}}\bar{\mathrm{H}}_\mathrm{j} + \bar{\mathrm{N}}_\mathrm{j} \end{aligned} \tag{6.5}$$

where $\bar{\mathrm{R}}\mathrm{p}_\mathrm{j}$ and $\bar{\mathrm{R}}_\mathrm{j}$ represent the received pilot and data signal at the *j*-th antenna respectively. $\bar{\mathrm{P}}$ and $\bar{\mathrm{S}}$ are the pilot and data signals respectively, $\bar{\mathrm{H}}\mathrm{p}_\mathrm{j}$, $\bar{\mathrm{H}}_\mathrm{j}$ and $\bar{\mathrm{N}}\mathrm{p}_\mathrm{j}$, $\bar{\mathrm{N}}_\mathrm{j}$ represent the channel parameters and the white Gaussian noise between the two transmit antennas and the Nr receive antennas for pilot and data signals respectively. The pilot elements of (6.5) can be expressed as:

$$\begin{aligned}
\bar{R}p_j &= \left[Rp_{j,kp}(n) \quad Rp_{j,kp+1}(n) \right]^T \\
\bar{H}p_j &= \begin{bmatrix} Hp_{1,j,kp}(n) \\ Hp_{2,j,kp}(n) \end{bmatrix} = \begin{bmatrix} Hp_{1,j,kp+1}(n) \\ Hp_{2,j,kp+1}(n) \end{bmatrix} \\
\bar{P} &= \begin{bmatrix} P_{1,kp}(n) & P_{2,kp}(n) \\ -P^*_{2,kp}(n) & P^*_{1,kp}(n) \end{bmatrix} = \begin{bmatrix} P_{1,kp}(n) & P_{2,kp}(n) \\ P_{1,kp+1}(n) & P_{2,kp+1}(n) \end{bmatrix}, \quad \bar{N}p_j = \begin{bmatrix} Np_{1,j,kp}(n) \\ Np_{2,j,kp+1}(n) \end{bmatrix}
\end{aligned} \tag{6.6}$$

The data elements are given as:

$$\begin{aligned}
\bar{R}_j &= \left[R_{j,k}(n) \quad R_{j,k}(n+1) \right]^T \\
\bar{H}_j &= \begin{bmatrix} H_{1,j,k}(n) \\ H_{2,j,k}(n) \end{bmatrix} \\
\bar{S} &= \begin{bmatrix} S_{1,k}(n) & S_{2,k}(n) \\ -S^*_{2,k}(n) & S^*_{1,k}(n) \end{bmatrix}, \quad \bar{N}p_j = \begin{bmatrix} N_{1,j,k}(n) \\ N_{2,j,k}(n) \end{bmatrix}
\end{aligned} \tag{6.7}$$

where k=0, 1,…, N_s-1.

Following the derivations made for SFBC-OFDM, the channel estimation parameters can be expressed as:

$$\tilde{H}p_j = \begin{bmatrix} \tilde{H}p_{1,j,kp}(n) \\ \tilde{H}p_{2,j,kp}(n) \end{bmatrix} = \begin{bmatrix} \tilde{H}p_{1,j,kp+1}(n) \\ \tilde{H}p_{2,j,kp+1}(n) \end{bmatrix} = \bar{P}^{-1}\bar{R}p_j = \begin{bmatrix} \dfrac{rp_{j,kp}p^*_{kp} - rp_{j,kp+1}p_{kp+1}}{|p_{kp}|^2 + |p_{kp+1}|^2} \\ \dfrac{rp_{j,kp}p^*_{kp+1} + rp_{j,kp+1}p_{kp}}{|p_{kp}|^2 + |p_{kp+1}|^2} \end{bmatrix} \tag{6.8}$$

Assuming that channel parameters remain constant over 2 OFDM symbols and over 2 SFBC and STBC adjacent blocks, the following can be derived using (6.5) and (6.8):

$$\begin{aligned}\tilde{S}_{1,k}(n) &= \sum_{j=1}^{N_r}(\tilde{H}p_{1,j,kp}(n)R_{j,k}(n) + \tilde{H}p_{2,j,kp}(n)R_{j,k}(n+1)) \\ &= \tilde{s}_{2k} = \sum_{j=1}^{N_r}(\tilde{h}p^{*}_{1,j,kp}r_{j,2k} + \tilde{h}p_{2,j,kp}r^{*}_{j,2k+1}) \\ \tilde{S}_{2,k}(n) &= \sum_{j=1}^{N_r}(\tilde{H}p^{*}_{2,j,kp}(n)R_{j,k}(n) + \tilde{H}p_{1,j,kp}(n)R^{*}_{j,k}(n+1)) \\ &= \tilde{s}_{2k+1} = \sum_{j=1}^{N_r}(\tilde{h}p^{*}_{2,j,kp}r_{j,2k} - \tilde{h}p_{1,j,kp}r^{*}_{j,2k+1})\end{aligned} \tag{6.9}$$

As stated earlier for other types of coding and from the above derivations, the proposed channel estimation method is very simple and therefore is cost and computation effective, because the channel is estimated with no matrix inversion at the receiver. Allocating a group of data subcarriers to a pilot tone slightly increases the complexity but the method is still cost effective due to its simplicity at the receiver. Moreover, at the transmitter side, only the pilot sequence needs to be added to the original data signal.

6.4.2 SFBC/STBC-OFDM for 4 Transmit Antennas

In this Section, the SFBC/STBC-OFDM is presented for 4 transmit antennas where pilot subcarriers are encoded according to the encoding rules of SFBC while data subcarriers are encoded according to the encoding rules of STBC. Contrary to Subsection 6.4.1, the channel parameters are assumed constant over 8 OFDM symbols and over 2 adjacent SFBC-STBC blocks or two STBC blocks. The encoding of the pilot and data subcarriers can be found in (6.10), (6.11) and Figure 6-8.

$$
\begin{aligned}
P_1 &= [\,p_0, -p_1, -p_2, -p_3, p_0^*, -p_1^*, -p_2^*, -p_3^*, \ldots, \\
&\quad p_{Np/2-4},\ -p_{Np/2-3},\ -p_{Np/2-2},\ -p_{Np/2-1}, p_{Np/2-4}^*,\ -p_{2Np/2-3}^*,\ -p_{Np/2-2}^*, -p_{Np/2-1}^*\,]^T \\
P_2 &= [\,p_1, p_0, p_3, -p_4, p_1^*, p_0^*, p_3^*, -p_2^*, \ldots, \\
&\quad p_{Np/2-3},\ p_{Np/2-4},\ p_{Np/2-1},\ -p_{Np/2-2}, p_{Np/2-3}^*,\ p_{2Np/2-4}^*, p_{Np/2-1}^*, -p_{Np/2-2}^*\,]^T \\
P_3 &= [\,p_2,\ -p_3,\ p_0, p_1, p_2^*,\ -p_3^*, p_0^*, p_1^*, \ldots, \\
&\quad p_{Np/2-2},\ -p_{Np/2-1},\ p_{Np/2-4}, p_{Np/2-3}, p_{Np/2-2}^*,\ -p_{2Np/2-1}^*, p_{Np/2-4}^*, p_{Np/2-3}^*\,]^T \\
P_4 &= [\,p_3,\ p_2,\ -p_1, p_0, p_3^*,\ p_2^*, -p_1^*, p_0^*, \ldots, \\
&\quad p_{Np/2-1},\ p_{Np/2-2},\ -p_{Np/2-3}, p_{Np/2-4}, p_{Np/2-1}^*,\ p_{2Np/2-2}^*, -p_{Np/2-3}^*, p_{Np/2-4}^*\,]^T
\end{aligned}
\tag{6.10}
$$

$$
\begin{aligned}
S_1(n) &= [\,s_0,\ s_4,\ \ldots,\ s_{4k}, \ldots, s_{4Ns-8}, s_{4Ns-4}\,]^T \\
S_2(n) &= [\,s_1,\ s_5,\ \ldots,\ s_{4k+1}, \ldots, s_{4Ns-7},\ s_{4Ns-3}\,]^T \\
S_3(n) &= [\,s_2,\ s_6,\ \ldots,\ s_{4k+2}, \ldots, s_{4Ns-6}, s_{4Ns-2}\,]^T \\
S_4(n) &= [\,s_3,\ s_7,\ \ldots,\ s_{4k+3}, \ldots, s_{4Ns-5},\ s_{4Ns-1}\,]^T \\
S_1(n+1) &= -S_2(n); S_2(n+1) = S_1(n); \quad S_3(n+1) = -S_4(n); S_4(n+1) = S_3(n); \\
S_1(n+2) &= -S_3(n); S_2(n+2) = S_4(n); \quad S_3(n+2) = S_1(n); \quad S_4(n+2) = -S_2(n); \\
S_1(n+3) &= -S_4(n); S_2(n+3) = -S_3(n); S_3(n+3) = S_2(n); \quad S_4(n+3) = S_1(n); \\
S_1(n+4) &= S_1^*(n); \quad S_2(n+5) = S_2^*(n); \quad S_3(n+4) = S_3^*(n); \quad S_4(n+4) = S_4^*(n); \\
S_1(n+5) &= -S_2^*(n); S_2(n+6) = S_1^*(n); \quad S_3(n+5) = -S_4^*(n); \quad S_4(n+5) = S_3^*(n); \\
S_1(n+6) &= -S_3^*(n); S_2(n+7) = S_4^*(n); \quad S_3(n+6) = S_1^*(n); \quad S_4(n+6) = -S_2^*(n); \\
S_1(n+7) &= -S_4^*(n); S_2(n+8) = -S_3^*(n); S_3(n+7) = S_2^*(n); \quad S_4(n+7) = S_1^*(n);
\end{aligned}
\tag{6.11}
$$

where k=0, 1, …, Ns-1.

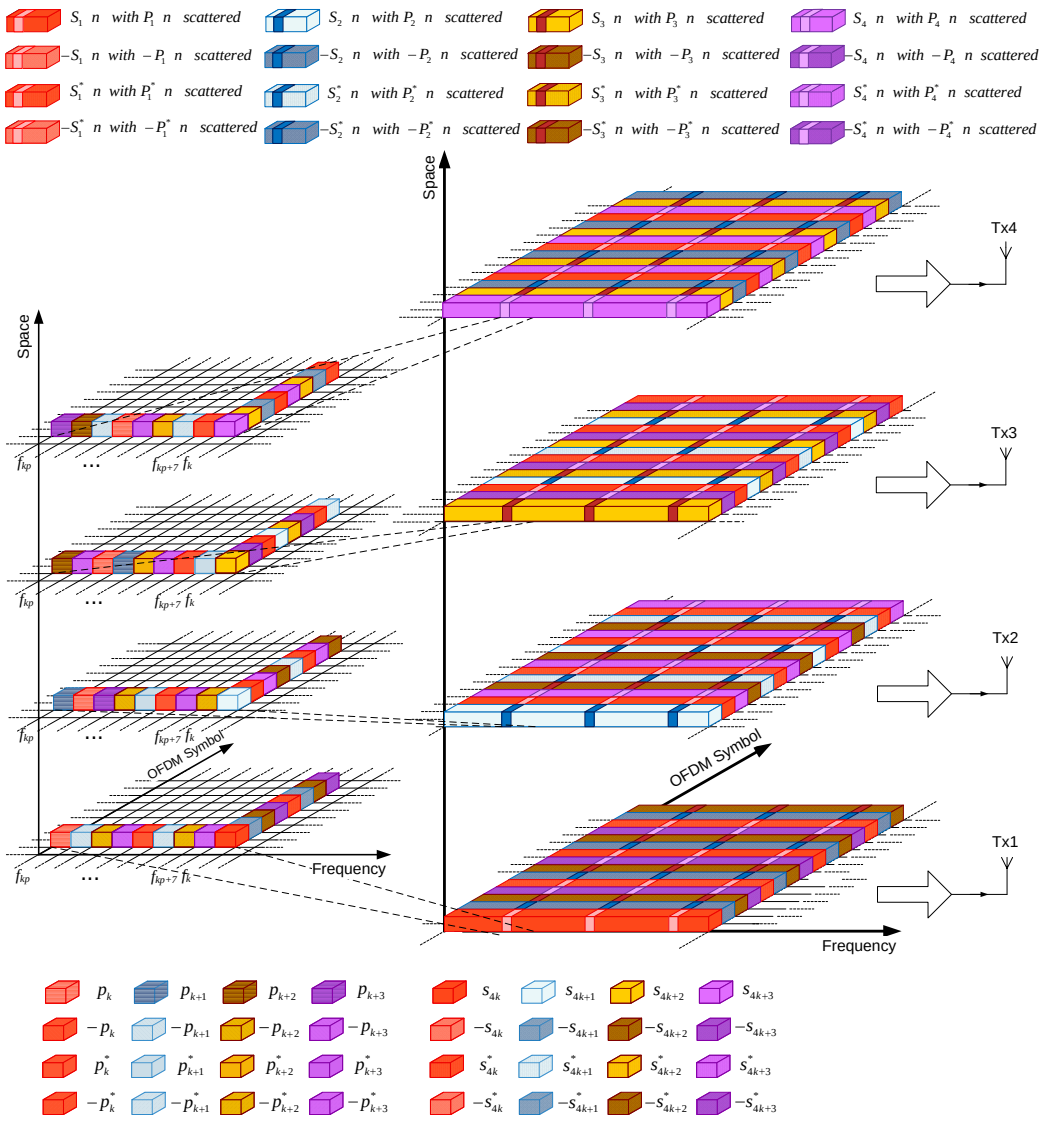

Figure 6-3: Organisation of Pilot and Data Symbol for 4 Transmit Antennas SFBC/STBC-OFDM

Once encoded, data is modulated using OFDM and transmitted through multipath Rayleigh frequency selective channels. Equation of the received pilot and data signals after FFT can be expressed as:

$$\begin{aligned} \bar{R}p_j &= \sum_{j=1}^{N_r} \bar{P}\bar{H}p_j + \bar{N}p_j \\ \bar{R}_j &= \sum_{j=1}^{N_r} \bar{S}\bar{H}_j + \bar{N}_j \end{aligned} \tag{6.12}$$

where $\bar{R}p_j, \bar{P}, \bar{H}p_j$ and $\bar{N}p_j$ represent the received pilot, pilot signal, channel parameters and white Gaussian noise at pilot subcarriers respectively. Also $\bar{R}_j$, $\bar{S}$, $\bar{H}_j$ and, $\bar{N}_j$ represent the received data signal, transmitted signal, channel parameters and the white Gaussian noise for data subcarriers respectively.

Pilot matrix $\bar{P}$ and vectors $\bar{R}p_j, \bar{H}p_j$ and $\bar{N}p_j$ can be expressed as:

$$\bar{R}p_j = \begin{bmatrix} Rp_{j,kp}(n) \\ Rp_{j,kp+1}(n) \\ Rp_{j,kp+2}(n) \\ Rp_{j,kp+3}(n) \\ Rp_{j,kp+4}(n) \\ Rp_{j,kp+5}(n) \\ Rp_{j,kp+6}(n) \\ Rp_{j,kp+7}(n) \end{bmatrix}, \bar{H}p_j = \begin{bmatrix} Hp_{1,j,kp}(n) \\ Hp_{2,j,kp}(n) \\ Hp_{3,j,kp}(n) \\ Hp_{4,j,kp}(n) \end{bmatrix}, \bar{N}p_j = \begin{bmatrix} Np_{1,j,kp}(n) \\ Np_{2,j,kp}(n) \\ Np_{3,j,kp}(n) \\ Np_{4,j,kp}(n) \\ Np_{5,j,kp}(n) \\ Np_{6,j,kp}(n) \\ Np_{7,j,kp}(n) \\ Np_{8,j,kp}(n) \end{bmatrix}$$

$$\bar{P} = \begin{bmatrix} P_{1,kp}(n) & P_{2,kp}(n) & P_{3,kp}(n) & P_{4,kp}(n) \\ -P_{2,kp}(n) & P_{1,kp}(n) & -P_{4,kp}(n) & P_{3,kp}(n) \\ -P_{3,kp}(n) & P_{4,kp}(n) & P_{1,kp}(n) & -P_{2,kp}(n) \\ -P_{4,kp}(n) & -P_{3,kp}(n) & P_{2,kp}(n) & P_{1,kp}(n) \\ P^*_{1,kp}(n) & P^*_{2,kp}(n) & P^*_{3,kp}(n) & P^*_{4,kp}(n) \\ -P^*_{2,kp}(n) & P^*_{1,kp}(n) & -P^*_{4,kp}(n) & P^*_{3,kp}(n) \\ -P^*_{3,kp}(n) & P^*_{4,kp}(n) & P^*_{1,kp}(n) & -P^*_{2,kp}(n) \\ -P^*_{4,kp}(n) & -P^*_{3,kp}(n) & P^*_{2,kp}(n) & P^*_{1,kp}(n) \end{bmatrix} \quad (6.13)$$

where kp=0, 4,…, Np-4.

Similarly receive signal, channel gain, transmitted signal and white Gaussian noise for data subcarriers are given in (6.14).

$$\bar{R}_j = \begin{bmatrix} R_{j,k}(n) \\ R_{j,k}(n+1) \\ R_{j,k}(n+2) \\ R_{j,k}(n+3) \\ R_{j,k}(n+4) \\ R_{j,k}(n+5) \\ R_{j,k}(n+6) \\ R_{j,k}(n+7) \end{bmatrix}, \bar{H}_j = \begin{bmatrix} H_{1,j,k}(n) \\ H_{2,j,k}(n) \\ H_{3,j,k}(n) \\ H_{4,j,k}(n) \end{bmatrix}, \bar{N}_j = \begin{bmatrix} N_{1,j,k}(n) \\ N_{2,j,k}(n) \\ N_{3,j,k}(n) \\ N_{4,j,k}(n) \\ N_{5,j,k}(n) \\ N_{6,j,k}(n) \\ N_{7,j,k}(n) \\ N_{8,j,k}(n) \end{bmatrix}$$

$$\bar{S} = \begin{bmatrix} S_{1,k}(n) & S_{2,k}(n) & S_{3,k}(n) & S_{4,k}(n) \\ -S_{2,k}(n) & S_{1,k}(n) & -S_{4,k}(n) & S_{3,k}(n) \\ -S_{3,k}(n) & S_{4,k}(n) & S_{1,k}(n) & -S_{2,k}(n) \\ -S_{4,k}(n) & -S_{3,k}(n) & S_{2,k}(n) & S_{1,k}(n) \\ S^*_{1,k}(n) & S^*_{2,k}(n) & S^*_{3,k}(n) & S^*_{4,k}(n) \\ -S^*_{2,k}(n) & S^*_{1,k}(n) & -S^*_{4,k}(n) & S^*_{3,k}(n) \\ -S^*_{3,k}(n) & S^*_{4,k}(n) & S^*_{1,k}(n) & -S^*_{2,k}(n) \\ -S^*_{4,k}(n) & -S^*_{3,k}(n) & S^*_{2,k}(n) & S^*_{1,k}(n) \end{bmatrix} \quad (6.14)$$

where k=0, 1, …, Ns-1.

As described in Chapters 4 and 5, channel parameters at pilot subcarriers are first estimated to initiate the joint iterative channel estimation process. Due to the fact that pilot symbols are known at the receiver and assuming that channel parameters remain constant over 8 OFDM symbols (n_t=8 for S_{4c}) therefore $hp_{i,j,kp}(n)=hp_{i,j,kp}(n+x)$, with x=1, 2, …, 8 and over 9 adjacent subcarriers at the initiation stage. In the next iteration, channel is still assumed constant over 8 OFDM symbols but only over 2 adjacent subcarriers due to the fact that after initiation, adjacent blocks are STBC-OFDM.

Thus with the help of (6.12), (6.13) and (6.14), estimated channel parameters can be derived as given in (6.15).

$$\tilde{h}p_{1,j,kp} = \frac{rp_{j,kp}p^*_{kp} - rp_{j,kp+1}p^*_{kp+1} - rp_{j,kp+2}p^*_{kp+2} - rp_{j,kp+3}p^*_{kp+3}}{2\left(|p_{kp}|^2 + |p_{kp+1}|^2 + |p_{kp+2}|^2 + |p_{kp+3}|^2\right)} +$$
$$\frac{rp_{j,kp+4}p_{kp} - rp_{j,kp+5}p_{kp+1} - rp_{j,kp+6}p_{kp+2} - rp_{j,kp+7}p_{kp+3}}{2\left(|p_{kp}|^2 + |p_{kp+1}|^2 + |p_{kp+2}|^2 + |p_{kp+3}|^2\right)}$$
$$\tilde{h}p_{2,j,kp} = \frac{rp_{j,kp}p^*_{kp+1} + rp_{j,kp+1}p^*_{kp} + rp_{j,kp+2}p^*_{kp+3} - rp_{j,kp+3}p^*_{kp+2}}{2\left(|p_{kp}|^2 + |p_{kp+1}|^2 + |p_{kp+2}|^2 + |p_{kp+3}|^2\right)} +$$
$$\frac{rp_{j,kp+4}p_{kp+1} + rp_{j,kp+5}p_{kp} + rp_{j,kp+6}p_{kp+3} - rp_{j,kp+7}p_{kp+2}}{2\left(|p_{kp}|^2 + |p_{kp+1}|^2 + |p_{kp+2}|^2 + |p_{kp+3}|^2\right)}$$
$$\tilde{h}p_{3,j,kp} = \frac{rp_{j,kp}p^*_{kp+2} - rp_{j,kp+1}p^*_{kp+3} + rp_{j,kp+2}p^*_{kp} + rp_{j,kp+3}p^*_{kp+1}}{2\left(|p_{kp}|^2 + |p_{kp+1}|^2 + |p_{kp+2}|^2 + |p_{kp+3}|^2\right)} +$$
$$\frac{rp_{j,kp+4}p_{kp+2} - rp_{j,kp+5}p_{kp+3} + rp_{j,kp+6}p_{kp} + rp_{j,kp+7}p_{kp+1}}{2\left(|p_{kp}|^2 + |p_{kp+1}|^2 + |p_{kp+2}|^2 + |p_{kp+3}|^2\right)}$$
$$\tilde{h}p_{4,j,kp} = \frac{rp_{j,kp}p^*_{kp+3} + rp_{j,kp+1}p^*_{kp+2} - rp_{j,kp+2}p^*_{kp+1} + rp_{j,kp+3}p^*_{kp}}{2\left(|p_{kp}|^2 + |p_{kp+1}|^2 + |p_{kp+2}|^2 + |p_{kp+3}|^2\right)} + \quad (6.15)$$
$$\frac{rp_{j,kp+4}p_{kp+3} + rp_{j,kp+5}p_{kp+2} - rp_{j,kp+6}p_{kp+1} + rp_{j,kp+7}p_{kp}}{2\left(|p_{kp}|^2 + |p_{kp+1}|^2 + |p_{kp+2}|^2 + |p_{kp+3}|^2\right)}$$

Estimated channel coefficients are used at the receiver to create a new matrix $\ddot{H}p_j$ and a new received vector $\ddot{R}_j$ such that:

$$\ddot{H}p_j = \begin{bmatrix} \tilde{H}p^*_{1,j,kp} & \tilde{H}p^*_{2,j,kp} & \tilde{H}p^*_{3,j,kp} & \tilde{H}p^*_{4,j,kp} & \tilde{H}p_{1,j,kp} & \tilde{H}p_{2,j,kp} & \tilde{H}p_{3,j,kp} & \tilde{H}p_{4,j,kp} \\ \tilde{H}p^*_{2,j,kp} & -\tilde{H}p^*_{1,j,kp} & -\tilde{H}p^*_{4,j,kp} & \tilde{H}p^*_{3,j,kp} & \tilde{H}p_{2,j,kp} & -\tilde{H}p_{1,j,kp} & -\tilde{H}p_{4,j,kp} & \tilde{H}p_{3,j,kp} \\ \tilde{H}p^*_{3,j,kp} & \tilde{H}p^*_{4,j,kp} & -\tilde{H}p^*_{1,j,kp} & -\tilde{H}p^*_{2,j,kp} & \tilde{H}p_{3,j,kp} & \tilde{H}p_{4,j,kp} & -\tilde{H}p_{1,j,kp} & -\tilde{H}p_{2,j,kp} \\ \tilde{H}p^*_{4,j,kp} & -\tilde{H}p^*_{3,j,kp} & \tilde{H}p^*_{2,j,kp} & -\tilde{H}p^*_{1,j,kp} & \tilde{H}p_{4,j,kp} & -\tilde{H}p_{3,j,kp} & \tilde{H}p_{2,j,kp} & -\tilde{H}p_{1,j,kp} \end{bmatrix} \quad (6.16)$$

$$\ddot{R}_j = [R_{j,k}(n) \quad R_{j,k}(n+1) \quad R_{j,k}(n+2) \quad R_{j,k}(n+3) \quad R^*_{j,k}(n+4) \quad R^*_{j,k}(n+5) \quad R^*_{j,k}(n+6) \quad R^*_{j,k}(n+7)]^T \quad (6.17)$$

The receiver uses the constructed matrix $\ddot{H}p_j$ and the constructed vector $\ddot{R}_j$ for the combining purposes described in (6.18) .

$$\tilde{S} = \begin{bmatrix} \tilde{s}_{4k} \\ \tilde{s}_{4k+1} \\ \tilde{s}_{4k+2} \\ \tilde{s}_{4k+3} \end{bmatrix} = \sum_{j=1}^{N_r} \ddot{H}p_j \ddot{R}_j \tag{6.18}$$

where $\tilde{s}_{4k}$, $\tilde{s}_{4k+1}$, $\tilde{s}_{4k+2}$ and $\tilde{s}_{4k+3}$ can be found in (6.19).

$$\begin{aligned}
\tilde{s}_{4k} &= \sum_{j=1}^{N_r} (\tilde{h}p^*_{1,j,kp} r_{j,4k} + \tilde{h}p^*_{2,j,kp} r_{j,4k+1} + \tilde{h}p^*_{3,j,kp} r_{j,4k+2} + \tilde{h}p^*_{4,j,kp} r_{j,4k+3} + \\
&\qquad \tilde{h}p_{1,j,kp} r^*_{j,4k+4} + \tilde{h}p_{2,j,kp} r^*_{j,4k+5} + \tilde{h}p_{3,j,kp} r^*_{j,4k+6} + \tilde{h}p_{4,j,kp} r^*_{j,4k+7}) \\
\tilde{s}_{4k+1} &= \sum_{j=1}^{N_r} (\tilde{h}p^*_{2,j,kp} r_{j,4k} - \tilde{h}p^*_{1,j,kp} r_{j,4k+1} - \tilde{h}p^*_{4,j,kp} r_{j,4k+2} + \tilde{h}p^*_{3,j,kp} r_{j,4k+3} + \\
&\qquad \tilde{h}p_{2,j,kp} r^*_{j,4k+4} - \tilde{h}p_{1,j,kp} r^*_{j,4k+5} - \tilde{h}p_{4,j,kp} r^*_{j,4k+6} + \tilde{h}p_{3,j,kp} r^*_{j,4k+7}) \\
\tilde{s}_{4k+2} &= \sum_{j=1}^{N_r} (\tilde{h}p^*_{3,j,kp} r_{j,4k} + \tilde{h}p^*_{4,j,kp} r_{j,4k+1} - \tilde{h}p^*_{1,j,kp} r_{j,4k+2} - \tilde{h}p^*_{2,j,kp} r_{j,4k+3} + \\
&\qquad \tilde{h}p_{3,j,kp} r^*_{j,4k+4} + \tilde{h}p_{4,j,kp} r^*_{j,4k+5} - \tilde{h}p_{1,j,kp} r^*_{j,4k+6} - \tilde{h}p_{2,j,kp} r^*_{j,4k+7}) \\
\tilde{s}_{4k+3} &= \sum_{j=1}^{N_r} (\tilde{h}p^*_{4,j,kp} r_{j,4k} - \tilde{h}p^*_{3,j,kp} r_{j,4k+1} + \tilde{h}p^*_{2,j,kp} r_{j,4k+2} - \tilde{h}p^*_{1,j,kp} r_{j,4k+3} + \\
&\qquad \tilde{h}p_{4,j,kp} r^*_{j,4k+4} - \tilde{h}p_{3,j,kp} r^*_{j,4k+5} + \tilde{h}p_{2,j,kp} r^*_{j,4k+6} - \tilde{h}p_{1,j,kp} r^*_{j,4k+7})
\end{aligned} \tag{6.19}$$

From Subsection 6.4.1 and 6.4.2, it can be seen that when SFBC is used to encode pilot subcarriers and STBC for data subcarriers, complexity of the systems remain the same and complexity is kept to an acceptable level. Moreover, it can be seen that similar to STBC-OFDM and SFBC-OFDM no matrix inversion is required at the receiver.

6.4.3 Simulation Results for SFBC/STBC-OFDM

The performance of the proposed SFBC/STBC-OFDM combination algorithm has been evaluated according to the specification described in Chapter 4

and 5. A set of 192 data subcarriers was used with various number of pilot subcarriers for 2 and 4 transmit antennas and 1 and 2 receive antennas. Similar modulation order to the one used for STBC-OFDM and SFBC-OFDM were used and specific simulation parameters can be found in Table 4-1 of Chapter 4, Section 4.6

In this section, SFBC is used to encode pilot symbols therefore, in order to follow similar group decoding procedure as the one described in Chapter 5, two and eight pilot subcarriers were assigned to each group of data for 2 and 4 transmit antennas respectively.

Figure 6-4 and Figure 6-5 show the performance results for 2 and 4 transmit antennas and 1 receive antenna for various number of pilot subcarriers (8, 12, 16 and 24) and different modulation orders for pilot and data subcarriers. Indeed, pilot were first modulated using similar modulation to the one used for data subcarriers (16QAM). Subsequently, simulation was performed such that BPSK was used to modulate pilot subcarriers. From the figures, it can be seen that the combination achieves between 2 to 10dB difference between the proposed channel estimation strategy and the case where CSI is known at the receiver.

Similar conclusions can be made for two receive antennas using 64QAM as illustrated in Figure 6-6 and Figure 6-7. When the same modulation order is used for the pilot and data subcarriers, 4 to 10 dB difference is obtained. Performance improves when lower modulation is used for pilot subcarriers while only 2 dB difference is obtained for the case where the number of pilot subcarriers is equal to 24 and 4 transmit antennas are used.

Finally, effect of the number of pilot symbols on the channel estimation has been investigated. From Figure 6-4 to Figure 6-7, it can be said that results improve when the number of pilot subcarriers increase.

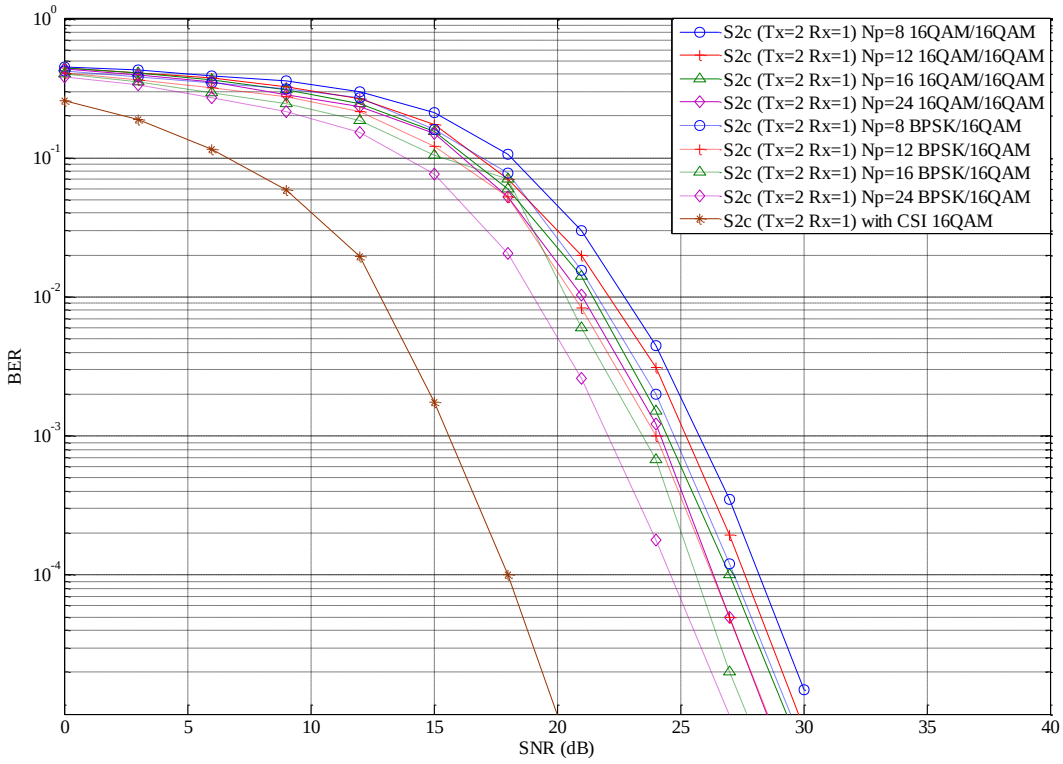

Figure 6-4: Effect of the use of Different Modulation and Pilot Length for 2 Transmit and 1 Receive Antennas

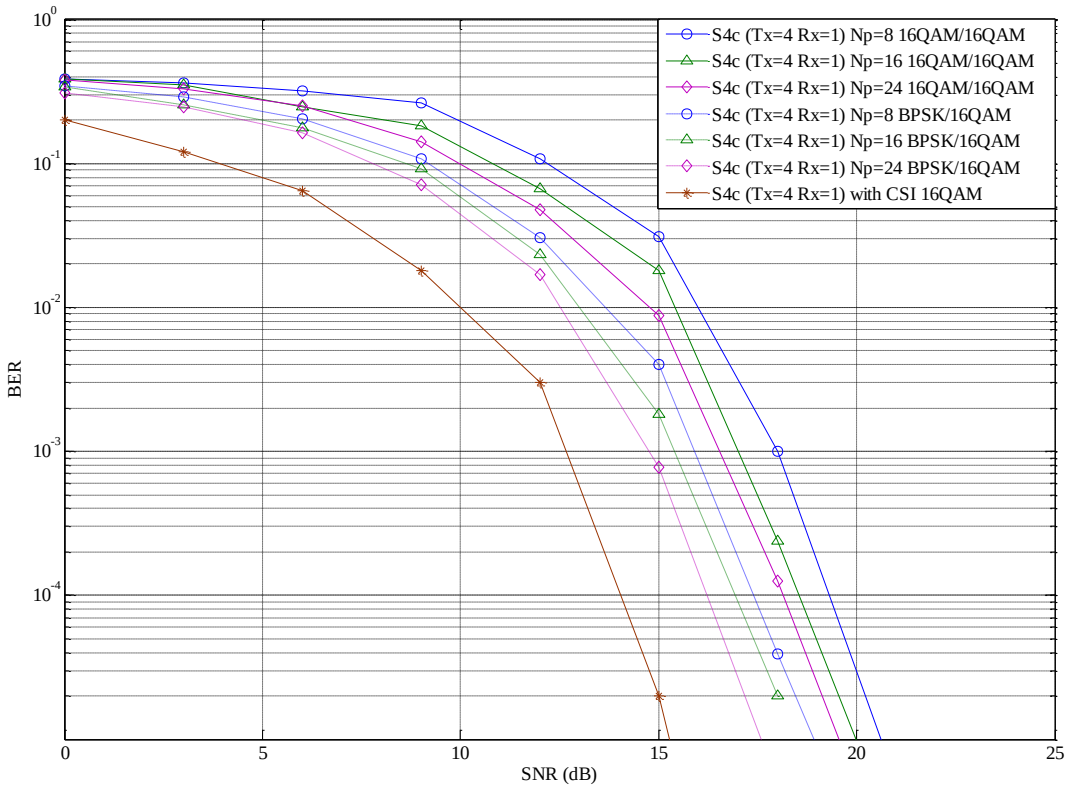

Figure 6-5: Effect of the use of Different Modulation and Pilot Length for 4 Transmit and 1 Receive Antennas

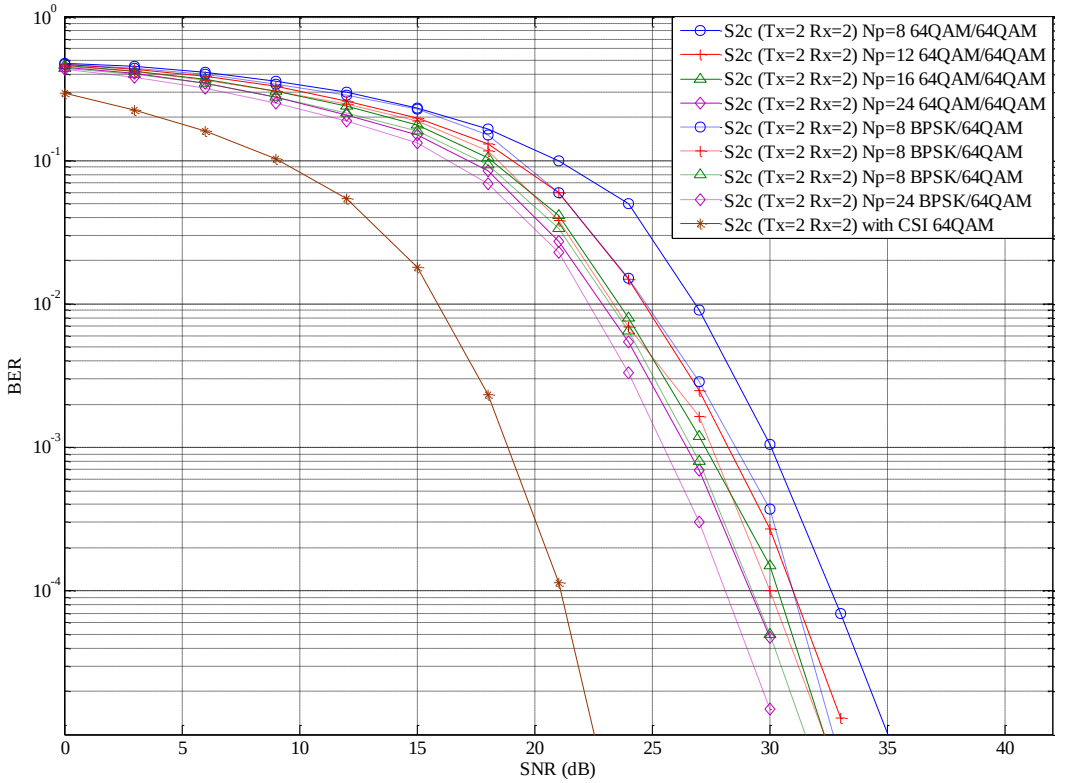

Figure 6-6: Effect of the use of Different Modulation and Pilot Length for 2 Transmit and 2 Receive Antennas

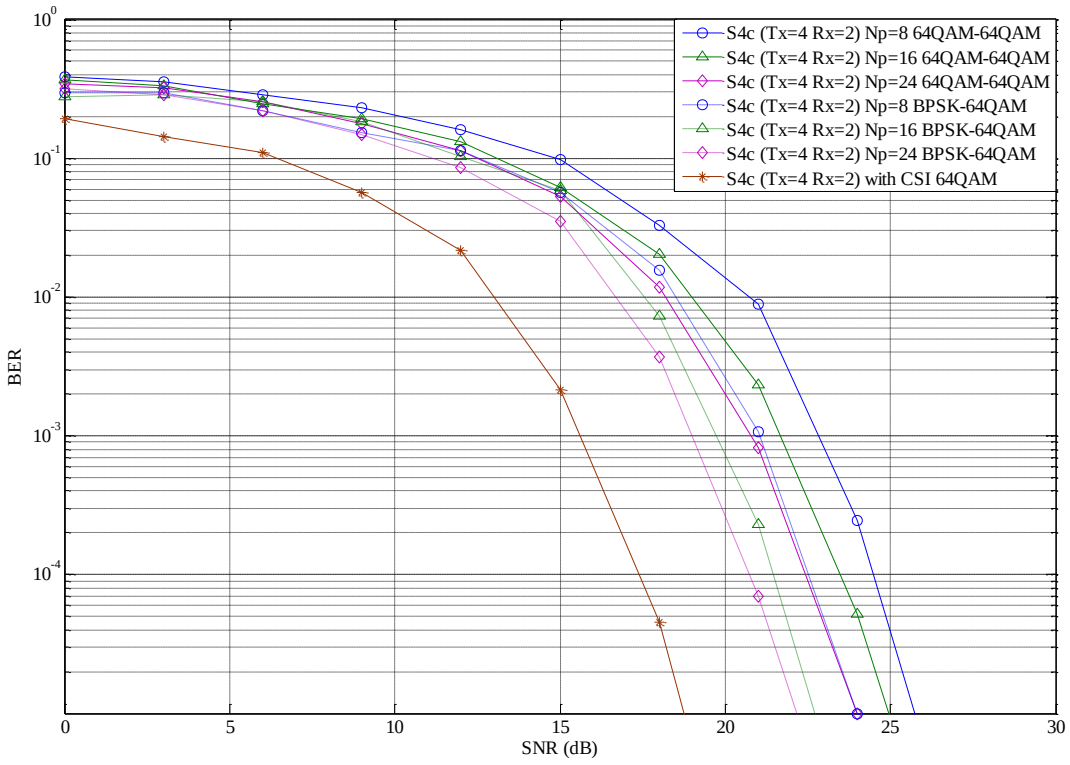

Figure 6-7: Effect of the use of Different Modulation and Pilot Length for 4 Transmit and 2 Receive Antennas

6.5 STBC Pilot Aided Channel Estimation for SFBC-OFDM Systems

Channel estimation method with pilot subcarriers coded according to STBC-OFDM rules and data subcarriers coded according to SFBC-OFDM is presented in this Section.

6.5.1 STBC/SFBC-OFDM for 2 Transmit Antennas

Pilot and data coding for STBC/SFBC-OFDM systems can be found in Figure 6-8 and corresponding vectors can be found in (6.20) and (6.21).

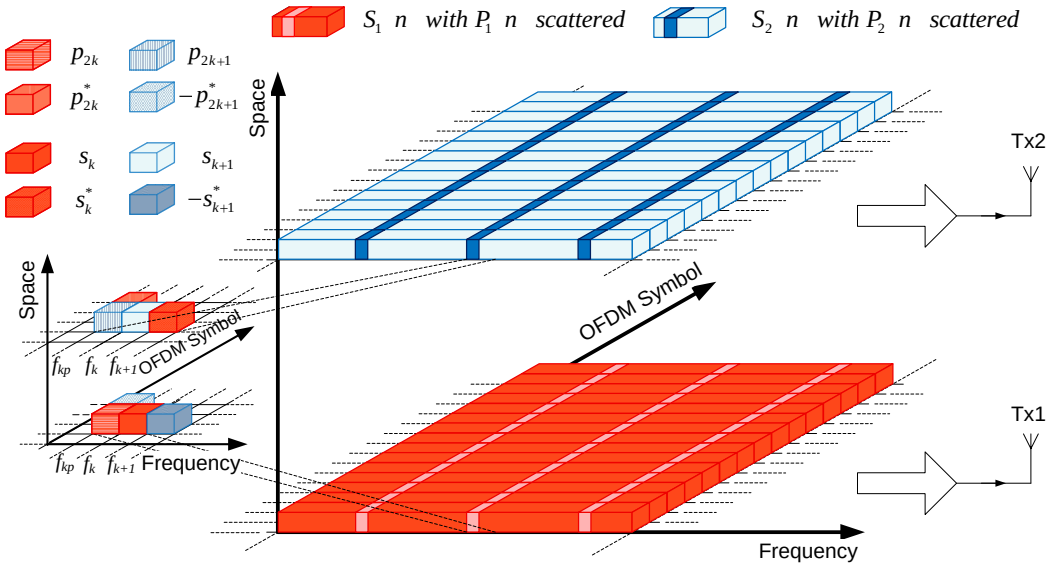

Figure 6-8: Organisation of Pilot and Data Symbol for 2 Transmit Antennas

$$
\begin{aligned}
P_1(n) &= [p_0,\ p_2,\ldots,\ p_{2Np-4},\ p_{2Np-2}]^T \\
P_2(n) &= [p_1,\ p_3,\ \ldots,\ p_{2Np-3},\ p_{2Np-1}]^T \\
P_1(n+1) &= [-p_1^*,\ -p_3^*,\ldots,\ -p_{2Np-3}^*,\ -p_{2Np-1}^*]^T = -P_2^*(n) \\
P_2(n+1) &= [p_0^*,\ p_2^*,\ \ldots,\ p_{2Np-4}^*,\ p_{2Np-2}^*]^T = P_1^*(n)
\end{aligned}
\tag{6.20}
$$

$$
\begin{aligned}
S_1 &= [s_0,\ -s_1^*,\ \ldots,\ s_k,\ -s_{k+1}^*,\ldots,\ s_{Ns-2},-s_{Ns-1}^*]^T \\
S_2 &= [s_1,\ s_0^*,\ \ldots,\ s_{k+1},\ s_k^*,\ldots,\ s_{Ns-1},\ s_{Ns-2}^*]^T
\end{aligned}
\tag{6.21}
$$

In a similar way, the received pilot and data symbols can be expressed by the 1xNp and 1xNs vectors:

$$
\begin{aligned}
Rp_j(n) &= [rp_{j,0},\ rp_{j,2},\ \ldots,\ rp_{j,2Np-4},\ rp_{j,2Np-2}]^T \\
Rp_j(n+1) &= [rp_{j,1}^*,\ rp_{j,3}^*,\ \ldots,\ rp_{j,2Np-3}^*,\ rp_{j,2Np-1}^*]^T
\end{aligned}
\tag{6.22}
$$

$$
R_j\ \ n\ = [r_{j,0},\ r_{j,1},\ \ldots,\ r_{j,2Ns-2},\ r_{j,2Ns-1}]^T \tag{6.23}
$$

From (6.1), and with the help of (6.20), (6.21), (6.22) and (6.23) , the received equations can be expressed as:

$$\begin{aligned} Rp_{j,k}(n) &= rp_{j,2kp} = hp_{1,j,2kp}p_{2kp} + hp_{2,j,2kp}p_{2kp+1} \\ Rp_{j,k}(n+1) &= rp_{j,2kp+1} = -hp_{1,j,2kp}p^{*}_{2kp+1} + hp_{2,j,2kp}p^{*}_{2kp} \end{aligned} \tag{6.24}$$

$$\begin{aligned} r_{j,k} &= h_{1,j,k}s_k + h_{2,j,k}s_{k+1} \\ r_{j,k+1} &= -h_{1,j,k+1}s^{*}_{k+1} + h_{2,j,k+1}s^{*}_{k} \end{aligned} \tag{6.25}$$

Pilot sequence known at the receiver is then used to estimate the channel parameter at the pilot subcarriers. With the assumption that channel parameters remain constant over two adjacent subcarriers and two adjacent OFDM symbols, channel parameters can be expressed with the help of (6.24) as:

$$\begin{aligned} \tilde{H}p_{1,j,kp}(n) = \tilde{H}p_{1,j,kp}(n+1) = \tilde{h}p_{1,j,2kp} &= \frac{rp_{j,2kp}p^{*}_{2kp} - rp_{j,2kp+1}p_{2kp+1}}{\left|p_{2kp}\right|^2 + \left|p_{2kp+1}\right|^2} \\ \tilde{H}p_{2,j,kp}(n) = \tilde{H}p_{2,j,kp}(n+1) = \tilde{h}p_{2,j,2kp} &= \frac{rp_{j,2kp}p^{*}_{2kp+1} + rp_{j,2kp+1}p_{2kp}}{\left|p_{2kp}\right|^2 + \left|p_{2kp+1}\right|^2} \end{aligned} \tag{6.26}$$

The detection formulas for the data signals can be derived with the help of (6.25) and (6.26). Assuming $hp_{i,j,kp} = h_{i,j,k} = h_{i,j,k+1}$, equation (6.27) can be derived.

$$\begin{aligned} \tilde{S}_{1,k}(n) &= \sum_{j=1}^{N_r}(\tilde{H}p_{1,j,kp}(n)R_{j,k}(n) + \tilde{H}p_{2,j,kp}(n)R_{j,k}(n+1)) \\ &= \tilde{s}_k = \sum_{j=1}^{N_r}(\tilde{h}p^{*}_{1,j,kp}r_{j,k} + \tilde{h}p_{2,j,kp}r^{*}_{j,k+1}) \\ \tilde{S}_{2,k}(n) &= \sum_{j=1}^{N_r}(\tilde{H}p^{*}_{2,j,kp}(n)R_{j,k}(n) + \tilde{H}p_{1,j,kp}(n)R^{*}_{j,k}(n+1)) \\ &= \tilde{s}_{k+1} = \sum_{j=1}^{N_r}(\tilde{h}p^{*}_{2,j,kp}r_{j,k} - \tilde{h}p_{1,j,kp}r^{*}_{j,k+1}) \end{aligned} \tag{6.27}$$

Replacing the channels by the estimated expressions obtained in (6.26), (6.27) becomes:

$$\begin{aligned}\tilde{s}_k &= \frac{1}{\Delta_p}(Ap^*_{kp+1} + Bp_{kp}) \\ \tilde{s}_{k+1} &= \frac{1}{\Delta_p}(Bp_{kp+1} - Ap^*_{kp})\end{aligned} \tag{6.28}$$

where and A and B can be expressed as:

$$\begin{aligned}A &= \sum_{j=1}^{N_r}(rp_{j,kp}r^*_{j,2k+1} - rp^*_{j,kp+1}r_{j,2k}) \\ &= \Delta_h \quad p_{2kp+1}s_k - p_{2kp}s_{k+1} \quad + N_{j,1} \\ B &= \sum_{j=1}^{N_r}(rp^*_{j,2kp}r_{j,k} + rp_{j,2kp+1}r^*_{j,k+1}) \\ &= \Delta_h \quad p^*_{2kp}s_k + p^*_{2kp+1}s_{k+1} \quad + N_{j,2}\end{aligned} \tag{6.29}$$

where and $N_{j,1}$ and $N_{j,2}$ are white Gaussian Noise vectors.

Substituting (6.29) into (6.28) leads to:

$$\begin{aligned}\tilde{s}_k &= \Delta_h s_k + N_3 \\ \tilde{s}_{k+1} &= \Delta_h s_{k+1} + N_4\end{aligned} \tag{6.30}$$

where N_9 and N_{12} are noise terms.

6.5.2 STBC/SFBC-OFDM for 4 Transmit Antennas

In this Subsection, the case of 4 transmit antennas with N_r receive antennas is investigated where pilot and data subcarriers are encoded using STBC and SFBC respectively. Figure 6-9 shows the organisation of the pilot and data symbols through space, time and frequency and equivalent vectors can be found in (6.31) and (6.32). From the figure, it can be seen that channel parameters need to be assumed constant over n_t =8 OFDM symbols and over 9 or 16 adjacent subcarriers

according to the encoding of two adjacent blocks irrespective of whether a pilot subcarriers is adjacent to a SFBC block or 2 SFBC blocks are adjacent to each other.

$$
\begin{aligned}
&P_1(n) = \left[\, p_0,\ p_4,\ \ldots,\ p_{4kp}, \ldots, p_{4Np-8},\ p_{4Np-4} \,\right]^T \\
&P_2(n) = \left[\, p_1,\ p_5,\ \ldots,\ p_{4kp+1}, \ldots, p_{4Np-7},\ p_{4Np-3} \,\right]^T \\
&P_3(n) = \left[\, p_2,\ p_6,\ \ldots,\ p_{4kp+2}, \ldots, p_{4Np-6},\ p_{4Np-2} \,\right]^T \\
&P_4(n) = \left[\, p_3,\ p_7,\ \ldots,\ p_{4kp+3}, \ldots, p_{4Np-5},\ p_{4Np-1} \,\right]^T \\
&P_1(n+1) = -P_2(n);\ \ P_2(n+1) = P_1(n); \qquad P_3(n+1) = -P_4(n);\ P_4(n+1) = P_3(n); \\
&P_1(n+2) = -P_3(n);\ P_2(n+2) = P_4(n); \qquad P_3(n+2) = P_1(n);\ \ P_4(n+2) = -P_2(n); \\
&P_1(n+3) = -P_4(n);\ P_2(n+3) = -P_3(n);\ \ P_3(n+3) = P_2(n);\ \ P_4(n+3) = P_1(n); \\
&P_1(n+4) = P_1^*(n);\ \ P_2(n+4) = P_2^*(n); \quad P_3(n+4) = P_3^*(n);\ \ P_4(n+4) = P_4^*(n); \\
&P_1(n+5) = -P_2^*(n);\ P_2(n+5) = P_1^*(n); \quad P_3(n+5) = -P_4^*(n);\ P_4(n+5) = P_3^*(n); \\
&P_1(n+6) = -P_3^*(n);\ P_2(n+6) = P_4^*(n); \quad P_3(n+6) = P_1^*(n);\ \ P_4(n+6) = -P_2^*(n); \\
&P_1(n+7) = -P_4^*(n);\ P_2(n+7) = -P_3^*(n);\ P_3(n+7) = P_2^*(n);\ \ P_4(n+7) = P_1^*(n);
\end{aligned}
\tag{6.31}
$$

$$
\begin{aligned}
S_1 = [&s_0,\ -s_1,\ -s_2,\ -s_3,\ s_0^*,\ -s_1^*,\ -s_2^*,\ -s_3^*\ \ldots, \\
&s_{Ns/2-4},\ -s_{Ns/2-3},\ -s_{Ns/2-2},\ -s_{Ns/2-1},\ s_{Ns/2-4}^*,\ -s_{Ns/2-3}^*,\ -s_{Ns/2-2}^*,\ -s_{Ns/2-1}^*]^T \\
S_2 = [&s_1, s_0, s_3, -s_2,\ s_1^*, s_0^*, s_3^*, -s_2^*\ \ldots, \\
&s_{Ns/2-3},\ s_{Ns/2-4},\ s_{Ns/2-1},\ -s_{Ns/2-2},\ s_{Ns/2-3}^*,\ s_{Ns/2-4}^*,\ s_{Ns/2-1}^*,\ -s_{Ns/2-2}^*]^T \\
S_3 = [&s_2,\ -s_3, s_0, s_1,\ s_2^*,\ -s_3^*,\ s_0^*,\ s_1^*\ \ldots, \\
&s_{Ns/2-2},\ -s_{Ns/2-1},\ s_{Ns/2-4}, s_{Ns/2-3},\ s_{Ns/2-2}^*,\ -s_{Ns/2-1}^*,\ s_{Ns/2-4}^*,\ s_{Ns/2-3}^*]^T \\
S_4 = [&s_3,\ s_2,\ -s_1,\ s_0,\ s_3^*,\ s_2^*,\ -s_1^*,\ s_0^*\ \ldots, \\
&s_{Ns/2-1},\ s_{Ns/2-2},\ -s_{Ns/2-3}, s_{Ns/2-4},\ s_{Ns/2-1}^*,\ s_{Ns/2-2}^*,\ -s_{Ns/2-3}^*,\ s_{Ns/2-4}^*]^T
\end{aligned}
\tag{6.32}
$$

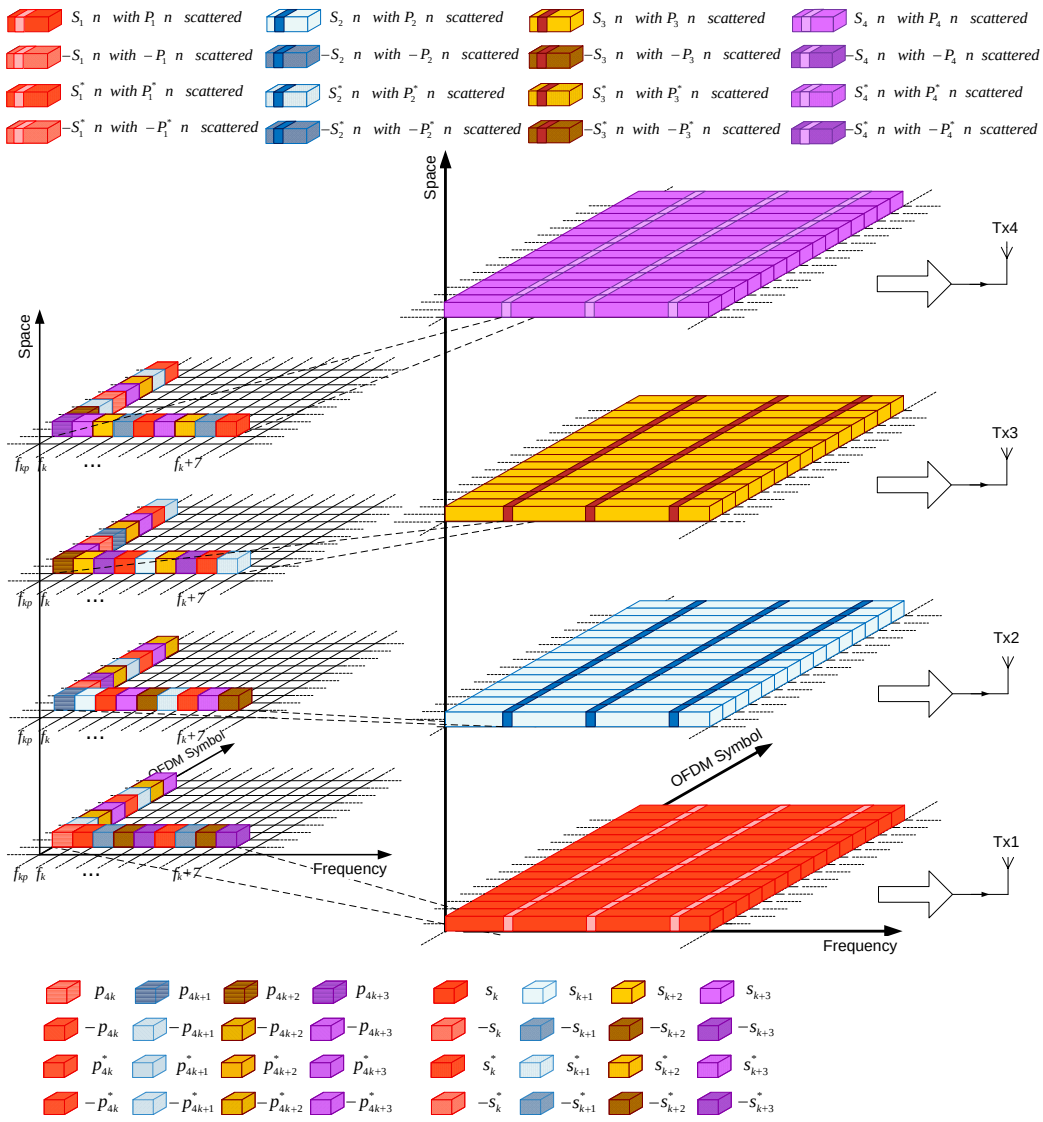

Figure 6-9: Organisation of Pilot and Data Symbol for 4 Transmit Antennas

Transmitted signal is then received and received pilot and data signals after FFT can be expressed as:

$$
\begin{aligned}
rp_{j,4kp} &= hp_{1,j,4kp}\,p_{4kp} + hp_{2,j,4kp}\,p_{4kp+1} + hp_{3,j,4kp}\,p_{4kp+2} + hp_{4,j,4kp}\,p_{4kp+3} \\
rp_{j,4kp+1} &= -hp_{1,j,4kp+1}\,p_{4kp+1} + hp_{2,j,4kp+1}\,p_{4kp} - hp_{3,j,4kp+1}\,p_{4kp+3} + hp_{4,j,4kp+1}\,p_{4kp+2} \\
rp_{j,4kp+2} &= -hp_{1,j,4kp+2}\,p_{4kp+2} + hp_{2,j,4kp+2}\,p_{4kp+3} + hp_{3,j,4kp+2}\,p_{4kp} - hp_{4,j,4kp+2}\,p_{4kp+1} \\
rp_{j,4kp+3} &= -hp_{1,j,4kp+3}\,p_{4kp+3} - hp_{2,j,4kp+3}\,p_{4kp+2} + hp_{3,j,4kp+3}\,p_{4kp+1} + hp_{4,j,4kp+3}\,p_{4kp} \\
rp_{j,4kp+4} &= hp_{1,j,4kp+4}\,p^{*}_{4kp} + hp_{2,j,4kp+4}\,p^{*}_{4kp+1} + hp_{3,j,4kp+4}\,p^{*}_{4kp+2} + hp_{4,j,4kp+4}\,p^{*}_{4kp+3} \\
rp_{j,4kp+5} &= -hp_{1,j,4kp+5}\,p^{*}_{4kp+1} + hp_{2,j,4kp+5}\,p^{*}_{4kp} - hp_{3,j,4kp+5}\,p^{*}_{4kp+3} + hp_{4,j,4kp+5}\,p^{*}_{4kp+2} \\
rp_{j,4kp+6} &= -hp_{1,j,4kp+6}\,p^{*}_{4kp+2} + hp_{2,j,4kp+6}\,p^{*}_{4kp+3} + hp_{3,j,4kp+6}\,p^{*}_{4kp} - hp_{4,j,4kp+6}\,p^{*}_{4kp+1} \\
rp_{j,4kp+7} &= -hp_{1,j,4kp+7}\,p^{*}_{4kp+3} - hp_{2,j,4kp+7}\,p^{*}_{4kp+2} + hp_{3,j,4kp+7}\,p^{*}_{4kp+1} + hp_{4,j,4kp+7}\,p^{*}_{4kp}
\end{aligned}
\tag{6.33}
$$

$$
\begin{aligned}
r_{j,k} &= h_{1,j,k}s_k + h_{2,j,k}s_{k+1} + h_{3,j,k}s_{k+2} + h_{4,j,k}s_{k+3} \\
r_{j,k+1} &= -h_{1,j,k+1}s_{k+1} + h_{2,j,k+1}s_k - h_{3,j,k+1}s_{k+3} + h_{4,j,k+1}s_{k+2} \\
r_{j,k+2} &= -h_{1,j,k+2}s_{k+2} + h_{2,j,k+2}s_{k+3} + h_{3,j,k+2}s_k - h_{4,j,k+2}s_{k+1} \\
r_{j,k+3} &= -h_{1,j,k+3}s_{k+3} - h_{2,j,k+3}s_{k+2} + h_{3,j,k+3}s_{k+1} + h_{4,j,k+3}s_k \\
r_{j,k+4} &= h_{1,j,k+4}s^{*}_k + h_{2,j,k+4}s^{*}_{k+1} + h_{3,j,k+4}s^{*}_{k+2} + h_{4,j,k+4}s^{*}_{k+3} \\
r_{j,k+5} &= -h_{1,j,k+5}s^{*}_{k+1} + h_{2,j,k+5}s^{*}_k - h_{3,j,k+5}s^{*}_{k+3} + h_{4,j,k+5}s^{*}_{k+2} \\
r_{j,k+6} &= -h_{1,j,k+6}s^{*}_{k+2} + h_{2,j,k+6}s^{*}_{k+3} + h_{3,j,k+6}s^{*}_k - h_{4,j,k+6}s^{*}_{k+1} \\
r_{j,k+7} &= -h_{1,j,k+7}s^{*}_{k+3} - h_{2,j,k+7}s^{*}_{k+2} + h_{3,j,k+7}s^{*}_{k+1} + h_{4,j,k+7}s^{*}_k
\end{aligned}
\tag{6.34}
$$

Where kp=0, 1,…, Np-1 and k=0, 4, …, Ns-4.

From (6.33), channel estimation equations can be derived such that:

$$\begin{aligned}
\tilde{h}p_{1,j,kp} &= \frac{rp_{j,kp}p_{kp}^{*} - rp_{j,kp+1}p_{kp+1}^{*} - rp_{j,kp+2}p_{kp+2}^{*} - rp_{j,kp+3}p_{kp+3}^{*}}{2\left(\left|p_{kp}\right|^2 + \left|p_{kp+1}\right|^2 + \left|p_{kp+3}\right|^2 + \left|p_{kp+4}\right|^2\right)} + \\
&\quad \frac{rp_{j,kp+4}p_{kp} + rp_{j,kp+5}p_{kp+1} + rp_{j,kp+6}p_{kp+2} + rp_{j,kp+7}p_{kp+3}}{2\left(\left|p_{kp}\right|^2 + \left|p_{kp+1}\right|^2 + \left|p_{kp+3}\right|^2 + \left|p_{kp+4}\right|^2\right)} \\
\tilde{h}p_{2,j,kp} &= \frac{rp_{j,kp}p_{kp+1}^{*} + rp_{j,kp+1}p_{kp}^{*} + rp_{j,kp+2}p_{kp+3}^{*} - rp_{j,kp+3}p_{kp+2}^{*}}{2\left(\left|p_{kp}\right|^2 + \left|p_{kp+1}\right|^2 + \left|p_{kp+3}\right|^2 + \left|p_{kp+4}\right|^2\right)} + \\
&\quad \frac{rp_{j,kp+4}p_{kp+1} + rp_{j,kp+5}p_{kp} + rp_{j,kp+6}p_{kp+3} - rp_{j,kp+7}p_{kp+2}}{2\left(\left|p_{kp}\right|^2 + \left|p_{kp+1}\right|^2 + \left|p_{kp+3}\right|^2 + \left|p_{kp+4}\right|^2\right)} \\
\tilde{h}p_{3,j,kp} &= \frac{rp_{j,kp}p_{kp+2}^{*} - rp_{j,kp+1}p_{kp+3}^{*} + rp_{j,kp+2}p_{kp}^{*} + rp_{j,kp+3}p_{kp+1}^{*}}{2\left(\left|p_{kp}\right|^2 + \left|p_{kp+1}\right|^2 + \left|p_{kp+3}\right|^2 + \left|p_{kp+4}\right|^2\right)} + \\
&\quad \frac{rp_{j,kp+4}p_{kp+2} - rp_{j,kp+5}p_{kp+3} + rp_{j,kp+6}p_{kp} + rp_{j,kp+7}p_{kp+1}}{2\left(\left|p_{kp}\right|^2 + \left|p_{kp+1}\right|^2 + \left|p_{kp+3}\right|^2 + \left|p_{kp+4}\right|^2\right)} \\
\tilde{h}p_{4,j,kp} &= \frac{rp_{j,kp}p_{kp+3}^{*} + rp_{j,kp+1}p_{kp+2}^{*} - rp_{j,kp+2}p_{kp+1}^{*} + rp_{j,kp+3}p_{kp}^{*}}{2\left(\left|p_{kp}\right|^2 + \left|p_{kp+1}\right|^2 + \left|p_{kp+3}\right|^2 + \left|p_{kp+4}\right|^2\right)} + \\
&\quad \frac{rp_{j,kp+4}p_{kp+3} + rp_{j,kp+5}p_{kp+2} - rp_{j,kp+6}p_{kp+1} + rp_{j,kp+7}p_{kp}}{2\left(\left|p_{kp}\right|^2 + \left|p_{kp+1}\right|^2 + \left|p_{kp+3}\right|^2 + \left|p_{kp+4}\right|^2\right)}
\end{aligned} \tag{6.35}$$

Based on (6.34), the formulas of the combined signals can be written as:

$$\begin{aligned}
\tilde{s}_k &= \frac{1}{2\Delta_p}(Ap_{kp} + Bp_{kp+1} + Cp_{kp+2} + Dp_{kp+3} + \\
&\qquad Ep_{kp}^{*} + Fp_{kp+1}^{*} + Gp_{kp+2}^{*} + Hp_{kp+3}^{*}) \\
\tilde{s}_{k+1} &= \frac{1}{2\Delta_p}(-Bp_{1,kp} + Ap_{kp+1} + Dp_{kp+2} - Cp_{kp+3} - \\
&\qquad Fp_{kp}^{*} + Ep_{kp+1}^{*} + Hp_{kp+2}^{*} - Gp_{kp+3}^{*}) \\
\tilde{s}_{k+3} &= \frac{1}{2\Delta_p}(-Cp_{1,kp} - Dp_{kp+1} + Ap_{kp+2} + Bp_{kp+3} - \\
&\qquad Gp_{kp}^{*} - Hp_{kp+1}^{*} + Ep_{kp+2}^{*} + Fp_{kp+3}^{*}) \\
\tilde{s}_{k+4} &= \frac{1}{2\Delta_p}(-Dp_{1,kp} + Cp_{kp+1} - Bp_{kp+2} + Ap_{kp+3} - \\
&\qquad Hp_{kp}^{*} + Gp_{kp+1}^{*} - Fp_{kp+2}^{*} + Ep_{kp+3}^{*})
\end{aligned} \tag{6.36}$$

and A, B, C, D, E, F, G and H are given as:

$$
\begin{aligned}
A &= \sum_{j=1}^{N_r}(r_{j,kp}^{*}r_{j,k} + r_{j,kp+1}^{*}r_{j,k+1} + r_{j,kp+2}^{*}r_{j,k+2} + r_{j,kp+3}^{*}r_{j,k+3} + \\
&\qquad r_{j,kp+4}r_{j,k+4}^{*} + r_{j,kp+5}r_{j,k+5}^{*} + r_{j,kp+6}r_{j,k+6}^{*} + r_{j,kp+7}r_{j,k+7}^{*}) \\
&= 2\Delta_h(p_{kp}^{*}s_k + p_{kp+1}^{*}s_{k+1} + p_{kp+2}^{*}s_{k+2} + p_{kp+3}^{*}s_{k+3}) + N_{j,1} \\
B &= \sum_{j=1}^{N_r}(-r_{j,kp+1}^{*}r_{j,k} + r_{j,kp}^{*}r_{j,k+1} + r_{j,kp+3}^{*}r_{j,k+2} - r_{j,kp+2}^{*}r_{j,k+3} - \\
&\qquad r_{j,kp+5}r_{j,k+4}^{*} + r_{j,kp+4}r_{j,k+5}^{*} + r_{j,kp+7}r_{j,k+6}^{*} - r_{j,kp+6}r_{j,k+7}^{*}) \\
&= 2\Delta_h(p_{kp+1}^{*}s_k - p_{kp}^{*}s_{k+1} + p_{kp+3}^{*}s_{k+2} - p_{kp+2}^{*}s_{k+3}) + N_{j,2} \\
C &= \sum_{j=1}^{N_r}(-r_{j,kp+2}^{*}r_{j,k} - r_{j,kp+3}^{*}r_{j,k+1} + r_{j,kp}^{*}r_{j,k+2} + r_{j,kp+1}^{*}r_{j,k+3} - \\
&\qquad r_{j,kp+6}r_{j,k+4}^{*} - r_{j,kp+7}r_{j,k+5}^{*} + r_{j,kp+4}r_{j,k+6}^{*} + r_{j,kp+5}r_{j,k+7}^{*}) \\
&= 2\Delta_h(p_{kp+2}^{*}s_k - p_{kp+3}^{*}s_{k+1} - p_{kp}^{*}s_{k+2} + p_{kp+1}^{*}s_{k+3}) + N_{j,3} \\
D &= \sum_{j=1}^{N_r}(-r_{j,kp+3}^{*}r_{j,k} + r_{j,kp+2}^{*}r_{j,k+1} - r_{j,kp+1}^{*}r_{j,k+2} + r_{j,kp}^{*}r_{j,k+3} - \\
&\qquad r_{j,kp+7}r_{j,k+4}^{*} + r_{j,kp+6}r_{j,k+5}^{*} - r_{j,kp+5}r_{j,k+6}^{*} + r_{j,kp+4}r_{j,k+7}^{*}) \\
&= 2\Delta_h(p_{kp+3}^{*}s_k + p_{kp+2}^{*}s_{k+1} - p_{kp+1}^{*}s_{k+2} - p_{kp}^{*}s_{k+3}) + N_{j,4} \\
E &= \sum_{j=1}^{N_r}(r_{j,kp+4}^{*}r_{j,k} + r_{j,kp+5}^{*}r_{j,k+1} + r_{j,kp+6}^{*}r_{j,k+2} + r_{j,kp+7}^{*}r_{j,k+3} + \\
&\qquad r_{j,kp}r_{j,k+4}^{*} + r_{j,kp+1}r_{j,k+5}^{*} + r_{j,kp+2}r_{j,k+6}^{*} + r_{j,kp+3}r_{j,k+7}^{*}) \\
&= 2\Delta_h(p_{kp}s_k + p_{kp+1}s_{k+1} + p_{kp+2}s_{k+2} + p_{kp+3}s_{k+3}) + N_{j,5} \\
F &= \sum_{j=1}^{N_r}(-r_{j,kp+5}^{*}r_{j,k} + r_{j,kp+4}^{*}r_{j,k+1} + r_{j,kp+7}^{*}r_{j,k+2} - r_{j,kp+6}^{*}r_{j,k+3} - \\
&\qquad r_{j,kp+1}r_{j,k+4}^{*} + r_{j,kp}r_{j,k+5}^{*} + r_{j,kp+3}r_{j,k+6}^{*} - r_{j,kp+2}r_{j,k+7}^{*}) \\
&= 2\Delta_h(p_{kp+1}s_k - p_{kp}s_{k+1} + p_{kp+3}s_{k+2} - p_{kp+2}s_{k+3}) + N_{j,6} \\
G &= \sum_{j=1}^{N_r}(-r_{j,kp+6}^{*}r_{j,k} - r_{j,kp+7}^{*}r_{j,k+1} + r_{j,kp+4}^{*}r_{j,k+2} + r_{j,kp+5}^{*}r_{j,k+3} - \\
&\qquad r_{j,kp+2}r_{j,k+4}^{*} - r_{j,kp+3}r_{j,k+5}^{*} + r_{j,kp}r_{j,k+6}^{*} + r_{j,kp+1}r_{j,k+7}^{*}) \\
&= 2\Delta_h(p_{kp+2}s_k - p_{kp+3}s_{k+1} - p_{kp}s_{k+2} + p_{kp+1}s_{k+3}) + N_{j,7} \\
H &= \sum_{j=1}^{N_r}(-r_{j,kp+7}^{*}r_{j,k} + r_{j,kp+6}^{*}r_{j,k+1} - r_{j,kp+5}^{*}r_{j,k+2} + r_{j,kp+4}^{*}r_{j,k+3} - \\
&\qquad r_{j,kp+3}r_{j,k+4}^{*} + r_{j,kp+2}r_{j,k+5}^{*} - r_{j,kp+1}r_{j,k+6}^{*} + r_{j,kp}r_{j,k+7}^{*}) \\
&= 2\Delta_h(p_{kp+3}s_k + p_{kp+2}s_{k+1} - p_{kp+1}s_{k+2} - p_{kp}s_{k+3}) + N_{j,8}
\end{aligned}
\tag{6.37}
$$

where and $N_{j,1}$, $N_{j,2}$, …, $N_{j,8}$ and N_9 to N_{12} are noise terms.

Substituting (6.37) into (6.36), the final equations for the signal detections can be derived and expressed as:

$$\begin{aligned} \tilde{s}_k &= \Delta_h s_k + N_9 \\ \tilde{s}_{k+1} &= \Delta_h s_{k+1} + N_{10} \\ \tilde{s}_{k+2} &= \Delta_h s_{k+2} + N_{11} \\ \tilde{s}_{k+3} &= \Delta_h s_{k+3} + N_{12} \end{aligned} \tag{6.38}$$

where N_9, N_{10}, N_{11} and N_{12} are noise terms.

Following the same procedure used in the preceding Subsection, derivations are simple and inverse matrix at the receiver is not necessary which reduces the algorithm complexity.

6.5.3 Simulation Results for STBC/SFBC-OFDM

Simulations results for STBC/SFBC-OFDM are proposed for 2 and 4 transmit antennas and 1 and 2 receive antennas. Simulation results were obtained under the same system parameters as Subsection 6.4.3.

Simulation results are presented for different modulation orders, for pilot and data subcarriers. In addition, different number of transmit and receive antennas have been used as well as different number of pilot subcarriers. The difference between the ideal case where CSI is known at the receiver and the iterative channel estimation technique is about 2 to 10dB. Moreover, from the Figure 6-10 to Figure 6-13, it can be seen that reducing the modulation order of the pilot subcarrier leads to 2 to 3dB improvement compared to the case where same

modulation order is used. An improvement of 2-3 dB is also possible when higher number of pilot subcarriers is used.

From the Figure 6-10 to Figure 6-13, it can also be noticed that increasing the number of transmit or receive antennas improves the performances as well as the use of a lower modulation order. As concluded in Chapter2, low modulation orders perform better than higher ones at the cost of bandwidth inefficiency.

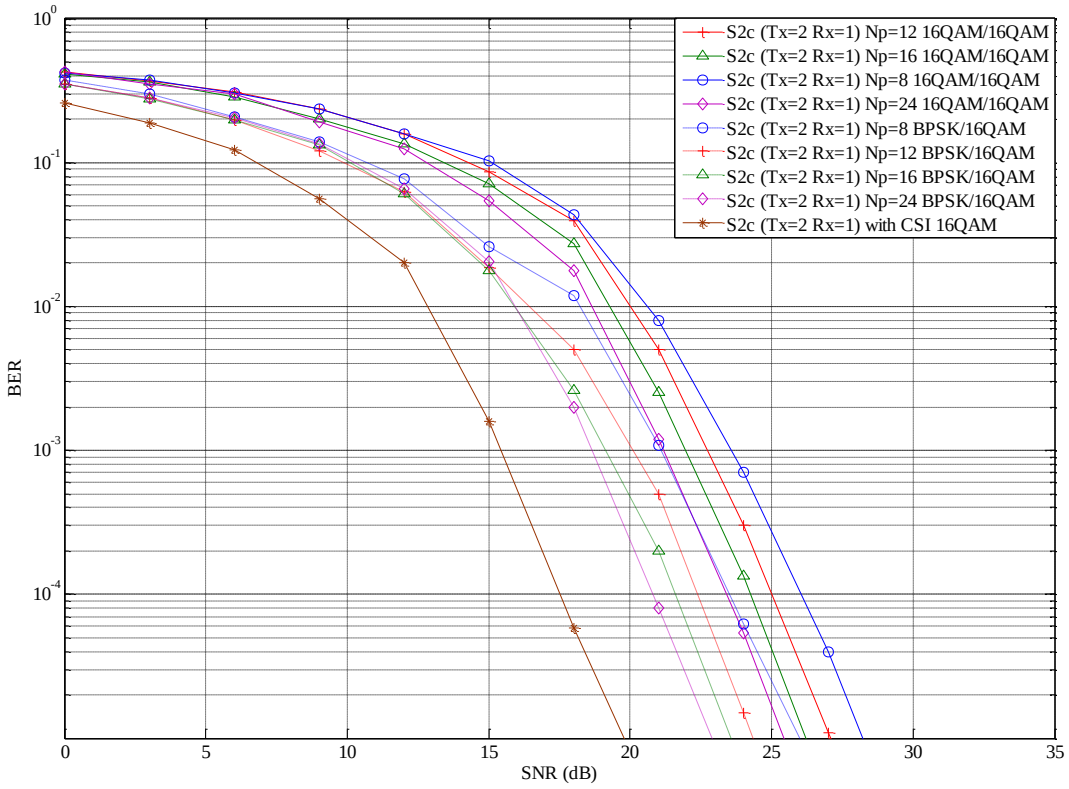

Figure 6-10: Effect of the use of Different Modulation and Pilot Length for 2 Transmit and 1 Receive Antennas

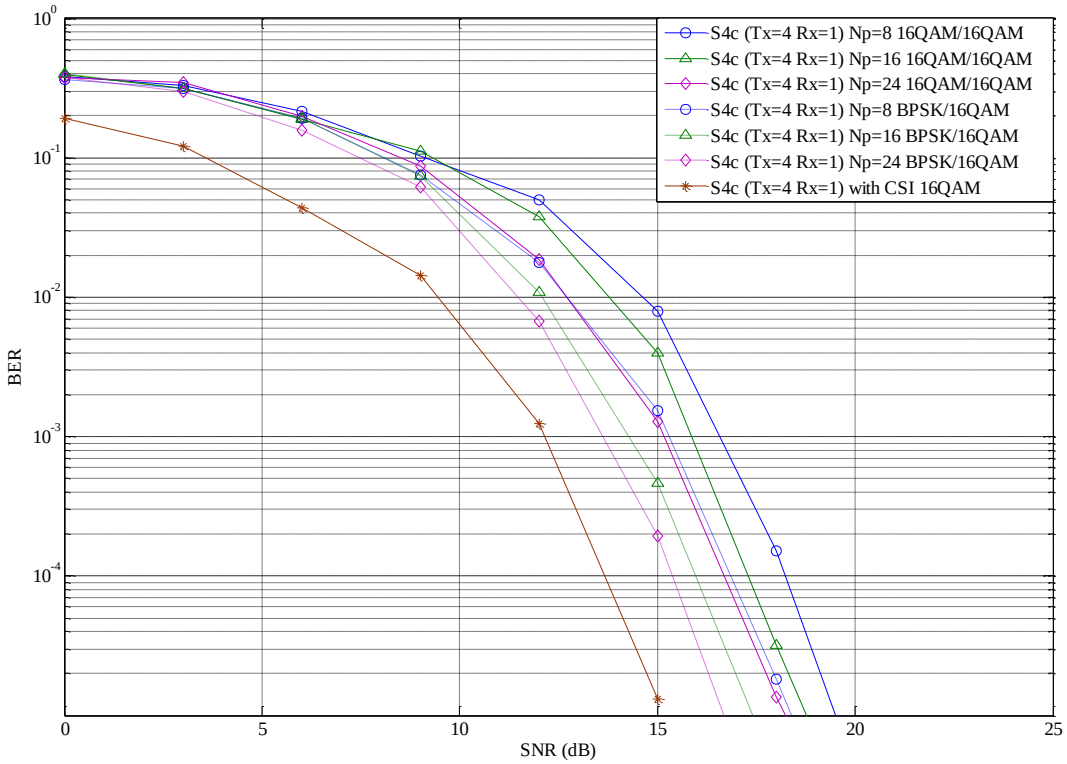

Figure 6-11: Effect of the use of Different Modulation and Pilot Length for 4 Transmit and 1 Receive Antennas

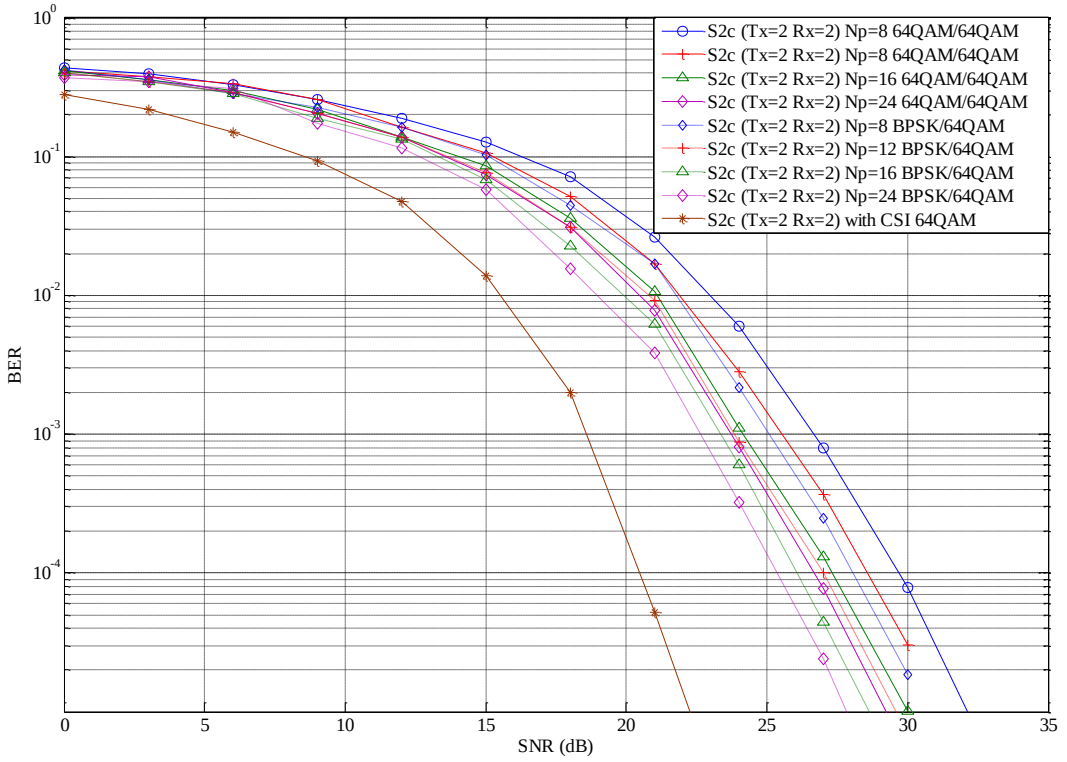

Figure 6-12: Effect of the use of Different Modulation and Pilot Length for 2 Transmit and 2 Receive Antennas

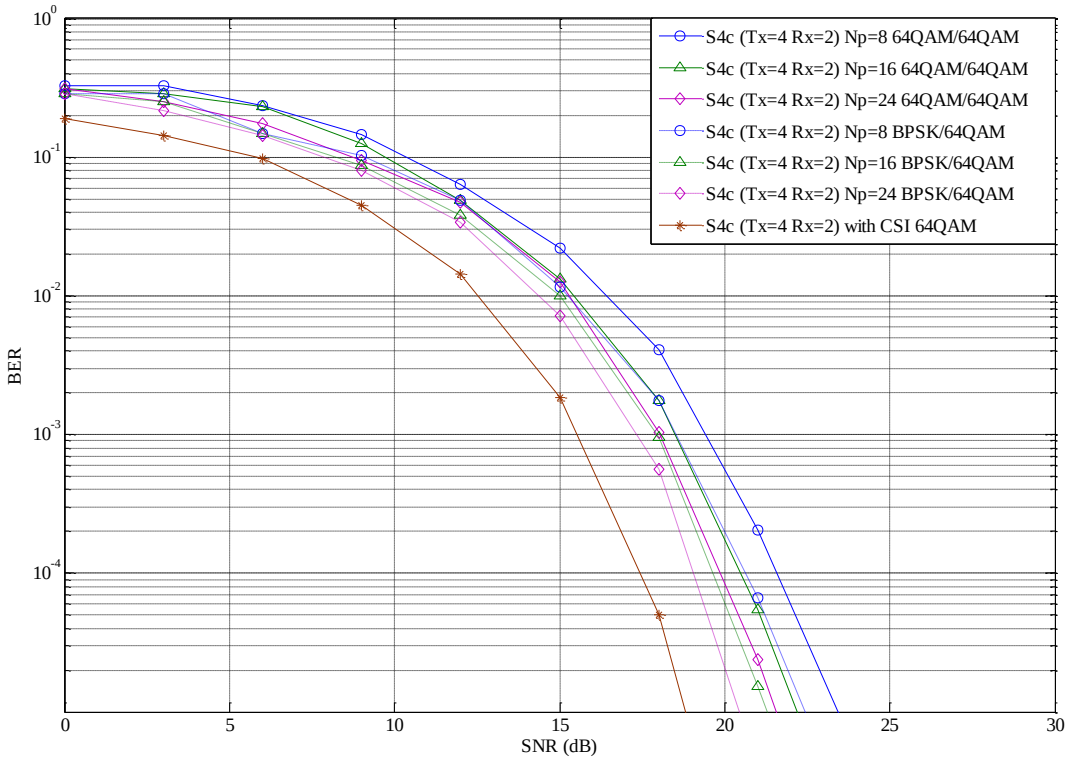

Figure 6-13: Effect of the use of Different Modulation and Pilot Length for 4 Transmit and 2 Receive Antennas

6.6 Performance Comparison of the Different Algorithms

In this Subsection, comparison results are analysed for scenarios where modulation order is kept unchanged and then made different for pilot and data subcarriers. In addition, the 4 methods presented in this work are compared for 2 and 4 transmit antennas with 1 and 2 receive antennas with 8 pilot subcarriers (Np=8).

From Figure 6-14 to Figure 6-17, it can be seen that the STBC/SFBC-OFDM channel estimation algorithm achieves the best performance with only 3 to 6 dB penalty when compared with the ideal case where CSI is known at the receiver. Then, STBC/STBC-OFDM in Chapter 4 is the second best algorithm, followed by SFBC/SFBC-OFDM in Chapter 5, and finally SFBC/STBC-OFDM. Results were

predictable due to the fact that in Chapter 5, it has been mentioned that SFBC-OFDM perform better than STBC-OFDM when comparison is based on similar amount of groups used. In the case of STBC/SFBC-OFDM, the systems takes advantage of the good performance achieved by SFBC-OFDM with higher number of groups used as pilot subcarriers are encoded using STBC. The worst case scenario, SFBC/STBC-OFDM, offer the creation of less groups due to the fact that pilot subcarriers are encoded using SFBC.

Finally, it can be seen that the modulation order of the system causes an upward or downward shift in the performance curve, but results remain unchanged in terms of STBC/SFBC-OFDM. Using higher modulation order implies higher BER but more efficient use of bandwidth while low modulation order reduces the BER at the cost of bandwidth inefficiency.

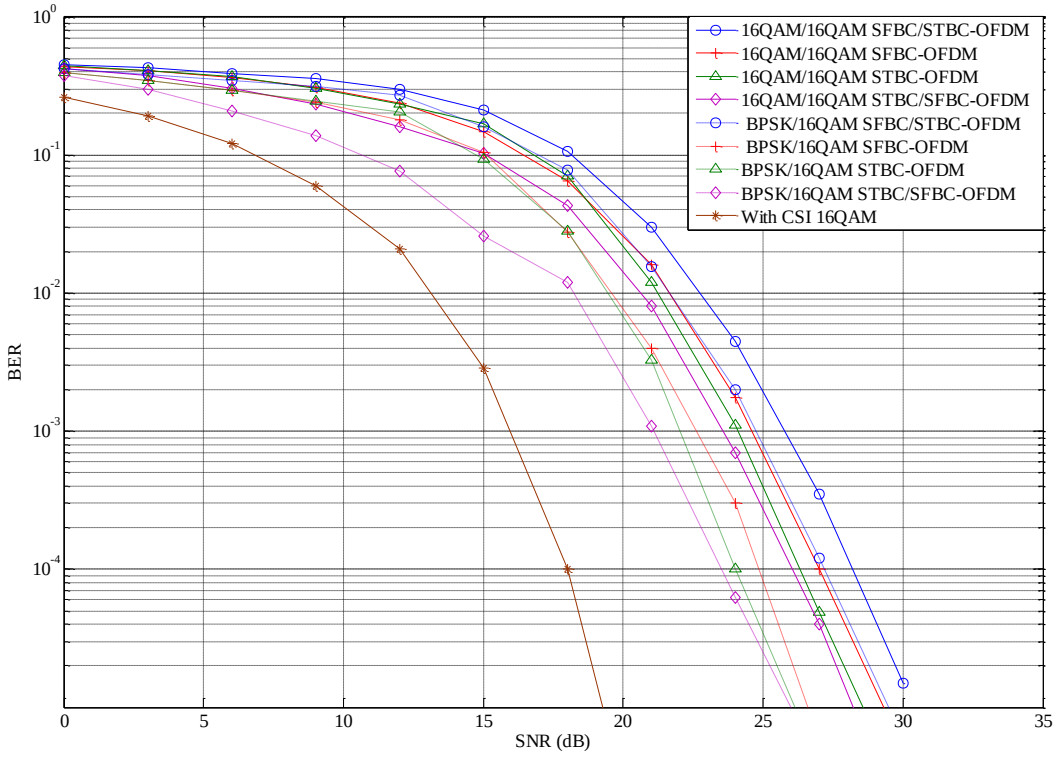

Figure 6-14: Performance Comparison of the 4 Schemes for 2 Transmit and 1 Receive Antennas

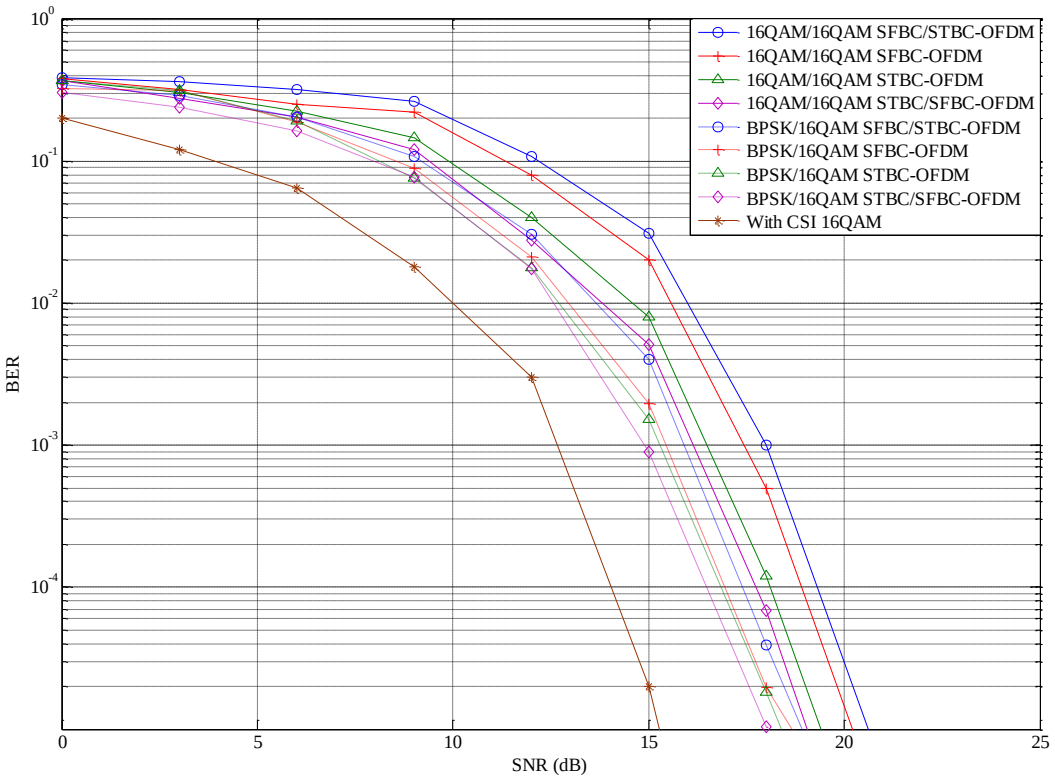

Figure 6-15: Performance Comparison of the 4 Schemes for 4 Transmit and 1 Receive Antennas

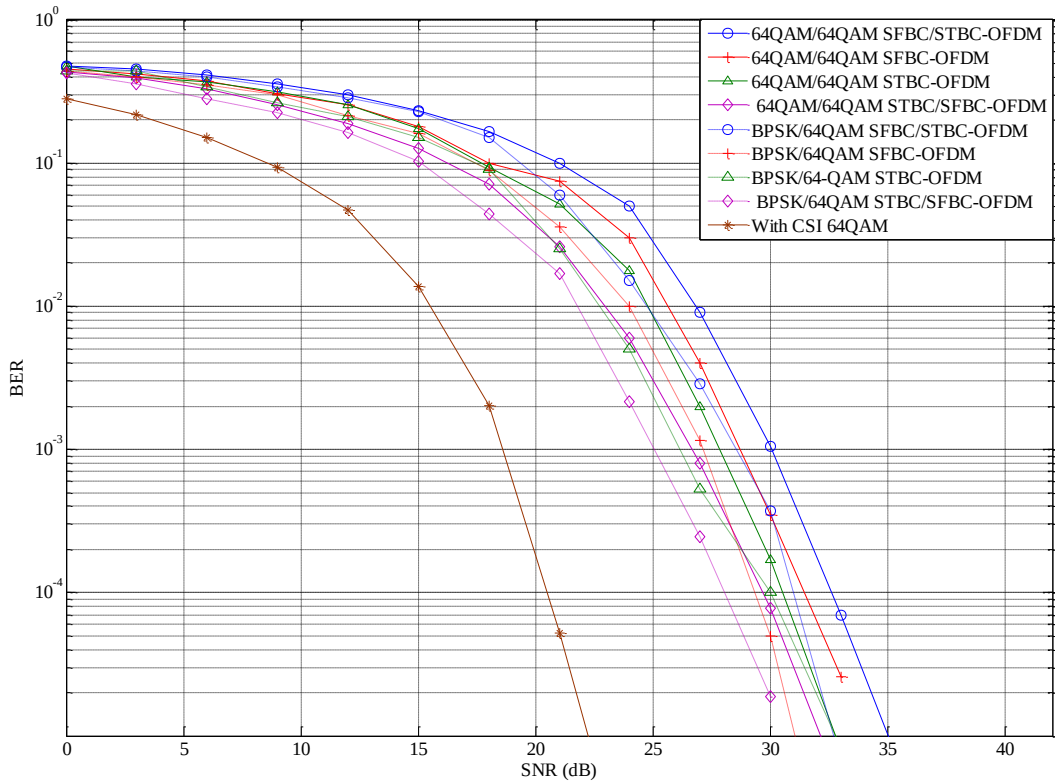

Figure 6-16: Performance Comparison of the 4 Schemes for 2 Transmit and 2 Receive Antennas

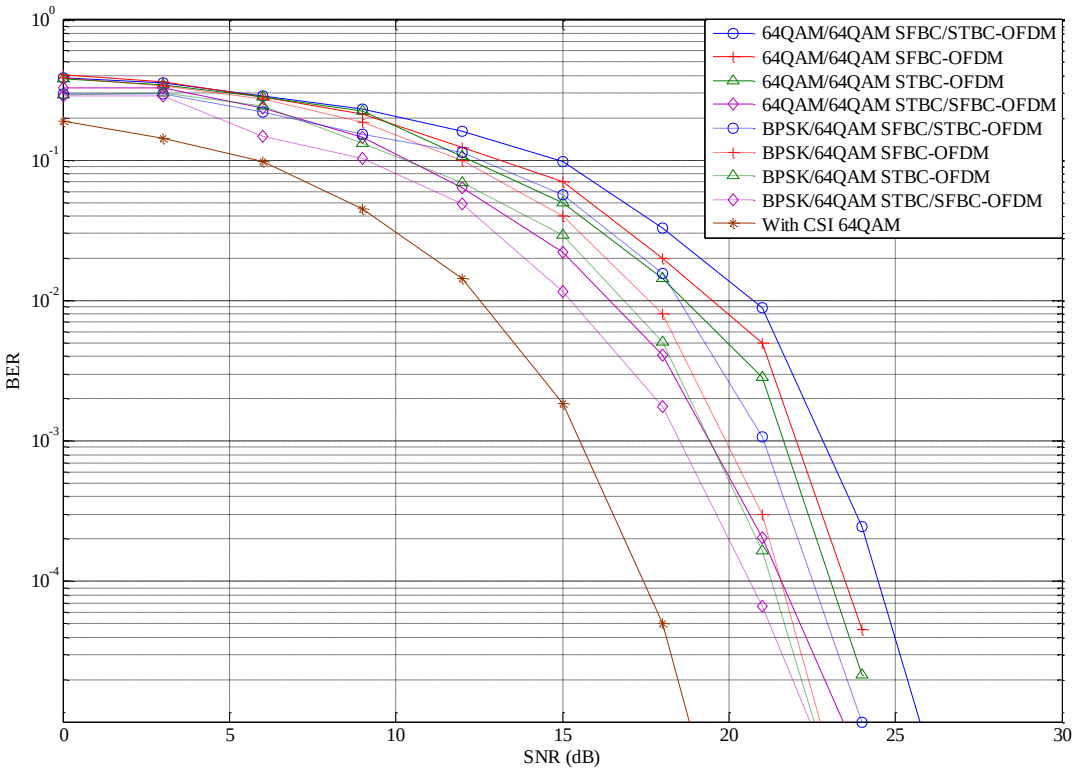

Figure 6-17: Performance Comparison of the 4 Schemes for 4 Transmit and 2 Receive Antennas

6.7 Conclusions

In this Chapter, a new channel estimation method is proposed based on the combination of the two methods proposed in Chapters 4 and 5. Alternating the type of coding at the pilot and data subcarriers allows improvement of the results without increasing the complexity. The method has been simulated under various conditions, different number of transmit and receive antennas, different modulation order at the pilot and data subcarriers. Finally, comparison of all the proposed methods was made and analysis was given.

The system proposed in this Chapter offers an efficient and computation-effective algorithm where the use of groups helps to improve the performance of the system without increasing the complexity at the receiver. All groups are

decoded simultaneously and using STBC to encode the pilot subcarrier offers the possibility to generate more groups due to the fact that symbols are coded across OFDM symbols. Limitation of the training sequence offers trade-off between accurate channel estimation and efficient bandwidth usage as more pilots would allow the algorithm to perform more accurate channel estimation at the cost of less transmitted data or more ISI.

Furthermore, the comparison Subsection show that STBC/SFBC-OFDM algorithm gives better performance which is due to the fact that SFBC performs slightly better than STBC and that STBC coding for pilot allows the creation of higher number of groups at the receiver. The other combination, SFBC/STBC-OFDM has a negative impact on channel estimation due to the fact that STBC/STBC offers the creation of a high number of decoding groups. On the other hand, SFBC reduces the number of decoding groups due to its coding over subcarrier which therefore reduces the quality of the channel estimation technique. For example, if 8 pilot subcarriers are allocated for 2 transmit antennas, in STBC/SFBC-OFDM, the number of groups generated would be Ns/8 whereas in SFBC/STBC-OFDM, only Ns/(8/n_t) is generated. As stated earlier, higher number of groups, better channel estimation and improved data recovery is achieved.

In this chapter, the problem of SFBC-OFDM in terms of generating less decoding group than STBC-OFDM for the same number of pilot subcarriers has been addressed by combining STBC and SFBC for pilot and data respectively. The level of accuracy observed when STBC is used to estimate channel parameters is similar to the level of accuracy achieved by SFBC-OFDM systems in low mobility scenarios. The significant difference, however, is that STBC offers the possibilities to generate higher number of groups of data at the cost of a

slight increase in the complexity of the system while achieving higher bandwidth efficiency. Indeed, higher number of group reduces the error propagation from one symbol block to another for the same number of pilot subcarrier, similar to that observed in SFBC-OFDM system.

7 Conclusions and Future Work

This chapter presents conclusions of the thesis and further work for the future.

7.1 General Summary of the Thesis

The constant demand of high speed data transmission over wireless communications for audio, video and internet applications has justified the necessity of upgrading proposed algorithms for narrowband systems to algorithms suitable for wideband systems. Many algorithms on the combination of MIMO with OFDM have been proposed due to its ability to enable a much more reliable and robust transmission in the harsh wireless environment by coding over space, time, and frequency domains. However, most of the work proposed in the literature assumes channel parameters are known at the receiver.

This thesis has first provided in Chapter 2, an extensive overview of MIMO wireless technologies, including Space-Time Block Codes, Quasi-Orthogonal Space-Time Block Codes and Differential Space-Time Block Codes. Simulation results have been presented as well as a comparison of different coding techniques highlighting advantages and disadvantages of each coding method for narrowband MIMO systems. The thesis has then reviewed MIMO-OFDM technology, the combination of MIMO with OFDM, for wideband MIMO systems in Chapter 3. Investigations into OFDM and STBC-OFDM have led to the development of a new iterative joint channel estimation and data detection technique for any number of transmit or receive antennas in Chapter 4. The joint scheme was

simulated according to the parameters defined in WiMax standard and can be adapted to any other wireless communications standards such as LTE and WLAN.

Chapter 5 of the thesis has presented a joint estimation and detection technique for SFBC-OFDM systems where symbols are coded over space and frequency instead of space and time (or OFDM symbols). Simulation results have been given as well as a comparison of SFBC-OFDM with STBC-OFDM. In order to appreciate the performances offered by coding through space and frequency, different simulation scenarios have been proposed where variation of the modulation order between pilot and data subcarriers, effect of the number of pilot subcarriers and effect of different channel conditions where delay spread of the channel is increased or reduced for fixed and mobile receivers have been considered. From the simulation results, it has been noticed that there exists a trade-off between SNR, complexity and bandwidth efficiency. Advantageously, the proposed method does not require any matrix inversion at the receiver and the system has been shown to be not sensitive to highly mobile environments.

In Chapter 6, a new MIMO-OFDM system with channel estimation is proposed based on combination of STBC-OFDM and SFBC-OFDM for pilot and data. Alternating the type of coding, STBC and SFBC at the pilot and data subcarriers allow improvement of the performance without increasing the complexity at the receiver. Simulation results have confirmed that STBC/SFBC-OFDM achieves better performance than other types of combinations of STBC and SFBC proposed in the thesis due to their efficient use of pilot subcarriers.

Moreover, throughout Chapter 4, 5 and 6 a new decoding scheme has been proposed which offers an efficient and computation-effective algorithm where the

use of grouping helps improving the performance of the system without increasing the complexity at the receiver as all groups are decoded simultaneously. Simulation results have shown that a higher number of pilot subcarrier, thus a higher number of groups, leads to a lower BER. Length of the training sequence offers trade-off between accurate channel estimation and efficient bandwidth usage as more pilots would allow the algorithm to perform more accurate channel estimation at the cost of less transmitted data or more Intersymbol Interference.

7.2 Results and Conclusions

A new iterative joint channel estimation and data detection scheme has been proposed for MIMO-OFDM systems. Investigations of STBC-OFDM were first conducted and simulations results for different number of transmit and receive antennas were obtained. The proposed joint estimation and data detection scheme has 6 to 9 dB loss in SNR when modulation type and order for pilot and data subcarriers are the same. However, BER performances improve when the simplest BPSK is used to modulate pilot subcarriers while data subcarriers are modulated with different modulation schemes. Effect of the number of pilot subcarriers on the proposed technique was also investigated and it was noticed that the performance of the system could be improved by 1 to 3dB. The proposed simultaneous group detection method proved to be faster than the traditional decoding process where symbols are decoded one by one. From the simulated detection times for STBC-OFDM system, it can be seen that the time saved grow exponentially with the number of pilot subcarriers.

SFBC-OFDM has been shown to be a good candidate for future mobile communications. Indeed, the obtained simulation results have confirmed its advantages of being robust in a mobile environment and memory efficient due to the fact that SFBC is coded over space and frequency and therefore only one OFDM symbol is required to decode SFBC block contrary to STBC-OFDM which requires n_t OFDM symbols to decode a STBC block. In addition, it has been shown that SFBC-OFDM performs better than STBC-OFDM when the number of group is the same. SFBC/SFBC-OFDM needs to regroup n_t pilot subcarriers per group to initiate the channel estimation while STBC/STBC-OFDM requires only one pilot subcarrier per group to initiate the estimation process and recover the data. It has also been noticed that the detection time of the SFBC-OFDM reduces linearly with the number of pilot subcarriers and that the number of receive antennas does not affect the performance of the system in term of decoding speed.

In a mixed use of STBC-OFDM and SFBC-OFDM for pilot and data subcarriers, simulation results have shown that STBC/SFBC-OFDM performs better than STBC-OFDM and SFBC-OFDM by 1 to 2dB, whilst SFBC/STBC-OFDM has the worst performance due to the fact that fewer groups are used to decode the OFDM symbols. Performances of the four different combinations of STBC and SFBC for pilots and data subcarriers vary between 1 and 3 dB.

7.3 Future Work

Research within wireless communications is vast and endless in possibilities. The work in this thesis has focused on the design of a joint channel estimation and data detection algorithm for different MIMO-OFDM systems using STBC and

SFBC. While the research is comprehensive, there remains further work which could be done to further enhance system performance in simulation and real time operation. Specifically these include adaptive modulation and coding, interpolation for channel estimation and implementation schemes in FPGA.

7.3.1 Adaptive Modulation for Pilot and Data Subcarriers

In order to always achieve the best performance through the channel, modulation order at the transmitter should be adjustable. The system adapts the modulation scheme to suit the transmission environment in order to maximise the channel capacity. In this thesis, similar work has been done where different modulation orders have been used for pilot and data subcarriers. Simulation results have shown that performance of the system can be improved by 1 to 3 dB when lower modulation is used for pilot subcarriers. A feedback bit would be required from the receiver to the transmitter to know the status of the channel. Adaptive modulation for pilots and data can be implemented by the use of a selectable multi-level modulation scheme.

7.3.2 Adaptive MIMO Coding for Pilots and Data

Chapter 6 of this thesis has proposed a new MIMO-OFDM process where pilot and data subcarriers follow two different types of MIMO coding, one over space and time (STBC-OFDM) and the other over space and frequency (SFBC-OFDM). Using different coding schemes for pilot and data subcarriers has been demonstrated as a promising technique as STBC/SFBC-OFDM technique can outperform STBC-OFDM system by 1 to 2 dB. Choice of MIMO-OFDM coding schemes of pilot and data subcarriers can also be made adaptive to channel conditions. For example, SFBC-OFDM is more robust than STBC-OFDM in

mobile environment and thus can be selected for channels with high Doppler effects.

7.3.3 Interpolation Method for MIMO Channel Estimation

In this thesis, performance of a new iterative joint channel estimation and data detection for MIMO-OFDM systems has been evaluated. Further work can be conducted on the use of an interpolation method to estimate the channel parameters at data subcarriers instead of using the iterative scheme. The proposed method could still be used to initiate the channel estimation process at pilot subcarriers but instead of using the recovered signal as a new set of pilot symbols, channel estimation between two pilot subcarriers could be achieved using an interpolation method such as the proposed in [98, 99].

7.3.4 FPGA Implementation of the Proposed Joint Schemes for MIMO-OFDM

In this thesis 4 types of MIMO-OFDM systems have been investigated and the proposed schemes have been verified by Matlab simulations. With advances in FPGA technology, hardware based simulations have received more attention due to their huge performance advantages over software based simulations [100]. It can take many hours to do a computer based simulation to obtain an error rate above 10^{-6} for a given signal to noise ratio, particularly when simulating a complex MIMO communications link. But such an error rate can be obtained within minutes for an implemented hardware solution. Hardware based simulations not only offer real-time simulations but also enable the designers to effectively and accurately evaluate the hardware architectures of algorithms and systems. Therefore, further research should be conducted to implement the

proposed MIMO-OFDM systems and joint schemes in FPGA. This will indeed be done in a university sponsored project aiming at building a MIMO-OFDM platform or testbed.

7.3.5 Limitation of the Proposed Channel Estimation Technique

In this thesis, a new iterative channel estimation has been proposed for three types of coding techniques, STBC-OFDM, SFBC-OFDM and a combination of both. Due to the advances in FPGA technology, further research should be conducted to implement the proposed MIMO-OFDM systems and joint schemes in FPGA. However, in order to implement the proposed technique, three aspects must be considered carefully. First, the computation efficiency of the algorithm which in the STBC case increases with the number of antennas used must be considered. This is because as high computation algorithm would imply higher power consumption and higher memory usage. Then, a trade-off needs to be found between pilot subcarrier and bandwidth efficiency as higher number of pilot would reduce the number of data transmitted per OFDM symbols for lower BER. Finally, synchronisation of the received data should be considered especially in frequency selective channels. This is because data will suffer from the channel delay and therefore, data symbols transmitted at one frequency f might be detected at the receiver at a different frequency $f+\Delta f$. Therefore, synchronisation should be considered with extra care and a synchronisation technique should be embedded into the system. However, this could increase the complexity of the system.

References

[1] B. Lu and X. Wang, "Space-time code design in OFDM systems," in *IEEE Conference on Global Telecommunications*, vol.2, pp. 1000-1004, *2000.*

[2] L. Zhiqiang, X. Yan and G. B. Giannakis, "Space-time-frequency coded OFDM over frequency-selective fading channels," *IEEE Transactions on Signal Processing*, vol. 50, pp. 2465-2476, 2002.

[3] Z. Wei, X. Xia and K. Ben Letaief, "Space-Time/Frequency Coding for MIMO-OFDM in Next Generation Broadband Wireless Systems," *IEEE Wireless Communications* , vol. 14, pp. 32-43, 2007.

[4] J. Mietzner, R. Schober, L. Lampe, W. H. Gerstacker, "Multiple-antenna techniques for wireless communications - a comprehensive literature survey," *IEEE Communications Surveys & Tutorials* , vol. 11, pp. 87-105, 2009.

[5] S. M. Alamouti, "A simple transmit diversity technique for wireless communications," *IEEE Journal on Selected Areas in Communications*, vol. 16, pp. 1451-1458, 1998.

[6] W. Huiming, X. Xiang-Gen, Y. Qinye and L. Bin, "A family of space-time block codes achieving full diversity with linear receivers," *IEEE Transactions on Communications*, vol. 57, pp. 3607-3617, 2009.

[7] E. Basar and U. Aygolu, "High-rate full-diversity space-time block codes for three and four transmit antennas," *IET Communications*, vol. 3, pp. 1371-1378, 2009.

[8] A. Slaney and Y. Sun, "Space-time coding for wireless communications: an overview," *IEE Proceedings in Communications*, vol. 153, pp. 509-518, 2006.

[9] "IEEE Standard for Information technology--Telecommunications and information exchange between systems-Local and metropolitan area networks-Specific requirements Part 11: Wireless LAN Medium Access Control (MAC) and Physical Layer (PHY) Specifications Amendment 5: Enhancements for Higher Throughput," *IEEE Std 802.11n-2009 (Amendment to IEEE Std 802.11-2007 as amended by IEEE Std 802.11k-2008, IEEE Std 802.11r-2008, IEEE Std 802.11y-2008, and IEEE Std 802.11w-2009)*, pp. c1-502, 2009.

[10] S. N. Diggavi, N. Al-Dhahir, A. Stamoulis and A. R. Calderbank, "Great expectations: the value of spatial diversity in wireless networks," *Proceedings of the IEEE*, vol. 92, pp. 219-270, 2004.

[11] R. D. Murch and K. B. Letaief, "Antenna systems for broadband wireless access," *IEEE Communications Magazine*, vol. 40, pp. 76-83, 2002.

[12] S. P. Alex and L. M. A. Jalloul, "Performance Evaluation of MIMO in IEEE802.16e/WiMAX," *IEEE Journal of Selected Topics in Signal Processing*, vol. 2, pp. 181-190, 2008.

[13] Z. Kan, H. Lin, L. Gang, C. Hanwen, W. Wang and M. Dohler, "Beyond 3G Evolution," *IEEE Vehicular Technology Magazine*, vol. 3, pp. 30-36, 2008.

[14] W. Fan, A. Ghosh, C. Sankaran, P. Fleming, F. Hsieh, S. Benes, "Mobile WiMAX systems: performance and evolution," *IEEE Communications Magazine,* vol. 46, pp. 41-49, 2008.

[15] J. Ming and L. Hanzo, "Multiuser MIMO-OFDM for Next-Generation Wireless Systems," *Proceedings of the IEEE,* vol. 95, pp. 1430-1469, 2007.

[16] D. Agrawal, V. Tarokh, A. Naguib and N. Seshadri, "Space-time coded OFDM for high data-rate wireless communication over wideband channels," in *IEEE Conference on Vehicular Technology*, vol.3, pp. 2232-2236, *1998*.

[17] M. Uysal, N. Al-Dhahir and C. N. Georghiades, "A space-time block-coded OFDM scheme for unknown frequency-selective fading channels," *IEEE Communications Letters* , vol. 5, pp. 393-395, 2001.

[18] H. Bolcskei and A. J. Paulraj, "Space-frequency coded broadband OFDM systems," in *IEEE Conference on Wireless Communications and Networking*, vol.1, pp. 1-6, *2000.*

[19] H. El Gamal, A. R. Hammons, L. Youjian, M. P. Fitz and O. Y. Takeshita, "On the design of space-time and space-frequency codes for MIMO frequency-selective fading channels," *IEEE Transactions on Information Theory,* vol. 49, pp. 2277-2292, 2003.

[20] W. Su, Z. Safar and K. J. R. Liu, "Full-rate full-diversity space-frequency codes with optimum coding advantage," *IEEE Transactions on Information Theory,* vol. 51, pp. 229-249, 2005.

[21] L. Keonkook, K. Youngok, K. Joonhyuk, "A novel orthogonal space-time-frequency block code for OFDM systems," *IEEE Communications Letters*, vol. 13, pp. 652-654, 2009.

[22] M. Fozunbal, S. W. McLaughlin and R. W. Schafer, "On space-time-frequency coding over MIMO-OFDM systems," *IEEE Transactions on Wireless Communications,* vol. 4, pp. 320-331, 2005.

[23] D. Astely, E. Dahlman, A. Furuskar, Y. Jading, M. Lindstrom and S. Parkvall, "LTE: the evolution of mobile broadband - [LTE part II: 3GPP release 8]," *IEEE Communications Magazine,* vol. 47, pp. 44-51, 2009.

[24] L. Hun-Hee, B. Myung-Sun, K. Jee-Hoon and S. Hyoung-Kyu, "Efficient detection scheme in MIMO-OFDM for high speed wireless home network system," , *IEEE Transactions on Consumer Electronics,* vol. 55, pp. 507-512, 2009.

[25] N. Sarmadi, S. Shahbazpanahi and A. B. Gershman, "Blind Channel Estimation in Orthogonally Coded MIMO-OFDM Systems: A Semidefinite Relaxation Approach," , *IEEE Transactions on Signal Processing,* vol. 57, pp. 2354-2364, 2009.

[26] Z. Jian-Kang and M. Wing-Kin, "Full Diversity Blind Alamouti Space-Time Block Codes for Unique Identification of Flat-Fading Channels," *IEEE Transactions on Signal Processing* , vol. 57, pp. 635-644, 2009.

[27] W. Feng, W. P. Zhu and M. N. S. Swamy, "A Semiblind Channel Estimation Approach for MIMO-OFDM Systems," *IEEE Transactions on Signal Processing,* vol. 56, pp. 2821-2834, 2008.

[28] F. Delestre and Y. Sun, "MIMO-OFDM with pilot-aided channel estimation for WiMax systems," in *IEEE 6th International Conference on Wireless and Mobile Computing, Networking and Communications*, pp. 586-590, 2010.

[29] F. Delestre and Y. Sun, "A channel estimation method for MIMO-OFDM Mobile WiMax systems," in *IEEE 7th International Symposium on Wireless Communication Systems*, pp. 956-960, *2010*.

[30] F. Delestre and Y. Sun, "Pilot Aided Channel Estimation for MIMO-OFDM Systems," *London Communication Symposium*, UCL 2009.

[31] K. Meng-Lin and H. Chia-Chi, "A Refined Channel Estimation Method for STBC/OFDM Systems in High-Mobility Wireless Channels," *IEEE Transactions on Wireless Communications*, vol. 7, pp. 4312-4320, 2008.

[32] M. Abuthinien, S. Chen and L. Hanzo, "Semi-blind Joint Maximum Likelihood Channel Estimation and Data Detection for MIMO Systems," *IEEE Signal Processing Letters*, vol. 15, pp. 202-205, 2008.

[33] D. Torrieri and M. C. Valenti, "Efficiently decoded full-rate space-time block codes," *IEEE Transactions on Communications*, vol. 58, pp. 480-488, 2010.

[34] G. J. Foschini and M. J. Gans, "On Limits of Wireless Communications in a Fading Environment when UsingMultiple Antennas," *Wireless Personal Communication*, vol. 6, pp. 311-335, 1998.

[35] E. Telatar, "Capacity of multi-antenna Gaussian channels," *European Transactions on Telecommunications*, vol. 10, pp. 585–595, 1999.

[36] V. Tarokh, H. Jafarkhani and A. R. Calderbank , "Space-time block coding for wireless communications: performance results," *IEEE Journal on Selected Areas in Communications*, vol. 17, pp. 451-460, 1999.

[37] V. Tarokh, H. Jafarkhani and A. R. Calderbank, "Space-time block codes from orthogonal designs," *IEEE Transactions on Information Theory*, vol. 45, pp. 1456-1467, 1999.

[38] V. Tarokh, A. Naguib, N. Seshadri and A. R. Calderbank, "Space-time codes for high data rate wireless communication: performance criteria in the presence of channel estimation errors, mobility, and multiple paths," *IEEE Transactions on Communications*, vol. 47, pp. 199-207, 1999.

[39] H. Jafarkhani, "A quasi-orthogonal space-time block code," *IEEE Transactions on Communications*, vol. 49, pp. 1-4, 2001.

[40] H. Jafarkhani, "A quasi-orthogonal space-time block code," in *IEEE Conference on Wireless Communications and Networking*, vol.1, pp. 42-45, 2000.

[41] S. J. Alabed, J. M. Paredes and A. B. Gershman, "A Low Complexity Decoder for Quasi-Orthogonal Space Time Block Codes," *IEEE Transactions on Wireless Communications*, vol. 10, pp. 988-994, 2011.

[42] L. A. Dalton and C. N. Georghiades, "A full-rate, full-diversity four-antenna quasi-orthogonal space-time block code," *IEEE Transactions on Wireless Communications*, vol. 4, pp. 363-366, 2005.

[43] D. N. Dao and C. Tellambura, "A general method to decode ABBA quasi-orthogonal space-time block codes," *IEEE Communications Letters*, vol. 10, pp. 713-715, 2006.

[44] V. Tarokh and H. Jafarkhani, "A differential detection scheme for transmit diversity," *IEEE Journal on Selected Areas in Communications*, vol. 18, pp. 1169-1174, 2000.

[45] D. B. Smith and L. W. Hanlen, "New group product differential unitary space-time codes with simplified design and detection," *IEEE Transactions on Wireless Communications*, vol. 7, pp. 4825-4830, 2008.

[46] T. Rappaport, "Wireless Communications: Principles and Practice," *2nd ed.Prentice Hall,* 2001.

[47] B.Vucetic and J.Yuan, "Space-Time Coding," *John Wiley & Sons Ltd,* 2003.

[48] H. Lee, "Robust full-diversity full-rate quasi-orthogonal STBC for four transmit antennas," IEEE *Electronics Letters,* vol. 45, pp. 1044-1045, 2009.

[49] H. Jafarkhani and V. Tarokh, "Multiple transmit antenna differential detection from generalized orthogonal designs," *IEEE Transactions on Information Theory,* vol. 47, pp. 2626-2631, 2001.

[50] B. L. Hughes, "Differential space-time modulation," *IEEE Transactions on Information Theory,* vol. 46, pp. 2567-2578, 2000.

[51] B. M. Hochwald and T. L. Marzetta, "Unitary space-time modulation for multiple-antenna communications in Rayleigh flat fading," *IEEE Transactions on Information Theory,* vol. 46, pp. 543-564, 2000.

[52] E. Biglieri, J. Proakis and S. Shamai, "Fading channels: information-theoretic and communications aspects," *IEEE Transactions on Information Theory,* vol. 44, pp. 2619-2692, 1998.

[53] A. R. Jafri, A. Baghdadi and M. Jezequel, "Parallel MIMO Turbo Equalization," *IEEE Communications Letters,* vol. 15, pp. 290-292, 2011.

[54] K. Ui-kun and I. Gi-hong, "Cyclic delay diversity with frequency domain turbo equalization for uplink fast fading channels," *IEEE Communications Letters,* vol. 13, pp. 184-186, 2009.

[55] C. Won-Joon and J. M. Cioffi, "Multiple input/multiple output (MIMO) equalization for space-time block coding," in *IEEE Pacific Rim Conference on Communications, Computers and Signal Processing*, pp. 341-344, *1999*.

[56] C. Won-Joon and J. M. Cioffi, "Space-time block codes over frequency selective Rayleigh fading channels," in *IEEE 50th Conference on Vehicular Technology*, vol.5, pp. 2541-2545, *1999*.

[57] L. Ye, J. H. Winters and N.R. Sollenberger, "Signal detection for MIMO-OFDM wireless communications," in *IEEE International Conference on Communications*, vol.10, pp. 3077-3081, 2001.

[58] K. P. Kongara, K. Ping-Heng, P. J. Smith, L. M. Garth and A. Clark, "Block-Based Performance Measures for MIMO OFDM Beamforming Systems," *IEEE Transactions on Vehicular Technology,* vol. 58, pp. 2236-2248, 2009.

[59] G. Bauch, "Space-time block codes versus space-frequency block codes," in *the 57th IEEE Semiannual Conference on Vehicular Technology*, vol.1, pp. 567-571, *2003*.

[60] C. Tsung-Hui, M. Wing-Kin and C. Chong-Yung, "Maximum-Likelihood Detection of Orthogonal Space-Time Block Coded OFDM in Unknown Block Fading Channels," *IEEE Transactions on Signal Processing,* vol. 56, pp. 1637-1649, 2008.

[61] H. Bolcskei, "MIMO-OFDM wireless systems: basics, perspectives, and challenges," *IEEE Wireless Communications* , vol. 13, pp. 31-37, 2006.

[62] L. Sili, B. Narasimhan and N. Al-Dhahir, "A Novel SFBC-OFDM Scheme for Doubly Selective Channels," *IEEE Transactions on Vehicular Technology,* vol. 58, pp. 2573-2578, 2009.

[63] I. B. W. A. W. Group., " Channel Models for Fixed Wireless Applications," vol. IEEE 802.16a-03/01, 2003.

[64] R. W. Chang, "Synthesis of band-limited orthogonal signals for multichannel data transmission," *Bell Systems Technical Journal,* pp. 1775–1796, 1966.

[65] C. Sungkeun, P. Myonghee, L. Sungeun, B. Keuk-Joon and H. Daesik, "A new PAPR reduction technique for OFDM systems using advanced peak windowing method," *IEEE Transactions on Consumer Electronics,* vol. 54, pp. 405-410, 2008.

[66] Y. Wang and Z. Luo, "Optimized Iterative Clipping and Filtering for PAPR Reduction of OFDM Signals," *IEEE Transactions on Communications,* vol. 59, pp. 33-37, 2011.

[67] K. F. Lee and D. B. Williams, "A space-frequency transmitter diversity technique for OFDM systems," in *Conference on Global Telecommunications*, vol.3, pp. 1473-1477, *2000.*

[68] L. Ye, N. Sheshadri and S. Ariyavisitakul, "Channel estimation for OFDM systems with transmitter diversity in mobile wireless channels," *IEEE Journal on Selected Areas in Communications,* vol. 17, pp. 461-471, 1999.

[69] A. Ghosh, D. R. Wolter, J. G. Andrews and R. Chen, "Broadband wireless access with WiMax/802.16: current performance benchmarks and future potential," *IEEE Communications Magazine ,* vol. 43, pp. 129-136, 2005.

[70] A. Ghosh, *R. Ratasuk, B. Mondal, N. Mangalvedhe and T. Thomas,* "LTE-advanced: next-generation wireless broadband technology," *IEEE Wireless Communications,* vol. 17, pp. 10-22, 2010.

[71] E. Beres and R. Adve, "Blind Channel Estimation for Orthogonal STBC in MISO Systems," *IEEE Transactions on Vehicular Technology,* vol. 56, pp. 2042-2050, 2007.

[72] H. Bolcskei, R. W. Heath and A. J. Paulraj, "Blind equalization in OFDM-based multi-antenna systems," in *the IEEE Symposium on Adaptive Systems for Signal Processing, Communications, and Control*, pp. 58-63, 2000.

[73] V. Choqueuse, A. Mansour, G. Burel, L. Collin and K. Yao, "Blind Channel Estimation for STBC Systems Using Higher-Order Statistics," *IEEE Transactions on Wireless Communications,* vol. 10, pp. 495-505, 2011.

[74] M. Morelli and U. Mengali, "A comparison of pilot-aided channel estimation methods for OFDM systems," *IEEE Transactions on Signal Processing,* vol. 49, pp. 3065-3073, 2001.

[75] J. Won Gi, P. Kyung Hyun and C. Yong Soo, "An efficient channel estimation technique for OFDM systems with transmitter diversity," in *The 11th IEEE International Symposium on Personal, Indoor and Mobile Radio Communications*, vol.2, pp. 1246-1250, *2000.*

[76] G. L. Stuber, J. R. Barry, S. W. McLaughlin, L. Ye, M. A. Ingram and T. G. Pratt, "Broadband MIMO-OFDM wireless communications," *Proceedings of the IEEE,* vol. 92, pp. 271-294, 2004.

[77] L. Ye, "Simplified channel estimation for OFDM systems with multiple transmit antennas," *IEEE Transactions on Wireless Communications,* vol. 1, pp. 67-75, 2002.

[78] "IEEE Standard for Local and metropolitan area networks Part 16: Air Interface for Broadband Wireless Access Systems," *IEEE Std 802.16-2009 (Revision of IEEE Std 802.16-2004)*, pp. C1-2004, 2009.

[79] "IEEE 802.16a-03/01 Channel Models for Fixed Wireless Applications," 2003.

[80] R. V. Nee and R. Prasad, *OFDM for Wireless Multimedia Communications*, 2000

[81] J. Yunho, K. Jiho, L. Seongjoo, Y. Hongil and K. Jaeseok, "Design and Implementation of MIMO-OFDM Baseband Processor for High-Speed Wireless LANs," *IEEE Transactions on Circuits and Systems II: Express Briefs*, vol. 54, pp. 631-635, 2007.

[82] H. Dogan, H. A. Cirpan and E. Panayirci, "Iterative Channel Estimation and Decoding of Turbo Coded SFBC-OFDM Systems," *IEEE Transactions on Wireless Communications*, vol. 6, pp. 3090-3101, 2007.

[83] G. Feifei, Z. Yonghong, A. Nallanathan and N. Tung-Sang, "Robust subspace blind channel estimation for cyclic prefixed MIMO ODFM systems: algorithm, identifiability and performance analysis," *IEEE Journal on Selected Areas in Communications*, vol. 26, pp. 378-388, 2008.

[84] C. Shin, R. W. Heath and E. J. Powers, "Blind Channel Estimation for MIMO-OFDM Systems," *IEEE Transactions on Vehicular Technology*, vol. 56, pp. 670-685, 2007.

[85] F. Delestre, E. Masoud, Y. Sun and A. Slaney, "Detection scheme for space-time block codes wireless communications without channel state information," in *11th IEEE Singapore International Conference on Communication Systems*, pp. 77-81, *2008*.

[86] S. D. Muruganathan and A. B. Sesay, "A Low-Complexity Decision-Directed Channel-Estimation Scheme for OFDM Systems With Space-Frequency Diversity in Doubly Selective Fading Channels," *IEEE Transactions on Vehicular Technology*, vol. 58, pp. 4277-4291, 2009.

[87] L. Deneire, P. Vandenameele, L. Van der Perre, B. Gyselinckx and M. Engels, "A low complexity ML channel estimator for OFDM," in *IEEE International Conference on Communications*, vol.5, pp. 1461-1465, 2001.

[88] H. Minn, K. Dong In and V. K. Bhargava, "A reduced complexity channel estimation for OFDM systems with transmit diversity in mobile wireless channels," *IEEE Transactions on Communications*, vol. 50, pp. 799-807, 2002.

[89] L. Tingting, W. Mao, L. Yan, S. Feng, W. Jianxin, S. Weixin, C. Qian, "A Minimum-Complexity High-Performance Channel Estimator for MIMO-OFDM Communications," *IEEE Transactions on Vehicular Technology*, vol. 59, pp. 4634-4639, 2010.

[90] A. D. Marousis and P. Constantinou, "An efficient channel estimation scheme for realistic SFBC MISO OFDM systems," in *First European Conference on Antennas and Propagation*, pp. 1-6, *2006*.

[91] "IEEE 802.16a-03/01 Channel Models for Fixed Wireless Applications," 2003.

[92] M. Torabi, S. Aissa and M. R. Soleymani, "On the BER Performance of Space-Frequency Block Coded OFDM Systems in Fading MIMO Channels," *IEEE Transactions on Wireless Communications*, vol. 6, pp. 1366-1373, 2007.

[93] H. Zamiri-Jafarian and S. Pasupathy, "Robust and Improved Channel Estimation Algorithm for MIMO-OFDM Systems," *IEEE Transactions on Wireless Communications,* vol. 6, pp. 2106-2113, 2007.

[94] C. Hsiao-Yun, K. Meng-Lin, J. Shyh-Jye and H. Chia-Chi, "A Robust Channel Estimator for High-Mobility STBC-OFDM Systems," *IEEE Transactions on Circuits and Systems I: Regular Papers,* vol. 57, pp. 925-936, 2010.

[95] P. Jung-Hyun, O. Mi-Kyung and P. Dong-Jo, "New Channel Estimation Exploiting Reliable Decision-Feedback Symbols for OFDM Systems," in *IEEE International Conference on Communications*, pp. 3046-3051, *2006*.

[96] G. Yi and K. B. Letaief, "Low complexity channel estimation for space-time coded wideband OFDM systems," *IEEE Transactions on Wireless Communications,* vol. 2, pp. 876-882, 2003.

[97] T. Y. Al-Naffouri, O. Awoniyi, O. Oteri and A. Paulraj, "Receiver design for MIMO-OFDM transmission over time variant channels," in *IEEE Conference on Global Telecommunications*, vol.4, pp. 2487-2492, *2004*.

[98] L. Seung Joon, "On the training of MIMO-OFDM channels with least square channel estimation and linear interpolation," *IEEE Communications Letters*, vol. 12, pp. 100-102, 2008.

[99] D. Cescato and H. Bolcsksei *, et al.,* "Algorithms for Interpolation-Based QR Decomposition in MIMO-OFDM Systems," *IEEE Transactions on Signal Processing,* vol. 59, pp. 1719-1733, 2011.

[100] Z. En, H. Xiaolin, C. Jianping, Z. Zhan and H. Kayama, "FPGA implementation and experimental performances of a novel timing synchronization method in MIMO-OFDM systems," in *14th IEEE Asia-Pacific Conference on Communications*, pp. 1-5, *2008*.